

Nanostructure Formation during Lipid Digestion

A thesis submitted for the degree of
Doctor of Philosophy

Submitted by

Stephanie Phan

Bachelor of Pharmaceutical Sciences (Honours)

Monash University



Drug Delivery, Disposition and Dynamics
Monash Institute of Pharmaceutical Sciences
Monash University (Parkville Campus)
381 Royal Parade, Parkville
Victoria 3052, Australia

August 2015

To my dearest husband, Kevin James Rietmyk

Copyright Notice

© Stephanie Phan. Except as provided in the Copyright Act 1968, this thesis may not be reproduced in any form without the written permission of the author.

Contents

Abstract	I
Declaration of Authorship.....	II
Publications.....	IV
Communications	V
Acknowledgements.....	VI
List of Abbreviations.....	VIII
Thesis Structure.....	IX
Chapter 1. Introduction	1
1.1 Declaration.....	2
1.2 Self-assembled Structures Formed during Lipid Digestion: Characterization and Implications for Oral Lipid-based Drug Delivery Systems	3
1.3 A Statement of the Problem.....	4
1.4 Lipid Digestion and Absorption	5
1.5 Enhancement of Absorption of Lipophilic Poorly Water-Soluble Drugs by Lipids	6
1.6 Lipid and Lipid-Based Formulation Classification Systems.....	7
1.7 Self-Assembled Structures in Lipid Systems	9
1.8 Techniques for the Study of Structures During Digestion	12
1.8.1 Microscopy Techniques.....	12
1.8.1.1 Light Microscopy	12
1.8.1.2 Cross Polarised Light Microscopy (CPLM)	14
1.8.1.3 Freeze Fracture Electron Microscopy (FFEM).....	14
1.8.1.4 Cryogenic-Transmission Electron Microscopy (cryo-TEM).....	15
1.8.1.5 Cryogenic Field Emission Scanning Electron Microscopy (cryo-FESEM)	16
1.8.2 Scattering Techniques.....	17
1.8.2.1 Polarised and Depolarised Dynamic Light Scattering (DLS).....	17
1.8.2.2 Small and Wide Angle X-ray Scattering (SAXS/WAXS).....	18

1.8.2.3 Small Angle Neutron Scattering (SANS).....	19
1.8.3 Spectroscopic Techniques.....	19
1.8.3.1 Nuclear Magnetic Resonance (NMR) Spectroscopy	19
1.8.3.2 Raman Spectroscopy and Multiplex Coherent Anti-Stokes Raman Scattering (CARS) Microspectroscopy	20
1.8.3.3 Electron Paramagnetic Resonance (EPR) Spectroscopy	20
1.9. Self-Assembled Structures in Digesting Lipid Systems	21
1.9.1 Equilibrium ‘Assembled’ Studies	21
1.9.2 <i>In Vitro</i> Dynamic Studies in Real Time.....	27
1.9.2.1 Approaches and Models for <i>In Vitro</i> Digestion	27
1.9.2.2 Structures Formed During <i>In Vitro</i> Digestion Studies	29
1.9.3 <i>Ex Vivo</i> Studies	32
1.9.4 <i>In Vivo</i> Studies	35
1.10 Current Limitations in Characterising Structural Aspects of Lipolysis	35
1.11 Hypotheses.....	36
1.12 Aims	38
1.13 References	39
Chapter 2. General Materials and Experimental Techniques.....	47
2.1 Materials.....	48
2.1.1 Lipids.....	48
2.1.2 General Materials	48
2.2 Preparation of Digestion Buffer and Simulated Intestinal Fluid.....	49
2.3 Preparation of Equilibrium Systems.....	49
2.4 <i>In Vitro</i> Lipolysis.....	49
2.5 Methods for Characterising Liquid Crystalline Structures	50
2.5.1 Small Angle X-ray Scattering (SAXS).....	50
2.5.2 Small Angle Neutron Scattering (SANS)	52
2.5.4. Dynamic Light Scattering (DLS).....	53

2.5.4 Cryogenic Transmission Electron Microscopy (cryo-TEM)	54
2.6 High Performance Liquid Chromatography (HPLC)	55
2.7 References	56
Chapter 3. Disposition and Crystallization of Saturated Fatty Acid in Mixed Micelles	58
3.1 Declaration	59
3.2 Disposition and Crystallization of Saturated Fatty Acids in Mixed Micelles of Relevance to Lipid Digestion.....	61
3.3 Introduction	62
3.4 Experimental.....	65
3.5 Results and Discussion.....	69
3.6 Conclusion.....	76
3.7 Supporting Information	78
3.8 References	85
Chapter 4. How Relevant Are Assembled Equilibrium Samples in Understanding Structure Formation during Lipid Digestion?.....	89
4.1 Declaration	90
4.2 How Relevant Are Assembled Equilibrium Samples in Understanding Structure Formation during Lipid Digestion?	91
4.3 Introduction	92
4.4 Experimental.....	93
4.5 Results	96
4.6 Discussion	105
4.7 Conclusion.....	108
4.8 Supporting Information	109
4.9 References	111
Chapter 5. Structural Aspects of Digestion of Medium Chain Triglycerides.....	114
5.1 Declaration	115

5.2 Structural Aspects of Digestion of Medium Chain Triglycerides Studied in Real Time using sSAXS and cryo-TEM	116
5.3 Introduction	117
5.4 Experimental.....	120
5.5 Results	123
5.6 Discussion	134
5.7 Conclusion.....	138
5.8 References	139
Chapter 6. Immobilised Lipase for Enhanced Structural Resolution	142
6.1 Declaration	143
6.2 Immobilised Lipase for <i>In Vitro</i> Lipolysis Experiments.....	144
6.3 Introduction	145
6.4 Experimental.....	147
6.5 Results	151
6.6 Discussion	156
6.7 Conclusion.....	159
6.8 Supporting Information	160
6.9 References	162
Chapter 7. Summary and Perspectives.....	165
7.1 Summary of Findings.....	166
7.2 Future Directions	167
7.3 References	169

Abstract

An increasing number of new drug compounds are poorly water-soluble in nature, leading to limited solubility and absorption in the gastrointestinal tract, and hence low and variable bioavailability. Lipid-based formulations are increasingly viewed as an avenue to enhance the delivery of such drug molecules. During the digestion of formulation components, the lipolysis products disperse in the gastrointestinal environment and self-assemble into colloidal phases, enabling drug solubilisation.

Traditionally, the focus of research in these formulations has been on the compositional aspects, due to a lack of methods to study structure formation in real-time. To address this current shortcoming, the research undertaken in this thesis examines structure formation in the gastrointestinal tract during lipid digestion. Two approaches have been examined; equilibrium and dynamic studies. In equilibrium studies, bile salt/phospholipid mixed micelles upon incorporation of monoglycerides and fatty acids were studied by scattering and microscopy techniques to determine the influence of pH, temperature and lipid chain length on self-assembly behaviour. An *in vitro* lipolysis model coupled to synchrotron small angle X-ray scattering was employed for structural studies in real-time, where structure formation was linked to composition using pH stat titration, cryogenic-transmission electron microscopy and high performance liquid chromatography. In addition, the possibility of using an immobilised lipase to address drawbacks in the use of porcine pancreatic lipase for *in vitro* lipolysis experiments, particularly in terms of scattering measurements was investigated.

The studies described in this thesis have provided new approaches and insights into structure formation during lipid digestion and further understanding for the rational design of lipid-based drug formulations.

Declaration of Authorship

In accordance with Monash University Doctorate Regulation 17/Doctor of Philosophy and Master of Philosophy (MPhil) regulations the following declarations are made:

I hereby declare that this thesis contains no material which has been accepted for the award of any other degree or diploma at any university or equivalent institution and that, to the best of my knowledge and belief, this thesis contains no material previously published or written by another person, except where due reference is made in the text of the thesis.

This thesis includes four original papers published in peer reviewed journals and one unpublished manuscript. The core theme of the thesis is the understanding of nanostructure formation during lipid digestion. The ideas, development and writing up of all the papers in the thesis were the principle responsibility of myself, the candidate, working within the theme of Drug Delivery, Disposition and Dynamics, under the supervision of Professor Ben J. Boyd.

The inclusion of co-authors reflects the fact that the work came from active collaboration between researchers.

In the case of Chapters 1, 3, 4, 5 and 6, my contribution to the work involved the following:

Thesis chapter	Publication title	Publication status	Nature and extent of candidate's contribution
1	Self-assembled structures formed during lipid digestion: Characterisation and implications for oral lipid-based drug delivery systems	Published	Manuscript preparation
3	Disposition and crystallization of fatty acid in mixed micelles of relevance to lipid digestion	Published	Research design, performance of data collection and analysis, manuscript preparation
4	How relevant are assembled equilibrium samples in understanding structure formation during lipid digestion?	Published	Research design, performance of data collection and analysis, manuscript preparation
5	Structural aspects of digestion of medium chain triglycerides studied in real time using sSAXS and cryo-TEM	Published	Research design, performance of data collection and analysis, manuscript preparation
6	Immobilised lipase for in vitro lipolysis experiments	Published	Research design, performance of data collection and analysis, manuscript preparation

I have renumbered sections of submitted or published papers in order to generate a consistent presentation within the thesis.

Signed:



Date: 21/08/15

Publications

First author

1. Phan S., Hawley A., Mulet X, Waddington L., Prestidge C.A., Boyd B.J., *Structural aspects of digestion of medium chain triglycerides studied in real time using sSAXS and cryo-TEM*. Pharm Res, 2013. **30**(12): p.3088-3100.
2. Phan S., Salentinig S., Prestidge C.A., Boyd B.J., Self-assembled structures formed during lipid digestion: Characterisation and implications for oral lipid-based drug delivery systems. Drug Delivery and Transl Res, 2013. **4**(3): p.275-294.
3. Phan S., Salentinig S., Gilbert E.P., Darwish T.A., Hawley A., Nixon-Luke R., Bryant G., Boyd B.J., *Disposition and crystallization of fatty acid in mixed micelles of relevance to lipid digestion*. J Colloid Interface Sci, 2015. **449**: p.160-166.
4. Phan S., Salentinig S., Hawley A., Boyd B.J., *Immobilised lipase for in vitro lipolysis experiments*. J Pharm Sci, 2015. **104**(4) p:1311-1318.
5. Phan S., Salentinig S., Hawley A., Boyd B.J., *How relevant are assembled equilibrium samples in understanding structure formation during lipid digestion?* Eur J Pharm Biopharm, 2015 (published online 23/07/15, DOI: 10.1016/j.ejpb.2015.07.015).

Second author

1. Salentinig S., Phan S., Khan J., Hawley A., Boyd B.J., *Formation of highly organised nanostructures during the digestion of milk*. ACS Nano, 2013. **7**(12): p. 10904-10911.
2. Salentinig S., Phan S., Darwish T.A., Kirby N., Boyd B.J., Gilbert E.P., *pH-responsive micelles based on caprylic acid*. Langmuir, 2014. **30**(25): p. 7296-303.
3. Salentinig S., Phan S., Hawley A., Boyd B.J., *Self-assembly structure formation during the digestion of human breast milk*. Angewandte Chem Int Ed, 2014 **54**(5): p. 1600-1603.

Communications

1. Phan S., Mulet X., Boyd B.J., *Effect of dietary lipids on bile salt micelles*. Poster presentation, AUS-CRS Conference 5th Annual Meeting 2011, Hamilton Island, Australia.
2. Phan S., Mulet X., Hawley A., Waddington L., Boyd B.J., *Linking structure and composition during digestion of lipid-based drug formulations*. Poster presentation, Drug Delivery Australia Meeting 2012, Melbourne, Australia.
3. Phan S., Mulet X., Boyd B.J., *Real time SAXS studies for understanding structure in digesting lipid systems*. Oral presentation, 5th International Small-Angle Scattering Conference 2012, Sydney, Australia.
4. Phan S., Mulet X., Hawley A., Waddington L., Boyd B.J., *Strategies for linking structure and composition during digestion of lipid-based drug formulations*. Poster presentation, Australia Colloid and Interface Symposium 2013, Noosa, Australia.
5. Phan S., Hawley A., Boyd B.J., *Solid state characterization of drug precipitation during digestion of super-SNEDDS lipid based drug delivery system using synchrotron SAXS/WAXS*. Poster presentation, 40th Annual Meeting & Exposition of the Controlled Release Society 2013, Honolulu, Hawaii, USA.
6. Phan S., Salentinig S., Boyd B.J., *Nanostructure formation during the digestion of milk*. Oral presentation, 8th Annual Higher Degrees by Research Symposium 2013, Melbourne, Australia.
7. Phan S., Salentinig S., Boyd B.J., *Nanostructure formation during lipid digestion*. Oral presentation, 29th Australian Colloid and Surface Science Student Conference 2014, Melbourne, Australia.
8. Phan S., Salentinig S., Boyd B.J., Kirby N., Darwish T.A., Gilbert E.P., *Structural investigation into the influence of lipolysis products on the structure of bile salt micelles*. Poster presentation, 5th FIP Pharmaceutical Sciences World Congress 2014, Melbourne, Australia.
9. Phan S., Salentinig S., Hawley A., Boyd B.J., *Immobilised lipase for in vitro lipolysis experiments*. Poster presentation, 10th Biennial Globalization of Pharmaceutics Education Network Conference 2014, Heksinki, Finland.

Acknowledgements

First and foremost, I would like to express my sincere gratitude to Doctor Father Ben Boyd for your guidance and encouragement. You often said that a PhD is much more than a project and I appreciate the countless opportunities I have had to learn, travel and grow, both professionally and personally. Your wealth of knowledge, dedication, and hardworking attitude (as evidenced by your ability to not look like a zombie during beamtimes and stamina to party harder than us at conferences) is admirable, and it has been an honour to work in such a productive and fun working environment.

I would also like to thank Stefan Salentinig for the many discussions, scientific and not so scientific, and your good sense of humour. It has been amusing having you around in the office and working in the lab with you! Xavier Mulet, thanks for believing in me and for being my 'digestion assistant' during my first 24 hour beamtime, I couldn't have done it without you.

Thanks to our collaborators, Nigel Kirby, Adrian Hawley and Stephen Mudie from the SAXS/WAXS beamline at the Australian Synchrotron for being so accommodating with our complicated and fiddly setups in such a small workspace, and for technical support at odd hours in the night. Thanks to Lynne Waddington, from CSIRO, for assistance with cryo-TEM measurements. I appreciate your enthusiasm and the entertaining conversations we had as we hunted down vesicles and liquid crystalline phases in my samples.

Thanks to the Boyd group family – Tri-Hung Nguyen, Charlie Dong, Jason Liu, Oliver Montagnat, Graham Webster, Kathy Lee, Khay Fong, Adam Tilley, Josephine Chong, Kristian Tangso, Jamal Khan, Joanne Du, Nicolas Alcaraz, Linda Hong and Tang Li for your friendship, troubleshooting help with various equipment, and for sharing in the trials and triumphs in the lab.

The Australian Postgraduate Award and the Australian Research Council are acknowledged for financial support.

To my family, and especially my parents, thank you for your support, patience, making sure I am always well fed and for your unfailing love. Your encouragement, hard work and sacrifices over the years have given me the opportunity to pursue my dreams, and for that I am eternally grateful.

And finally to Kevin Rietwyk, whom I met just as I was beginning my research career, I did not know at the time I would be embarking on another adventure! I have found you to be a constant source of joy, strength and inspiration, and I am sincerely grateful for your compassion, generosity and enduring love.

List of Abbreviations

4-BPBA, 4-bromophenylboronic acid

BS, bile salt

CALB, lipase B from *Candida antarctica*

Cryo-TEM, cryogenic-transmission electron microscopy

DLS, dynamic light scattering

DDLS, depolarized dynamic light scattering

FA, fatty acid

GIT, gastrointestinal tract

HPLC, high performance liquid chromatography

LCT, long chain triglyceride

MCT, medium chain triglyceride

MG, monoglyceride

PL, phospholipid

SANS, small angle neutron scattering

SAXS, small angle X-ray scattering

sSAXS, synchrotron small angle X-ray scattering

SIF, simulated intestinal fluid

TBU, tributyrin units

TG, triglyceride

Thesis Structure

The chapters of this thesis have been directly reproduced from published or submitted manuscripts. Chapter 1 is a review introducing lipid digestion, lipid self-assembled structures and the use for lipid-based formulations for the delivery of poorly water-soluble drugs, to enhance drug solubilisation and absorption in the gastrointestinal tract. It summarises the various experimental approaches that have been applied to the study of structure formation during digestion of these formulations, and concludes with the hypotheses and aims of this thesis. As this review was published before the decision to study immobilised lipase in Chapter 6, it does not include literature on relevant aspects of immobilised lipases. Instead, such a literature study has been inserted in Section 1.10 so that it supports the subsequently stated hypotheses and aims.

Chapter 2 is a relevant materials and experimental techniques section which contains a more detailed description of the methods that have been employed, developed and validated. The experimental chapters (Chapter 3, 4, 5 and 6) have been ordered systematically.

Chapter 3 is the first experimental chapter, which investigates the likely structure formation in the gastrointestinal tract during lipid digestion in equilibrium systems containing lipolysis products of increasing carbon chain length. Studying equilibrium systems was a logical starting point for this thesis as it addresses past work which have taken this approach and serves as a basis to understand the subsequent chapters. The studies were performed in a controlled manner which provides a framework for understanding how factors such as pH, temperature and lipid chain length, influence self-assembly behaviour of these lipids.

Chapter 4 builds on the previous chapter and probes similarities and differences in colloidal structures formed under equilibrium and dynamic conditions. *In vitro* lipolysis experiments are more complex than equilibrium experiments due to dispersion of the digestion medium and the addition of lipase, which initiates digestion of triglyceride and production of amphiphilic lipolysis products as the reaction progresses. Hence, the study of structure formation using synchrotron small angle X-ray scattering (sSAXS) during lipolysis of triglyceride emulsions in real-time were anticipated to be more *in vivo* relevant than equilibrium systems.

Chapter 5 continues to use the *in vitro* lipolysis model coupled to sSAXS and focusses on linking composition and real-time structure formation during the digestion of medium chain triglycerides. These lipids have generated interest due to their great solubilising capacity for highly lipophilic drugs, and so the structure formation in these systems and the influence of

lipid:bile salt ratio was of interest in this thesis and adds understanding for the rational design of lipid-based formulations.

The porcine pancreatic lipase used in these studies is a crude extract containing many proteins that contribute to a high level of 'background' scattering in the same regime as the colloidal structures, limiting determination of structure to particles with strong 'Bragg peaks' in the scattering profiles. In order to overcome this problem, possible use of immobilised lipase that could be separated from the digestion mixture was proposed. Hence, Chapter 6 investigates the potential for lipase immobilised onto micrometre sized polymer beads that can be separated from the solution during measurements to improve the quality of scattering data during *in vitro* lipolysis.

The thesis is concluded in Chapter 7 with a summary and perspectives chapter

Chapter 1. Introduction

Chapter 1. Introduction

This chapter is a review on the current state of knowledge of colloidal structures generated during lipid digestion. It focuses on lipid-based drug formulations, techniques for studying lipid structures during digestion, and spans from ‘assembled’ phase diagram approaches, to contemporary real-time methods. This chapter has been published as: Phan S., Salentinig S., Prestidge C.A., Boyd B.J., *Self-assembled structures formed during lipid digestion: Characterisation and implications for oral lipid-based drug delivery systems*. Drug Delivery and Transl Res, 2013. 4(3): p.275-294.

1.1 Declaration

Declaration by candidate:

In the case of Chapter 1, the nature and extent of my contribution to the work was the following:

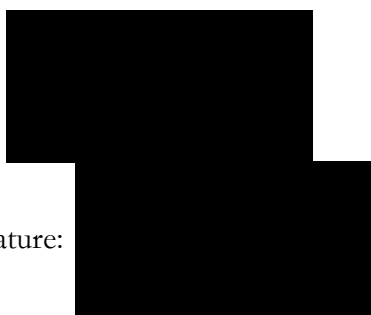
Nature of contribution	Extent of contribution
Manuscript preparation	80%

The following co-authors contributed to the work:

Name	Nature of contribution
Stefan Salentinig	Input into manuscript preparation
Clive A. Prestidge	Input into manuscript preparation
Ben J. Boyd	Supervision, intellectual input, input into manuscript preparation

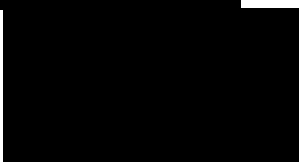
The undersigned hereby certify that the above declaration correctly reflects the nature and extent of the candidate’s and co-authors’ contributions to this work.

Candidate’s signature:



Date: 21/08/15

Main supervisor’s signature:



Date: 21/08/15

1.2 Self-assembled Structures Formed during Lipid Digestion: Characterization and Implications for Oral Lipid-based Drug Delivery Systems

Stephanie Phan ¹, Stefan Salentinig ¹, Clive A. Prestidge ², Ben J. Boyd ^{1,3}

¹ Drug Delivery, Disposition and Dynamics, Monash Institute of Pharmaceutical Sciences, Monash University (Parkville Campus), 381 Royal Parade, Parkville, VIC 3052, Australia

² Ian Wark Research Institute, University of South Australia (Mawson Lakes Campus), SA, Australia

Received and published online 18th September 2013

Citation: Drug Deliv. and Transl. Res. (2014) 4:275–294

DOI: 10.1007/s13346-013-0168-5

Abstract

There is increasing interest in the use of lipid-based formulations for the delivery of poorly water-soluble drugs. After ingestion of the formulation, exposure to the gastrointestinal environment results in dispersion and digestion processes, leading to the production of amphiphilic digestion products that form self-assembled structures in the aqueous environment of the intestine. These structures are crucial for the maintenance of drug in a solubilized state prior to absorption. This review describes the structural techniques used to study such systems, the structures formed in assembled ‘equilibrium’ compositions where components are combined in expected ratios representative of the endpoint of digestion, structures formed using dynamic *in vitro* ‘non-equilibrium’ digestion models where the composition and hence structures present change over time, and observations from *ex vivo* aspirated samples. Possible future directions towards an improved understanding of structural aspects of lipid digestion are proposed.

1.3 A Statement of the Problem

The discovery of poorly water-soluble drug candidates in drug discovery programs often poses problems during development due to reduced systemic exposure after oral administration. It has been known for some time that the co-administration of lipophilic drugs with natural or synthetic lipids may enhance drug absorption and bioavailability. For lipophilic and highly permeable drugs, this has been attributed to enhanced drug solubilisation and dissolution in the small intestine due to the presence of endogenous and exogenous lipid, lipid digestion products and colloidal structures thereof (Figure 1.1) [1, 2]. Consequently lipid-based formulations for poorly water-soluble drugs are becoming an increasingly popular avenue to improve absorption.

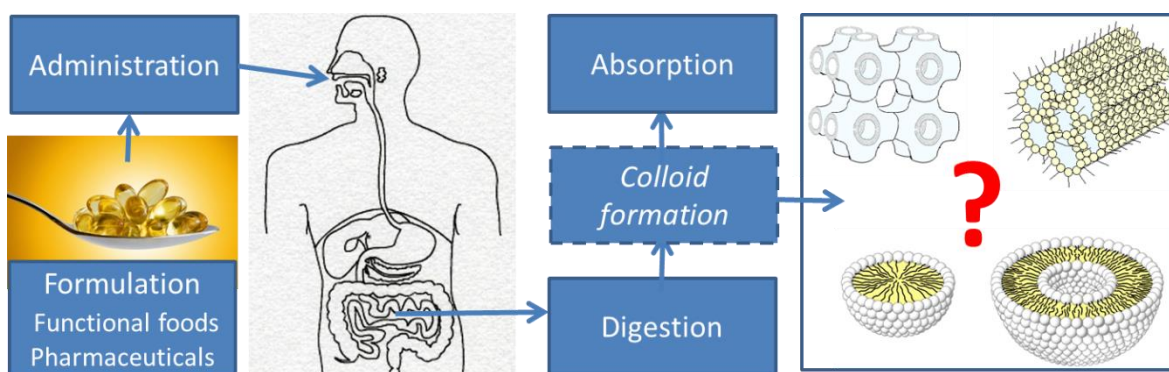


Figure 1.1: Formulation, digestion and colloid formation are all linked in the process of improving bioavailability for poorly water-soluble drugs when administered with digestible lipids and lipid formulations.

Despite the recognition that the formation of self-assembled structure is an important determinant of drug solubilizing capacity in the gastrointestinal tract, and are hence critical to drug absorption [3, 4], the literature to date has largely focussed on composition during digestion rather than structure. *In vitro* digestion models have been developed to determine the composition of digesting lipid media; the digestion process can be followed by titration, and digested lipids and solubilized and precipitated drug concentrations can be determined analytically [5-11]. The focus on composition rather than structure has been in part due to the fact that digestion is a dynamic process, and a major challenge in the field has been a lack of

methods to study structure formation in real time. Thus, this thesis focuses on structure formation during lipid digestion, and linking structure with composition.

1.4 Lipid Digestion and Absorption

Enzymatic digestion of lipids takes place in the gastrointestinal tract (GIT) under the action of gastric lipase from chief cells lining gastric mucosa [12, 13], and lipase and co-lipase from the pancreas [14]. Partial digestion of dietary triglycerides (TG) to diglyceride (DG) and fatty acid (FA) occurs in the stomach by the gastric lipase [15], which is assisted by mechanical mixing to form a crude emulsion, however most lipid digestion occurs in the small intestine, where the TGs are digested by water-soluble pancreatic lipase/co-lipase at the oil-water interface [16]. This enzyme stereospecifically hydrolyses the ester bonds linking the FA to glycerol at the Sn1 and Sn3 position to nominally produce two FAs and a 2-monoglyceride (MG) [17]. However, it is possible, and perhaps likely, that digestion occurs to a greater extent, and it has been reported that the molar ratio of MG:FA in human intestinal fluids may be as high as 1:6 [18, 19]. Rautureau *et al.* suggest that this could be due to faster absorption of MG compared to FA [20]. Due to the presence of free fatty acid, a strong pH effect on the structure formation and transformation can be expected as the pH changes through the digestive tract [21-24]

Endogenous amphiphilic molecules, including phospholipids (PL), cholesterol (chol) and bile salts (BS), are secreted in bile from the gall bladder into the small intestine, and act as emulsifying agents to solubilise lipids by the formation of a variety of structures including liquid crystals, vesicles and mixed micelles. Bile salts are derived from cholesterol, and their structure consists of a non-planar steroid ring with variations in the number, position and stereochemistry of the hydroxyl groups in the steroid nucleus, and amino-acid conjugation (Figure 1.2) [25, 26]. They have polar and non-polar sides and are capable of self-assembly to form globular, elongated and disc-like micelles in combination with lecithin [27-29]. Mixed micelles act to remove digestion products from the oil-water interface as FA and MG have high interfacial activity and can replace the lipase from the oil-water interface [30-32]. Although discussion still persists on the exact mechanism of lipid absorption, it is generally accepted that lipid is absorbed from this mixed colloidal phase, most likely from micelles, via partitioning into the membrane of intestinal epithelial cells (enterocytes).

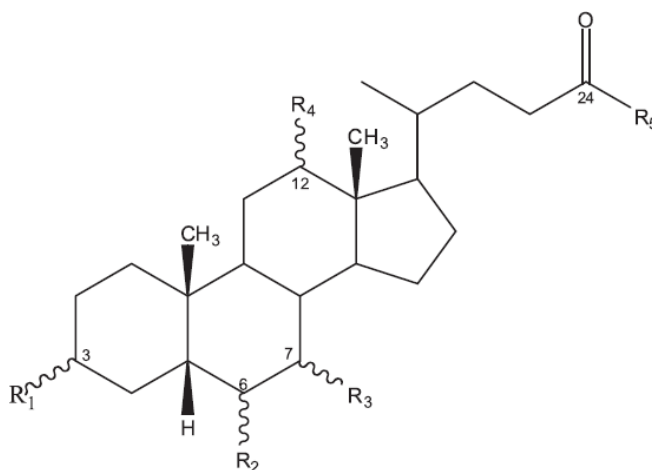


Figure 1.2: General structure of bile salt where variation in OH and H groups occurs at the R¹-R⁴ positions and variation in amino acid conjugation occurs at the R⁵ position. Figure reproduced from [26].

1.5 Enhancement of Absorption of Lipophilic Poorly Water-Soluble Drugs by Lipids

Lipophilic drugs with low aqueous solubility, less than 100 µg/mL, often have limited or variable absorption and bioavailability [33]. Solubility becomes an issue in cases where the dissolution rate is so slow that the time required for dissolution to occur is longer than the transit time past the site of absorption. The dose:solubility ratio is an important measure of solubility and is defined as the volume of gastrointestinal fluid required to dissolve the administered dose [34]. Solubility in the GIT depends on the physicochemical properties of the drug molecules, including aqueous solubility, molecular weight, crystalline form, drug lipophilicity and pK_a, and solvent variables such as the presence of endogenous surfactants and co-ingested food, counter-ions, surface tension, buffer capacity, osmolarity and pH of the GIT.

The role of co-administered dietary and formulation lipids in enhancing lipophilic, poorly water-soluble drug absorption is well known [1, 2, 7, 35-37]. In both cases there is the potential to enhance drug solubilisation by utilising the body's natural lipid digestion process to increase biliary secretion of BS, PL and cholesterol. These surfactants lower the surface tension of gastrointestinal (GI) fluids [35] and solubilise drug via the formation of dispersed colloidal structures [38, 39]. Micellar solubilisation enhances luminal solubility by up to 1000

fold [40]. In the case of lipid-based drug formulations, exogenous lipids may also intercalate into the BS/PL structures and promote micellar swelling, thus further increasing the solubilising capacity [36]. For example, these self-assembled structures have been shown to increase the uptake of tocopherol into Caco-2 cells [41].

The potential for enhanced bioavailability is influenced by factors such as lipid chain length, lipid class, lipid concentration, degree of saturation, characteristics of colloidal structures formed and the degree of dispersion [36]. While digestion of the lipid is accepted as a necessary step for overall improved drug absorption, digestion of the lipid vehicle may result in drug precipitation [36] and potentially reduced bioavailability. The addition of solid substrates, such as silica-lipid hybrid microparticles, to modify digestion kinetics and prevent precipitation of drug through providing a competitive adsorptive surface has also been reported as a strategy to prevent precipitation [42, 43]. Balancing the propensity for precipitation against that for solubilisation has been the major aim of research in the field for over a decade.

1.6 Lipid and Lipid-Based Formulation Classification Systems

A classification of biological lipids was proposed by Small in 1968 (Figure 1.3). Lipids were organised based on their physical properties and interactions in bulk aqueous systems, and at the air-water or oil-water interface [44]. Importantly, in the context of this review, the classification system is based principally on the self-assembly behaviour of the lipids.

Polar class I lipids are insoluble, non-swelling amphiphiles. They contain a long aliphatic chain or large bulky aromatic structure and have at least one hydrophilic group, allowing them to spread to form a stable monomolecular film. They include di- and triglycerides, long-chain protonated fatty acids and alcohols, waxes, sterol esters, phytols, retinols, fat-soluble vitamins and cholesterol.

Class II lipids are insoluble, swelling amphiphiles. They self-assemble to form well-defined liquid crystal phases in bulk liquids and/or monolayers at air/water interfaces depending on temperature, chain length, saturation, branching and substitution. Examples include lecithin and products of triglyceride hydrolysis; monoglyceride and fatty acids.

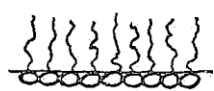
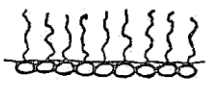
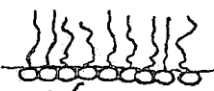
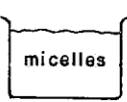
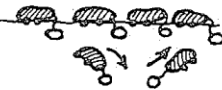
<u>CLASS</u>	<u>INTERACTION IN WATER</u>	
	<u>BULK</u>	<u>SURFACE</u>
NON-POLAR LIPIDS	 crystals or oil in water	 will not spread to form monolayer
POLAR LIPIDS		
I. Insoluble non-swelling amphiphiles	 crystals or oil in water	 spreads to form stable monolayer
II. Insoluble swelling amphiphiles	 Liquid crystals (LC) in water	 spreads to form stable monolayer
III. Soluble amphiphiles		
A) <i>Lyotropic meso- morphism</i>	 micelles	 form unstable film
B) <i>No Lyotropic meso- morphism</i>	 micelles	 form unstable film

Figure 1.3: Classification of lipids. Figure reproduced from [44].

Class IIIA soluble amphiphiles have a clear polarity between the hydrophobic and hydrophilic components of the molecule, and can form liquid crystalline phases when combined with water. This class includes anionic, cationic and non-ionic detergents and lyso-lecithin. Type B are aromatic compounds that do not form liquid crystalline phases. They include bile salts, saponins, rosin soaps and phenanthrene sulfonic acids.

In the case of lipid-based formulations for poorly water-soluble drugs, Pouton has proposed a classification system based not on structure formation, but rather on composition, dispersibility in the aqueous environment and the likely requirement for digestion [45]. Formulations range from Type I, which are oils requiring digestion, to Type IV which represent more complex formulations and contain hydrophilic surfactants and co-solvents and

no oils. The formulation performance and drug fate will be dictated by changes that occur during dispersion, dilution of the formulation in the GIT and digestion. There are advantages and disadvantages for each type, for example, Type I formulations are digestible and less likely to induce drug precipitation on dilution but do not disperse in water, whereas Type IV formulations are highly dispersible but drug is more likely to precipitate on dilution due to loss of solubility and the presence of hydrophilic excipients. Self-emulsifying drug delivery systems (SEDDS) can form micro or nano-emulsifying drug delivery systems [2, 37, 45, 46] and newer formulations include supersaturated-self emulsifying drug delivery systems (super-SEDDS) [47-49]. These contain cosolvents and surfactants or polymers, which aim to generate and maintain supersaturated drug and prevent precipitation. Cyclosporine A (Sandimmune Neoral) and HIV protease inhibitors, ritonavir and saquinavir have successfully been marketed as self-emulsifying drug delivery systems for oral delivery as capsules [37, 46].

While the scheme proposed by Pouton conveniently categorises the formulations in terms of dispersibility and likely digestibility, it is principally focussed on the pre-administration form of the formulation, and does not necessarily inform on colloidal structure formed *in vivo* with or without digestion, even though these are considered to be important determinants of *in vivo* outcome in terms of bioavailability. In particular, there are many examples where the simpler Type I and Type II formulations, which disperse poorly, outperform the more complex Type III and IV systems in terms of drug absorption and bioavailability. A scheme based on likely formation of particular colloidal structures and not on starting composition *per se* may prove ultimately more useful in providing a predictive framework, but this will not be possible until pre-absorptive structure formation and the link to bioavailability can be firmly established.

1.7 Self-Assembled Structures in Lipid Systems

A variety of self-assembled structures may be formed when biocompatible amphiphilic lipids are added to water (Figure 1.4) [50]. The structures formed depend on factors such as lipid structure and concentration, thermodynamic parameters such as temperature and pressure, and the presence of additives [51, 52]. The type of structure formed depends on the manner in which the individual amphiphiles self-assemble to pack to prevent direct contact between water and hydrophobic chains. The geometry of packing can be described by the critical packing parameter [53], which is defined as the ratio of the surfactant tail volume (V) to the product of effective area per molecule at the interface (a) and the surfactant tail length (l).

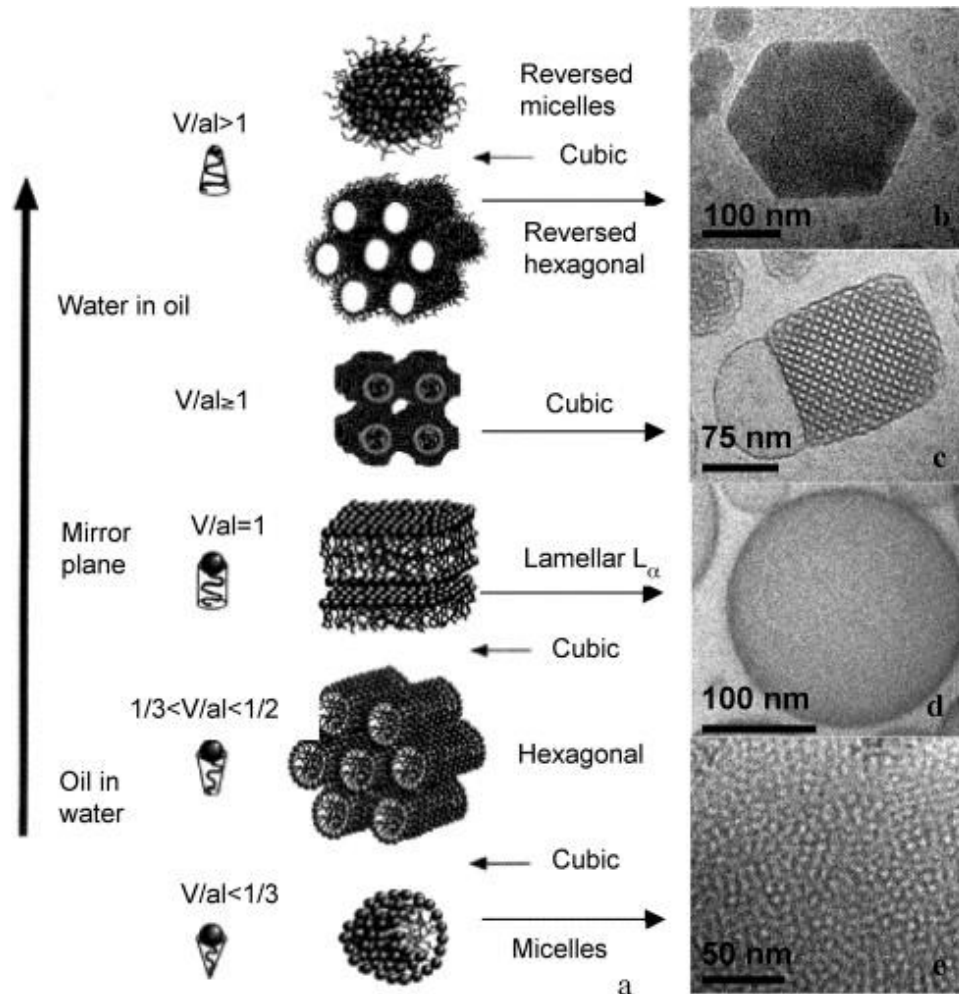


Figure 1.4: (a) The sequence of phases as a function of the critical packing parameter (V/al). Direct or aqueous colloidal structures are formed at $V/al < 1$ followed by a mirror plane at $V/al = 1$ and reverse, or oil-continuous structures at $V/al > 1$. (b) Cryo-TEM of a dispersed reversed hexagonal H_2 phase [54]. (c) Cryo-TEM for a dispersed reversed bicontinuous cubic V_2 phase of space group $Im\bar{3}m$, adapted from [55]. Dispersion made from Dimodan U (a commercial monoglyceride comprising mainly monolinolein). (d) Cryo-TEM of a vesicle, which can be obtained by dispersion of a fluid lamellar L_α liquid crystalline phase (obtained from a mixture of Dimodan U and sodium stearylactylate). (e) Cryo-TEM of a micelle dispersion (obtained from a polysorbate 80 solution). Figure reproduced from [55].

Cone shaped amphiphiles with a large polar head compared to the chain have positive mean curvature and form Type I or normal structures that curve towards the lipid regions, with oil-in-water micelles being the simplest structure. Inverted wedge shaped amphiphiles with a small polar head and large chain have energetically unfavourable contact between the aqueous

and lipid regions. They have negative mean curvature and form Type II or inverse structures where the interfacial curvature curves towards the aqueous region, allowing the chains to splay and reducing the area of the interface [56, 57] (Figure 1.5). Inverse phases are more biologically relevant and are often stable at physiological temperatures and in excess water [58]. They are formed by increasing temperature, increasing salt concentration, decreasing hydration and also by lipids with bulky hydrophobic groups [58].

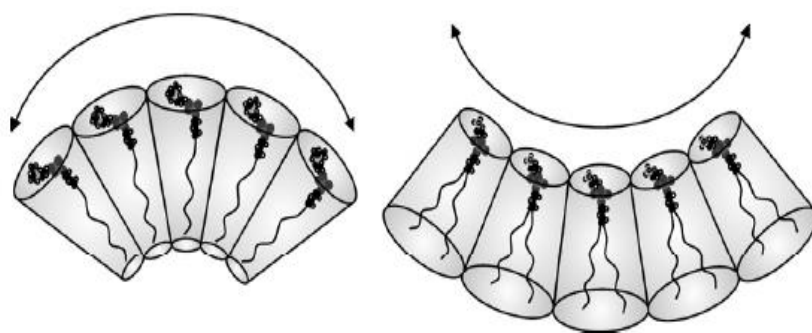


Figure 1.5: Illustration of how lipid geometry creates positive (left) and negative (right) mean curvature and affects packing [56].

Liquid crystalline mesophases often form when insoluble swelling amphiphiles (Small's Type II lipids) are added to water. The mesophases include the viscous reversed bicontinuous cubic (V_2) and reversed hexagonal phases (H_2). The V_2 phases (of which three different variants have been observed), consist of a pair of continuous but non-intersecting water channels separated by a lipid bilayer [50]. The H_2 phase is composed of rod-shaped inverse micelles packed in a hexagonal pattern and in contrast to the V_2 phase, the water channels are closed in the H_2 phase [50]. The inverse micellar (L_2) mesophase consists of inverse micelles and the fluid lamellar phase (L_2) consists of amphiphiles forming stacked bilayers. The inverse micellar cubic phase (I_2) has been proposed to consist of two different-sized inverse micelle populations packed into a cubic array [59].

1.8 Techniques for the Study of Structures during Digestion

On exposure to GI fluids, and with the aid of digestion, lipids display rich phase behaviour with many of the aforementioned self-assembled structures existing at various points during the digestion process either in isolation or in co-existence [60, 61]. These processes are both elegant and complex – an essentially unstructured oil is transformed through often highly geometrically ordered liquid crystalline structures and ultimately to relatively simple micellar assemblies. These nanostructures themselves consist of complex and dynamic composition containing lipid digestion products, endogenous amphiphilic molecules and drug molecules, which will also influence the self-assembly behaviour [3, 62, 63]. Consequently a range of techniques have been proposed for interrogating the complex structural and compositional aspects of digesting lipid systems. These techniques and their advantages and limitations are discussed in the following section.

1.8.1 Microscopy Techniques

1.8.1.1 Light Microscopy

Regular light microscopy can be used to observe the size and surface texture of oily droplets on exposure to enzymes. The first reports of liquid crystalline phases formed during *in vitro* lipid digestion were made by Patton and Carey, using simple light microscopy (Figure 1.6) [60, 64]. The presence of unilamellar vesicles was confirmed. It was proposed that as digestion occurs, digestion products ‘bud off’ from the surface of TG+DG emulsion and form colloidal structures in the presence of bile salt in the intestinal lumen. Due to the resolution limit of light microscopy given by the wavelength of light, it does not provide specific information about compositional or structural detail in the nanometer-dimensions relevant for these self-assembled aggregates.

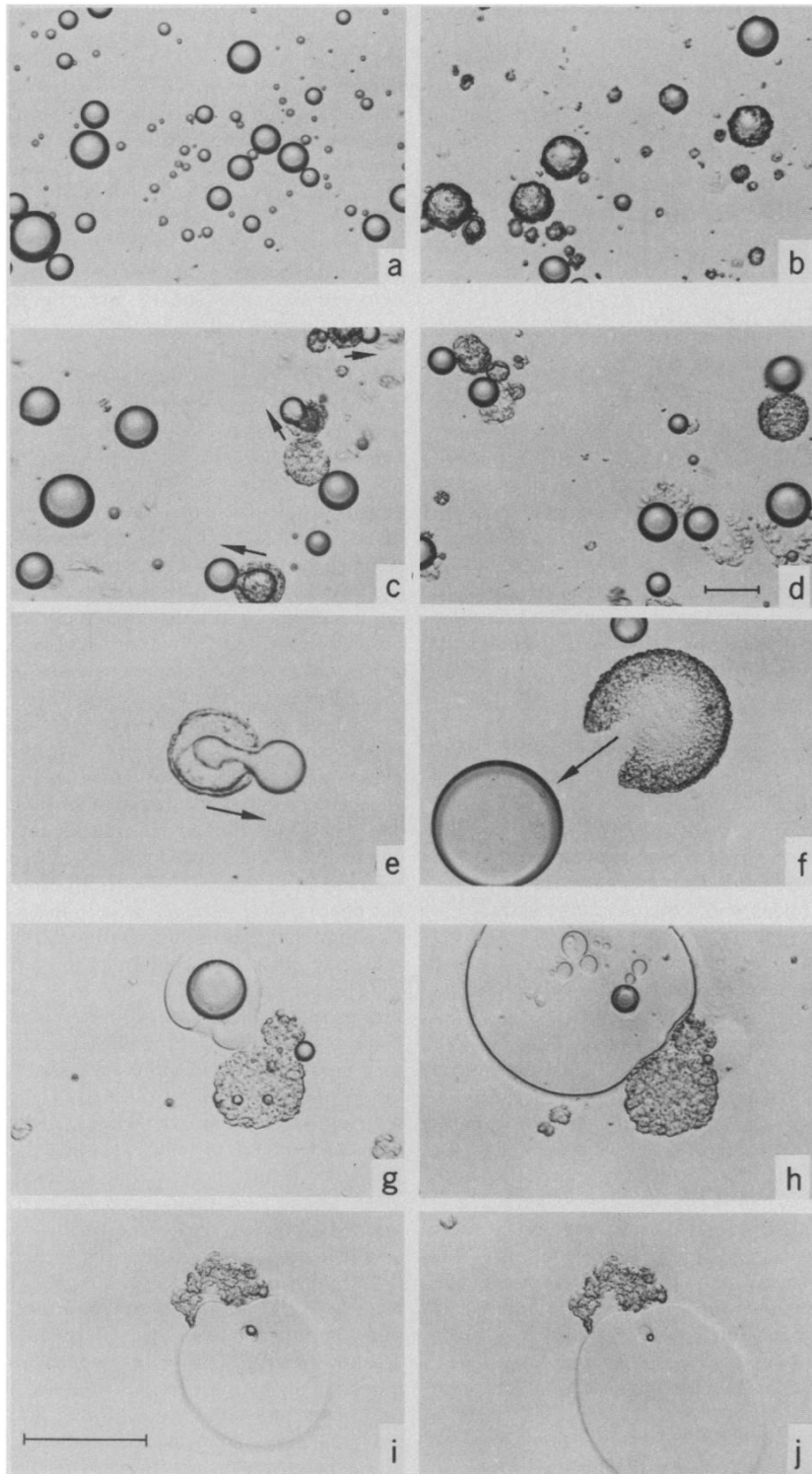


Figure 1.6: The sequence of events during digestion of olive oil viewed using light microscopy [60]. Undigested oil droplets are ‘ejected’ from lamellar liquid crystalline ‘shell’ structures formed at the interface over the first five minutes (c-f); at later times, a ‘viscous isotropic phase’ likely to be the V_2 cubic phase is observed (g-j).

1.8.1.2 Cross Polarised Light Microscopy (CPLM)

CPLM can be used to distinguish between anisotropic liquid crystalline phases (such as lamellar and hexagonal) which display optically birefringent textures under cross polarised light, and isotropic liquid crystalline phases (including cubic) which are characterised by a dark background. Scattering techniques, such as SAXS described below, are often used in combination with CPLM to further discriminate between the anisotropic and isotropic phases. The technique is simple and factors such as time, temperature, pH and concentrations of reactants can be controlled. Disadvantages include difficulties in extracting any compositional information at interfaces, and that the physical mixing of intestinal contents that occurs *in vivo* cannot be simulated on a microscope slide, as it was noted that crudely mixed lipid and well dispersed droplets undergo lipolysis at different rates [64].

1.8.1.3 Freeze Fracture Electron Microscopy (FFEM)

FFEM has been used to study fat digestion since the 1980s [61, 65-67]. Lamellae and vesicles have been observed at the surface of a digesting oil droplet (Figure 1.7) [65]. Freeze fracture electron microscopy overcomes some shortcomings of traditional TEM; production of artefacts due to fixation techniques, inability to halt lipolysis precisely, and lipid solubilisation and extraction by chemical dehydrants and embedments [68, 69]. It preserves water-dependent lipid phases and the rate of freezing (100 K/s) allows a snapshot view of dynamic lipolysis [70] rather than information about the global sample. The sample (intestinal tissue and luminal contents) is frozen between two copper planchets by immersion in liquid nitrogen or exposure to a jet of liquefied propane (-160 °C). These conditions allow for sample preservation, and a replica of the sample surface is made by evaporating platinum and carbon onto the fractured surface. The 'mask' is cleaned and mounted onto a copper grid so that it can be viewed by electron microscope.

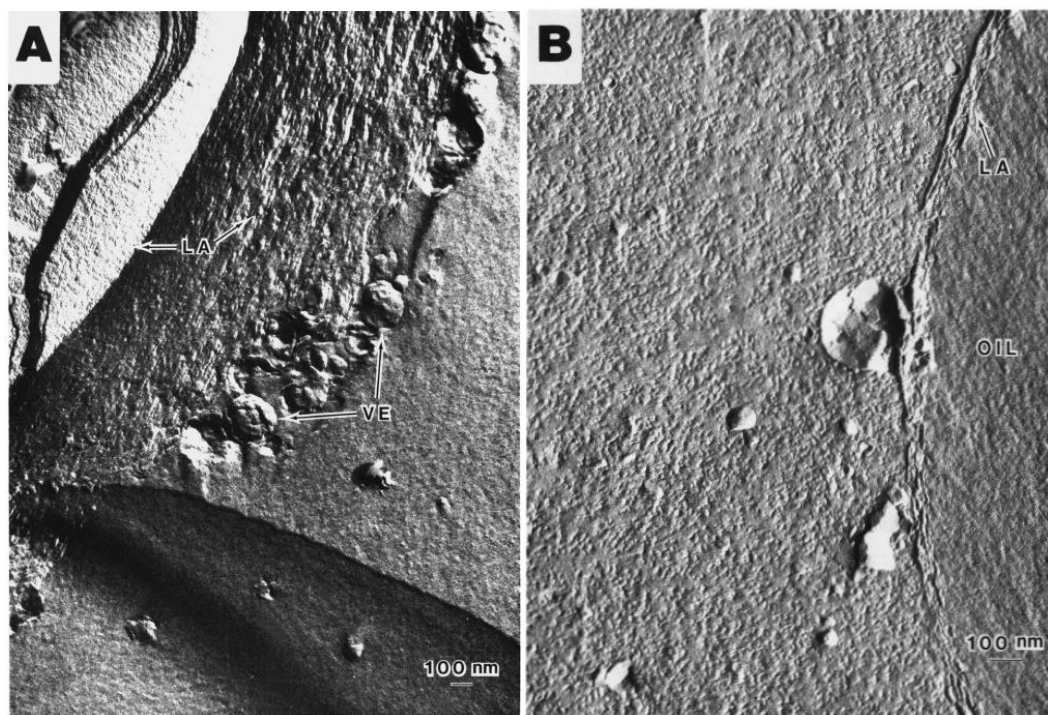


Figure 1.7: Morphology of lamellae and vesicles generated at the surface of large triolein droplets in the presence of (A) pancreatic lipase and 17 mM taurodeoxycholate (B) 42 mM pig gallbladder bile and pig pancreatic juice. Samples viewed by freeze fracture electron microscopy after 2 hr digestion [65].

1.8.1.4 Cryogenic-Transmission Electron Microscopy (cryo-TEM)

Cryo-TEM allows direct viewing of the sample and provides information about the morphology (size and shape) of complex systems and internal structure of soft nanostructured materials, with resolution to 1-2 nm [71]. However as for all microscopy techniques, it only allows visualisation of a small portion of the sample size rather than global information about the sample. Cryo-TEM was used for example to study phases and aggregate structures formed in sodium cholate+glycerol monooleate+water systems [72]. The technique has also been applied to view structures formed during *in vitro* digestions or in *ex vivo* aspirates. In *in vitro* digestion, samples can be taken during lipolysis and treated with a lipase inhibitor prior to being loaded on a carbon grid supported by a copper grid [11, 73, 74]. The sample is then blotted with filter paper to obtain a thin liquid film which is then immediately quenched in liquid ethane at $-180\text{ }^{\circ}\text{C}$ and transferred to liquid nitrogen ($-196\text{ }^{\circ}\text{C}$) to ensure immediate vitrification. The grid is then viewed by electron microscopy at low doses to prevent sample

damage. Vitrification ensures samples are preserved in their native environment, and has advantages in that it avoids issues associated with normal sample preparation, such as artefacts induced by staining, fixation and adsorption.

1.8.1.5 Cryogenic Field Emission Scanning Electron Microscopy (cryo-FESEM)

Cryo-FESEM has been used for investigating the three dimensional morphology of nanostructured aqueous dispersions of amphiphilic lipids such as monoglycerides, phospholipids, urea-based lipids and glycolipids [75] and bulk and rigid mesophases [76, 77]. These self-assembled structures include cubosomes, hexosomes, micellarcubosomes, sponge phases and microemulsion droplets. It is possible to view the internal structure and characterise the 3D and surface structure of cubosomes and hexosomes (Figure 1.8 and 1.9) [78, 79]. Cryo-FESEM has not directly been used to date to investigate colloidal structures resulting from lipolysis as cryo-TEM (for 2D information) combined with a complementary technique such as small angle X-ray scattering provides sufficient evidence to confirm the external and internal morphology.

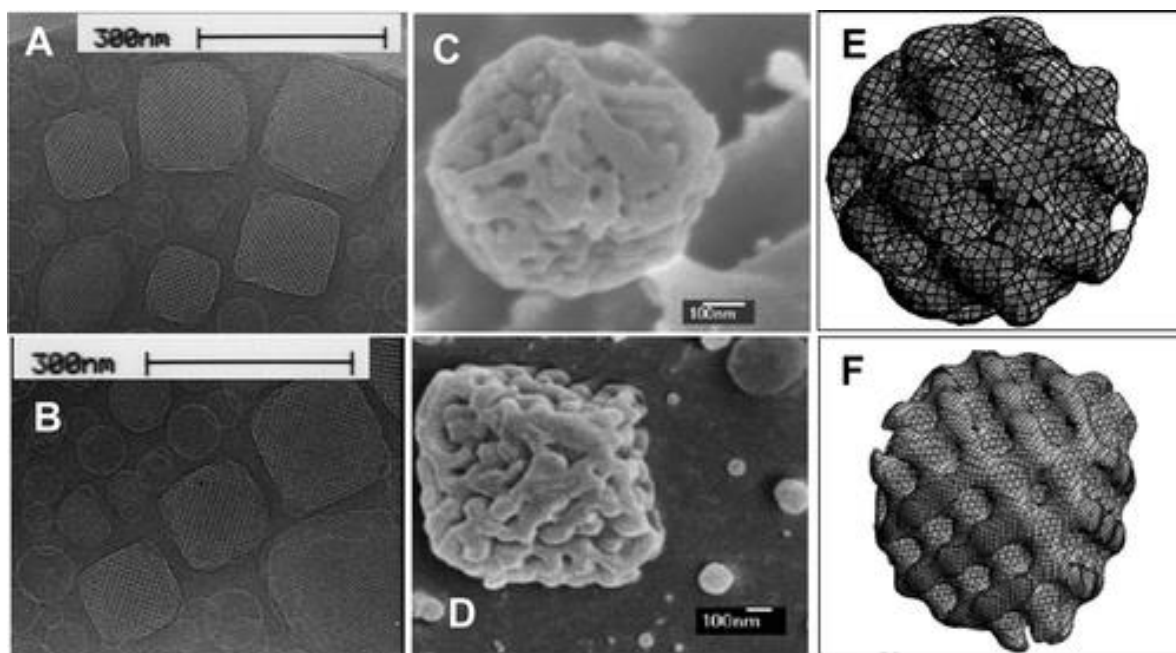


Figure 1.8: Images of phytantriol cubosomes obtained using (A and B) cryo-TEM (C and D) cryo-FESEM (E and F) models. Reproduced from [79].

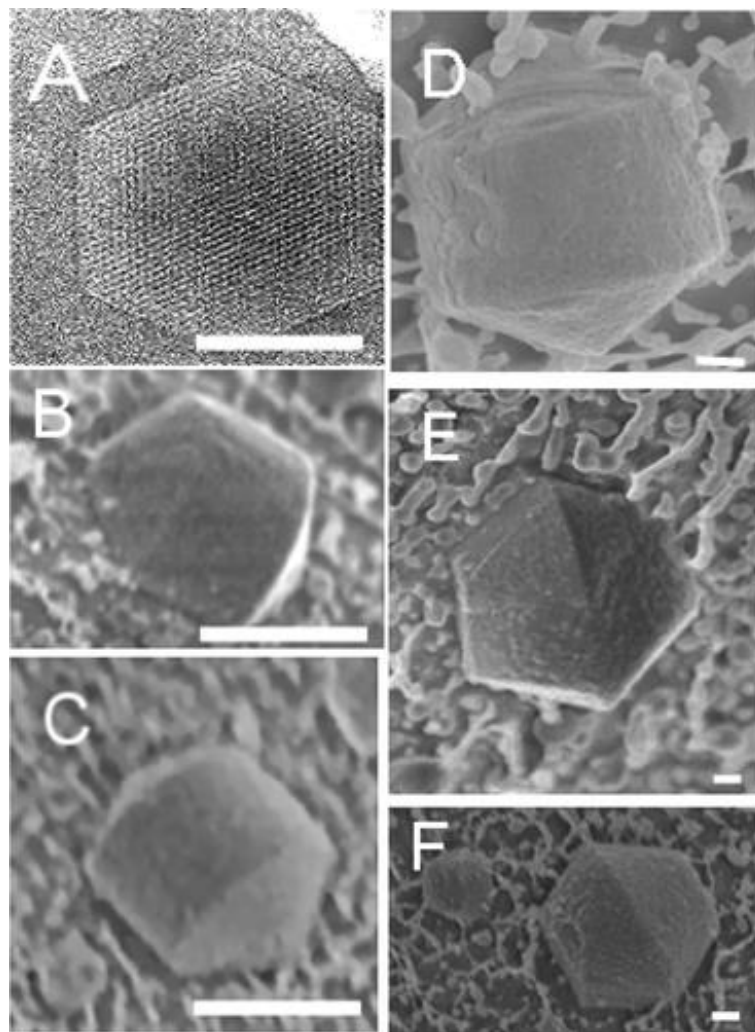


Figure 1.9: Images of phytantriol hexosomes obtained using (A) cryo-TEM (B-F) cryo-FESEM [79].

1.8.2 Scattering Techniques

1.8.2.1 Polarised and Depolarised Dynamic Light Scattering (DLS)

Dynamic light scattering is a technique commonly used to characterise particle size and size distribution of colloidal systems, for example, micelles and vesicles and emulsions [61, 67, 80]. This technique has been used to determine the changes in particle dimensions and size distribution occurring during the digestion process. Understanding the effect of lipid digestion products and drug molecules on the structure of colloidal particles generate during digestion of lipid-based drug formulations can aid in understanding the degree of saturation of particles with such components and hence drug and lipid absorption tendency. A coherent primary laser beam is focused on the sample cell and the autocorrelation function of the photocurrent

is recorded at a fixed angle. From the detected intensity correlation functions, a mean diffusion coefficient can be calculated using cumulant analysis [81].

Depolarized dynamic light scattering (DDLS) is a special technique that can be used to study optically anisotropic particles (e.g. elongated micelles) as occurring at the end of the lipid digestion process. In the case of DDLS, the primary and the scattered beam are directed through crossed polarizers. In this case, scattering is only detected from optically anisotropic particles. Correlation functions are recorded at different angles and the translational and rotational diffusion coefficients are evaluated from the angular dependence of the decay-rate of the depolarized field correlation function [11, 82].

1.8.2.2 Small and Wide Angle X-ray Scattering (SAXS/WAXS)

SAXS has become the most recognised technique used to characterise bulk and dispersed liquid crystals and other colloidal structures in solution [83]. SAXS provides non-invasive morphological information from typically 1 nm to several hundreds of nm ($\theta < 10^\circ$). Variations of the scattering intensity depending on the scattering angle are caused by inhomogeneities in the electron density within the sample (e.g. due to colloids having different electron density than the bulk average). Information on size, shape and distribution of colloids in solution can be obtained with this technique. In addition, in the case of liquid crystalline samples, SAXS can also be used to identify the structure type depending on the dimensions using a ‘structure pattern recognition’ approach. The angular position of maxima in the diffracted signal follow Bragg’s law $n\lambda = 2d\sin(\theta)$ where n is an integer, λ the wavelength of the X-rays, d the spacing between the lattice planes and θ the scattering angle [84]. The positions of the Bragg peaks are reciprocally related to the separation between molecules or lattice planes in the sample. The ratio of the peak position is unique for each type of structure and has been used to identify the structure of liquid crystals [85].

SAXS has successfully been used to study structures and colloidal phase transitions in digesting lipid systems. Systems containing mixtures intended to simulate digested systems (containing eg. fatty acids, monoglycerides, bile salts and phospholipids) have been studied via a phase diagram approach using SAXS [3, 62, 72, 86-88], as well as in a dynamic setting using benchtop or synchrotron source to follow structural changes during digestion [11, 39, 73].

When the recording of the scattering intensity is increased to wider angles ($\theta > 10^\circ$), thereby covering the size range from a few nanometers down to one angstrom, the technique is referred to as wide-angle X-ray diffraction (WAXS) or more commonly just XRD (X-ray diffraction). WAXS is used to analyse atomic and molecular arrangements and can be used for example to study the arrangements of molecules or drug crystallization [89]. Information about drug/additive crystallinity and precipitation during dispersion and digestion can be obtained. WAXS or XRD has also been applied in the pharmaceutical industry in the areas of protein crystallography and drug crystallization [90]. Time-resolved XRD was used by Caffrey *et al.* in 1989 to study lipid phase transitions [91].

1.8.2.3 Small Angle Neutron Scattering (SANS)

SANS is a non-disruptive and non-invasive technique used for materials characterisation and provides information about structure generally over the same size range as SAXS. Instead of scattering arising from electron density differences in the sample, the neutrons are scattered by the atomic nuclei and their change in direction and energy is measured [92]. A unique feature of SANS is contrast variation, which is based on the differences in scattering of hydrogen and deuterium. Samples can be prepared with a mixture of H₂O and D₂O so that particular components are rendered transparent to neutrons and selected molecules or protein areas can be deuterated to change their scattering contrast relative to the bulk average. The major disadvantages of SANS are that neutron sources are large scale infrastructure not readily accessible to many researchers, with limited time available for experiment. They also typically have much lower flux than SAXS sources (even lab sources) meaning that kinetic studies are often not feasible.

1.8.3 Spectroscopic Techniques

1.8.3.1 Nuclear Magnetic Resonance (NMR) Spectroscopy

NMR spectroscopy is used to determine the physical and chemical properties of atoms or molecules in their environment and exploits magnetic properties of certain atomic nuclei. It has been used to study simple and mixed BS micelles [93] and to characterise the physical state and chemical compositions of structures formed in aqueous systems of BS+cholesterol+mixed intestinal lipids [88]. In these experiments, single lipid components

were synthesised and selectively deuterated to distinguish it from ordinary hydrogen by mass. In a ternary phase diagram approach a large micellar phase, lamellar and cubic phase formed by sodium taurocholate and monoolein in water have been discovered using ^2H NMR, in combination with CPLM and XRD [80].

1.8.3.2 Raman Spectroscopy and Multiplex Coherent Anti-Stokes Raman Scattering (CARS) Microspectroscopy

Raman spectroscopy yields information about the vibrational modes of a molecule to determine the molecular structure. A monochromatic laser beam is focused on the sample, and the scattered light is measured. It is a non-invasive, however due to weak spontaneous Raman scattering, imaging is slow. The technique provides information on lipid chain conformation and chain environment, but not the total structure. For example, Raman spectroscopy has been used to study mixed BS+MG micelles [94].

CARS is a more recently introduced non-invasive technique used to observe and quantify compositional evolution of digesting systems. It uses two pulsed laser sources to generate a coherent beam to produce a signal with Anti-Stokes frequency. This technique overcomes the weak signals obtained with Raman spectroscopy, has submicrometer spatial resolution, is chemically sensitive, has millimolar sensitivity and does not require labelling. The contrast in the images results from molecular vibrations, where different molecules have unique vibrational signatures, thus it can be used to distinguish different chemical species. In digestion related systems, CARS was used to image the bioactive molecule, undigested oil and lipolytic products forming around the edge of the oil droplet [95]. It was possible to map evolution of the digestion process to specify locations at which lipolytic products are generated, and quantitatively map concentrations of model lipophilic drugs, progesterone and Vitamin D₃ within an oil droplet during digestion.

1.8.3.3 Electron Paramagnetic Resonance (EPR) Spectroscopy

EPR spectroscopy uses the presence of paramagnetic molecules and is based on the interaction of electron spin in a magnetic field. EPR spectroscopy has been applied to monitor partitioning of a spin-labelled lipophilic model drug in between different colloid phases in real time during digestion of lipid-based formulations [96]. The resulting spectra

changed during digestion, indicating that the model drug was redistributed between the oil phase, and mixed bile salt+phospholipid micelles. EPR is non-invasive, requires paramagnetic labelling, allows measurement of micropolarity and microviscosity, microacidity and oxygen content, however it is not spatially resolved. EPR spectroscopy has also been used to study structures of bile salt+lecithin mixed micelles [97].

1.9. Self-Assembled Structures in Digesting Lipid Systems

Given the aforementioned processing of lipids and lipid-based formulations, their propensity to self-assemble to supramolecular aggregates or structures and the techniques used to study their self-assembled structures, the main remainder of this chapter then is to address what is actually known about structure formation during digestion, and in particular how this might be impacted by formulation and physiological variables.

1.9.1 Equilibrium 'Assembled' Studies

Equilibrium studies of the self-assembly structures in biologically relevant mixtures that represent certain stages of the lipid digestion process have been used to try to develop an understanding of intermolecular structures occurring in this process. The assumption made in such equilibrium studies is that structure in digesting systems is only dictated by composition at that point in time and that structures present in real digesting mixtures are not subject to non-equilibrium effects. The equilibrium studies are not able to simulate the *in vivo* environment where gastric and intestinal motility, as well as dilution and digestion reactions all play a role in changing the local composition in a continuous manner throughout the digestion process.

Model systems studied vary widely in complexity, and the influence of parameters such as composition, pH, osmotic pressure or addition of guest molecules of various nature on the formation and transformation of self-assembled structures has been studied. The resulting phase-diagrams are intended to provide the basis of understanding of intermolecular interactions during triglyceride digestion under controlled conditions. Specifically, varying conditions such as MG and FA concentrations systematically to present progressive changes in composition expected during digestion might reasonably be expected to add to our understanding of structure formation and progression during lipid digestion. However, few

such direct systematic studies have been completed, with select few compositions usually investigated in single studies, limiting consensus in the structure-digestion field. Table 1.1 summarizes selected equilibrium studies with the focus on self-assembly of lipid digestion components.

Table 1.1: Structures formed in equilibrium studies on assembled systems under static conditions.

System	Structural Technique	Observations and comments	Ref.
<i>Gastrointestinal micellar environment prior to lipid digestion</i>			
PC+NaC	Cryo-TEM, Turbidity measurements	With increasing [cholate], vesicular structures changed size and more multilamellar vesicles were seen. Open vesicles, large bilayer sheets and long flexible cylindrical micelles at phase boundaries. At higher [cholate], vesicles transition to optically clear mixed micelles	[98]
Lecithin+NaTDC	SAXS, EPR spectroscopy	100% lecithin forms bilayers (multilamellar vesicles) 100% NaTDC forms simple BS micelles which are globular With increasing [lecithin] in NaTDC micelles, structure transforms from globular micelles → mixed, oblate, ellipsoidal structure	[97]
<i>Long chain (C₁₈) length lipids</i>			
MO+OA+NaO interactions with BS	Microscopy with polarizing filters	In presence of BS, micelles and liquid crystalline phases present	[99]
MO+OA+BS+chol	CPLM, Freeze fracture EM, DLS	Mixed micelles, L _α , cholesterol monohydrate crystals and cholesterol saturated micelles, cholesterol and intestinal lipids mixed micelles and unilamellar vesicles	[61]
MO+OA+BS	Freeze fracture EM	Pure LP+BS produced unilamellar vesicles. At high [LP], multilamellar vesicles are present	[65]
MO+OA (1:2 and 1:6)+SIF (fed state)	Cryo-TEM, DLS	SIF without lipolysis products contained micelles. SIF with lipolysis products contained vesicles and other colloidal structures. Structures in 1:6 media were more numerous and more well defined in shape and size	[35]
MO+OA (1:2 and 1:6)+SIF (fed state with lyso-PC+chol)	Cryo-TEM, DLS	Lyso-PC forms micelles, so micelles dominate Increasing MG level forms uni and multivesicular structures	[90]
Monostearin+NaCmixed micellar solution	Raman spectroscopy	Gel phase, cubic phase (noted 'C') and L _α	[94]
SIF(fasted and fed state)+MO+OA	DLS	LCT provided vesicles, swollen mixed micelles. At low lipid loads and low BS/PC, vesicle phase was responsible for small proportion of solubilisation capacity. At higher lipid loads and high BS/PC, proportion of lipid load in vesicle phase increases.(cf. MT – vesicles, mixed micelles, simple micelles)	[3]
MO+OA+BS+PC	Cryo-TEM	Micelles, uni and bilamellar vesicles with deformed internal structure, bilayer fragments and multicompart ment vesicles at high BS+PC	[100]
MO+NaO; MO+OA	CPLM, Cryo-TEM,	Large L _α in MO/NaO/water system. Stable	[101]

	SAXS, NMR	vesicles are dominant aggregates at high [water]. Also has a H ₂ , L ₂ and cubic gyroid phase H ₂ at low water content in MO /OA/water system. Also Fd3m, and L ₂	
OA+NaO+MO, ΔpH	SAXS, Cryo-TEM, DLS	With increasing OA at low pH: C → H ₂ → Fd3m → L ₂ → emulsion With increasing pH at high enough OA+MO+water system: L ₂ → Fd3m → H ₂ → C → vesicles	[23]
MO+DO+water	CPLM, SAXS, NMR	L ₂ at high [MO], reduction of MO favours formation of H ₂ when DO content is 4-30% and water content <27 wt %. Below this, cubic and L _α appear. There was also a large emulsion region	[102]
1. Sunflower oil MG+glycerol 2. MO+chol 3. NaO+ sunflower oil	Microscopy, XRD	1. C, L ₂ , gel phase, or coagel (crystals+water) 2. MO+water: L _α → C occurs. Addition of chol can cause C → L _α 3. L _α , C, liquid region	[103]
NaTC+MO	NMR, XRD, CPLM, DLS	Large micellar phase, L _α , C	[80]
MG+OA and linoleic acid	CPLM, XRD	Increased solubilisation of TG or OA in C formed by MG and water: H ₂ → L ₂ H ₂ not easily dispersed by bile salt solutions whereas C phase is, L _α can be dispersed without BS. Sunflower oil MG+SBO TG+water: L _α , C, H ₂ , L ₂ MO+OA+aqueous buffer:C, H ₂ , L ₂	[104]
Oleate+OA+BS±MO	SANS	At high [lipid], globular mixed micelles with repulsive electrostatic interactions Cholyglycine+MO+oleate+OA transition to vesicles at lower concentrations Cholyglycine+ oleate+OA has elongated and tablet-like micelles at low concentrations	[105]

Shorter chain length lipids

MG+FA (mixed C ₈ +C ₁₀) +BS+PC	DLS only	MCT: vesicles, mixed micelles, simple micelles (cflCT = vesicles, mixed micelles in above section))	[3]
MG+FA(C _{8, 12})+BS+lyso-PC	CPLM, DLS	With decreasing MG/FA, structures changed from liquid crystalline phase → L ₁ (mixed micelles and vesicles) All systems L ₁ at high dilution. This region reduced with chain length: C8: L _α , C12: L _α , C	[87]
MG+FA (C ₁₂)+BS+PC+Chol	CPLM, SAXS	C	[62]
MG+FA (C ₁₄) BS+PC+Chol	NMR, XRD	L _α (vesicles), micelles	[88]

Abbreviations: BS (bile salt), C (cubic phase), chol (cholesterol), FA (fatty acid), H₂ (reversed hexagonal phase), L_α (lamellar phase), L₁ (micellar phase), L₂ (reversed micellar phase), LP (lipolytic products), MG (monoglyceride), MO (monoolein), NaC (sodium cholate), NaO (sodium oleate), OA (oleic acid), PC (phosphatidyl choline), SBO (soybean oil), SIF (simulated intestinal fluid), TG (triglyceride)

The complexity evident in the compositions studied and the approaches to their structural interrogation makes the drawing of trends across the literature extremely difficult to make. Nevertheless some major trends are apparent, particularly with chain length of the lipid, BS concentration, lipolytic products:BS ratio.

Pre-digestion state: SIF (simulated intestinal fluid) containing BS and PL in a 4:1 ratio, without lipolytic products has been reported to contain only micelles [3, 35] and the addition of exogenous lipid digestion products to the systems changes the phase behaviour. Other reports have indicated that in SIF where the total BS content is low, that vesicles are apparent [106], but the *in vivo* significance is not clear. It is likely that the consensus indicates a micellar phase in pre-digestion systems, and higher structure formation on addition of lipolytic products to the micellar systems.

Incorporation of medium chain lipid digestion products: Medium chain triglyceride (MCT) digestion products (eg. monocaprylin, monocaprin and their representative FA) intercalate into the BS+PL micelles to swell them and form mixed micelles and vesicles (dispersed lamellar phase) when there is a high lipid:BS ratio [3, 62, 87, 88]. This is in agreement with reports that when the molar ratio of lipid:BS>1, micelles and vesicles are present [107].

Incorporation of long chain lipid digestion products: Increase in chain length or unsaturation results in less polar digestion products that are capable of displaying more complex phase behaviour. They form liquid crystalline phases such as bicontinuous and micellar cubic phases, or inverted hexagonal phases, in addition to the structures reported in the MCT system. Dilution with SIF was seen to impact phase behaviour. In highly dilute conditions, with low quantities of MG/FA, short and long chain systems behaved similarly and formed a colloidal liquid consisting of vesicles and swollen mixed micelles that are optically clear [62, 87]. Enhanced drug solubility was observed in lipid-containing simulated digested systems, and for the phases observed upon dilution with SIF, however, this benefit decreased with dilution. Lamellar and cubic phases had a greater solubilisation capacity for hydrocortisone compounds, which were used to represent poorly water-soluble drugs [87].

Monoglycerides formed during lipid digestion are known to assemble into a large variety of liquid crystalline structures and microemulsions in combination with oil and water [108] and other digestion components, such as FA, BS and PL [3, 23, 61, 65, 72, 90, 94, 99, 100, 102-105]. The formation of liquid crystalline structures in MG systems occurs when the number of carbons in the lipid tail exceeds 12 [109].

Influence of digestion stoichiometry: Phase behaviour has also been shown to be influenced by the MG:FA ratio. The 1:2 ratio expected when triglyceride is stoichiometrically digested to one MG and two FA molecules is most commonly used, however it has been noted that when the monoolein:oleic acid ratio was increased 1:6, colloidal structures were more numerous and more well defined in shape and size than in a 1:2 ratio [35]. There is evidence that the digestion of TG, particularly MCT, proceeds past the 1:2 ratio, consequently equilibrium studies at this ratio provide at best a snapshot at some point towards the end of digestion, but possibly not at complete digestion.

Influence of pH: In many fats and oils, oleic acid (OA) is one of the main fatty-acid components. The phase diagram for the oleic acid–monoolein–water (OA+MO+H₂O) system in bulk has been described previously and bicontinuous cubic phase, inversed hexagonal, inverse micellar cubic phase (Fd3m symmetry) and the inverse micellar phase can be observed with increasing OA concentration in the presence of excess water [101]. In the sodium oleate (NaO)+MO+H₂O system, the vesicle phase was dominating [110].

This rich phase behaviour has also been observed in the dispersed MO+OA system. At sufficiently high OA concentration, the internal structure of the dispersed particles was found to strongly depend on the pH of the aqueous phase. The increase in pH leads to the *in situ* transformation of OA to NaO within the structure of the particles representing the OA+NaO+MO+H₂O system. Increasing pH leads to a decrease in the critical packing parameter, inducing structural transformations from emulsified inverse micellar phase, through micellar cubosomes, hexosomes, and bicontinuous cubosomes to vesicles [23]. The reversible transition from liquid crystalline structures to vesicles occurs at intestinal pH values between pH 7 and 8. The apparent pK_a for OA in MO determined by SAXS was found to be between 6 and 7 which is within the physiological pH range of the intestine, and depends somewhat on composition and colloidal environment [23].

In the last step of digestion, mixed micelles and vesicles are formed by MG, FA and BS, depending on the composition. The early model presenting only micelles [111] has been modified during the years [67, 112, 113].

A phase diagram has been presented, showing the co-existence of vesicles and micelles as a function of BS concentration [112]. Increasing BS favours the formation of micelles. The shape of the micelles can be cylindrical or globular and elongation occurs as well as transition to vesicles upon dilution [27-29, 98, 113].

The addition of BS to dispersed MO+OA systems showed a transfer of the BS into the interface of the self-assembled structure, where it contributed to the packing of the molecules. Increasing BS concentration has been found to lead to decrease the critical packing parameter of the system thus leading to a more hydrophilic interface. The transition from liquid crystalline structures to vesicles occurred at high BS concentration [11].

1.9.2 *In Vitro* Dynamic Studies in Real Time

1.9.2.1 Approaches and Models for *In Vitro* Digestion

Early approaches to study *in vitro* digestion of lipid systems simply involved exposing lipid to lipase containing aqueous phase on a microscope slide, and structure formation was observed under the microscope (Figure 1.6) [60, 64]. However, lipid digestion is a highly dynamic process *in vivo*. Lipids are emulsified by antral contraction waves and retroulsive jet motions caused by muscle contractions in the stomach [114, 115]. Material transfer into and out of the system occurs due to bile salt addition and product absorption. Osmolality, pH and viscosity of the digestive juice all vary at different stages of the digestion process [116]. Consequently, more complex *in vitro* models have been developed to try to mimic some of these variables to better probe behaviour during digestion.

In vitro lipid digestion models simulating *in vivo* conditions of the digestive environment in the GIT have been used to study the digestion profiles of TGs with varying alkyl-chain length and in the form of self-emulsifying drug delivery vehicles [6-8, 38, 73, 74, 100, 117, 118]. A schematic of one such model used is presented in Figure 1.10. Briefly, lipid formulation is dispersed in simulated fasted or fed intestinal fluid in a thermostatted glass vessel, at 37°C. The pH value is adjusted, often to 6.5 or 7.5 depending on the model, a compromise between the optimum pH for pancreatic lipase activity ($6 < \text{pH} < 10$) [119] and duodenal pH ($5.0 < \text{pH} < 6.5$) [120]. Pancreatic lipase and co-lipase are added to initiate digestion, causing the production of fatty acids from the triglycerides, decreasing pH. A pH electrode, pH-stat meter controller and autoburette maintain the pre-defined pH value via titration with NaOH. The volume of NaOH used is an indication of the extent of digestion, assuming stoichiometric reaction between FA and NaOH. Although models used by different research groups vary in geometry, reagent concentrations and degree of agitation, [121] the concept as described is the most common.

Depending on the model, calcium is added either as a bolus at the start or continuously during digestion, as it is thought to influence the digestion via formation of soaps with free fatty acids and facilitate removal of digestion products from the surface of the digesting oil droplet, which would otherwise hinder lipase activity [10, 24, 60]. Thus there are a number of potential variables associated with using that model that may lead to differences in structure formation during the digestion process even for the same formulation. The Lipid Formulation Classification System Consortium has been established to develop a standardised *in vitro* model and method for the assessment of lipid-based formulations [122] albeit without acknowledgement of the structural aspects of the digestion process.

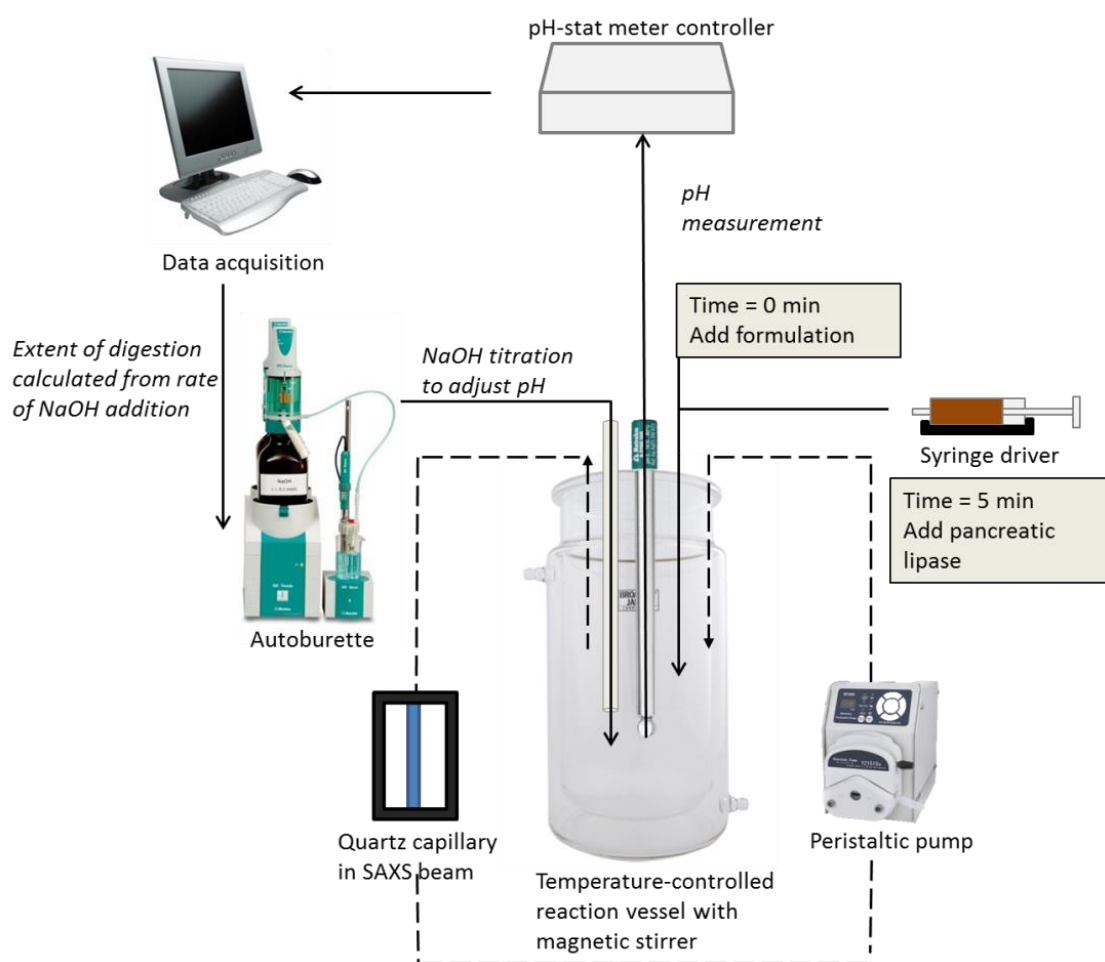


Figure 1.10: Schematic of an *in vitro* digestion apparatus. The reaction vessel is connected to pH stat comprising a burette and pH meter, and a syringe driver can be used to automate enzyme addition. A flow through cell with peristaltic pump can be fitted to provide *in situ* measurements of structure by eg. SAXS. Modified with permission from [39].

In some reports, digesting samples have been removed during lipolysis and treated with lipase inhibitor before subjecting the samples to scrutiny using a range of techniques for structure and composition. Light microscopy [60, 64, 86], freeze fracture electron microscopy [65, 66], cryo-TEM [74, 100], CARS [95] and scattering methods [11, 86] have all been used to study formation and transformation in self-assembled structures during lipolysis as summarized in Table 1.2.

Alternatively, *in situ* flow-through experiments have been performed using SAXS as the structural interrogation technique [39]. These approaches avoid the need for sample inhibition, and alleviate concerns of artefacts being introduced during sample retrieval treatment and storage. In this case the digestion vessel is fitted with a flow-through cell and pump, as illustrated in Figure 1.10. The X-ray source can be from a benchtop instrument or a synchrotron source [123]. Synchrotron SAXS is advantageous as the higher flux enables probing of structures in shorter time scales, to monitor structural changes in real time. There is also the potential for application to an *in vivo* scattering model, whereby a quartz capillary is surgically inserted into the intestine of a rat, and placed in the path of an X-ray beam for *in situ* SAXS experiments.

1.9.2.2 Structures Formed During In Vitro Digestion Studies

Early *in vitro* digestion models provided information about the chemical composition during digestion, but no data on colloidal structure formation [39]. In recent years, these models have been used in combination with cryo-TEM [11, 74, 100], SAXS and XRD to study self-assembly during the lipid digestion process. The current published studies are summarised in Table 1.2.

Colloidal phases produced *in vitro* in digesting SNEDDS systems containing long chain triglycerides (LCT), DG, MG and FA were studied using SAXS [73] and cryo-TEM [74]. At defined time points during the digestion experiment, samples were taken and enzyme inhibitor was added to halt the digestion process. SAXS measurements showed the initial formation of a lamellar phase, and after 60 min a transition to an inverse hexagonal phase occurred in response to compositional changes.

The presence of these phases has been reported in studies on assembled equilibrium systems, as well as *in situ* digestion using long chain (LC) lipids. In the latter, a flow-through mode was

added to the *in vitro* digestion model, where the digestion medium was continuously pumped through a quartz capillary, which was placed in the X-ray beam from a synchrotron source to study structural evolution in real-time during the LC SNEDDS digestion [39]. The model was validated by adding dispersions of the non-digestible lipid, phytantriol, and digestible, GMO, to the digestion procedure, as they produce known structure when subjected to bile salts and lipolytic enzymes.

Table 1.2: Structures formed during dynamic *in vitro* digestion studies.

System	Structural technique	Observations and comments	Ref.
<i>Long chain triglycerides</i>			
Olive oil+BS+human pancreatic lipase/colipase	Light microscopy	Lipolytic products+BS+lipase/colipase gives birefringent L_{α} phase (Ca^{2+} and ionised FA), and viscous isotropic phase (MG, protonated FA)	[60]
Olive oil+NaTDC or NaTC/ $CaCl_2$; Human and porcine pancreatic lipase	Light microscopy	Without BS, the fat digestion product phases are relatively stable With free Ca^{2+} , unsaturated BS micelles and pancreatic lipase, shell of crystalline product forms around digesting fat droplet At pH 6.5 – 7, amorphous isotropic pool dominates At pH 7.5 tubular projections of lamellar phase emerge and hexagonal phase	[64]
TG+pancreatic lipase+BS	Freeze fracture EM	On surface of digesting TG droplets, spherical vesicles and lamellar products are formed. These vesicles are more irregular than the ones found in the assembled systems At LP/BS ratio > 1, vesicles are present	[65]
Gum arabic-stabilized trioleylglycerol emulsion; <i>In vitro</i> digestion without BS and colipase	Freeze fracture EM	pH and droplet size influence phase morphology At pH 8.3, homogenous spherical vesicles \rightarrow partially hydrolysed droplets showed a crystalline “crust” and swollen L_{α} phase. Possible transitory hexagonal phase composed of tubular-lamellar elements At pH 7, amorphous “crust” on drop surface	[66]
Triolein	Flow through SAXS for time-resolved data, with sonication Cryo-TEM	Oil emulsion \rightarrow emulsified microemulsion $\rightarrow I_2$ (Fd3m symmetry) $\rightarrow H_2 \rightarrow C \rightarrow$ vesicles Increasing [BS] and pH decreases CPP	[11]
Triolein	<i>In vitro</i> digestion on microscope slide; CARS	Crystalline phase formed around oil droplet over 90 min digestion	[95]
<i>Long chain monoglyceride</i>			
MO+water+lipase+NaO/OA /DO	SAXS CPLM	MO+OA+water: $C \rightarrow H_2 \rightarrow I_2 \rightarrow L_2$ MO+DO+water: $H_2 \rightarrow I_2 \rightarrow L_2$	[86]

MO+NaO+water: $L_{\alpha} \rightarrow H_1$ **Long chain SNEDDS formulations**

LCT-based SNEDDS+lipase+SIF (fasted and fed)	Cryo-TEM – digestion samples inhibited for later imaging	Micelles present during entire lipolysis process Oil droplets \rightarrow spherical or elongated unilamellar vesicles, bilamellar vesicles, open vesicles, bilayer fragments Multilamellar vesicles dominate at high BS/PL conditions	[74, 100]
LCT-based SNEDDS+lipase+SIF (fasted)	Cryo-TEM SAXS	$L_{\alpha} \rightarrow H_2$	[73]
LCT-based SNEDDS+lipase+SIF (fasted)	SAXS (synchrotron) <i>in situ</i>	Sesame oil and maisine: $L_{\alpha} \rightarrow H_2$. Maisine forms more H_2 SNEDDS: $L_{\alpha} \rightarrow H_2$ (faster transition)	[39]

Abbreviations: BS (bile salt), C (cubic phase), DO (diolein), FA (fatty acid), H_1 (hexagonal phase), H_2 (reversed hexagonal phase), L_{α} (lamellar phase), L_1 (micellar phase), L_2 (reversed micellar phase), LP (lipolytic products), MCT (medium chain triglyceride), MG (monoglyceride), MO (monoolein), NaTDC (sodium taurodeoxycholate), LCT (long chain triglyceride), NaO (sodium oleate), OA (oleic acid), TG (triglyceride), SIF (simulated intestinal fluid), SNEDDS (self-nanoemulsifying drug delivery system)

Cryo-TEM imaging on samples taken during the digestion of the LC-SNEDDS system revealed the presence of intact oil droplets and micelles at the start of digestion, followed by the appearance of unilamellar vesicles 20-200nm in diameter, which co-existed with the micelles [74]. This is in agreement with previous reports in other LC systems [11, 65].

In vitro digestion of protein stabilized long- and medium chain triglyceride emulsions (triolein and MCT) under simulated *in vivo* conditions has been studied by time-resolved SAXS and DLS in combination with offline DDLS and cryo-TEM [11]. The results from this study show that the triolein emulsion transitioned through various phases such as emulsified microemulsion, inverse micellar cubic (Fd3m symmetry), inverse hexagonal and inverse bicontinuous cubic and finally vesicles in combination with anisotropic particles (e.g. elongated micelles). Contrary to this rich phase behaviour observed in the LCT system, MCT emulsions showed a direct transition to vesicles. Increasing pH and bile salt concentration had a similar influence on the colloidal structures by decreasing the critical packing parameter. The addition of hydrophobic components induced an increase in the critical packing parameter and might delay the digestion process.

1.9.3 *Ex Vivo* Studies

Of all the methods discussed, *ex vivo* studies would have a great advantage in that the sample represents real digestive medium. However it is important that the sampling position is accurately known. Furthermore, the absorption process will take place concurrently, thereby complicating interpretation of the data. A drawback is that uncertainty around artefacts induced by sampling and sample treatment unfortunately cannot be ignored. A limited number of studies have nevertheless been conducted using *ex vivo* samples as summarised in Table 1.3.

Table 1.3: Structures formed during *ex vivo* studies.

System	Structural technique	Observations and comments	Ref.
<i>Ex vivo</i> Killifish intestine after fat feeding	Freeze fracture EM	Rough-textured lamellae produced during digestion At LP/BS ratio > 1, vesicles are present	[65]
<i>Ex vivo</i> human aspirates after test meal	Freeze fracture electron microscopy DLS	Unilamellar vesicles, L ₂ liquid crystals, mixed micelles [67]	[67]
<i>Ex vivo</i> human aspirates after lipid emulsion administration	Particle sizing methods	Vesicles, mixed micelles isolated from duodenal contents collected after 2 hr digestion	[124]
<i>Ex vivo</i> human aspirates after heterogeneous meal administration	Cryo-TEM AFM DLS	Spherical micelles, worm like micelles, faceted vesicles, bilayers, oil droplets, membrane fragments	[125]

Freeze fracture electron microscopy revealed the presence of lamellar and vesicular structures in the intestinal contents of killifish after fat feeding [65]. Quantitation of the bile salt to lipid ratio over time correlated decreased lipid content to increased prevalence of micelles and decreased prevalence of vesicles. The overall results provided the concept schematic reproduced in Figure 1.11, which provides the basis for commonly published equivalent schematics in more recent literature [30].

The morphology of colloidal samples formed during digestion of a lipid-based formulation, and their similarity with *ex vivo* samples of human intestinal fluid after test meal has been previously studied by DLS, cryo-TEM and AFM [11, 74, 100, 124, 125]. The reported

colloidal species and the sequence of phase changes observed during lipid digestion are in good agreement, where at the beginning of lipid digestion, only oil droplets and protein were present, and unilamellar and bilamellar vesicles were seen to develop and dominate at the end of digestion. The observation of a bilayer fragment loosely associated with an oil droplet in *ex vivo* samples as seen in Panel B of Figure 1.12 suggests that vesicles ‘bud-off’ from the surfaces of the oil droplets [125].

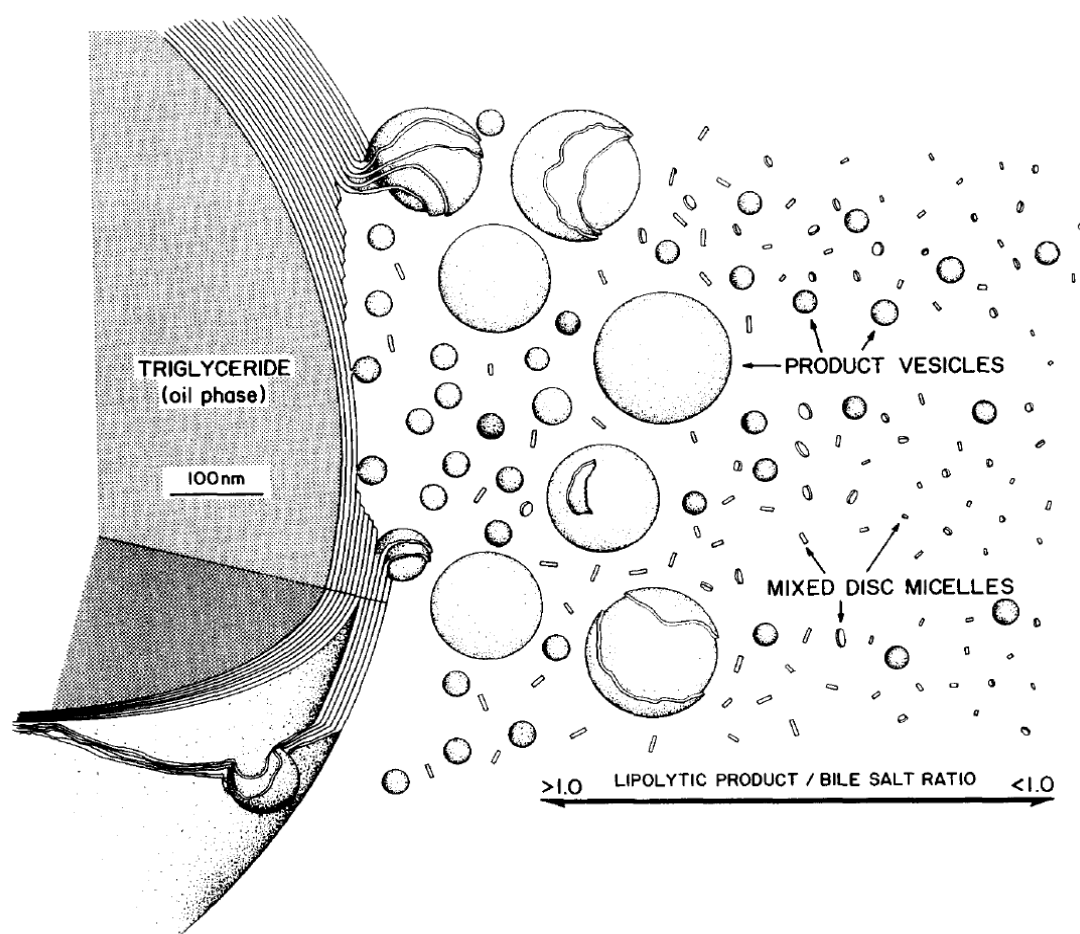


Figure 1.11: Schematic of structure formation during digestion of triglyceride on dilution with bile (reproduced from Rigler *et al.* [65]).

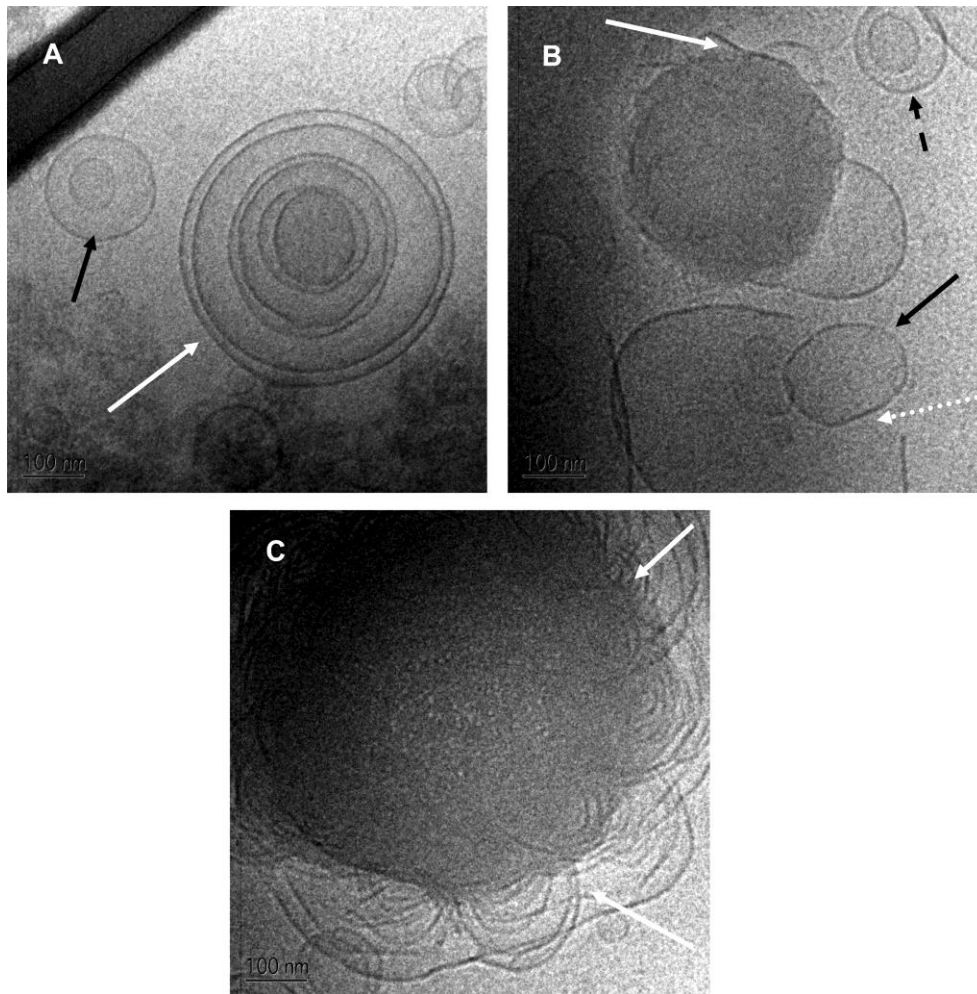


Figure 1.12: Cryo-TEM images from human aspirated intestinal content, reproduced from Müllertz *et al.* [125]. (A) A bilamellar vesicle (indicated with a black arrow) and a multilamellar vesicle (indicated by a white arrow). (B) A unilamellar vesicle (indicated by a black arrow), bilamellar vesicle (indicated by a dashed black arrow), and ruptured vesicle (indicated by a dashed white arrow) co-existing with an oil droplet with bilayer (indicated by a white arrow) closely located to their surface suggesting the lipolytic product phases accumulated on its surface. The bar represents 100 nm. (C) Oil droplet protrusions (bilayers) emerged from it (indicated by white arrows).

It is important to note that no cubic or hexagonal phases have been reported in the limited *ex vivo* studies in the literature. Potential reasons for this are that liquid crystalline phases are likely to only form transiently at the surface of the digesting oil droplet, requiring surface specific techniques for their identification and characterisation such as microbeam scattering techniques [126]. Alternatively, structures observed may also be subject to artefacts of non-

representative sampling. It is also possible that the nature of the techniques employed only provides an ‘average’ view of the structural information about the system of interest, meaning that small populations of highly ordered structures are not detectable at sufficient resolution. SAXS could be used to detect small proportions of highly ordered structures at the surface of particles in *ex vivo* samples, however this has not yet been performed to our knowledge.

1.9.4 *In Vivo* Studies

In vivo studies would circumvent issues/uncertainty in sampling techniques due to sample transformation such as in past *ex vivo* studies, and allow direct correlation of structure formation with formulation and drug/lipid absorption, and hence are the ‘end-game’ in the field. To our knowledge, there are no direct *in vivo* studies reported to date that reveal detail about structure formation during lipid digestion, in any species. This would require application of structure-revealing techniques such as *in vivo* scattering, *in vivo* imaging or *in situ* microscopic or spectroscopic techniques.

Future advances along these lines might be possible in animal models of lipid digestion as suggested previously for SAXS by Warren *et al.* [39], or may come from highly sensitive MRI studies that might elucidate nuclear environmental changes due to changes in self-assembled structure. It is likely that such studies will be developed over the coming years which will enable the gap in understanding structure formation as the link between formulation and outcome to be finally understood in the lipid-based drug delivery field.

1.10 Current Limitations in Characterising Structural Aspects of Lipolysis

Characterisation of colloidal structure during lipid digestion is essential to advance the understanding and to optimise performance of the lipid-based formulations for the oral delivery of poorly water-soluble drugs. The major techniques used for such studies have been freeze fracture electron microscopy, cryo-TEM and X-ray scattering; these techniques are undergoing improvements and more contemporary approaches are enabling higher resolution and faster kinetic studies during lipid digestion. Specifically, when combined with a high-intensity synchrotron X-ray source, SAXS provides real-time information with sub-seconds resolution of self-assembly in the highly dynamic environment in the digestion process. From a model perspective selected ‘assembled’ phase diagram approaches have been presented

providing a framework to understand self-assembly of components in a controlled manner. However the wide disparity in system composition and conditions between different studies makes it difficult to draw broader conclusions, other than that long chain lipid systems certainly display more variety of assembly modes compared to medium chain lipids. This observation is consistent with studies using *in vitro* digestion models.

The current *in vitro* digestion model utilises porcine pancreatin extract as the lipase source to simulate digestion in the small intestine [6, 39, 122, 127]. This crude extract contains other proteins and enzymes, such that when scattering techniques are applied to elucidate the colloidal species generated during lipolysis, the resolution of structures present may be confounded. Immobilised lipases are lipases that have been confined or localized by various methods, allowing them to be reused continuously and enhancing stability and activity [128, 129]. They are widely used as biocatalysts in the food, detergent, textile, cosmetic and pharmaceutical industries, however they have not yet been applied to digestions. In the context of *in vitro* lipolysis experiments, the immobilisation of lipase onto polymer beads is advantageous as the beads can be separated from the digesting medium, to improve the ability to study structural aspects using scattering methods.

It is envisioned that advancement to *in vivo* models will be the ultimate goal in understanding and controlling self-assembled structures and their implications for delivery of pharmaceutically active molecules.

1.11 Hypotheses

It is anticipated that characterisation of colloidal structure during lipid digestion will advance the understanding for optimisation of performance of the lipid-based formulations for the oral delivery of poorly water-soluble drugs. The hypotheses governing this thesis have been addressed in the subsequent chapters as indicated below:

Chapter 3: Disposition and Crystallization of Saturated Fatty Acid in Mixed Micelles

1. That the structure of mixed bile salt/phospholipid micelles depends on lipid composition and digestive conditions such as pH.

2. That intestinal fluids decrease the propensity of crystallisation of long chain lipolysis products.

Chapter 4: How Relevant Are Assembled Equilibrium Samples in Understanding Structure Formation during Lipid Digestion?

1. That colloidal structures formed will be different under equilibrium and dynamic conditions, and that the latter experiments are more *in vivo* relevant.
2. That colloidal structures formed during *in vitro* lipolysis depend on composition, fatty acid and monoglyceride chain length.
3. That emulsification of the lipid prior to *in vitro* lipolysis increases rate of lipolysis and structure formation.

Chapter 5: Structural Aspects of Digestion of Medium Chain Triglycerides

1. That medium chain lipolysis products can combine with intestinal fluids to form a vesicular phase during *in vitro* lipolysis.
2. That the addition of lipase inhibitor, 4-bromophenyl boronic acid, influences structure during lipolysis.

Chapter 6: Immobilised Lipase for Enhanced Structural Resolution

1. That an immobilised lipase is amenable for use in *in vitro* lipolysis experiments.
2. That the progress of lipolysis can be tracked by fatty acid analysis using HPLC and pH stat titration
3. That the use of immobilised lipase will provide enhanced detection limit for colloidal structure when studied by SAXS, and hence improve the current method for structural studies during *in vitro* lipolysis.

1.12 Aims

Chapter 3: Disposition and Crystallization of Saturated Fatty Acid in Mixed Micelles

1. To characterise the structure of mixed bile salt micelles upon incorporation of short, medium and long chain lipolysis products (monoglyceride and fatty acid) at varying temperature and pH.
2. To identify crystalline material in mixed bile salt micelles systems.

Chapter 4: How Relevant Are Assembled Equilibrium Samples in Understanding Structure Formation during Lipid Digestion?

1. To examine differences in colloidal structure formation under equilibrium conditions and dynamic conditions.
2. To determine the link between lipid composition and structure formation during dynamic *in vitro* lipolysis experiments compared to assembled systems.
3. To determine the effect of emulsification on the rate of lipolysis and structure formation.

Chapter 5: Structural Aspects of Digestion of Medium Chain Triglycerides

1. To characterise the structural aspects of *in vitro* lipolysis of medium chain triglyceride in real time.
2. To determine the influence of lipid content, bile salt content and lipase inhibitor on structure formation during *in vitro* lipolysis of medium chain triglyceride.

Chapter 6: Immobilised Lipase for Enhanced Structural Resolution

1. To assess the lipolytic activity of the immobilised lipase by pH stat titration.
2. To develop a HPLC assay to quantify fatty acid content during *in vitro* lipolysis.
3. To determine whether the detection limit for colloidal structures is enhanced after *in vitro* lipolysis with immobilised lipase compared to porcine pancreatin extract.

1.13 References

1. Humberstone, A.J. and Charman, W.N., *Lipid-based vehicles for the oral delivery of poorly water soluble drugs*. Adv Drug Deliv Rev, 1997. **25**(1): p. 103-128.
2. Gershanik, T. and Benita, S., *Self-dispersing lipid formulations for improving oral absorption of lipophilic drugs*. Eur J Pharm Biopharm, 2000. **50**(1): p. 179-188.
3. Kossena, G.A., et al., *Separation and characterization of the colloidal phases produced on digestion of common formulation lipids and assessment of their impact on the apparent solubility of selected poorly water-soluble drugs*. J Pharm Sci, 2003. **92**(3): p. 634-648.
4. Kossena, G.A., et al., *Influence of the intermediate digestion phases of common formulation lipids on the absorption of a poorly water-soluble drug*. J Pharm Sci, 2005. **94**(3): p. 481-492.
5. Sek, L., Porter, C.J.H., and Charman, W.N., *Characterisation and quantification of medium chain and long chain triglycerides and their in vitro digestion products, by HPTLC coupled with in situ densitometric analysis*. J Pharm Biomed Anal, 2001. **25**(3-4): p. 651-661.
6. Sek, L., et al., *Evaluation of the in-vitro digestion profiles of long and medium chain glycerides and the phase behaviour of their lipolytic products*. J Pharm Pharmacol, 2002. **54**(1): p. 29-41.
7. Kaukonen, A., et al., *Drug solubilization behavior during in vitro digestion of suspension formulations of poorly water-soluble drugs in triglyceride lipids*. Pharm Res, 2004. **21**(2): p. 254-260.
8. Kaukonen, A.M., et al., *Drug solubilization behavior during in vitro digestion of simple triglyceride lipid solution formulations*. Pharm Res, 2004. **21**(2): p. 245-253.
9. Zangenberg, N.H., et al., *A dynamic in vitro lipolysis model II: Evaluation of the model*. Eur J Pharm Biopharm, 2001. **14**(3): p. 237-244.
10. Zangenberg, N.H., et al., *A dynamic in vitro lipolysis model I. Controlling the rate of lipolysis by continuous addition of calcium*. Eur J Pharm Sci, 2001. **14**(2): p. 115-122.
11. Salentinig, S., et al., *Transitions in the internal structure of lipid droplets during fat digestion*. Soft Matter, 2011. **7**(2): p. 650-661.
12. Borovicka, J., et al., *Regulation of gastric and pancreatic lipase secretion by CCK and cholinergic mechanisms in humans*. Am J Physiol Gastrointest Liver Physiol, 1997. **273**(2): p. 374-380.
13. Moreau, H., et al., *Immunocytolocalization of human gastric lipase in chief cells of the fundic mucosa*. Histochemistry, 1989. **91**(5): p. 419-423.
14. Thomson, A.B.R., et al., *Intestinal aspects of lipid absorption: In review*. Can J Phys Pharm, 1989. **67**(3): p. 179-191.
15. Hamosh, M., et al., *Fat digestion in the newborn: characterisation of lipase in gastric aspirates of premature and term infants*. J Clin Investig, 1981. **67**(3): p. 838-846.
16. Chapus, C., et al., *Mechanism of pancreatic lipase action. 1. Interfacial activation of pancreatic lipase*. Biochemistry, 1976. **15**(23): p. 4980-4987.

17. Widmaier, E.P.e.a., *Vander's human physiology: The mechanisms of body function*. 10 ed. 2006, New York: McGraw-Hill.
18. Persson, E., et al., *Simultaneous assessment of lipid classes and bile acids in human intestinal fluid by solid-phase extraction and HPLC methods*. J Lipid Res, 2007. **48**(1): p. 242-251.
19. Kalantzi, L., et al., *Canine intestinal contents vs. simulated media for the assessment of solubility of two weak bases in the human small intestinal contents*. Pharm Res, 2006. **23**(6): p. 1373-1381.
20. Rautureau, M., Bisalli, A., and Rambaud, J.C., *Bile salts and lipids in aqueous intraluminal phase during the digestion of a standard meal in normal man* Gastroenterol Clin Biol, 1981. **5**(4): p. 417-25.
21. Russell, T.L., et al., *Upper gastrointestinal pH in 79 healthy, elderly, north-American men and women*. Pharm Res, 1993. **10**(2): p. 187-196.
22. Evans, D.F., et al., *Measurement of gastrointestinal pH profiles in normal ambulant human-subjects*. Gut, 1988. **29**(8): p. 1035-1041.
23. Salentinig, S., Sagalowicz, L., and Glatter, O., *Self-assembled structures and pK(a) value of oleic acid in systems of biological relevance*. Langmuir, 2010. **26**(14): p. 11670-11679.
24. Vinarov, Z., et al., *In vitro study of triglyceride lipolysis and phase distribution of the reaction products and cholesterol: effects of calcium and bicarbonate*. Food Funct, 2012. **3**(11): p. 1206-1220.
25. Amenitsch, H., et al., *Bile salts form lyotropic liquid crystals*. Colloids Surf, A 2003. **213**(1): p. 79-92.
26. Holm, R., Müllertz, A., and Mu, H., *Bile salts and their importance for drug absorption*. Int J Pharm, 2013. **453**(1): p. 44-55.
27. Long, M.A., Kaler, E.W., and Lee, S.P., *Structural characterization of the micelle-vesicle transition in lecithin-bile salt-solutions*. Biophys J, 1994. **67**(4): p. 1733-1742.
28. Hjelm, R.P., Thiyagarajan, P., and Alkan, H., *A small-angle neutron-scattering study of the effects of dilution on particle morphology in mixtures of glycocholate and lecithin*. J Appl Crystallogr, 1988. **21**: p. 858-863.
29. Vinson, P.K., Talmon, Y., and Walter, A., *Vesicle-micelle transition of phosphatidylcholine and octyl glucoside elucidated by cryo-transmission electron-microscopy*. Biophys J, 1989. **56**(4): p. 669-681.
30. Porter, C.J.H., Trevaskis, N.L., and Charman, W.N., *Lipids and lipid-based formulations: Optimizing the oral delivery of lipophilic drugs*. Nat Rev Drug Discov, 2007. **6**(3): p. 231-248.
31. Reis, P., et al., *Competition between lipases and monoglycerides at interfaces*. Langmuir, 2008. **24**(14): p. 7400-7407.
32. Reis, P., et al., *Adsorption of polar lipids at the water-oil interface*. Langmuir, 2008. **24**(11): p. 5781-5786.
33. Chakraborty, S., et al., *Lipid - An emerging platform for oral delivery of drugs with poor bioavailability*. Eur J Pharm Biopharm, 2009. **73**(1): p. 1-15.

34. Horter, D. and Dressman, J.B., *Influence of physicochemical properties on dissolution of drugs in the gastrointestinal tract*. Adv Drug Deliv Rev, 1997. **25**(1): p. 3-14.
35. Kleberg, K., et al., *Biorelevant media simulating fed state intestinal fluids: Colloid phase characterization and impact on solubilization capacity*. J Pharm Sci, 2010. **99**(8): p. 3522-3532.
36. Porter, C.J.H. and Charman, W.N., *In vitro assessment of oral lipid based formulations*. Adv Drug Deliv Rev, 2001. **50**: p. S127-S147.
37. Pouton, C.W., *Lipid formulations for oral administration of drugs: Non-emulsifying, self-emulsifying and 'self-microemulsifying' drug delivery systems*. Eur J Pharm Biopharm, 2000. **11**: p. S93-S98.
38. Porter, C.J.H., et al., *Susceptibility to lipase-mediated digestion reduces the oral bioavailability of danazol after administration as a medium-chain lipid-based microemulsion formulation*. Pharm Res, 2004. **21**(8): p. 1405-1412.
39. Warren, D.B., et al., *Real time evolution of liquid crystalline nanostructure during the digestion of formulation lipids using synchrotron small-angle X-ray scattering*. Langmuir, 2011. **27**(15): p. 9528-9534.
40. Porter, C.J.H. and Charman, W.N., *Intestinal lymphatic drug transport: an update*. Adv Drug Deliv Rev, 2001. **50**(1-2): p. 61-80.
41. Folmer, B.M., et al., *Monocomponent hexa- and dodecaethylene glycol succinyl-tocopherol esters: Self-assembly structures, cellular uptake and sensitivity to enzyme hydrolysis*. Biochem Pharmacol, 2009. **78**(12): p. 1464-1474.
42. Tan, A., et al., *Hybrid nanomaterials that mimic the food effect: Controlling enzymatic digestion for enhanced oral drug absorption*. Angew Chem Int Ed, 2012. **51**(22): p. 5475-5479.
43. Tan, A., et al., *Silica nanoparticles to control the lipase-mediated digestion of lipid-based oral delivery systems*. Mol Pharm, 2010. **7**(2): p. 522-532.
44. Small, D.M., *A classification of biologic lipids based upon their interaction in aqueous systems*. J Am Oil Chem Soc, 1968. **45**(3): p. 108-&.
45. Pouton, C.W., *Formulation of poorly water-soluble drugs for oral administration: Physicochemical and physiological issues and the lipid formulation classification system*. Eur J Pharm Biopharm, 2006. **29**(3-4): p. 278-287.
46. Gursoy, R.N. and Benita, S., *Self-emulsifying drug delivery systems (SEDDS) for improved oral delivery of lipophilic drugs*. Biomed Pharmacother, 2004. **58**(3): p. 173-182.
47. Gao, P., et al., *Development of a supersaturable SEDDS (S-SEDDS) formulation of paclitaxel with improved oral bioavailability*. J Pharm Sci, 2003. **92**(12): p. 2386-2398.
48. Gao, P. and Shi, Y., *Characterization of supersaturable formulations for improved absorption of poorly soluble drugs*. AAPS J, 2012. **14**(4): p. 703-713.
49. Thomas, N., et al., *In vitro and in vivo performance of novel supersaturated self-nanoemulsifying drug delivery systems (super-SNEDDS)*. J Control Release, 2012. **160**(1): p. 25-32.

50. Kaasgaard, T. and Drummond, C.J., *Ordered 2-D and 3-D nanostructured amphiphile self-assembly materials stable in excess solvent*. *Phys Chem Chem Phys*, 2006. **8**(43): p. 4957-4975.
51. Fong, W.K., Hanley, T., and Boyd, B.J., *Stimuli responsive liquid crystals provide 'on-demand' drug delivery in vitro and in vivo*. *J Control Release*, 2009. **135**(3): p. 218-226.
52. Yaghmur, A., et al., *Effects of pressure and temperature on the self-assembled fully hydrated nanostructures of monoolein-oil systems*. *Langmuir*, 2010. **26**(2): p. 1177-1185.
53. Israelachvili, J.N., Mitchell, D.J., and Ninham, B.W., *Theory of self-assembly of hydrocarbon amphiphiles into micelles and bilayers*. *J Chem Soc Faraday Trans II*, 1976. **72**: p. 1525-1568.
54. Yaghmur, A., et al., *Emulsified microemulsions and oil-containing liquid crystalline phases*. *Langmuir*, 2005. **21**(2): p. 569-577.
55. Sagalowicz, L., et al., *Monoglyceride self-assembly structures as delivery vehicles*. *Trends Food Sci Technol*, 2006. **17**(5): p. 204-214.
56. Shearman, G.C., et al., *Inverse lyotropic phases of lipids and membrane curvature*. *J Phys Condens Matter*, 2006. **18**(28): p. S1105-S1124.
57. Seddon, J.M., et al., *Inverse micellar phases of phospholipids and glycolipids*. *Phys Chem Chem Phys*, 2000. **2**(20): p. 4485-4493.
58. Schwarz, U.S. and Gompper, G., *Bending frustration of lipid-water mesophases based on cubic minimal surfaces*. *Langmuir*, 2001. **17**(7): p. 2084-2096.
59. Seddon, J.M., et al., *An Fd3m lyotropic cubic phase in a binary glycolipid/water system*. *Langmuir*, 1996. **12**(22): p. 5250-5253.
60. Patton, J.S. and Carey, M.C., *Watching fat digestion*. *Science*, 1979. **204**(4389): p. 145-148.
61. Staggars, J.E., et al., *Physical-chemical behavior of dietary and biliary lipids during intestinal digestion and absorption. 1. Phase behavior and aggregation states of model lipid systems patterned after aqueous duodenal contents of health adult human-beings*. *Biochemistry*, 1990. **29**(8): p. 2028-2040.
62. Kossena, G.A., et al., *A novel cubic phase of medium chain lipid origin for the delivery of poorly water soluble drugs*. *J Control Release*, 2004. **99**(2): p. 217-229.
63. Salentinig, S., et al., *pH-driven colloidal transformations based on the vasoactive drug nicergoline*. *Langmuir*, 2014. **30**(49): p. 14776-14781.
64. Patton, J.S., et al., *The light-microscopy of triglyceride digestion*. *Food Microstruct*, 1985. **4**(1): p. 29-41.
65. Rigler, M.W., Honkanen, R.E., and Patton, J.S., *Visualization by freeze fracture, in vitro and in vivo, of the products of fat digestion*. *J Lipid Res*, 1986. **27**(8): p. 836-57.
66. Rigler, M.W. and Patton, J.S., *The production of liquid-crystalline product phases by pancreatic lipase in the absence of bile salts: A freeze-fracture study*. *Biochimica Et Biophysica Acta*, 1983. **751**(3): p. 444-454.

67. Hernell, O., Stagers, J.E., and Carey, M.C., *Physical-chemical behavior of dietary and biliary lipids during intestinal digestion and absorption. 2 Phase-analysis and aggregation states of luminal lipids during duodenal fat digestion in healthy adult human-beings*. *Biochemistry*, 1990. **29**(8): p. 2041-2056.
68. Weibull, C., Christiansson, A., and Carlemalm, E., *Extraction of membrane-lipids during fixation, dehydration and embedding of acholeplasma-laidlawii-cells for electron-microscopy*. *J Microsc Oxford*, 1983. **129**(FEB): p. 201-207.
69. Dermier, G.B., *An autoradiographic and biochemical study of oleic acid absorption by intestinal slices including determinations of lipid loss during preparation for electron microscopy*. *J Ultrastruct Res*, 1968. **22**(3-4): p. 312-&.
70. Muller, M., Meister, N., and Moor, H., *Freezing in a propane jet and its application in freeze-fracturing*. *Mikroskopie*, 1980. **36**(5-6): p. 129-140.
71. Danino, D., *Cryo-TEM of soft molecular assemblies*. *Curr Opin Colloid Interface Sci*, 2012. **17**(6): p. 316-329.
72. Gustafsson, J., et al., *Phase behavior and aggregate structure in aqueous mixtures of sodium cholate and glycerol monooleate*. *J Colloid Interface Sci*, 1999. **211**(2): p. 326-335.
73. Fatouros, D.G., et al., *Structural development of self nano emulsifying drug delivery systems (SNEDDS) during in vitro lipid digestion monitored by small-angle X-ray scattering*. *Pharm Res*, 2007. **24**(10): p. 1844-1853.
74. Fatouros, D.G., Bergenstahl, B., and Müllertz, A., *Morphological observations on a lipid-based drug delivery system during in vitro digestion*. *Eur J Pharm Biopharm*, 2007. **31**(2): p. 85-94.
75. Yaghmur, A. and Glatter, O., *Characterization and potential applications of nanostructured aqueous dispersions*. *Adv Colloid Interface Sci*, 2009. **147–148**(0): p. 333-342.
76. Tan, G., et al., *Cryo-field emission scanning electron microscopy imaging of a rigid surfactant mesophase*. *Langmuir*, 2008. **24**(19): p. 10621-10624.
77. Fong, W.-K., et al., *Controlling the nanostructure of gold nanorod–lyotropic liquid-crystalline hybrid materials using near-infrared laser irradiation*. *Langmuir*, 2012. **28**(40): p. 14450-14460.
78. Rizwan, S.B., et al., *Characterisation of bicontinuous cubic liquid crystalline systems of phytantriol and water using cryo field emission scanning electron microscopy (cryo FESEM)*. *Micron*, 2007. **38**(5): p. 478-485.
79. Boyd, B.J., et al., *Self-assembled geometric liquid-crystalline nanoparticles imaged in three dimensions: Hexosomes are not necessarily flat hexagonal prisms*. *Langmuir*, 2007. **23**(25): p. 12461-12464.
80. Svaerd, M., et al., *Micelles, vesicles, and liquid crystals in the monoolein-sodium taurocholate-water system: phase behavior, NMR, self-diffusion, and quasi-elastic light scattering studies*. *J Phys Chem*, 1988. **92**(8): p. 2261-2270.
81. Koppel, D.E., *Analysis of macromolecular polydispersity in intensity correlation spectroscopy: The method of cumulants*. *J Chem Phys*, 1972. **57**(11): p. 4814-&.

82. Berne, B.J.P., R., *Dynamic Light Scattering*. 1976, New York: Wiley-Interscience.
83. Hyde, S., *Handbook of Applied Surface and Colloid Chemistry*, ed. Holmberg, K. 2001: John Wiley & Sons, Ltd. 299-332.
84. Bragg, W.L. and Thomson, J.J., *The diffraction of short electromagnetic waves by a crystal*. Proc Cam Philos Soc, 1914. **17**: p. 43-57.
85. Seddon, J.M., et al., *Structural studies of liquid crystals by X-ray diffraction*, in *Handbook of liquid crystals set*. 2008, Wiley-VCH Verlag GmbH. p. 635-679.
86. Borné, J., Nylander, T., and Ehan, A., *Effect of lipase on different lipid liquid crystalline phases formed by oleic acid based acylglycerols in aqueous systems*. Langmuir, 2002. **18**(23): p. 8972-8981.
87. Kossena, G.A., et al., *Probing drug solubilization patterns in the gastrointestinal tract after administration of lipid-based delivery systems: A phase diagram approach*. J Pharm Sci, 2004. **93**(2): p. 332-348.
88. Westerman, P.W., *Physicochemical characterization of a model digestive mixture by 2H NMR*. J Lipid Res, 1995. **36**(12): p. 2478-2492.
89. Boetker, J., et al., *Structural elucidation of rapid solution-mediated phase transitions in pharmaceutical solids using in situ synchrotron SAXS/WAXS*. Mol Pharm, 2012. **9**(9): p. 2787-2791.
90. Fatouros, D.G., et al., *Physicochemical characterization of simulated intestinal fed-state fluids containing lyso-phosphatidylcholine and cholesterol*. Dissolution Technol, 2009. **16**(3): p. 47-50.
91. Caffrey, M., *The study of lipid phase-transition kinetics by time-resolved X-ray diffraction*. Annu Rev Biophys Biophys Chem, 1989. **18**: p. 159-186.
92. Lopez-Rubio, A. and Gilbert, E.P., *Neutron scattering: a natural tool for food science and technology research*. Trends Food Sci Technol, 2009. **20**(11-12): p. 576-586.
93. Small, D.M., Penkett, S.A., and Chapman, D., *Studies on simple and mixed bile salt micelles by nuclear magnetic resonance spectroscopy*. Biochimica Et Biophysica Acta, 1969. **176**(1): p. 178-&.
94. Ljusbergwahren, H. and Larsson, K., *A Raman-spectroscopy study of mixed bile salt-monoglyceride micelles*. Chem Phys Lipids, 1981. **28**(1): p. 25-32.
95. Day, J.P., et al., *Label-free imaging of lipophilic bioactive molecules during lipid digestion by multiplex coherent anti-Stokes Raman scattering microspectroscopy*. J Am Chem Soc, 2010. **132**(24): p. 8433-8439.
96. Rube, A., Klein, S., and Mader, K., *Monitoring of in vitro fat digestion by electron paramagnetic resonance spectroscopy*. Pharm Res, 2006. **23**(9): p. 2024-2029.
97. Muller, K., *Structural aspects of bile salt-lecithin mixed micelles*. Hepatology, 1984. **4**(5): p. S134-S137.
98. Walter, A., et al., *Intermediate structures in the cholate-phosphatidylcholine vesicle micelle transition*. Biophys J, 1991. **60**(6): p. 1315-1325.

99. Hofmann, A.F., *Molecular association in fat digestion: Interaction in bulk of monoolein, oleic acid, and sodium oleate with dilute, micellar bile salt solutions*. Adv Chem Ser, 1968(84): p. 53-&.
100. Fatouros, D.G., et al., *Colloidal structures in media simulating intestinal fed state conditions with and without lipolysis products*. Pharm Res, 2009. **26**(2): p. 361-374.
101. Borné, J., Nylander, T., and Khan, A., *Phase behavior and aggregate formation for the aqueous monoolein system mixed with sodium oleate and oleic acid*. Langmuir, 2001. **17**(25): p. 7742-7751.
102. Borné, J., Nylander, T., and Khan, A., *Microscopy, SAXD, and NMR studies of phase behavior of the monoolein-diolein-water system*. Langmuir, 2000. **16**(26): p. 10044-10054.
103. Larsson, K., Gabrielsson, K., and Lundberg, B., *Phase behavior of some aqueous systems involving monoglycerides, cholesterol and bile-acids*. J Sci Food Agric, 1978. **29**(10): p. 909-914.
104. Lindstrom, M., et al., *Aqueous lipid phases of relevance to intestinal fat digestion and absorption*. Lipids, 1981. **16**(10): p. 749-754.
105. Hjelm, R.P., et al., *Structure of conjugated bile salt-fatty acid-monoglyceride mixed colloids: Studies by small-angle neutron scattering*. J Phys Chem B, 2000. **104**(2): p. 197-211.
106. Cohen, D.E., Angelico, M., and Carey, M.C., *Structural alterations in lecithin-cholesterol vesicles following interactions with monomeric and micellar bile salts: physical-chemical basis for subselection of biliary lecithin species and aggregative states of biliary lipids during bile formation*. J Lipid Res, 1990. **31**(1): p. 55-70.
107. Embleton, J.K. and Pouton, C.W., *Structure and function of gastro-intestinal lipases*. Adv Drug Deliv Rev, 1997. **25**(1): p. 15-32.
108. Qiu, H. and Caffrey, M., *The phase diagram of the monoolein/water system: metastability and equilibrium aspects*. Biomaterials, 2000. **21**(3): p. 223-234.
109. Lutton, E.S., *Phase behaviour of aqueous systems of monoglycerides*. J Am Oil Chem Soc, 1965. **42**(12): p. 1068-&.
110. Borné, J., Nylander, T., and Khan, A., *Vesicle formation and other structures in aqueous dispersions of monoolein and sodium oleate*. J Colloid Interface Sci, 2003. **257**(2): p. 310-320.
111. Hofmann, A.F. and Borgstrom, B., *Intraluminal phase of fat digestion in man: The lipid content of micellar and oil phases of intestinal content obtained during fat digestion and absorption*. J Clin Investig, 1964. **43**(2): p. 247-&.
112. Mazer, N.A., Benedek, G.B., and Carey, M.C., *Quasielastic light-scattering studies of aqueous biliary lipid systems. Mixed micelle formation in bile salt-lecithin solutions*. Biochemistry, 1980. **19**(4): p. 601-615.
113. Schurtenberger, P., Mazer, N., and Kanzig, W., *Micelle to vesicle transition in aqueous solutions of bile-salt and lecithin*. J Phys Chem, 1985. **89**(6): p. 1042-1049.
114. Armand, M., et al., *Physicochemical characteristics of emulsions during fat digestion in human stomach and duodenum*. Am J Physiol Gastrointest Liver Physiol, 1996. **271**(1): p. G172-G183.

115. Schulze, K., *Imaging and modelling of digestion in the stomach and the duodenum*. Neurogastroenterol Motil, 2006. **18**(3): p. 172-183.
116. Kalantzi, L., et al., *Characterization of the human upper gastrointestinal contents under conditions simulating bioavailability/bioequivalence studies*. Pharm Res, 2006. **23**(1): p. 165-176.
117. Christensen, J.O., et al., *Solubilisation of poorly water-soluble drugs during in vitro lipolysis of medium- and long-chain triacylglycerols*. Eur J Pharm Biopharm, 2004. **23**(3): p. 287-296.
118. Porter, C.J.H., et al., *Use of in vitro lipid digestion data to explain the in vivo performance of triglyceride-based oral lipid formulations of poorly water-soluble drugs: Studies with halofantrine*. J Pharm Sci, 2004. **93**(5): p. 1110-1121.
119. Gargouri, Y., Moreau, H., and Verger, R., *Gastric lipases: Biochemical and physiological studies* Biochimica Et Biophysica Acta, 1989. **1006**(3): p. 255-271.
120. Dressman, J.B., et al., *Upper gastrointestinal (GI) pH in young, healthy men and women*. Pharm Res, 1990. **7**(7): p. 756-761.
121. Larsen, A.T., Sassene, P., and Müllertz, A., *In vitro lipolysis models as a tool for the characterization of oral lipid and surfactant based drug delivery systems*. Int J Pharm, 2011. **417**(1-2): p. 245-255.
122. Williams, H.D., et al., *Toward the establishment of standardized in vitro tests for lipid-based formulations, part 1: Method parameterization and comparison of in vitro digestion profiles across a range of representative formulations*. J Pharm Sci, 2012. **101**(9): p. 3360-3380.
123. Dong, Y.D. and Boyd, B.J., *Applications of X-ray scattering in pharmaceutical science*. Int J Pharm, 2011. **417**(1-2): p. 101-111.
124. Armand, M., et al., *Digestion and absorption of 2 fat emulsions with different droplet sizes in the human digestive tract*. Am J Clin Nutri, 1999. **70**(6): p. 1096-1106.
125. Müllertz, A., et al., *Insights into intermediate phases of human intestinal fluids visualized by atomic force microscopy and cryo-transmission electron microscopy ex vivo*. Mol Pharm, 2012. **9**(2): p. 237-247.
126. Nozue, Y., Shinohara, Y., and Amemiya, Y., *Application of microbeam small- and wide-angle X-ray scattering to polymeric material characterization*. Polym. J, 2007. **39**(12): p. 1221-1237.
127. Fatouros, D.G. and Müllertz, A., *In vitro lipid digestion models in design of drug delivery systems for enhancing oral bioavailability*. Expert Opin Drug Metab Toxicol, 2008. **4**(1): p. 65-76.
128. Murty, V.R., Bhat, J., and Muniswaran, P.K.A., *Hydrolysis of oils by using immobilized lipase enzyme: A review*. Biotechnol Bioprocess Eng, 2002. **7**(2): p. 57-66.
129. Sharma, R., Chisti, Y., and Banerjee, U.C., *Production, purification, characterization, and applications of lipases*. Biotechnol Adv, 2001. **19**(8): p. 627-662.

Chapter 2. General Materials and Experimental Techniques

Chapter 2. General Materials and Experimental Techniques

2.1 Materials

2.1.1 Lipids

Captex 355 (MCT composed of 59% caprylic acid (C₈ fatty acid), 40% capric acid (C₁₀ fatty acid), <1% lauric acid (C₁₂ fatty acid) as stated in the product information) was obtained from Abitec Corporation (Janesville, WI, USA). Caprylic acid (C₈ fatty acid, 99%), capric acid (C₁₀ fatty acid), lauric acid (C₁₂ fatty acid, >99.5%), myristic acid (C₁₄ fatty acid, >99%), oleic acid (C_{18:1} fatty acid, >99%), monocaprylin (C₈ monoglyceride, 99%), monolaurin (C₁₂ monoglyceride, 99%) monoolein (C_{18:1} monoglyceride, 99%), tricaprylin (C₈ triglyceride, >99%), tripalmitin (C₁₆ triglyceride, >99%) and triolein (C_{18:1} triglyceride, >97% TLC) were purchased from Sigma Aldrich (St. Louis, MO, USA). Monomyristin (C₁₄ monoglyceride >97%), tributyrin (C₄ triglyceride, >98%), tricaprln (C₁₀ triglyceride, 98%), trilaurin (C₁₂ triglyceride, 98%) and trimyristin (C₁₄ triglyceride, 99%) was obtained from TCI Co. Ltd (Kawaguchi, Saitama, Japan). Phospholipid (1,2-dioleoyl-sn-glycero-3-phosphocholine, DOPC) was from Trapeze Association Pty Ltd (Clayton, Victoria, Australia). Lipids were used without further purification.

2.1.2 General Materials

Tris maleate (reagent grade), bile salt (sodium taurodeoxycholate, >95%), 4-bromophenylboronic acid (4-BPBA, >95%), NaOH (p.a. grade) and HCl (p.a. grade) were purchased from Sigma Aldrich (St. Louis, MO, USA). Sodium azide was purchased from Merck Schuchardt OHG (Eduard-Buchner-Straße, Hohenbrunn, Germany). Sodium chloride (>99%) was purchased from Chem Supply (Gillman, SA, Australia). USP grade pancreatin extract was purchased from Southern Biologicals (Nunawading, Victoria, Australia). Novozym[®] 435 was obtained from Novozymes (Bagsvaerd, Denmark). Calcium chloride (>99%) was obtained from Ajax Finechem (Seven Hills, NSW, Australia). HPLC grade methanol (MeOH) was purchased from Merck. Trifluoroacetic acid (TFA) was obtained from Pierce (Rockford, Illinois, USA). Water used was sourced from a Millipore water purification system using a Quantum[™] EX Ultrapure Organex cartridge (Millipore, Sydney, Australia).

2.2 Preparation of Digestion Buffer and Simulated Intestinal Fluid

Digestion buffer was prepared with 50 mM Tris maleate, 5 mM $\text{CaCl}_2 \cdot 2\text{H}_2\text{O}$, 150 mM NaCl, 6 mM NaN_3 as anti-microbial agent, and adjusted to pH 6.5. Bile salt (sodium taurodeoxycholate) and phospholipid (DOPC) were prepared in buffer at concentrations of 5 mM:1.25 mM and 20 mM:5 mM to simulate fasted and fed intestinal fluid, where the mean values and 4:1 BS:PL ratio represent intestinal contents after digestion [1, 2]. The phospholipid was dissolved in chloroform in a round bottom flask and the chloroform was removed by evaporation under vacuum to leave a thin film. Bile salt and digestion buffer were added and the solution was placed in a sonicator bath for 30 min, before it was stored at 4 °C to equilibrate overnight.

2.3 Preparation of Equilibrium Systems

The equilibrium systems reflecting the endpoint of the lipid digestion process were prepared by adding 10 mM monoglycerides and 20 mM fatty acids [2-5] to bile salt/phospholipid (BS/PL) micelles simulating the gastrointestinal state at the nominal end point of digestion of triglycerides. The 1:2 ratio of monoglyceride to fatty acid represents the nominal end point of digestion of the corresponding triglyceride.

Sonication with a tip sonicator (Misonix, New York) for 30 s at 100 W was used to solubilise the components. Samples were equilibrated for 24 hr and pH was adjusted with 1 M NaOH and HCl.

2.4 *In Vitro* Lipolysis

In vitro lipolysis experiments were performed using a pH-stat auto titrator (Metrohm, Switzerland), similar to previous report [6-10]. A schematic diagram of the model can be found in Chapter 1, Figure 1.10. Titration of fatty acids with a pH stat is frequently used to evaluate digestion of lipid-based formulations to examine drug disposition, solubilisation and precipitation, with the aim to achieve *in vitro-in vivo* correlations.

Pancreatin extracts were prepared by adding 4 g of porcine pancreatin powder to 5 mL of digestion buffer to achieve an activity of 10 000 TBU/mL. The suspension was magnetically

stirred for 15 min, and centrifuged for 15 min at 3500 rpm at 25 °C. Fresh pancreatin extracts were prepared each day and the supernatant was kept at room temperature prior to use.

Lipid was added to the fasted simulated intestinal fluid in the thermostatted digestion vessel at 37 °C, and magnetically stirred for 5 min for complete mixing and thermal equilibration. The pH was adjusted to 6.500 ± 0.003 , chosen as a compromise between the optimum for pancreatic lipase activity pH (6 – 10) [11] and duodenal pH (5.0 – 6.5) [12]. On addition of lipase (~1000 TBU/mL digest) the pH-stat titrated the digestion with 0.6 M NaOH in order to maintain pH 6.500 ± 0.003 . Lipolysis was allowed to proceed for a set time period, in which the degree of enzymatic digestion of the lipid was reflected in the volume of NaOH used to neutralize the fatty acids liberated during lipolysis.

A blank digestion without lipid but with bile salt micelles present was performed as a background experiment, to account for fatty acids that were produced from phospholipids and was subtracted from the profiles for the lipolysis experiments.

Where required during digestion, lipolysis was inhibited by the addition of lipase inhibitor (0.5 M 4-bromophenylboronic acid in methanol).

2.5 Methods for Characterising Liquid Crystalline Structures

2.5.1 Small Angle X-ray Scattering (SAXS)

SAXS is a well-established technique for the characterisation of colloidal structures in the nanometer range. A collimated X-ray beam of wavelength, λ , is focused onto the sample and scattered by variations in electron density in the sample (i.e. between the bulk and self-assembled structures). The angular scattering intensity provides non-invasive morphological information for structures with a spatial dimension typically 1 nanometer to several hundreds of nanometers, examples of which are in Figure 2.1. The scattering pattern is converted to a plot of intensity vs. the magnitude of the scattering vector, q , by $q = (4\pi/\lambda)\sin(\theta/2)$. This scattering expresses the arrangement of the amphiphilic molecules in a crystal lattice and is described by Bragg's Law, $2d\sin\theta = n\lambda$, where d is the interplanar distance between two reflecting planes and λ is the wavelength. The characteristic reciprocal spacings ratio of the Bragg peaks is correlated with previously documented Miller indices for known mesophases for the identification of the liquid crystalline mesophase present [13]. The q values at which the peaks are located can be used to calculate the interplanar spacing, d , between two

reflecting planes of the liquid crystal phase by $d = 2\pi/q$. This calculation, and the absolute location of the peaks allows for the calculation of the mean lattice parameter, a , of the crystal unit cell.

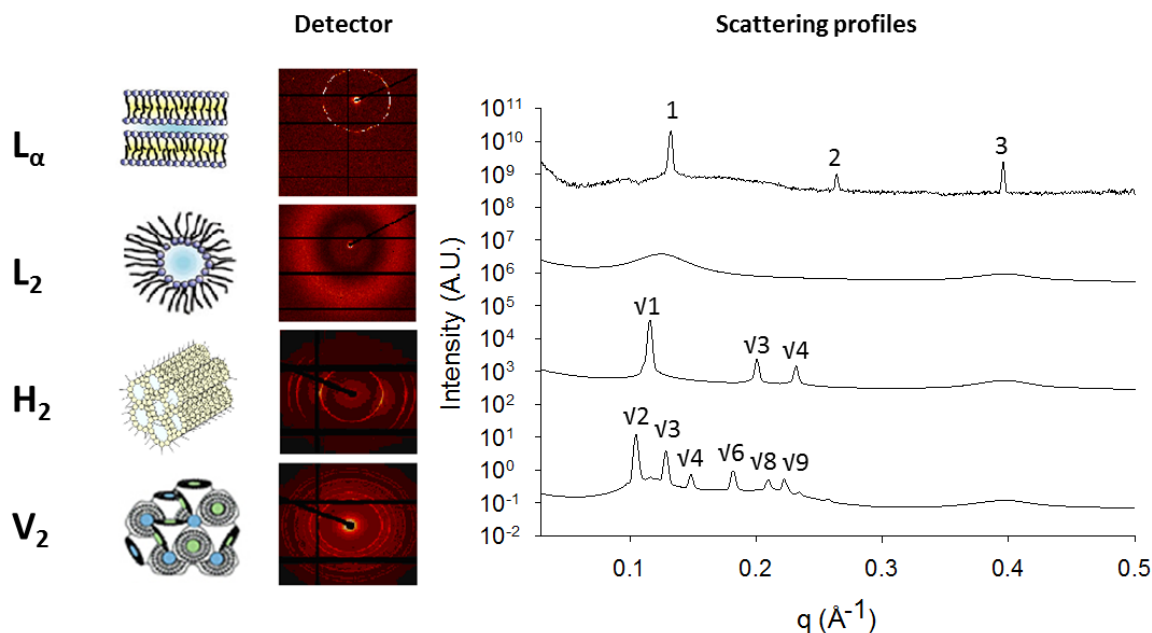


Figure 2.1: A 3-dimensional schematic of the unit cells of the lamellar (L_α), reversed micellar (L_2), reversed hexagonal (H_2) and reversed bicontinuous cubic (V_2) phase (left), their characteristic SAXS scattering patterns (middle) and scattering profiles (right) [14, 15].

In this thesis, SAXS was used to characterise structure in both equilibrium and dynamic digesting samples. SAXS measurements were performed at the SAXS/WAXS beamline at the Australian Synchrotron [16].

For equilibrium samples, samples were loaded into 1.5 mm diameter quartz capillaries which were inserted into a thermostatted metal heating block in the X-ray beam, which was controlled by a Peltier system accurate to ± 0.1 °C, for measurements taken at 37 °C. An X-ray beam with a wavelength of 1.1271 Å (11 keV) was selected. The sample to detector distance was adjusted to achieve the required q range, and the details are listed in the chapters. The 2D SAXS patterns were collected over 2 s using a Pilatus 1M detector (active area 169×179 mm² with a pixel size of 172 μm) and q -calibration was performed using silver behenate. 2D scattering patterns were integrated into the 1D scattering function $I(q)$ using the in-house

developed software package scatterBrain. Scattering curves are plotted as a function of relative X-ray intensity, $I(q)$, versus q .

The high-intensity and high-flux synchrotron X-ray source enabled real-time information with sub-second resolution of self-assembly in the highly dynamic environment in the digestion process and with higher resolution than a benchtop instrument. To monitor changes in nanostructure in real-time during *in vitro* lipolysis, the pH stat digestion vessel was fitted with silicon tubing (total volume <1 mL) to enable continuous flow of the digestion medium via peristaltic pump at a rate of 10 mL/min, through a 1.5 mm diameter quartz capillary. The capillary was fixed in a thermostatted metal heating block in the X-ray beam, which was controlled by a Peltier system accurate to ± 0.1 °C, for measurements taken at 37 °C. A remotely-operated syringe driver was used to deliver 1 mL of pancreatin extract over several seconds into the vessel to initiate digestion.

2.5.2 Small Angle Neutron Scattering (SANS)

In neutron scattering experiments, a beam of neutrons is passed through a sample, and the neutrons are scattered by nuclei of the atoms. Small angle neutron measurements can elucidate structural features in the nanometer range similar to SAXS measurements, hence SANS measurements were used to complement SAXS data, specifically to elucidate particle shape and fatty acid disposition using contrast variation approaches. Fully deuterated fatty acid, where the hydrogen atoms were replaced with deuterium atoms to provide isotopic contrast, were synthesised by collaborators at ANSTO. Deuterium has a greater scattering length density than hydrogen, which when incorporated into mixed bile salt micelles with hydrogenated components, allowed for contrast matching to enable localisation of the deuterated fatty acid.

SANS experiments were performed on the Quokka instrument at OPAL [17] at the Australian Nuclear Science and Technology Organisation (ANSTO). A wavelength of 5.0 Å and 10% wavelength resolution was used. Two instrument configurations were used with a source-to-sample distance of 8 m and sample-to-detector distances of 8 m and 2 m, the latter with a 300 mm detector offset to increase the maximum accessible q range. These configurations provide a continuous q range of 0.01 to 0.5 Å⁻¹ where q is the length of the scattering vector, defined by $q = (4\pi/\lambda)\sin(\theta/2)$, where λ is the wavelength and θ , the scattering angle. All samples were enclosed in Hellma cuvettes with a 1 mm path length. Samples were studied at several

temperatures with temperature control provided by a Julabo thermostatted bath. All data were corrected for blocked beam measurements, normalised and radially averaged using a package of macros in Igor software (Wavemetrics, Lake Oswego, Oregon, USA) and modified to accept HDF5 data files from Quokka. Scattering curves are plotted as a function of absolute (SANS) intensity, I , versus q .

A Guinier plot of the SANS data where $\ln(I)$ is plotted against q^2 was produced to determine the radius of gyration (R_g). This provides information about the particle size and was obtained from the slope of the Guinier plot, where the q range of $qR_g < 1.3$ was used to attain a reliable fit [18].

2.5.4. Dynamic Light Scattering (DLS)

Fixed angle, non-polarised DLS measurements were performed on a Malvern Zetasizer NanoZS to determine the hydrodynamic radius (R_H) and particle size distribution of mixed bile salt micelles. Samples were centrifuged for 5 min at 3500 rpm prior to the measurement to remove any trace dust particles. A laser power of 4 mW was used at a back scattering angle of 173° at room temperature. The average diffusion coefficient, D , was obtained by the cumulant analysis of the correlation functions [19]. The mean hydrodynamic radius R_H was deduced from the diffusion coefficient using the Stokes–Einstein equation:

$$R_H = \frac{k_B T}{6\pi\eta D}$$

where k_B is the Boltzmann constant, where T the absolute temperature and η is the viscosity of the solvent, (H_2O or D_2O). The polydispersity index (PDI) of the size distribution was determined from the second cumulant:

$$PDI = \frac{\mu_2}{\bar{\Gamma}^2}$$

where μ_2 is the second cumulant and $\bar{\Gamma}$ the mean of the inverse decay time.

Depolarized dynamic light scattering (DDLS) was used to confirm the presence of anisotropic particles observed by SANS and SAXS. DDLS measurements were performed on an ALV-5022F spectrometer, using a vertically-polarized Helium Neon laser (wavelength 633 nm). The scattered light passed through a crossed polarizer which was carefully adjusted to achieve

minimum scattered intensity. Correlation functions were collected at different scattering angles between 20° and 90°. At each angle, 10 measurements of 1 min duration were performed, and the average of the data sets was taken for each angle. DDLS takes advantage of the fact that the light scattered from optically homogeneous spherical particles maintains the same polarization as the incident light. However, optically anisotropic particles such as cylindrical micelles lead to depolarised scattering, which passes through the crossed polarizer to the detector. The scattering is angular dependent, allowing for the determination of the translational (D_T) and rotational diffusion (D_R) of the particles. The correlation function measured in DDLS is a combination of these parameters, and the decay rate of the depolarized field correlation function, Γ , is given by:

$$\Gamma = q^2 D_T + 6D_R$$

Γ was determined from the correlation function by cumulant expansion [19].

2.5.4 Cryogenic Transmission Electron Microscopy (cryo-TEM)

Cryo-TEM was used to directly observe the colloidal structures present in the digestion sample, as it provides information about particle size, shape and internal structure. Cryo-TEM was used to complement the scattering data. Vitrification of the sample provides a snapshot of the dispersed particles in their native environment and the technique avoids the issues associated with normal TEM sample preparation, including artefacts produced by staining, fixation and adsorption.

A laboratory-built humidity-controlled vitrification system was used to prepare the samples for cryo-TEM. Humidity was kept close to 80% for all experiments and ambient temperature was 22 °C.

Copper grids (200-mesh) coated with perforated carbon film (Lacey carbon film: ProSciTech, Qld, Australia) were glow discharged in nitrogen to render them hydrophilic. Aliquots (4 μ L) of the sample were pipetted onto each grid prior to plunging. After 30 s adsorption time the grid was blotted manually using Whatman 541 filter paper, for approximately 2 s. Blotting time was optimised for each sample. The grid was then plunged into liquid ethane cooled by liquid nitrogen to ensure immediate vitrification. Frozen grids were stored in liquid nitrogen until required.

The samples were examined using a Gatan 626 cryoholder (Gatan, Pleasanton, CA, USA) and Tecnai 12 Transmission Electron Microscope (FEI, Eindhoven, The Netherlands) at an operating voltage of 120 kV. At all times low dose procedures were followed, using an electron dose of 8-10 electrons/Å² for all imaging to prevent sample damage. Images were recorded using a FEI Eagle 4k×4k CCD camera at magnifications ranging from 15 000× to 50 000×. Images were recorded using a Megaview III CCD camera and AnalySIS camera control software (Olympus).

Negative stain TEM was used to determine crystallinity. Carbon coated 300-mesh copper grids were glow-discharged in nitrogen to render the carbon film hydrophilic. A 4 µL aliquot of the sample was pipetted onto each grid. After 30 s adsorption time the excess was drawn off using Whatman 541 filter paper, followed by staining with 2% aqueous potassium phosphotungstate at pH 7.2, for 10 s. Grids were air-dried until needed.

2.6 High Performance Liquid Chromatography (HPLC)

Several techniques have been used to separate and analyze lipid digestion products including HPTLC, GC and HPLC-MS. However, these have shortcomings such as long run times, labour intensive, high cost, requirement of specialized equipment and use of volatile solvents. Reversed phase HPLC using refractive index detection has recently been shown to be a useful tool to determine lipid composition following *in vivo* digestion that it is simple and non-destructive [20]. Thus this method was employed to separate and analytically quantify the production of medium chain fatty acids during digestion, for correlation with the total amount of fatty acid produced as indicated by the pH stat titration. Samples (200 µL) were taken during digestion for analysis of fatty acid content by HPLC. To halt digestion in the sample, lipase inhibitor (20 µL of 0.05 M 4-BPBA in methanol) was added to eppendorf tubes, where the methanol was evaporated off prior to addition of samples.

Reversed-phase high performance liquid chromatography (HPLC) - Samples were analysed for medium chain fatty acid content and separated by an isocratic reversed-phase HPLC method using a 4.6 × 150 mm Phenomenex Luna C₈ (2) (5 µm, 100 Å) analytical column, with a 15 × 3 mm Brownlee RP-18 (7 µm) guard column. The HPLC system consisted of a Shimadzu CBM-20A system controller, LC-20AD solvent delivery module, SIL-20A auto sampler and a CTO-20A column oven set at 40 °C, coupled to a RID-10A differential refractometric detector (Shimadzu Corp., Kyoto, Japan). An injection volume of 40 µL was used to separate caprylic

acid and capric acid using a mobile phase consisting of MeOH/water (75:25 v/v) with 0.1% TFA (v/v of total mobile phase) at a flow rate of 1 mL/min.

Preparation of standards and samples - A stock solution of caprylic and capric acid was prepared at a concentration of 10 mg/mL in methanol. A set of standards containing 0.1, 0.2, 0.5, 1.0 and 2.0 mg/mL of both lipids was prepared by mixing and dilution of the stock solution in the mobile phase. All stock solutions and standards were stored at 4 °C before analysis. Calibration curves were prepared by plotting the area under the curve against known concentration of standard solutions. Lipolysis samples were diluted in mobile phase prior to HPLC analysis. Unknown sample concentrations were calculated from the standard equation $y = mx + c$, as determined by the linear regression of the unweighted standard curve.

Assay validation - Validation of the HPLC assay was run over three days. Intra-assay accuracy was determined by replicate analysis (n=5) of standard solutions of lipids at three concentrations (0.1, 1.0 and 2.0 mg/mL). Inter-assay accuracy was determined on three separate days. The data were expressed as a percentage of the measured concentration over the theoretical concentration, where mean accuracy was within $\pm 15\%$ of the theoretical concentration. Intra-assay precision (repeatability) and inter-assay precision (reproducibility) were calculated in all three runs for each lipid at all three concentrations and expressed as the coefficient of variation (% CV) of replicate assays. Linearity was performed on standard curves for each run and linearity was fulfilled when the correlation coefficient (r^2) of the regression line was >0.99 .

2.7 References

1. Hernell, O., Staggars, J.E., and Carey, M.C., *Physical-chemical behavior of dietary and biliary lipids during intestinal digestion and absorption. 2 Phase-analysis and aggregation states of luminal lipids during duodenal fat digestion in healthy adult human-beings*. *Biochemistry*, 1990. **29**(8): p. 2041-2056.
2. Fatouros, D.G., et al., *Colloidal structures in media simulating intestinal fed state conditions with and without lipolysis products*. *Pharm Res*, 2009. **26**(2): p. 361-374.
3. Hofmann, A.F., *Molecular association in fat digestion: Interaction in bulk of monoolein, oleic acid, and sodium oleate with dilute, micellar bile salt solutions*. *Adv Chem Ser*, 1968(84): p. 53-&.
4. Kleberg, K., et al., *Biorelevant media simulating fed state intestinal fluids: Colloid phase characterization and impact on solubilization capacity*. *J Pharm Sci*, 2010. **99**(8): p. 3522-3532.

5. Kossena, G.A., et al., *Separation and characterization of the colloidal phases produced on digestion of common formulation lipids and assessment of their impact on the apparent solubility of selected poorly water-soluble drugs*. J Pharm Sci, 2003. **92**(3): p. 634-648.
6. Warren, D.B., et al., *Real time evolution of liquid crystalline nanostructure during the digestion of formulation lipids using synchrotron small-angle X-ray scattering*. Langmuir, 2011. **27**(15): p. 9528-9534.
7. Kaukonen, A., et al., *Drug solubilization behavior during in vitro digestion of suspension formulations of poorly water-soluble drugs in triglyceride lipids*. Pharm Res, 2004. **21**(2): p. 254-260.
8. Kaukonen, A.M., et al., *Drug solubilization behavior during in vitro digestion of simple triglyceride lipid solution formulations*. Pharm Res, 2004. **21**(2): p. 245-253.
9. Sek, L., et al., *Evaluation of the in-vitro digestion profiles of long and medium chain glycerides and the phase behaviour of their lipolytic products*. J Pharm Pharmacol, 2002. **54**(1): p. 29-41.
10. Williams, H.D., et al., *Toward the establishment of standardized in vitro tests for lipid-based formulations, part 1: Method parameterization and comparison of in vitro digestion profiles across a range of representative formulations*. J Pharm Sci, 2012. **101**(9): p. 3360-3380.
11. Gargouri, Y., Moreau, H., and Verger, R., *Gastric lipases: Biochemical and physiological studies* Biochimica Et Biophysica Acta, 1989. **1006**(3): p. 255-271.
12. Dressman, J.B., et al., *Upper gastrointestinal (GI) pH in young, healthy men and women*. Pharm Res, 1990. **7**(7): p. 756-761.
13. Kulkarni, C.V., et al., *Monoolein: A magic lipid?* Phys Chem Chem Phys, 2011. **13**(8): p. 3004-3021.
14. Boyd, B.J., et al., *Self-assembled geometric liquid-crystalline nanoparticles imaged in three dimensions: Hexosomes are not necessarily flat hexagonal prisms*. Langmuir, 2007. **23**(25): p. 12461-12464.
15. Holmberg K, J.B., Kronberg B, Lindman B, *Surfactants and Polymers in Aqueous Solution (Second Edition)*. 2002, Chichester: John Wiley & Sons Ltd.
16. Kirby, N.M., et al., *A low-background-intensity focusing small-angle X-ray scattering undulator beamline*. J Appl Crystallogr, 2013. **46**: p. 1670-1680.
17. Gilbert, E.P., Schulz, J.C., and Noakes, T.J., *'Quokka' - The small-angle neutron scattering instrument at OPAL*. Phys B, 2006. **385-86**: p. 1180-1182.
18. Svergun, D.I. and Koch, M.H.J., *Small-angle scattering studies of biological macromolecules in solution*. Rep Prog Phys, 2003. **66**(10): p. 1735-1782.
19. Koppel, D.E., *Analysis of macromolecular polydispersity in intensity correlation spectroscopy - Method of cumulants*. J Chem Phys, 1972. **57**(11): p. 4814-4820.
20. Lee, K.W., Porter, C.J., and Boyd, B.J., *A simple quantitative approach for the determination of long and medium chain lipids in bio-relevant matrices by high performance liquid chromatography with refractive index detection*. AAPS PharmSciTech, 2013. **14**(3): p. 927-34.

Chapter 3. Disposition and Crystallization of Saturated Fatty Acid in Mixed Micelles

Chapter 3. Disposition and Crystallization of Saturated Fatty Acid in Mixed Micelles

The work presented in this chapter has been published as: Phan S., Salentinig S., Gilbert E.P., Darwish T.A., Hawley A., Nixon-Luke R., Bryant G., Boyd B.J., *Disposition and crystallization of fatty acid in mixed micelles of relevance to lipid digestion*. J Colloid Interface Sci, 2015. **449**: p.160-166.

3.1 Declaration

Declaration by candidate:

In the case of Chapter 3, the nature and extent of my contribution to the work was the following:

Nature of contribution	Extent of contribution
Research design, performance of data collection and analysis, manuscript preparation	75%

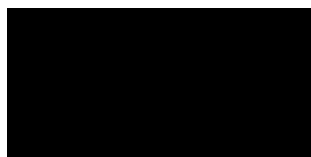
The following co-authors contributed to the work:

Name	Nature of contribution
Stefan Salentinig	Supervision, intellectual input, input into manuscript preparation
Elliot P. Gilbert	Intellectual input on SANS operation, input into manuscript preparation
Tamim A. Darwish	Synthesis of deuterated fatty acids, input into manuscript preparation
Adrian Hawley	Intellectual input on SAXS operation
Reece Nixon-Luke	Performance of DDLS data collection
Gary Bryant	Input into manuscript preparation
Ben J. Boyd	Supervision, intellectual input, input into manuscript preparation

Chapter 3. Disposition and Crystallization of Saturated Fatty Acid in Mixed Micelles

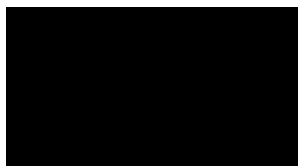
The undersigned hereby certify that the above declaration correctly reflects the nature and extent of the candidate's and co-authors' contributions to this work.

Candidate's signature:



Date: 21/08/15

Main supervisor's signature:



Date: 21/08/15

3.2 Disposition and Crystallization of Saturated Fatty Acids in Mixed Micelles of Relevance to Lipid Digestion

Stephanie Phan ¹, Stefan Salentinig ¹, Elliot Gilbert ², Tamim A. Darwish ³, Adrian Hawley ⁴, Reece Nixon-Luke ⁵, Gary Bryant ⁵, Ben J. Boyd ^{1,6}

¹ Monash Institute of Pharmaceutical Sciences, Monash University, 381 Royal Parade, Parkville, VIC 3052, Australia

² Bragg Institute and ³National Deuteration Facility, Australian Nuclear Science and Technology Organisation, Locked Bag 2001, Kirrawee DC, NSW 2232, Australia

⁴ SAXS/WAXS beamline, Australian Synchrotron, 800 Blackburn Road, Clayton, VIC 3168, Australia

⁵ Centre for Molecular and Nanoscale Physics, School of Applied Sciences, RMIT University, GPO Box 2476, Melbourne, Victoria 3001, Australia

⁶ ARC Centre of Excellence in Convergent Bio-Nano Science and Technology, Monash Institute of Pharmaceutical Sciences, Monash University (Parkville Campus), 381 Royal Parade, Parkville, VIC 3052, Australia

Received 9th October 2014 and published online 18th November 2014

Citation: *J. Colloid Interface Sci.* (2015) 449:160-166

DOI: 10.1016/j.jcis.2014.11.026

Abstract

During lipolysis of triglyceride by lipase, monoglyceride and fatty acids are produced which combine with gastrointestinal fluids to form self-assembled structures. These solubilize hydrophobic food components to promote their absorption. The aim of this study was a detailed understanding of structure formation from triglyceride digestion products with saturated short-, medium- and long chain fatty acids. Complementary characterization methods have been applied comprising small angle X-ray and neutron scattering – the latter

Chapter 3. Disposition and Crystallization of Saturated Fatty Acid in Mixed Micelles

involving the contrast matching technique using fully deuterated fatty acids – polarized and depolarized dynamic light scattering and cryogenic-transmission electron microscopy. Shape, size and solubilization capacity of the self-assembled structures was dependent on composition and lipid chain length. Crystallization of fatty acid was observed when the solubility limit in the mixed bile salt micelles was exceeded; however, increasing pH and temperature increased the fatty acid solubility. The results provide insight into structure formation and crystallization of incorporated lipolysis products; this is important for a detailed understanding of food structure and nutrition, as well as the rational design of lipid-based drug delivery systems.

Keywords: lipolysis, lipid digestion, lipid-based drug delivery, synchrotron small angle X-ray scattering, small angle neutron scattering, cryogenic transmission electron microscopy

Abbreviations:

BS, bile salt

Cryo-TEM, cryogenic-transmission electron microscopy

DDLS, depolarized dynamic light scattering

DLS, dynamic light scattering

FA, fatty acid

MG, monoglyceride

SANS, small angle neutron scattering

SAXS, small angle X-ray scattering

3.3 Introduction

Triglyceride lipids are responsible for 30% of the daily calorie intake in the Western diet [1, 2]. The digestion of triglycerides by lipases in the gastro-intestinal tract leads to generation of fatty acids and monoglycerides. These digestion products are required for membrane

synthesis, elements of cells and tissues, production of signaling compounds and a source of energy [1]. They impact lipid metabolism and are important in metabolic diseases, where fatty acid-binding protein expression is altered in conditions such as atherosclerosis, type 2 diabetes and obesity [3]. Fatty acids can also affect the development and progression of cancer and cardiovascular disease [4-6].

In the small intestine, fatty acid and monoglyceride combine with endogenous amphiphilic molecules secreted from the gallbladder, such as bile salt, cholesterol and phospholipid. These mixtures spontaneously self-assemble into thermodynamically stable structures such as mixed micelles of varying size and shape, vesicles and more complex liquid crystalline phases [7-9]. This structure formation has been confirmed *in vivo* in killifish [10] and human duodenal aspirates following a lipid-rich meal [9, 11-13]. The phase behavior has been studied in systems containing combinations of bile salt, monoglyceride and cholesterol, where it has been shown that colloidal structure and size depends on composition [14-17]. Bile salt micelles have been shown to elongate with increasing proportions of phospholipid, finally resulting in vesicles [18-20]. Bile salt micelles have also been found to increase in size with addition of monoglyceride and fatty acid [7].

Such structures facilitate transport of hydrophobic molecules in the gastrointestinal tract and uptake through the enterocyte membrane. They have high solubilizing capacity for hydrophobic molecules including cholesterol, dietary lipids [21, 22] and fat-soluble vitamins A, D, E and K [23, 24], and thus act as their carrier to prevent precipitation and enhance bioavailability. They also have a high solubilization capacity for hydrophobic drugs, which makes them potential vehicles for drug delivery [7, 25]. Co-administration of drugs with lipids has been proposed to reduce precipitation of the former during lipid digestion and increase bioavailability, rendering them of interest in the drug delivery field [26, 27].

Many saturated triglycerides are present in the Western diet [28], and the fatty acids produced on their digestion in the gut have melting points higher than physiological temperature e.g. C₁₂, C₁₄, C₁₆ and C₁₈ [29]. They are protonated at physiological pH, which can result in crystallization of lipid and excretion in the faeces, rather than absorption [30, 31]. The melting points of C₈ and C₁₀ fatty acids are lower than physiological temperature enabling them to be better solubilized and absorbed than long chain fatty acids. However there is a lack of understanding of the influence of structure formation on crystallization of saturated fatty acids and monoglycerides in biologically relevant multi-component systems containing bile

Chapter 3. Disposition and Crystallization of Saturated Fatty Acid in Mixed Micelles

salt, phospholipid, monoglyceride and fatty acid under physiological pH conditions. Solubilization of lipid digestion products such as fatty acids is required for uptake and use by the body; thus crystallization is undesirable. In this study, the shape and size of the resulting colloidal structures and the crystallization of saturated fatty acids in biologically relevant mixtures have been studied using scattering methods and electron microscopy.

The pH in the gastrointestinal tract has been shown to vary between 2 and 8 [32] (Figure 3.1), which will influence the partition coefficient of fatty acid between the aqueous bulk phase and the lipid areas of the colloidal structure, and potentially induce crystallization of the fatty acid. In addition, pH has an impact on the protonation state of the fatty acid which can modify the packing geometry based on the effective charge per molecule at the interface [33-36], thus influencing the size and shape of structures.

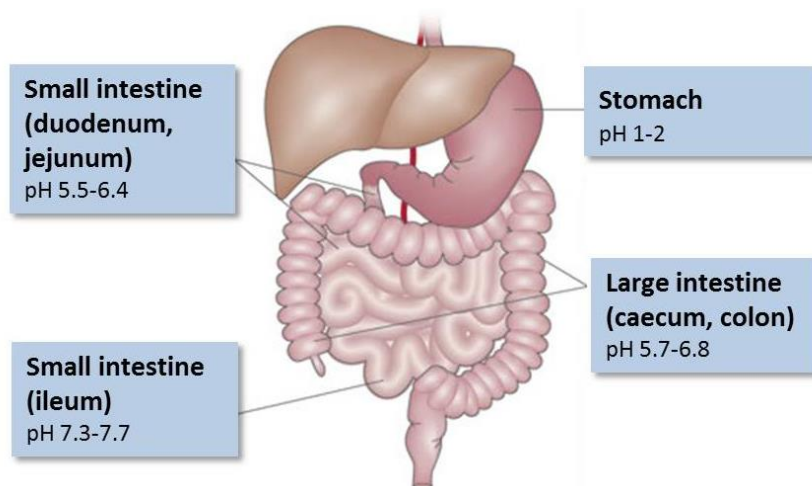


Figure 3.1: Variation in pH in the gastrointestinal tract. Image adapted with permission from [37].

To the best of our knowledge, this is the first study investigating the disposition and crystallization of lipolysis products in mixed micellar structures in biologically relevant conditions of the human intestine. An understanding of how intermolecular assembly of digestion products is influenced by composition, lipid chain length, pH and temperature will provide insight into the digestion process, and further the understanding for the delivery of hydrophobic molecules, including drugs, to the body.

3.4 Experimental

Materials

Deuterated caprylic acid (C_8 fatty acid, $C_8HD_{15}O_2$), lauric acid (C_{12} fatty acid, $C_{12}HD_{23}O_2$), and myristic acid (C_{14} fatty acid, $C_{14}HD_{27}O_2$), were prepared as described below. Monomyristin (C_{14} monoglyceride >97%) was obtained from TCI Co. Ltd (Kawaguchi, Saitama, Japan). Bile salt (sodium taurodeoxycholate >95%), monocaprylin (C_8 monoglyceride 99%), monolaurin (C_{12} monoglyceride 99%), tris maleate (reagent grade), NaOH (p.a. grade) and HCl (p.a. grade) were purchased from Sigma Aldrich (St. Louis, MO, USA). Phospholipid (1,2-dioleoyl-sn-glycero-3-phosphocholine, DOPC) was from Trapeze Association Pty. Ltd.. (Clayton, Victoria, Australia). Sodium chloride was purchased from Chem Supply (Gillman, SA, Australia). Sodium azide was purchased from Merck Schuchardt OHG (Eduard-Buchner-Straße, Hohenbrunn, Germany). Ultra-pure water (resistivity >18 M Ω cm) was used for the preparation of all samples.

Deuteration method

The deuteration of the three fatty acids were achieved following a procedure published elsewhere [36]. In summary, a mixture of the appropriate acid, Pt/activated carbon and NaOD in D_2O was subjected to two hydrothermal H/D exchange cycles in a Parr pressure reactor at 220 °C (23 bar) for 3 days each. Thin layer chromatography was used (referenced with the protonated compound) to develop separation protocols. Purification of the deuterated compounds was performed on silica gel columns, eluted with the appropriate solvents. 1H NMR (400 MHz), and 2H NMR (61.4 MHz) spectra were recorded on a Bruker 400 MHz spectrometer at 298 K. More details on the characterization are presented in the Supporting Information. The 1H NMR and 2H NMR spectra, as well as the mass spectrometry data are shown in Figures SI-3.1 – SI- 3.6.

Sample preparation

Fed simulated intestinal fluid was prepared using bile salt (BS, sodium taurodeoxycholate) and phospholipid (PL, DOPC) concentrations at a ratio of 20 mM:5 mM to represent concentrations relevant after food intake, in digestion buffer (50 mM Tris maleate, 150 mM NaCl, 6 mM NaN_3 as an antibacterial agent) [38-41]. The PL was weighed into a round bottom flask and dissolved in chloroform which was subsequently evaporated to produce a

thin film of PL. BS and digestion buffer was added, and the PL and BS were dispersed in a sonicator bath for 30 min. The equilibrium systems reflecting the endpoint of the lipid digestion process were prepared by adding 10 mM monoglycerides (C_8 , C_{12} or C_{14}) and 20 mM deuterated fatty acids (C_8 , C_{12} or C_{14}) [7, 42-44] to high levels of bile salt/phospholipid (BS/PL) micelles expected in the fed state simulating the gastrointestinal state at the nominal end point of digestion of triglycerides (C_8 , C_{12} or C_{14}). The 1:2 ratio of monoglyceride to fatty acid represents the nominal end point of digestion of the corresponding triglyceride, and thus is most commonly used. However there is evidence that digestion can proceed past this, thus it may not necessarily be entirely reflective of the end point of digestion but some transient composition towards the end of digestion [9, 43, 45, 46].

Sonication with a tip sonicator for 30 s at 100 W was used to solubilize the components. Samples were equilibrated for 24 hr and pH was adjusted with concentrated NaOH and HCl.

Small angle neutron scattering (SANS)

SANS experiments were performed on the Quokka instrument at OPAL [47] at a wavelength of 5.0 Å and 10% wavelength resolution. Two instrument configurations were used with a source-to-sample distance of 8 m and sample-to-detector distances of 8 m and 2 m, the latter with a 300 mm detector offset to increase maximum q . These configurations provide a continuous q range of 0.01 - 0.5 Å⁻¹ where q is the length of the scattering vector, defined by $q = (4\pi/\lambda)\sin(\theta/2)$, where λ is the wavelength and θ , the scattering angle. 250 µL samples were enclosed in Hellma cuvettes with a 1 mm path length. Samples were studied at several temperatures with control provided with a Julabo thermostatted bath. All data were corrected for blocked beam measurements, normalized and radially averaged using a package of macros in Igor software (Wavemetrics, Lake Oswego, Oregon, USA) and modified to accept HDF5 data files from Quokka. Scattering curves are plotted as a function of absolute (SANS) intensity, I , versus q .

A Guinier plot of the SANS data where $\ln(I)$ is plotted against q^2 was produced to determine the radius of gyration (R_g). This provides information about the particle size and was obtained from the slope of the Guinier plot, where the q range used was $qR_g < 1.3$ for a reliable fit [48].

Small angle X-ray scattering (SAXS)

SAXS measurements were performed at the SAXS/WAXS beamline [49] at the Australian Synchrotron. An X-ray beam with a wavelength of 1.1271 Å (11 keV) was used. A sample to detector distance of 1651 mm covered the q -range $0.007 < q < 0.5 \text{ \AA}^{-1}$. 200 μL samples were drawn through a 1.5 mm diameter quartz capillary which was fixed in the X-ray beam. A thermostatted metal heating block controlled by a Peltier system accurate to $\pm 0.1 \text{ }^\circ\text{C}$ was used for measurements taken at 37 $^\circ\text{C}$. The 2D SAXS patterns were acquired over 1 s using a Pilatus 1M detector with active area $169 \times 179 \text{ mm}^2$ and with a pixel size of 172 μm . 2D scattering patterns were integrated into the 1D scattering function $I(q)$ using the in-house developed software package scatterBrain. Scattering curves are plotted as a function of relative X-ray intensity, I , versus q .

Dynamic light scattering (DLS)

DLS was used to determine the mean hydrodynamic radius (R_H) and the size distribution width of the particles. DLS measurements were performed on a Malvern Zetasizer NanoZS to determine the hydrodynamic radius (R_H) and particle size distribution. Samples were centrifuged for 5 min at 3500 rpm prior to the measurement to remove any trace dust particles. A laser power of 4 mW was used at a back scattering angle of 173° at room temperature. The average diffusion coefficient, D , was obtained by the cumulant analysis of the correlation functions [50]. The mean hydrodynamic radius R_H was deduced from the diffusion coefficient using the Stokes–Einstein equation:

$$R_H = \frac{k_B T}{6\pi\eta D}$$

where k_B is the Boltzmann constant, T the absolute temperature and η the viscosity of the solvent. The polydispersity index (PDI) of the size distribution was determined from the second cumulant:

$$PDI = \frac{\mu_2}{\bar{\Gamma}^2}$$

where μ_2 is the second cumulant and $\bar{\Gamma}$ the mean of the inverse decay time.

Depolarized dynamic light scattering (DDLS) was used to confirm the presence of anisotropic particles observed by SANS and SAXS. DDLS measurements were performed on an ALV-

5022F spectrometer, using a vertically polarized Helium Neon laser (wavelength 633 nm). The scattered light passed through a crossed polarizer which was carefully adjusted to achieve minimum scattered intensity. Correlation functions were collected at different scattering angles between 20° and 90°. At each angle, 10 measurements of 1 min duration were performed, and the average of the data sets was taken for each angle. DDLS takes advantage of the fact that the light scattered from optically homogeneous spherical particles maintains the same polarization as the incident light. However, optically anisotropic particles such as cylindrical micelles lead to depolarized scattering. The correlation function measured in DDLS is a combination of translational diffusion and rotational diffusion, and the decay rate of the depolarized field correlation function, Γ , is given by:

$$\Gamma = q^2 D_T + 6D_R$$

Γ was determined from the correlation function by cumulant expansion [50].

Cryogenic-transmission electron microscopy (cryo-TEM)

Cryo-TEM was used to view the samples. A laboratory-built humidity-controlled vitrification system was used to prepare the samples. Humidity was kept close to 80% for all experiments, and ambient temperature was 22 °C.

Copper grids (200-mesh) coated with perforated carbon film (Lacey carbon film: ProSciTech, Qld, Australia) were glow discharged in nitrogen to render them hydrophilic. Aliquots (4 μ L) of the sample were pipetted onto each grid prior to plunging. After 30 s adsorption time the grid was blotted manually using Whatman 541 filter paper, for approximately 2 s. Blotting time was optimized for each sample. The grid was then plunged into liquid ethane cooled by liquid nitrogen. Frozen grids were stored in liquid nitrogen until required.

The samples were examined using a Gatan 626 cryoholder (Gatan, Pleasanton, CA, USA) and Tecnai 12 Transmission Electron Microscope (FEI, Eindhoven, The Netherlands) at an operating voltage of 120 kV. At all times low dose procedures were followed, using an electron dose of 8-10 electrons/ \AA^2 for all imaging. Images were recorded using a FEI Eagle 4k \times 4k CCD camera at magnifications ranging from 15 000 \times to 50000 \times . Images were recorded using a Megaview III CCD camera and AnalySIS camera control software (Olympus.)

Negative stain TEM was used to determine crystallinity. Carbon coated 300-mesh copper grids were glow-discharged in nitrogen to render the carbon film hydrophilic. A 4 μL aliquot of the sample was pipetted onto each grid. After 30 s adsorption time the excess was drawn off using Whatman 541 filter paper, followed by staining with 2% aqueous potassium phosphotungstate at pH 7.2, for 10 s. Grids were air-dried until needed.

3.5 Results and Discussion

Small angle neutron scattering employing fully deuterated fatty acids to enable contrast variation, and small angle X-ray scattering together provide complementary approaches to elucidate structure and map the location of the fatty acid in mixed micelles. Since neutrons scatter from the atomic core, the replacement of hydrogen with deuterium, which has a much greater scattering length density, strongly enhances the contrast in SANS. The scattering contrast can be modified by the choice of solvent (i.e. $\text{D}_2\text{O}/\text{H}_2\text{O}$) or the selective deuteration of molecules. This study combines both contrast variation methods. Fully deuterated fatty acids in combination with non-deuterated monoglyceride, bile salt and phospholipid were used. Using D_2O as a solvent resulted in scattering arising primarily from the bile salt, phospholipid and monoglyceride, whereas in H_2O the scattering signal is primarily from the deuterated fatty acid. The X-ray and neutron scattering length densities of the components are summarized in Table SI-3.1.

Effect of lipid chain length and pH on solubilization of lipids and structure of bile salt mixed micelles

The size and shape, and presence of crystallized components from mixed bile salt micelles, upon the incorporation of the digestion products of C_8 , C_{12} and C_{14} triglycerides were studied. With increasing lipid chain length, the size of the micelles increased as might be expected.

While there was no evidence of crystallization in the C_8 and C_{12} system, crystallization was observed in the C_{14} system at pH 6.5, representative of duodenal pH. The Bragg peaks at $q = 0.15, 0.16, 0.19$ and 0.33 \AA^{-1} result from the presence of fatty acid/soap crystals where the fatty acid is protonated (Figure 3.2A). The peaks were absent at higher pH values, as the fatty acid is fully deprotonated and solubilized in the mixed bile salt micelles.

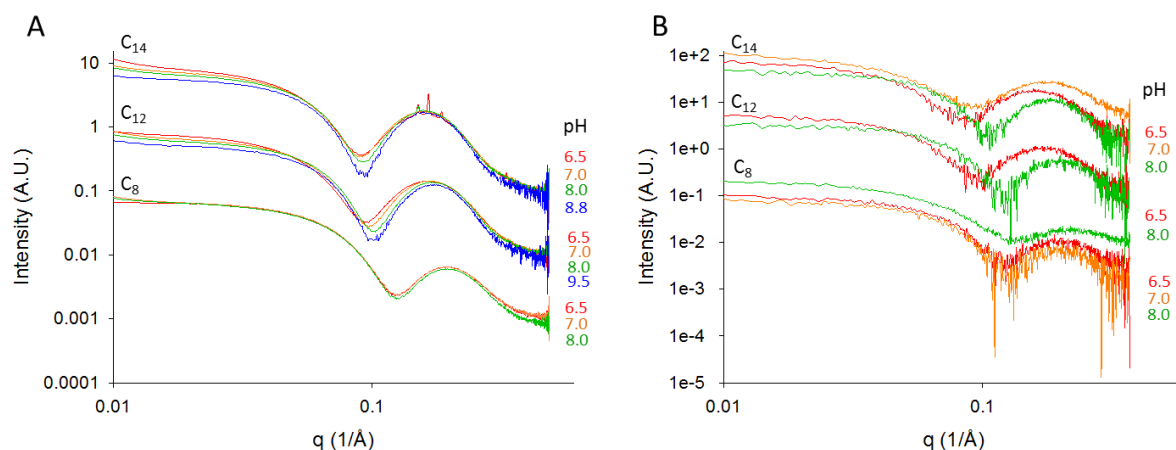


Figure 3.2: Increasing size was observed with increasing hydrocarbon chain length in C_8 , C_{12} , C_{14} MG+dFA systems in H_2O BS/PL micelles at varying pH values. Crystallinity was present in the C_{14} system at pH 6.5. SAXS measurements were performed at (A) 27 °C and (B) 37 °C.

The positions of Bragg peaks are consistent with values for crystalline C_{14} fatty acid (Figure 3.3A). The presence of crystalline material was confirmed with transmission electron microscopy in selected area diffraction mode with the negative stain phosphotungstic acid (Figure 3.3B).

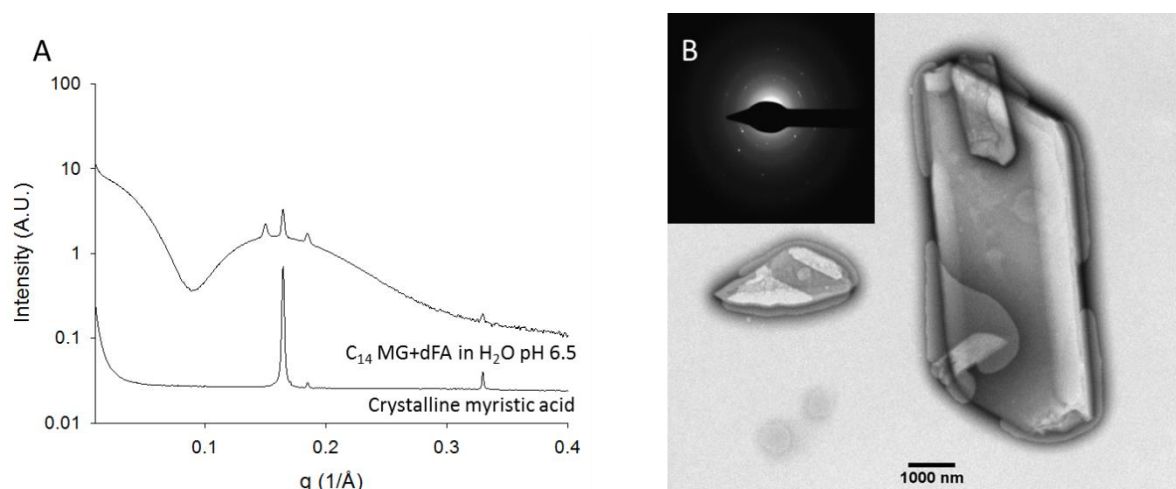


Figure 3.3: (A) Bragg peaks in the C_{14} MG+dFA H_2O system at pH 6.5 correlate to crystalline C_{14} fatty acid, as determined by SAXS measurements. (B) Diffraction from crystalline material was confirmed with electron microscopy using the negative stain phosphotungstic acid.

Chapter 3. Disposition and Crystallization of Saturated Fatty Acid in Mixed Micelles

SAXS measurements and electron diffraction on the C₁₄ samples prepared in D₂O, provided consistent results. At intestinal pH, no peaks were evident, however at lower pH, a Bragg peak at $q = 0.20 \text{ \AA}^{-1}$ was present which persisted until the temperature was raised to 60 °C (Figure SI-3.7). The crystallization behavior is attributed to the protonated state of the C₁₄ fatty acid at the low pH studied in these samples prepared in D₂O compared to the samples prepared in H₂O, and the differences in crystal polymorph may be due to the solvent used.

Crystallinity was not present when the sample temperature was increased to 37 °C, where SAXS measurements did not reveal Bragg peaks for any of the chain lengths studied in H₂O (Figure 3.2B). This suggests that the fatty acid is molten and solubilized in the mixed bile salt micelles at physiological pH and temperature, which is required to enable absorption of lipid, although the melting points of C₁₂ and C₁₄ fatty acid are higher, at 43.5 °C and 54.4 °C respectively [29]. The results suggest that the solvation of the fatty acids in the mixed bile salt micelles is sufficient to overcome the greater enthalpy of fusion for the longer chain saturated fatty acids.

Cryo-TEM was used to visualize the structures in the C₁₄ system in H₂O at pH 6.5 (Figure 3.4). The images show the presence of micelles and emulsified microemulsion droplets, the latter with dimensions of a few hundred nanometers in diameter. Microemulsions have been shown to occur in systems containing lipid, surfactant and water [51, 52].

Co-existing plate-like structures with well-defined edges were present, with dimensions from several hundreds of nanometers to microns, indicative of crystalline lipid. It has previously been reported that the addition of long chain lipid digestion products to mixed bile salt micelle systems, leads to an increase in hydrophobicity and decrease in solubility, resulting in crystallization [22].

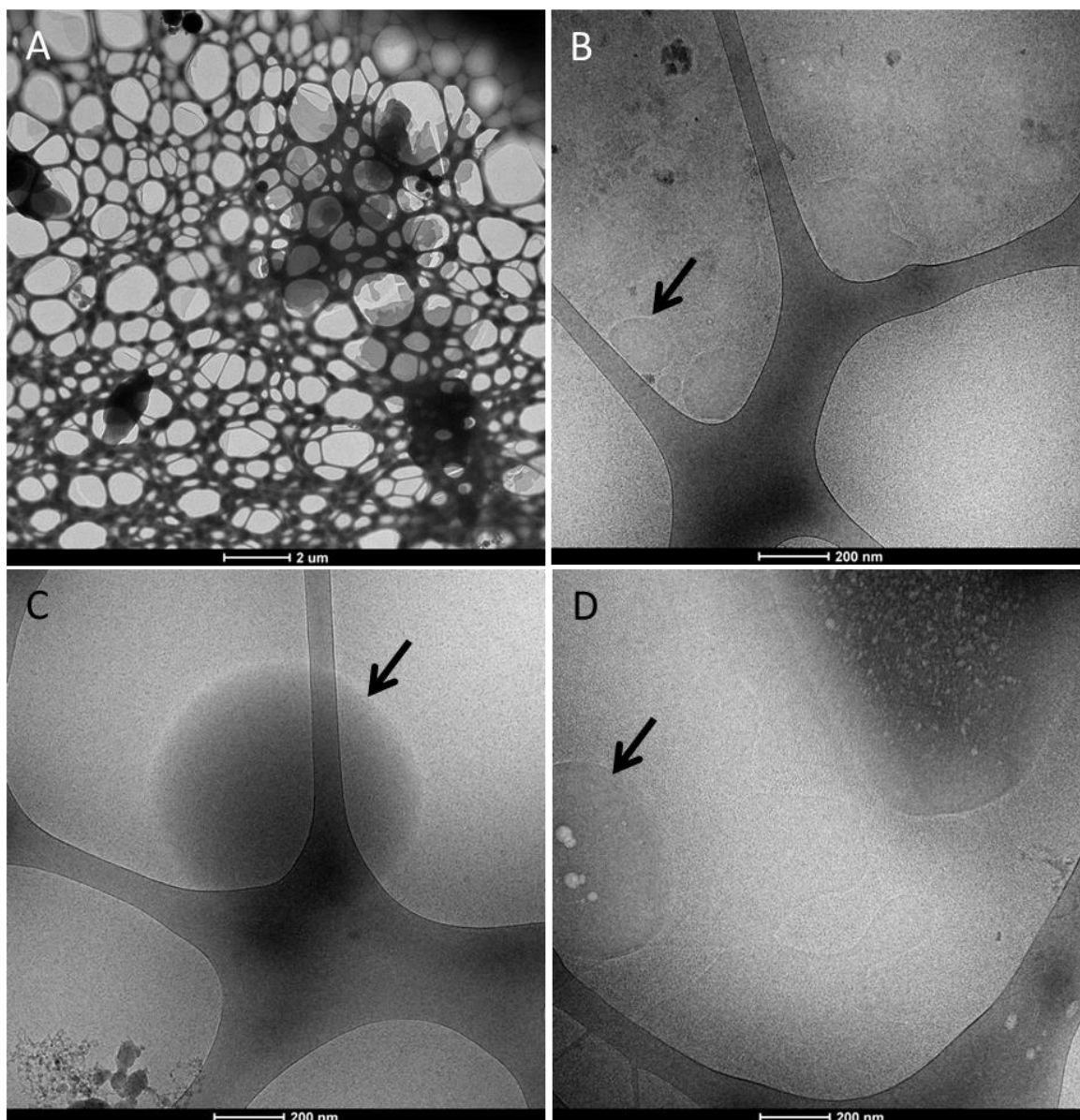


Figure 3.4: Cryo-TEM images of C_{14} MG+dFA system in H_2O BS/PL micelles at pH 6.5 show (A) many plate-like structures with well-defined edges indicative of crystalline material (B)-(D) large particles (indicated by arrows). Micelles were observed throughout the sample.

These results can have important implications for the absorption of saturated fatty acids. Crystallization of fatty acid in the small intestine is undesirable and it has previously been shown that protonated fatty acids and long chain fatty acids (C_{12} and longer) precipitate from intestinal contents and are subsequently excreted from the body rather than being absorbed [30, 31]. In a similar manner, cholesterol-rich vesicles were shown to produce cholesterol crystals which led to gallstone formation [20].

Localisation of components of mixed bile salt micelles using SANS

SANS experiments in combination with the contrast matching technique were used to study the location of components in the mixed bile salt micelles.

In all systems containing monoglyceride and fatty acid, an increase in the pH led to a decrease in the forward scattering in the D₂O and H₂O based systems (see Figure 3.5). To confirm the presence of elongated particles at low pH, DDLS measurements were performed on the C₁₂ system. At high pH the depolarized scattering was within the noise of the instrument, indicating that the particles are spherical. However, at low pH, the depolarized signal was well above the noise, confirming the results from SANS that the particles are elongated.

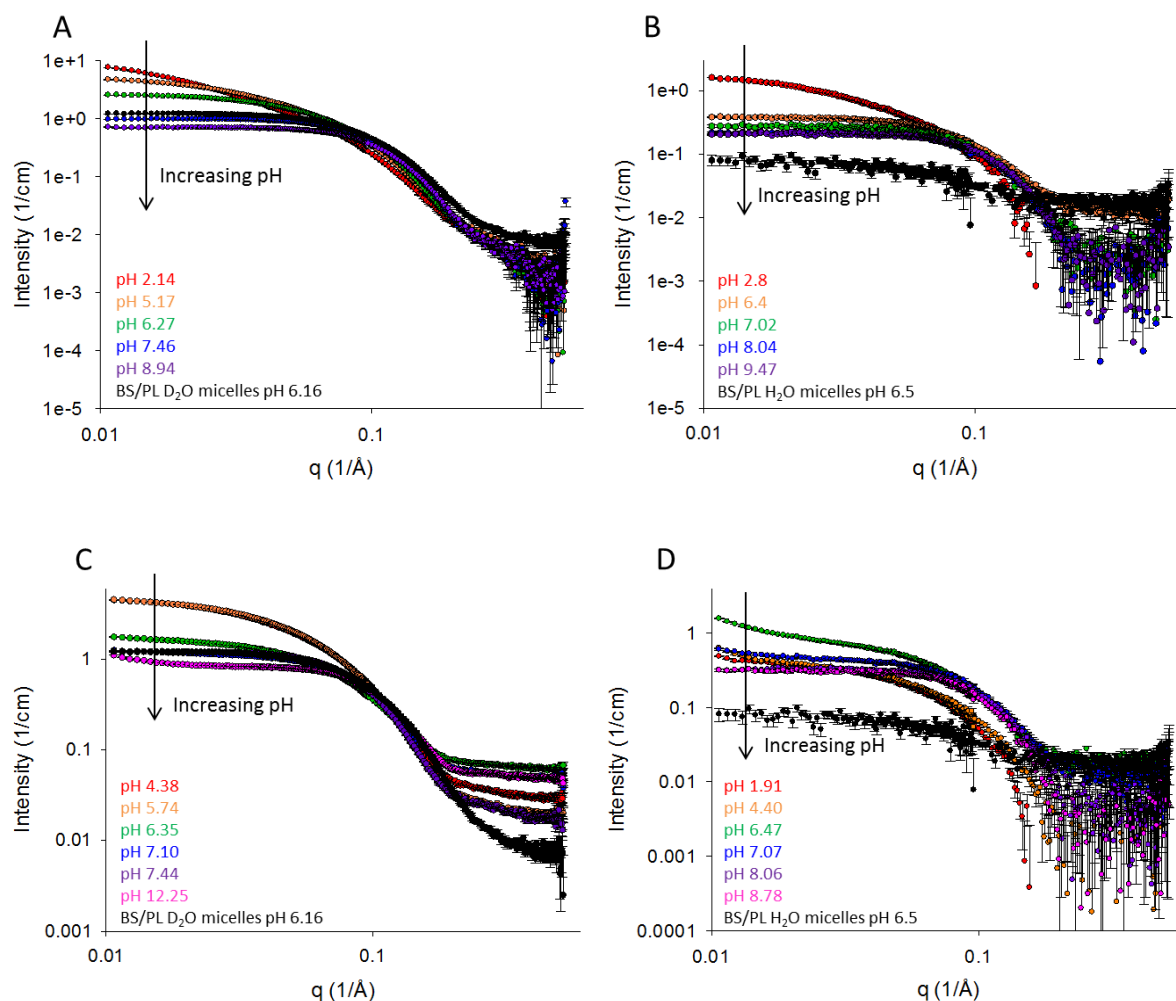


Figure 3.5: A transition from elongated to spherical particles was observed in C_{12} MG+dFA systems in (A) D_2O and (B) H_2O BS/PL micelles, and C_{14} MG+dFA systems in (C) D_2O and (D) H_2O BS/PL micelles. A decrease in the apparent size is observed with increasing pH. SANS measurements were performed at 27 °C.

Changing the pH did not influence the size of bile salt/phospholipid micelles in the absence of fatty acid/monoglyceride (Figure SI-3.8). Thus the influence of pH on structure formation can be attributed to the ionization state of the incorporated fatty acid, and changes in packing geometry of the fatty acids according to the critical packing parameter theory [33]. At low pH, the fatty acids are fully protonated and incorporation in the chain region of the existing structures, with overall reduced mean curvature is preferred, favouring elongation. At elevated pH, the fatty acids are fully deprotonated and pack to form highly curved spherical micelles

due to electrostatic repulsion and to minimize interactions of hydrocarbon tails with polar solvent.

The radius of gyration (R_g) was calculated from the SANS curves and is presented in Figure 3.6. The R_g for the mixed micelles decreased with increasing pH at both contrasts (i.e. in D_2O and H_2O). The hydrodynamic radii (R_H) from DLS measurements presented in the same figure confirm this trend. The corresponding correlation functions confirm essentially monomodal size distributions (Figure SI-3.9).

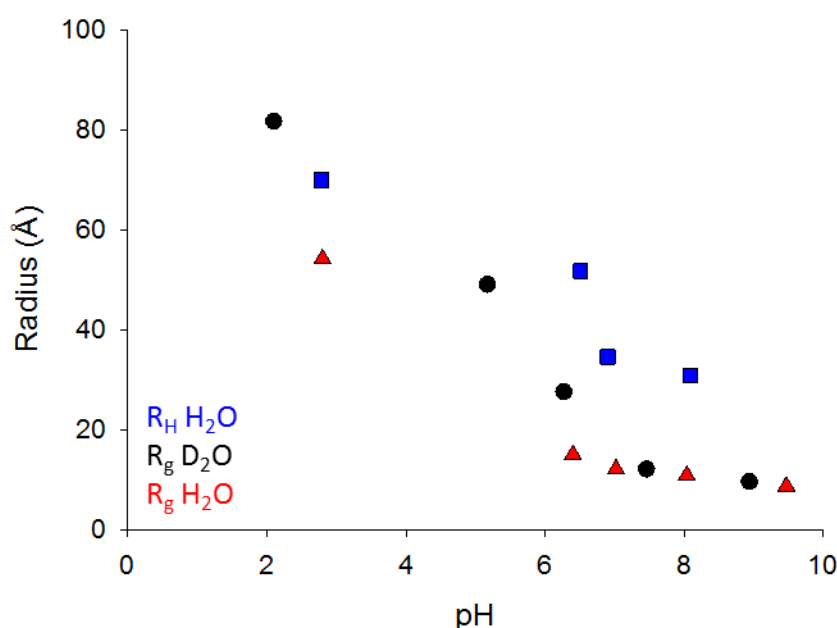


Figure 3.6: R_g and R_H for C_{12} MG+dFA systems in D_2O and H_2O show a decrease in the micellar size with increasing pH.

Comparing the R_g values in D_2O and H_2O at low pH, larger values were found in D_2O . In D_2O , the scattering arises from bile salt/phospholipid micelles and monoglyceride, whereas in H_2O , it arises primarily from the deuterated fatty acid. This disparity in size at low pH therefore suggests that the bile salt, phospholipid and monoglyceride are mainly located in a shell surrounding the core which is composed predominately of the deuterated fatty acid similar to the previous study in a shorter C_8 chain system [36]. At $pH > 7$, the disparity between the two values diminished, indicating an equal distribution of the fatty acid within the mixed micelles, whereby the C_{12} fatty acid remains part of the mixed micelles. This is in

contrast to the previous finding on the C₈ system where the fatty acid was redistributing from the micelles to the aqueous phase with increasing pH. This is consistent with reports that medium chain lipids have reduced capacity to be incorporated into, and swell, bile salt micelles [7].

The size and shape of BS/PL micelles was shown to vary with the addition of lipolysis products of C₈, C₁₂ and C₁₄ triglycerides under physiologically relevant pH conditions as summarized in Figure 3.7. With increasing lipid chain length, crystallization was observed under low pH conditions, but at elevated pH, lipids are solubilized in bile salt mixed micelles which may facilitate lipid absorption by the body.

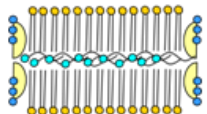
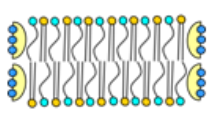
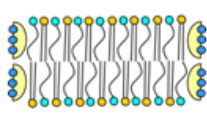
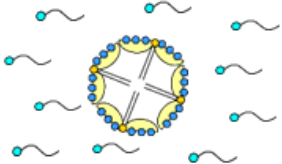
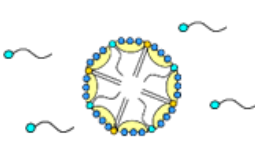
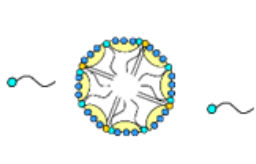
System (BS/PL micelles + MG + FA)	C ₈	C ₁₂	C ₁₄
Low pH (stomach)			
High pH (intestinal pH)			

Figure 3.7: Summary of phase behaviour of BS/PL micelles with the addition of lipolysis products of C₈, C₁₂ and C₁₄ triglycerides under physiologically relevant pH conditions. Figure adapted in part from [18, 53].

3.6 Conclusion

This study provides insight into likely structure formation during lipid digestion, where lipolytic products are solubilized by bile salts to form mixed micelles. These structures are important to promote the absorption of dietary lipids and vitamins. Self-assembly structure formation in bile salt/phospholipid micelles with incorporated monoglyceride and fatty acid, was seen to depend on composition, lipid chain length and pH; where increasing lipid chain length and decreasing pH increased the apparent size of the micelles. Crystallization of fatty

Chapter 3. Disposition and Crystallization of Saturated Fatty Acid in Mixed Micelles

acid in the C₁₄ system was observed, but this was dissipated at physiological temperature and with increasing pH. This is important as varying colloidal structures have different solubilization capacities for drug, and thus understanding of structure in lipid systems is critical for enabling rational design of lipid-based formulations.

Acknowledgements

The authors would like to thank Lynne Waddington for assistance with the cryo-TEM studies which were undertaken at CSIRO Materials Science and Engineering, Victoria, Australia.

This research was undertaken on the SAXS/WAXS beamline at the Australian Synchrotron, Victoria. Funding is acknowledged from the Australian Research Council under the Discovery Projects scheme DP120104032. BJB is a recipient of an Australian Research Council Future Fellowship (FT120100697).

3.7 Supporting Information

Scattering length densities of components

Table SI-3.1: Summary of chemical formula and X-ray and neutron scattering length densities (ρ) of the individual components. Also shown is the neutron contrast $\Delta\rho = (\rho - \rho_{\text{solvent}})$; the highest contrast (strongest scatterers) in D₂O and H₂O are underlined.

Component	Physical Density [g/cm ⁻³]	X-ray Scattering length density [Å ⁻²] × 10 ⁻⁷	Neutron Scattering length density [Å ⁻²] × 10 ⁻⁷	Neutron Contrast in H ₂ O $\Delta\rho$ (H ₂ O) × 10 ⁻⁷	Neutron Contrast in D ₂ O $\Delta\rho$ (D ₂ O) × 10 ⁻⁷
D ₂ O	1.1	93.7	63.8		
H ₂ O	1.0	94.7	-56.1		
C ₈ HD ₁₅ O ₂	0.9	76.4	58.0	<u>63.6</u>	-5.80
C ₁₂ HD ₂₃ O ₂	0.9	76.4	60.7	<u>66.3</u>	-3.10
C ₁₄ HD ₂₇ O ₂	0.9	76.4	61.6	<u>67.2</u>	-2.20
C ₁₁ H ₂₂ O ₄	0.9	84.3	3.49	9.10	<u>-60.3</u>
C ₁₅ H ₃₀ O ₄	0.9	84.9	2.12	7.73	<u>-61.7</u>
C ₁₇ H ₃₄ O ₄	0.9	85.1	1.62	7.23	<u>-62.2</u>
C ₂₆ H ₄₄ NO ₆ SNa	0.9	82.9	6.12	11.7	<u>-57.7</u>
C ₄₂ H ₈₂ NO ₈ P	0.9	84.7	2.38	7.99	<u>-61.4</u>

Preparation and characterisation of the deuterated fatty acids

Hydrothermal reactions were performed using a Mini Benchtop 4560 Parr Reactor (600 mL vessel capacity, 3000 psi maximum pressure, 350 °C maximum temperature). Thin layer chromatography was used (referenced with the protonated compound) to estimate the purity and to develop separation protocols. ^1H NMR (400 MHz), and ^2H NMR (61.4 MHz) spectra were recorded on a Bruker 400 MHz spectrometer at 298 K. Chemical shifts, in ppm, were referenced to the residual signal of the corresponding NMR solvent. Deuterium NMR was performed using the probe's lock channel for direct observation. For octanoic and myristic acids, methylsulfonylmethane was used as internal standard to quantify the extent of deuteration. The overall deuterium content (percentage) of a compound was calculated from the individual determinations at the different deuterated positions. This was performed by taking the sum of the percentage deuteration of each position multiplied by the number of protons/deuterium atoms at each of these positions and then dividing the answer by the total number of protons/deuterium in the compound (excluding any exchangeable protons, e.g., carboxylic acid).

Electrospray ionization mass spectra (ESI-MS) were recorded for all of the deuterated fatty acids on a 4000 QTrap AB Sciex spectrometer. The overall percentage deuteration of the molecules was calculated by MS using the isotope distribution analysis of the different isotopologues. This was calculated taking into consideration the ^{13}C natural abundance, whose contribution was subtracted from the peak area of each M+1 isotopologue to allow for accurate estimation of the percentage deuteration of each isotopologue.

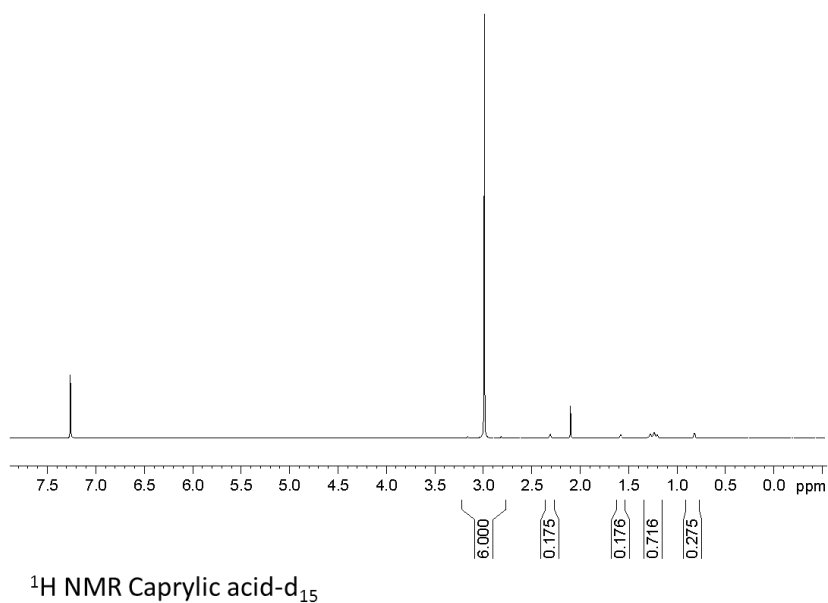


Figure SI-3.1: $^1\text{H NMR}$ (400MHz, CDCl_3 , methylsulfonylmethane as internal standard): δ_{H} 0.82 (0.275 H, br s, residual CH_3), 1.24 (0.716 H, br m, residual $4\times\text{CH}_2$), 1.58 (0.176 H, br s, residual $\underline{\text{CH}_2}\text{-(CH}_2\text{)COOH}$), 2.31 (0.175 H, br s, residual $\underline{\text{CH}_2}\text{COOH}$), 2.98 (6.000 H, s, $2\times\text{CH}_3$, internal standard).

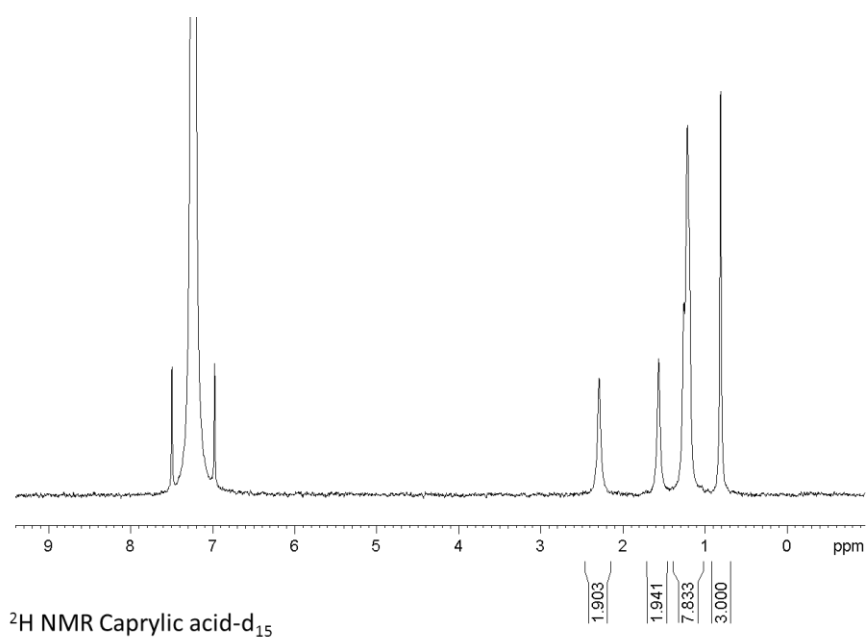


Figure SI-3.2: $^2\text{H NMR}$ (61.4 MHz, CDCl_3 , Figure SI-2): δ_{D} 0.81 (3.0D, s, CD_3), 1.21 (7.8, m, $4\times\text{CD}_2$), 1.57 (1.9D, s, $\underline{\text{CD}_2}\text{-(CD}_2\text{)COOH}$), 2.29 (1.9D, s, $\underline{\text{CD}_2}\text{COOH}$).

Isotope distribution for caprylic acid- d_{15} (ESI-MS, negative mode): 71.4% d_{15} , 22.6% d_{14} , 3.3% d_{13} (overall deuteration 98% D).

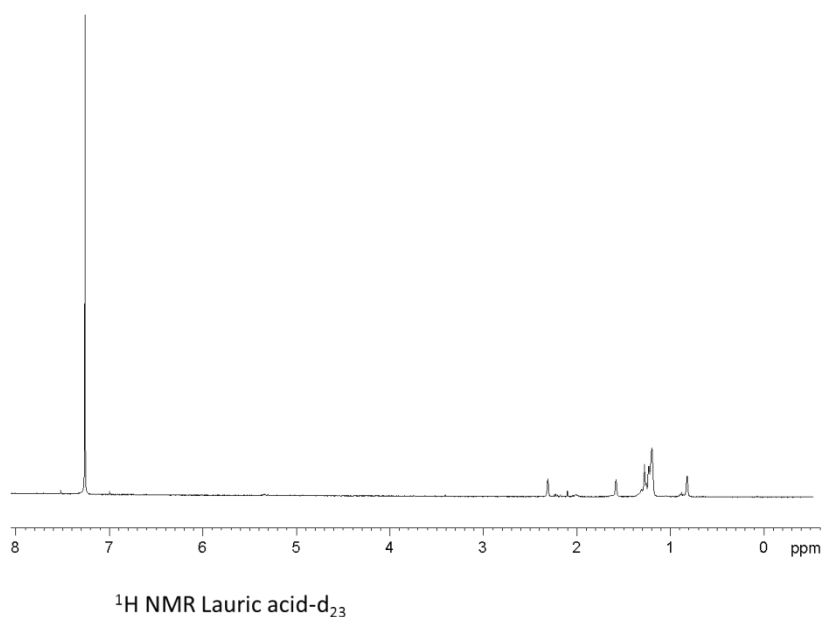


Figure SI-3.3: ^1H NMR (400MHz, CDCl_3): δ_{H} 0.82 (br s, residual CH_3), 1.23 (br m, residual $8 \times \text{CH}_2$), 1.58 (br s, residual $\underline{\text{CH}}_2\text{-(CH}_2\text{)COOH}$), 2.31 (br s, residual CH_2COOH).

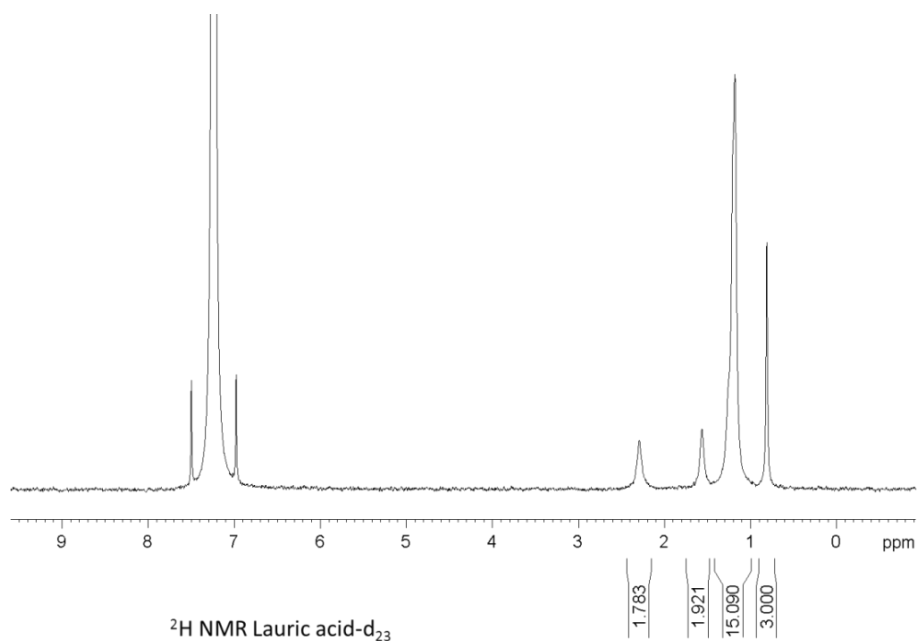


Figure SI-3.4: ^2H NMR (61.4 MHz, CDCl_3): δ_{D} 0.81 (3.0D, s, CD_3), 1.21 (15.0, m, $8 \times \text{CD}_2$), 1.57 (1.9D, s, $\underline{\text{CD}}_2\text{-(CD}_2\text{)COOH}$), 2.29 (1.7D, s, $\underline{\text{CD}}_2\text{COOH}$).

Isotope distribution lauric acid- d_{23} (ESI-MS, negative mode): 70.3% d_{23} , 24.5% d_{22} , 4.0% d_{21} , 0.7% d_{20} , 0.5% d_{19} (overall deuteration 98.4% D).

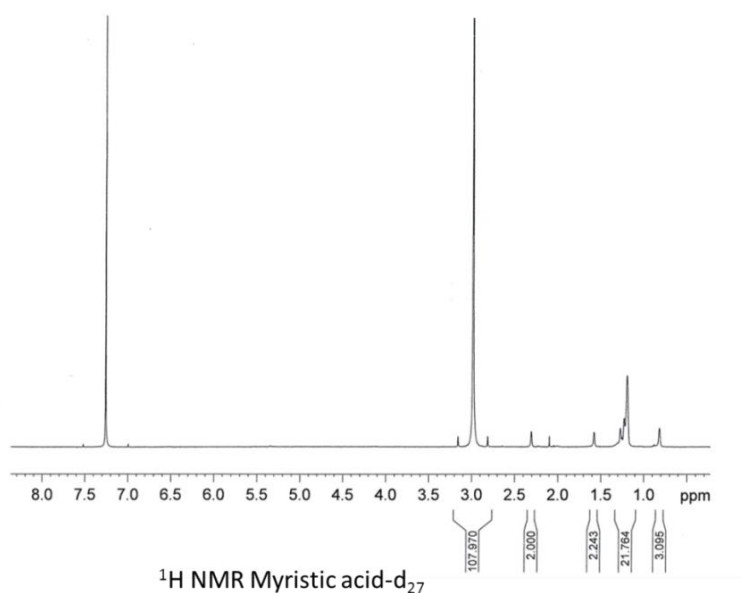


Figure SI-3.5: ^1H NMR (400MHz, CDCl_3 , methylsulfonylmethane as internal standard): δ_{H} 0.82 (0.172 H, br s, residual CH_3), 1.24 (1.209 H, br m, residual $10\times\text{CH}_2$), 1.58 (0.124 H, br s, residual $\text{CH}_2\text{-(CH}_2\text{)COOH}$), 2.32 (0.111 H, br s, residual CH_2COOH), 2.98 (6.000 H, s, $2\times\text{CH}_3$, internal standard).

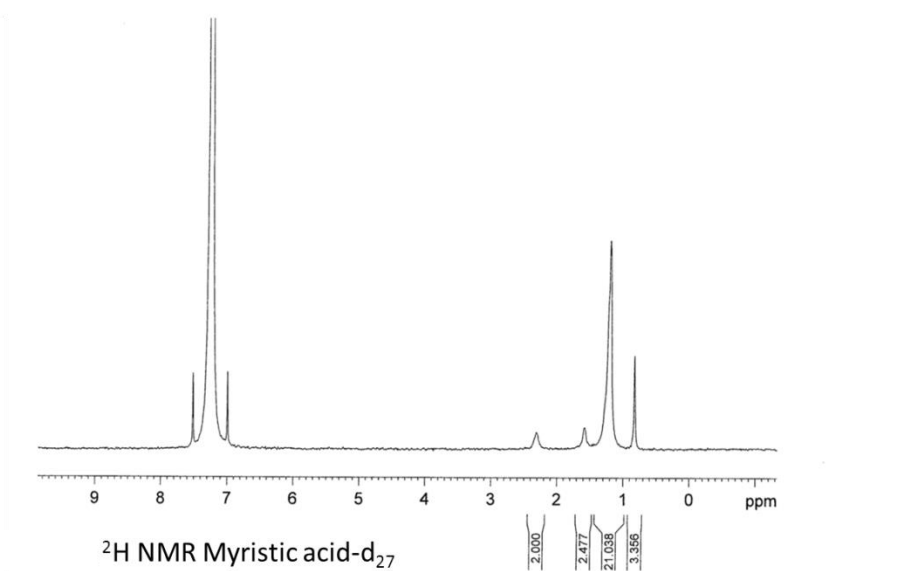


Figure SI-3.6: ^2H NMR (61.4 MHz, CDCl_3): δ_{D} 0.81 (3.3D, s, CD_3), 1.21 (21.0, m, $10\times\text{CD}_2$), 1.57 (2.4D, s, $\text{CD}_2\text{-(CD}_2\text{)COOH}$), 2.30 (2.0D, s, CD_2COOH).

Isotope distribution for myristic acid- d_{27} (ESI-MS, negative mode): 54.3% d_{27} , 34.3% d_{26} , 9.4% d_{25} , 2.1% d_{24} , (overall deuteration 97.8% D).

SAXS: Crystallinity in C_{14} system occurs at low pH

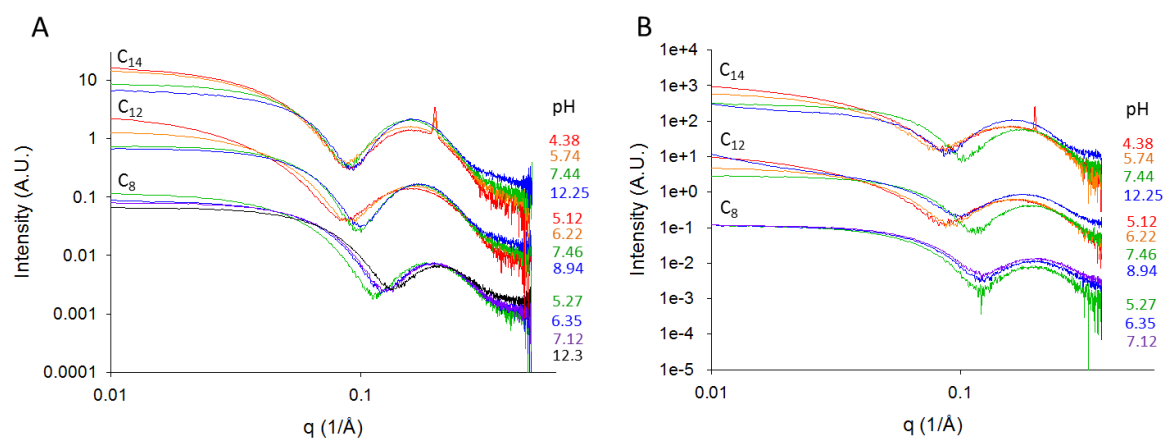


Figure SI-3.7: C_8 , C_{12} , C_{14} MG+dFA systems in D_2O BS/PL micelles at varying pH values. Increasing size was observed with increasing hydrocarbon chain length and crystallinity was present in the C_{14} system at pH 4.38 and 5.74. SAXS measurements were performed at A) 27 °C and B) 37 °C.

SANS control experiment: Bile salt micelles at varying pH values

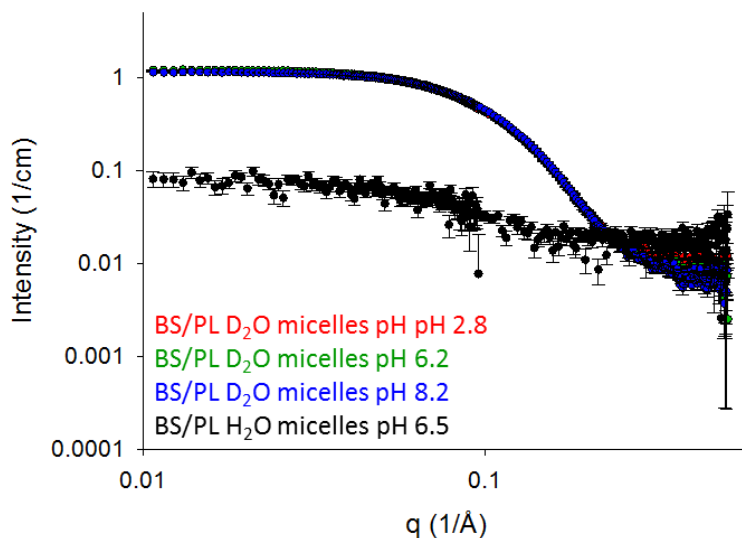


Figure SI-3.8: Shape and size of BS/PL micelles prepared in D₂O is independent of pH as indicated by SANS measurements at 27 °C (red green and blue line). The SANS curves for the BS/PL micelles in H₂O shows only a weak signal as the scattering length densities between BS, BL and H₂O are similar.

Dynamic light scattering: Correlation functions

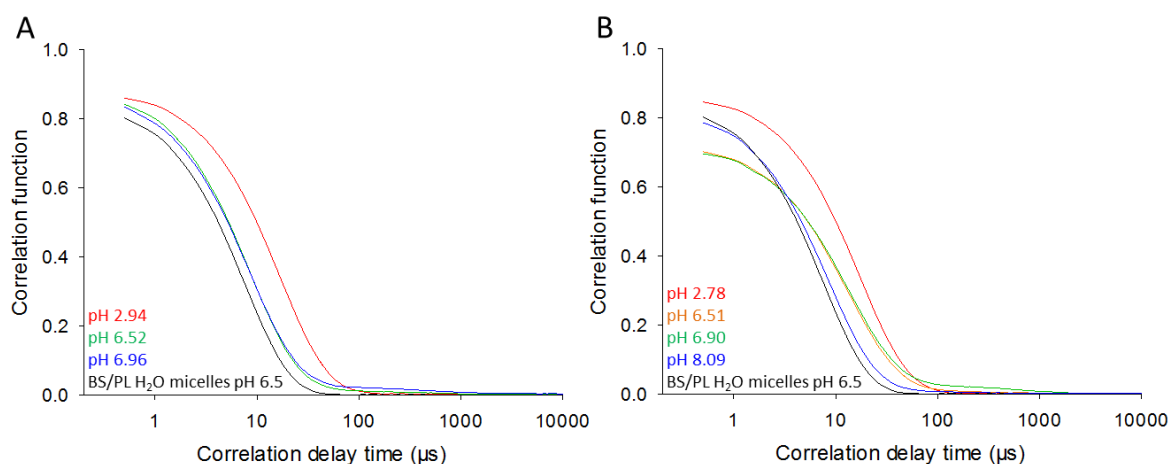


Figure SI-3.9: Intensity correlation functions from DLS for A) C₈ and B) C₁₂ MG+dFA systems in H₂O. A shift to shorter delay times (i.e. faster diffusion or smaller size) with increase in pH can be observed. The correlation functions show that the particles are rather monodisperse with one decay.

3.8 References

1. German, J.B. and Dillard, C.J., *Saturated fats: what dietary intake?* Am J Clin Nutri, 2004. **80**(3): p. 550-559.
2. Cordain, L., et al., *Origins and evolution of the Western diet: health implications for the 21st century.* Am J Clin Nutri, 2005. **81**(2): p. 341-54.
3. Cao, H.M., et al., *Identification of a lipokine, a lipid hormone linking adipose tissue to systemic metabolism.* Cell, 2008. **134**(6): p. 933-944.
4. Garaulet, M., et al., *Site-specific differences in the fatty acid composition of abdominal adipose tissue in an obese population from a Mediterranean area: Relation with dietary fatty acids, plasma lipid profile, serum insulin, and central obesity.* Am J Clin Nutri, 2001. **74**(5): p. 585-591.
5. Karki, S., et al., *The multi-level action of fatty acids on adiponectin production by fat cells.* Plos One, 2011. **6**(11).
6. Toren, P., Mora, B.C., and Venkateswaran, V., *Diet, obesity, and cancer progression: Are adipocytes the link?* Lipid Insights, 2013. **6**: p. 37-45.
7. Kossena, G.A., et al., *Separation and characterization of the colloidal phases produced on digestion of common formulation lipids and assessment of their impact on the apparent solubility of selected poorly water-soluble drugs.* J Pharm Sci, 2003. **92**(3): p. 634-648.
8. Patton, J.S. and Carey, M.C., *Watching fat digestion.* Science, 1979. **204**(4389): p. 145-148.
9. Staggers, J.E., et al., *Physical-chemical behavior of dietary and biliary lipids during intestinal digestion and absorption. 1. Phase behavior and aggregation states of model lipid systems patterned after aqueous duodenal contents of health adult human-beings.* Biochemistry, 1990. **29**(8): p. 2028-2040.
10. Rigler, M.W., Honkanen, R.E., and Patton, J.S., *Visualization by freeze fracture, in vitro and in vivo, of the products of fat digestion.* J Lipid Res, 1986. **27**(8): p. 836-57.
11. Hernell, O., Staggers, J.E., and Carey, M.C., *Physical-chemical behavior of dietary and biliary lipids during intestinal digestion and absorption. 2 Phase-analysis and aggregation states of luminal lipids during duodenal fat digestion in healthy adult human-beings.* Biochemistry, 1990. **29**(8): p. 2041-2056.
12. Hofmann, A.F. and Borgstrom, B., *Intraluminal phase of fat digestion in man: The lipid content of micellar and oil phases of intestinal content obtained during fat digestion and absorption.* J Clin Investig, 1964. **43**(2): p. 247-&.
13. Müllertz, A., et al., *Insights into intermediate phases of human intestinal fluids visualized by atomic force microscopy and cryo-transmission electron microscopy ex vivo.* Mol Pharm, 2012. **9**(2): p. 237-247.
14. Kossena, G.A., et al., *Probing drug solubilization patterns in the gastrointestinal tract after administration of lipid-based delivery systems: A phase diagram approach.* J Pharm Sci, 2004. **93**(2): p. 332-348.

Chapter 3. Disposition and Crystallization of Saturated Fatty Acid in Mixed Micelles

15. Borné, J., Nylander, T., and Khan, A., *Phase behavior and aggregate formation for the aqueous monoolein system mixed with sodium oleate and oleic acid*. Langmuir, 2001. **17**(25): p. 7742-7751.
16. Kossena, G.A., et al., *A novel cubic phase of medium chain lipid origin for the delivery of poorly water soluble drugs*. J Control Release, 2004. **99**(2): p. 217-229.
17. Gustafsson, J., et al., *Phase behavior and aggregate structure in aqueous mixtures of sodium cholate and glycerol monooleate*. J Colloid Interface Sci, 1999. **211**(2): p. 326-335.
18. Müller, K., *Structural aspects of bile salt-lecithin mixed micelles*. Hepatology, 1984. **4**(5): p. S134-S137.
19. Long, M.A., Kaler, E.W., and Lee, S.P., *Structural characterization of the micelle-vesicle transition in lecithin-bile salt-solutions*. Biophys J, 1994. **67**(4): p. 1733-1742.
20. Luk, A.S., Kaler, E.W., and Lee, S.P., *Structural mechanisms of bile salt-induced growth of small unilamellar cholesterol - Lecithin vesicles*. Biochemistry, 1997. **36**(19): p. 5633-5644.
21. Monte, M.J., et al., *Bile acids: Chemistry, physiology, and pathophysiology*. World J Gastroenterol, 2009. **15**(7): p. 804-816.
22. Carey, M.C. and Small, D.M., *The characteristics of mixed micellar solutions with particular reference to bile*. Am J Med, 1970. **49**(5): p. 590-608.
23. Hofmann, A.F. and Borgstrom, B., *Physico-chemical state of lipids in intestinal content during their digestion and absorption*. Fed Proc, 1962. **21**(1): p. 43-&.
24. Hofmann, A.F., *Function of bile salts in fat absorption - Solvent properties of dilute micellar solutions of conjugated bile salts*. Biochemical Journal, 1963. **89**(1): p. 57-&.
25. Kossena, G.A., et al., *Influence of the intermediate digestion phases of common formulation lipids on the absorption of a poorly water-soluble drug*. J Pharm Sci, 2005. **94**(3): p. 481-492.
26. Pouton, C.W., *Formulation of poorly water-soluble drugs for oral administration: Physicochemical and physiological issues and the lipid formulation classification system*. Eur J Pharm Biopharm, 2006. **29**(3-4): p. 278-287.
27. Porter, C.J.H., Trevaskis, N.L., and Charman, W.N., *Lipids and lipid-based formulations: Optimizing the oral delivery of lipophilic drugs*. Nat Rev Drug Discov, 2007. **6**(3): p. 231-248.
28. German, J.B. and Dillard, C.J., *Saturated fats: what dietary intake?* American Journal of Clinical Nutrition, 2004. **80**(3): p. 550-559.
29. Bockisch, M., *Fats and oils handbook*, 1998, AOCS Press.
30. Bracco, U., *Effect of triglyceride structure on fat absorption*. Am J Clin Nutri, 1994. **60**(6 Suppl): p. 1002S-1009S.
31. Small, D.M., *The effects of glyceride structure on absorption and metabolism* Annu Rev Nutr, 1991. **11**: p. 413-434.
32. Fallingborg, J., *Intraluminal pH of the human gastrointestinal tract*. Dan Med Bull, 1999. **46**(3): p. 183-196.

33. Israelachvili, J.N., Mitchell, D.J., and Ninham, B.W., *Theory of self-assembly of hydrocarbon amphiphiles into micelles and bilayers*. J Chem Soc Faraday Trans II, 1976. **72**: p. 1525-1568.
34. Salentinig, S., Sagalowicz, L., and Glatter, O., *Self-assembled structures and pK(a) value of oleic acid in systems of biological relevance*. Langmuir, 2010. **26**(14): p. 11670-11679.
35. Salentinig, S., et al., *Formation of highly organized nanostructures during the digestion of milk*. ACS Nano, 2013. **7**(12): p. 10904-10911.
36. Salentinig, S., et al., *pH-responsive micelles based on caprylic acid*. Langmuir, 2014. **30**(25): p. 7296-303.
37. Aron-Wisnewsky, J., Dore, J., and Clement, K., *The importance of the gut microbiota after bariatric surgery*. Nat Rev Gastroenterol Hepatol, 2012. **9**(10): p. 590-598.
38. Lee, K.W.Y., Porter, C.J.H., and Boyd, B.J., *The effect of administered dose of lipid-based formulations on the in vitro and in vivo performance of cinnarizine as a model poorly water-soluble drug*. J Pharm Sci, 2013. **102**(2): p. 565-578.
39. Porter, C.J.H., et al., *Use of in vitro lipid digestion data to explain the in vivo performance of triglyceride-based oral lipid formulations of poorly water-soluble drugs: Studies with halofantrine*. J Pharm Sci, 2004. **93**(5): p. 1110-1121.
40. Sek, L., Porter, C.J.H., and Charman, W.N., *Characterisation and quantification of medium chain and long chain triglycerides and their in vitro digestion products, by HPTLC coupled with in situ densitometric analysis*. J Pharm Biomed Anal, 2001. **25**(3-4): p. 651-661.
41. Kaukonen, A.M., et al., *Drug solubilization behavior during in vitro digestion of simple triglyceride lipid solution formulations*. Pharm Res, 2004. **21**(2): p. 245-253.
42. Hofmann, A.F., *Molecular association in fat digestion: Interaction in bulk of monoolein, oleic acid, and sodium oleate with dilute, micellar bile salt solutions*. Adv Chem Ser, 1968(84): p. 53-&.
43. Kleberg, K., et al., *Biorelevant media simulating fed state intestinal fluids: Colloid phase characterization and impact on solubilization capacity*. J Pharm Sci, 2010. **99**(8): p. 3522-3532.
44. Fatouros, D.G., et al., *Colloidal structures in media simulating intestinal fed state conditions with and without lipolysis products*. Pharm Res, 2009. **26**(2): p. 361-374.
45. Kalantzi, L., et al., *Canine intestinal contents vs. simulated media for the assessment of solubility of two weak bases in the human small intestinal contents*. Pharm Res, 2006. **23**(6): p. 1373-1381.
46. Persson, E.M., et al., *The effects of food on the dissolution of poorly soluble drugs in human and in model small intestinal fluids*. Pharm Res, 2005. **22**(12): p. 2141-2151.
47. Gilbert, E.P., Schulz, J.C., and Noakes, T.J., *'Quokka' - The small-angle neutron scattering instrument at OPAL*. Phys B, 2006. **385-86**: p. 1180-1182.
48. Svergun, D.I. and Koch, M.H.J., *Small-angle scattering studies of biological macromolecules in solution*. Rep Prog Phys, 2003. **66**(10): p. 1735-1782.
49. Kirby, N.M., et al., *A low-background-intensity focusing small-angle X-ray scattering undulator beamline*. J Appl Crystallogr, 2013. **46**: p. 1670-1680.

Chapter 3. Disposition and Crystallization of Saturated Fatty Acid in Mixed Micelles

50. Koppel, D.E., *Analysis of macromolecular polydispersity in intensity correlation spectroscopy - Method of cumulants*. J Chem Phys, 1972. **57**(11): p. 4814-4820.
51. Shah, D.O., *Micelles, microemulsions, and monolayers: Quarter century progress at the University of Florida*. Micelles, Microemulsions, and Monolayers (Int Symp), ed. Shah, D.O. 1998. 1-52.
52. Prajapati, H.N., Dalrymple, D.M., and Serajuddin, A.T.M., *A comparative evaluation of mono-, di- and triglyceride of medium chain fatty acids by lipid/surfactant/water phase diagram, solubility determination and dispersion testing for application in pharmaceutical dosage form development*. Pharm Res, 2012. **29**(1): p. 285-305.
53. Maji, S.K. and Haldar, S., *Effect of peptide architecture on the self-assembly properties of tripeptide based anionic surfactants issued from two different peptide sequences: Ala-Ala-Val and Ala-Pro-Val in aqueous media (pH 7.4)*. Colloid Surface A, 2012. **414**: p. 422-432.

**Chapter 4. How Relevant Are Assembled
Equilibrium Samples in Understanding
Structure Formation during Lipid
Digestion?**

Chapter 4. How Relevant Are Assembled Equilibrium Samples in Understanding Structure Formation during Lipid Digestion?

The work presented in this chapter has been published as: Phan S., Salentinig S., Hawley A., Boyd B.J., *How relevant are assembled equilibrium samples in understanding structure formation during lipid digestion?* Eur J Pharm Biopharm, 2015 (published online 23/07/15, DOI:10.1016/j.ejpb.2015.07.015).

4.1 Declaration

Declaration by candidate:

In the case of Chapter 4, the nature and extent of my contribution to the work was the following:

Nature of contribution	Extent of contribution
Research design, performance of data collection and analysis, manuscript preparation	85%

The following co-authors contributed to the work:

Name	Nature of contribution
Stefan Salentinig	Input into manuscript preparation
Adrian Hawley	Intellectual input on SAXS operation
Ben J. Boyd	Supervision, intellectual input, input into manuscript preparation

The undersigned hereby certify that the above declaration correctly reflects the nature and extent of the candidate's and co-authors' contributions to this work.

Candidate's signature:



Date: 21/08/15

Main supervisor's signature:



Date: 21/08/15

4.2 How Relevant Are Assembled Equilibrium Samples in Understanding Structure Formation during Lipid Digestion?

Stephanie Phan ¹, Stefan Salentinig ¹, Adrian Hawley ², Ben J. Boyd ¹

¹Monash Institute of Pharmaceutical Sciences, Monash University, 381 Royal Parade, Parkville, VIC 3052, Australia

² SAXS/WAXS beamline, Australian Synchrotron, 800 Blackburn Road, Clayton, VIC 3168, Australia

Received 1st May 2015 and published online 23rd July 2015

Citation: Eur. J. Pharm. Biopharm. (2015) 96:117-124

DOI: 10.1016/j.ejpb.2015.07.015

Keywords: lipid digestion, in vitro lipolysis, lipid-based drug delivery, small angle X-ray scattering, high performance liquid chromatography

Abstract

Lipid-based formulations are gaining interest for use as drug delivery systems for poorly water-soluble drug compounds. During digestion, the lipolysis products self-assemble with endogenous surfactants in the gastrointestinal tract to form colloidal structures, enabling enhanced drug solubilisation. Although earlier studies in the literature focus on assembled equilibrium systems, little is known about structure formation under dynamic lipolysis conditions. The purpose of this study was to investigate the likely colloidal structure formation in the small intestine after the ingestion of lipids, under equilibrium and dynamic conditions. The structural aspects were studied using small angle X-ray scattering and dynamic light scattering, and were found to depend on lipid composition, lipid chain length, prandial state and emulsification. Incorporation of phospholipids and lipolysis products into bile salt

micelles resulted in swelling of the structures. At insufficient bile salt concentrations, a co-existing lamellar phase was observed, due to a reduction in the solubilisation capacity for lipolysis products. Emulsification accelerated the rate of lipolysis and structure formation.

4.3 Introduction

Poorly water-soluble compounds dominate the number of newly-discovered drug molecules and require formulation approaches to enable oral delivery. For poorly water-soluble compounds, lipid formulations are increasingly seen as a potential formulation approach. The digestion of triglycerides in the gastrointestinal tract generates fatty acids and monoglycerides. These species combine with bile salts (BS) and phospholipid (PL) present in the small intestine, to generate colloidal aggregates such as mixed micelles and vesicles. Hydrophobic molecules such as dietary lipids, drugs and lipophilic vitamins can be solubilised into these structures, thereby increasing their solubility in the aqueous environment, for enhanced absorption and bioavailability.

The colloidal aspects of digestion of lipid formulations has received less attention due to a lack of methods to study structure formation during digestion in real-time. Consequently, formulation design is largely based on drug solubility in the formulation and not in the pre-absorptive colloidal milieu, meaning that these compounds are likely sub-optimally formulated. Thus a better understanding of the colloidal make-up in the gastrointestinal tract during digestion should assist in formulation design.

Past work in examining phase behaviour in digesting lipid systems has involved the mixing of medium- and long-chain lipid digestion products and endogenous amphiphilic molecules with water and bile salts [1-6]. These studies vary in the composition of guest molecules, osmotic pressure and pH conditions to simulate conditions in the small intestine. The structure in the resulting mixtures has been interrogated using techniques such as cryogenic transmission electron microscopy, freeze fracture electron microscopy, cross polarised light microscopy, small angle X-ray scattering, microscopy [7], where colloidal structure and size depend on lipid composition.

Whilst equilibrium studies provide a basis for understanding intermolecular interactions during lipolysis under controlled conditions, they potentially only provide a snapshot of the

structure at a given time during a highly dynamic process. In addition, the assumption with equilibrium studies is that the structure in digesting systems is only dictated by composition at that point in time, and that structures are not exposed to non-equilibrium effects such as gastric and intestinal motility, dilution and digestion reactions. *In vitro* lipolysis models have been developed which aim to better mimic *in vivo* conditions, and are capable of following the kinetics of digestion by determining the free fatty acid composition of digesting lipid media. Recent studies have utilised this model combined with synchrotron small angle X-ray scattering to enable the changes in nanostructure during lipid digestion to be elucidated in real-time [8, 9]. However, to the best of our knowledge, no studies exist which compare the two approaches, therefore the purpose of this study was to examine the structures formed at equilibrium, for a series of triglycerides of increasing chain length, compared with the composition and structures formed under non-equilibrium digestion conditions.

The increased complexity of the dynamic approach take into account variation in lipid composition due to digestion reactions and intestinal mobility, and it is envisioned that they will add to the current understanding of structure formation under more *in vivo* relevant conditions. This will be critical in progressing empirical formulation of lipid-based drug delivery systems to rational design.

4.4 Experimental

Materials

Tris maleate (reagent grade), bile salt (sodium taurodeoxycholate >95%), monocaprylin (C₈ monoglyceride, approx. 99%), monolaurin (C₁₂ monoglyceride, 99%), monoolein (C_{18:1} monoglyceride, 99%), caprylic acid (C₈ fatty acid, >99% by capillary gas chromatography), lauric acid (C₁₂ fatty acid, >99.5%), myristic acid (C₁₄ fatty acid, >99%) oleic acid (C_{18:1} fatty acid, >99%), tricaprylin (C₈ triglyceride, >99%), tripalmitin (C₁₆ triglyceride, >99%), and triolein (C_{18:1} triglyceride, >97% TLC) were purchased from Sigma Aldrich (St. Louis, MO, USA). Tricaprin (C₁₀ triglyceride, 98%), trilaurin (C₁₂ triglyceride, 98%) and trimyristin (C₁₄ triglyceride, 99%) were obtained from TCI Co. Ltd (Kawaguchi, Saitama, Japan). Phospholipid (dioleoylphosphatidyl choline, DOPC, >94%) was obtained from Trapeze Associates Pty Ltd. (Clayton, Victoria, Australia). Pancreatin extract was purchased from Southern Biologicals (Nunawading, Victoria, Australia) and had USP grade pancreatin activity.

Chapter 4. How Relevant Are Assembled Equilibrium Samples in Understanding Structure Formation during Lipid Digestion?

Calcium chloride (>99%) was obtained from Ajax Finechem (Seven Hills, NSW, Australia). Sodium chloride (>99%) was purchased from Chem Supply (Gillman, SA, Australia). Sodium azide was purchased from Merck Schuchardt OHG (Eduard-Buchner-StraÙe, Hohenbrunn, Germany). Water used was sourced from a Millipore water purification system using a Quantum™ EX Ultrapure Organex cartridge (Millipore, Australia).

Preparation of equilibrium samples

Simulated intestinal fluid was prepared using bile salt (BS, sodium taurodeoxycholate) and phospholipid (PL, DOPC) concentrations at a ratio of 5 mM:1.25 mM (fasted) and 20 mM:5 mM (fed), in digestion buffer pH 6.5 (50 mM Tris maleate, 150 mM NaCl, 5 mM CaCl₂·2H₂O, 6 mM NaN₃ as an antibacterial agent) [10-13]. The mean values and 4:1 BS:PL ratio represent intestinal contents after digestion [14, 15]. The PL was weighed into a round bottom flask and dissolved in chloroform which was subsequently evaporated to produce a thin film of PL. BS and digestion buffer were added, and the PL and BS were dispersed in a sonicator bath for 30 min. Equilibrium samples simulating the gastrointestinal state on digestion of triolein (C_{18:1} triglyceride), trilaurin (C₁₂ triglyceride) and tricaprylin (C₈ triglyceride) were prepared by adding monoglycerides (monoolein, monolaurin and monocaprylin) and fatty acids (oleic acid, lauric acid and caprylic acid) of the corresponding lipid chain length to simulated intestinal fluid, followed by tip sonication (Misonix, New York) for 30 s at 100 W.

Lipolysis model and *in vitro* lipolysis

In vitro digestion studies were performed using a pH-stat auto titrator (Radiometer, Copenhagen, Denmark), similar to previous reports [8, 13, 16, 17]. Lipids were added to 9 mL of the fasted or fed simulated intestinal fluid in the thermostatted digestion vessel at 37 °C at pH 6.5.

The lipid was introduced to the BS/PL micelles in two forms, in a pre-dispersed emulsion form in the micellar media, where the emulsion was formed by tip sonication (Misonix, New York) for 30 s at 100 W, or as a non-dispersed oil added directly to the BS/PL micelles as a bolus load and magnetically stirred. The sample was added to a thermostated vessel at 37 °C via water bath and magnetically stirred for 5 min for complete mixing and thermal equilibration and the pH was adjusted to 6.500 ± 0.003 , chosen as a compromise between the

optimum for pancreatic lipase activity pH (6 – 10) [18] and duodenal pH (5.0 – 6.5) [19]. On addition of pancreatin (7000 TBU/1 mL) the pH-stat titrated the digestion mixture with 0.2 M NaOH in order to maintain constant pH accounting for the free fatty acid products. Digestion was allowed to proceed for 30 min, in which the degree of enzymatic digestion of the lipid was reflected in the volume of NaOH used to neutralize the fatty acids. A blank digestion without lipid but with BS/PL micelles present was performed as a background experiment, to account for fatty acids that were produced from PLs and was subtracted from the profiles for the lipolysis experiments.

Synchrotron small angle X-ray scattering (SAXS) and flow-through *in vitro* lipolysis

SAXS measurements were performed on the SAXS/WAXS beamline [20] at the Australian Synchrotron. For equilibrium studies, samples were placed in 1.5 mm glass capillaries and inserted into a 37 °C thermostatted metal heating block controlled by a water bath accurate to ± 0.1 °C. An X-ray beam with a wavelength of 1.1271 Å (11 keV) was selected. The sample to detector distance was 1015 mm, covering a q -range of 0.014 – 0.65 Å⁻¹. The 2D SAXS patterns were collected using a Pilatus 1M detector (active area 169 × 179 mm² with a pixel size of 172 μm). Calibration was performed using silver behenate. The scattering pattern was converted to a plot of intensity versus length of the scattering vector, q , using the equation $q = (4\pi/\lambda)\sin(\theta/2)$ [21]. The d-spacing of the lamellar phase was calculated using the equation $d = 2\pi/q$ where q was the location of the first order lamellar peak. Buffer scattering was subtracted from all data.

To monitor changes in nanostructure in real-time during digestion, the digestion vessel was fitted with silicone tubing (total volume <1 mL) to enable continuous flow of the digestion medium via peristaltic pump at a rate of 10 mL/min, through a 1.5 mm diameter quartz capillary. The capillary was fixed in the X-ray beam. A remotely operated syringe driver was used to deliver 1 mL of pancreatin extract over several seconds into the vessel to initiate digestion. A 5 s acquisition time per 30 s for up to 60 min was used to yield the required information in flow through mode depending on the kinetics of digestion. The computer software ScatterBrain Analysis [20] was used to acquire and reduce 2D patterns to 1D curves.

Dynamic light scattering (DLS)

DLS measurements were performed on a Malvern Zetasizer NanoZS to determine the hydrodynamic radius (R_H) and particle size distribution. Samples were centrifuged for 5 min at 3500 rpm prior to the measurement to remove any trace dust particles. A laser power of 4 mW was used at a back scattering angle of 173° at room temperature. The average diffusion coefficient, D , was obtained by the cumulant analysis of the correlation functions [22]. The mean hydrodynamic radius R_H was deduced from the diffusion coefficient using the Stokes–Einstein equation:

$$R_H = \frac{k_B T}{6\pi\eta D}$$

where k_B is the Boltzmann constant, T the absolute temperature and η the viscosity of the solvent. The polydispersity index (PDI) of the size distribution was determined from the second cumulant:

$$PDI = \frac{\mu_2}{\bar{\Gamma}^2}$$

where μ_2 is the second cumulant and $\bar{\Gamma}$ the mean of the inverse decay time.

High performance liquid chromatography (HPLC)

HPLC with refractive index detection was employed to separate and quantify fatty acids during digestion for correlation with total fatty acid produced as indicated by the pH titration, as previously described [23].

4.5 Results

Structures formed in equilibrium systems

The equilibrium structures present in BS and BS/PL mixed micelles representing fasted and fed simulated intestinal fluids were studied using SAXS (Figure 4.1). The addition of PL to the BS micelles resulted in an increase in the size of the BS micelles, as indicated by a shift in the local minimum in q at approximately $0.05 < q < 0.08 \text{ \AA}^{-1}$ (indicated by the arrow in Figure 4.2). The size of the fed micelles was smaller than the corresponding fasted system. These trends

were confirmed with dynamic light scattering measurements (Table 4.1), and the correlation functions are presented in Figure SI-4.1.

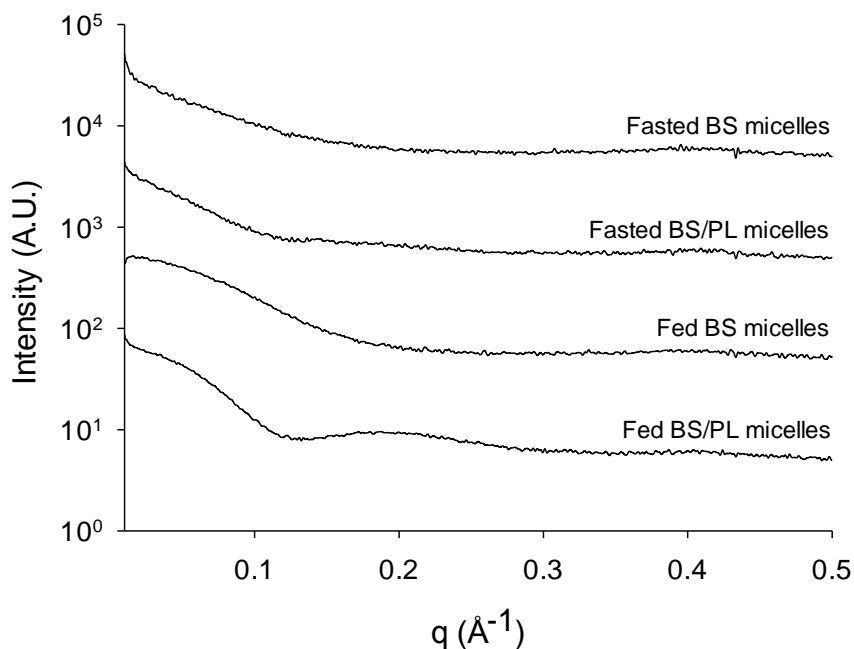


Figure 4.1: SAXS profiles for fasted BS (5 mM NaTDC) and BS/PL (5 mM NaTDC:1.25 mM DOPC) micelles, and fed BS (20 mM NaTDC) and BS/PL (20 mM NaTDC:5 mM DOPC) micelles, prepared in digestion buffer pH 6.5.

Table 4.1: Summary of hydrodynamic radius and PDI for fasted and fed BS and BS/PL micelles from DLS measurements.

Sample	Radius (nm)	PDI
Fasted BS micelles	2.5 ± 1.2	0.23
Fasted BS/PL micelles	4.3 ± 1.5	0.30
Fed BS micelles	2.4 ± 0.9	0.11
Fed BS/PL micelles	2.8 ± 1.0	0.18

Influence of the addition of lipolysis products on the structure of mixed bile salt micelles

SAXS measurements were performed on BS/PL mixed micelles upon the addition of the monoglyceride and fatty acid in a 1:2 molar ratio. These systems reflected the endpoint of digestion of triolein ($C_{18:1}$), trilaurin (C_{12}) and tricaprylin (C_8), where the chain lengths were selected to represent long, medium and short chain TGs respectively.

For the systems containing $C_{18:1}$ and C_{12} lipolysis products, the monoglyceride (MG) and fatty acids (FA) were incorporated into the fed state BS/PL micelles (Figure 4.2 and 4.3), with no evidence of any co-existing lamellar phase. However, in the fasted systems, a co-existing lamellar phase was formed in the $C_{18:1}$ system at the higher concentrations (MG:FA = 10:20 mM and 15:30 mM) with d-spacing of 47.5 Å, indicating a limit of solubilisation of the MG and FA between 5:10 and 10:20 mM. The lamellar phase was present in the fasted state for the C_{12} systems at all concentrations with d-spacing of 34.6 Å, indicating a solubilisation limit less than the 5:10 mM level.

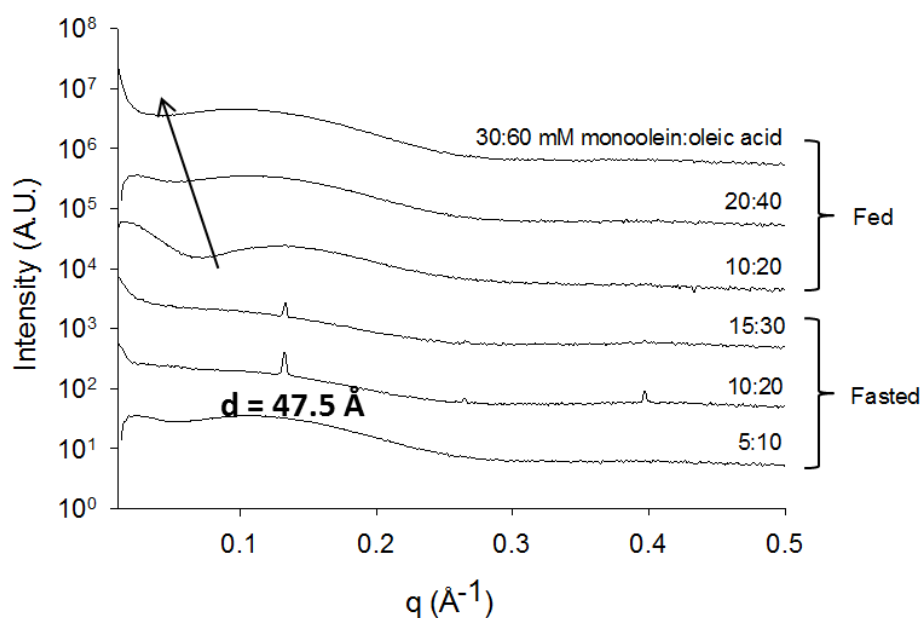


Figure 4.2: SAXS profiles of fasted and fed BS/PL mixtures with $C_{18:1}$ lipolysis products (monoolein:oleic acid) in the 1:2 mol ratio. The arrow indicates the decreasing q value for the minimum in the micellar scattering profiles, which indicates increasing size of micelles.

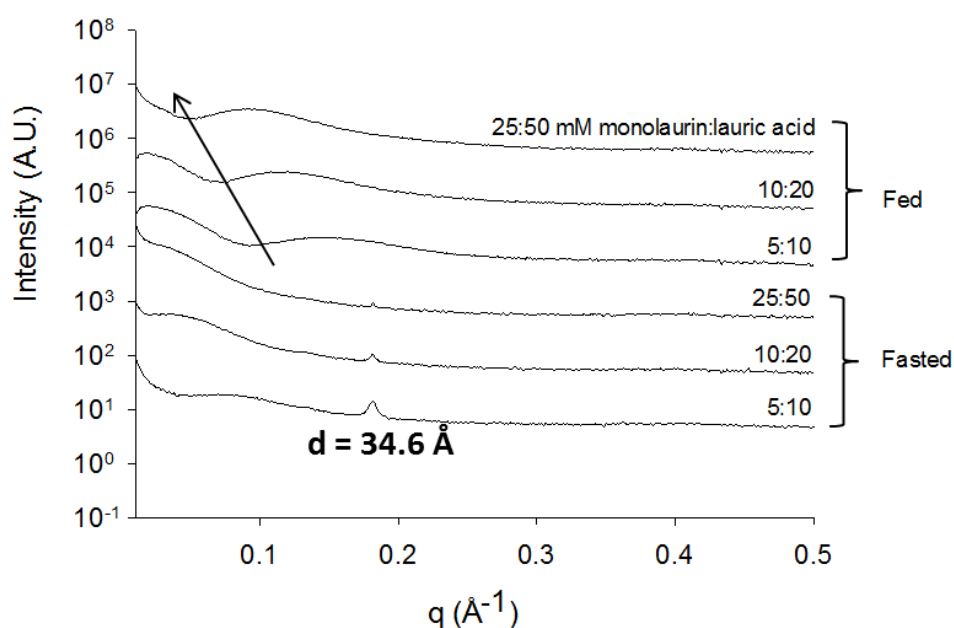


Figure 4.3: SAXS profiles of fasted and fed state BS/PL mixtures with C_{12} lipolysis products (monolaurin:lauric acid) in the 1:2 mol ratio. The arrow indicates the decreasing q value for the minimum in the micellar scattering profiles, which indicates increasing size of micelles.

In contrast to the $C_{18:1}$ and C_{12} systems, in the system containing 25:50 mM C_8 lipolysis products, a co-existing lamellar phase with a d-spacing of 29.6 \AA was present under both the fasted and fed conditions (Figure 4.4). As with the medium and longer chain systems, with increasing lipid loading, a shift in the local minimum in q at approximately $0.05 < q < 0.08 \text{ \AA}^{-1}$ (indicated by the arrow in Figure 4.4) occurred, indicating micelles formed with larger dimensions. This observation was confirmed with dynamic light scattering measurements (Table SI-4.1), and the correlation functions are presented in Figure SI-4.2.

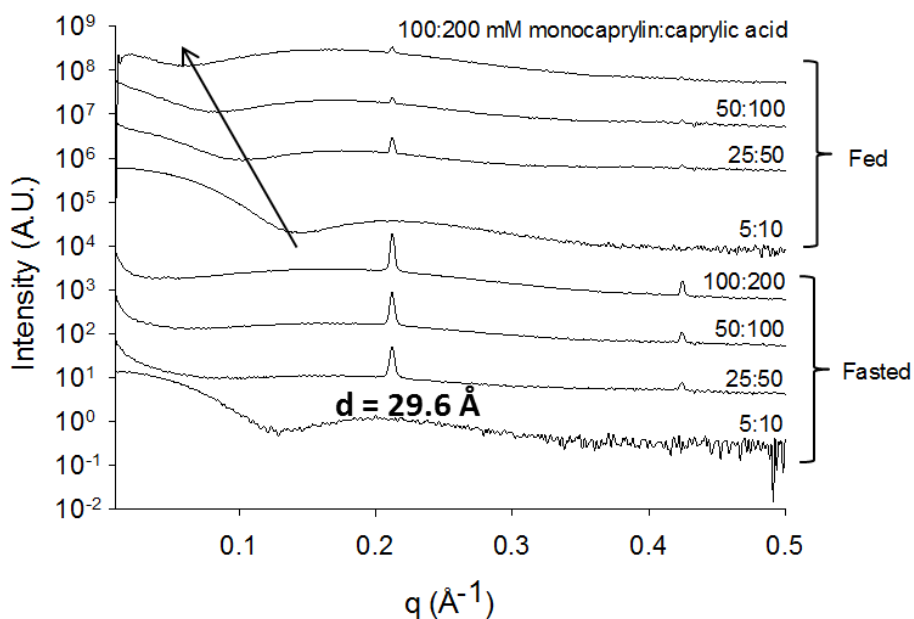


Figure 4.4: SAXS profiles of fasted and fed state BS/PL mixtures with C_8 lipolysis products (monocaprylin:caprylic acid) in the 1:2 mol ratio.

Structures formed during dynamic *in vitro* lipolysis

Dependence of lipid loading on structure formation during digestion of tricaprylin

The dependence of structure formation on the mass of lipid to be digested was examined during *in vitro* lipolysis of C_8 TG (Figure 4.5). Digestion of low lipid mass (5 mM) C_8 TG in fasted and fed states as bolus load and as an emulsion revealed no further structure formation from the mixed micelles that were initially present. At high lipid (50 mM) in both the fasted and fed state, a co-existing lamellar phase ($d=25.0 \text{ \AA}$) was present after 12 min at 40% digestion. The 50 mM digestion in the fasted state was repeated to enable sampling to quantify fatty acid liberated using HPLC. A strong correlation between the moles of fatty acid was found by pH stat titration and HPLC methods (Figure 4.5G).

Chapter 4. How Relevant Are Assembled Equilibrium Samples in Understanding Structure Formation during Lipid Digestion?

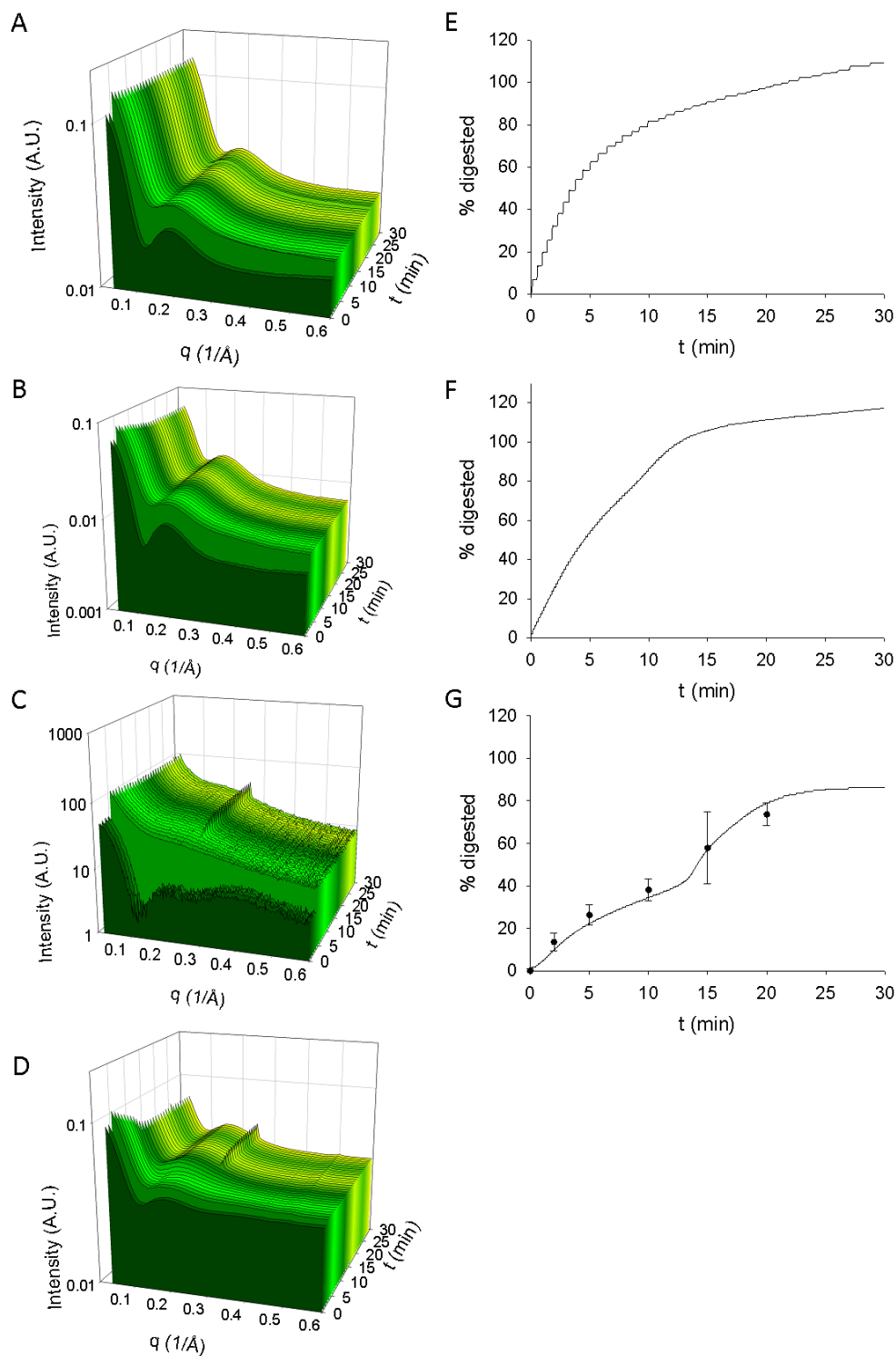


Figure 4.5: Digestion of A) 5 mM fed state and B) 25 mM fed state C) 50 mM fasted state D) 50 mM fed state C_8 TG as a bolus over 30 min at 37 °C studied by time-resolved SAXS (left) and the corresponding fatty acid content (right) by pH stat titration (line) and HPLC (closed circles, mean \pm range, $n=2$).

Effect of lipid chain length, prandial state (bile salt concentration) and emulsification on structure formation

In vitro digestions were performed for a series of triglycerides with a fixed concentration of lipid in the digest (5 or 50 mM) to determine the influence of lipid chain length and the oil/BS ratio on the resultant structures.

At fed state bile salt levels (20 mM), vesicles and micelles were observed due to an increase in hydrophilicity of the interface and a decrease in the critical packing parameter. Digestion of low concentration of short chain triglycerides revealed the presence of mixed micelles only, whereas triglycerides with carbon length $\geq C_{10}$ formed a co-existing lamellar phase even at low lipid loading. Triglycerides of chain lengths $\geq C_{12}$ are more hydrophobic than C_8 and C_{10} , and have melting points above physiological temperature [1, 24]. Hence these lipids were dispersed in the mixed micelles by tip sonication to form an emulsion prior to lipolysis experiments.

During *in vitro* digestion of 50 mM Captex 355 (~250 mg) as a bolus load in the fed state, time-resolved SAXS measurements revealed the formation of a lamellar peak after 15 min which was correlated with a change in the digestion kinetics as evident from the kink in the titration profile (Figure 4.6A).

When the lipid was presented as an emulsion prior to lipolysis, the rate of lipolysis increased such that the lamellar phase formed within several minutes due to rapid digestion of the triglyceride. The rapid digestion kinetics is indicated by the rapid titration of the sample with NaOH and subsequent plateau (Figure 4.6B).

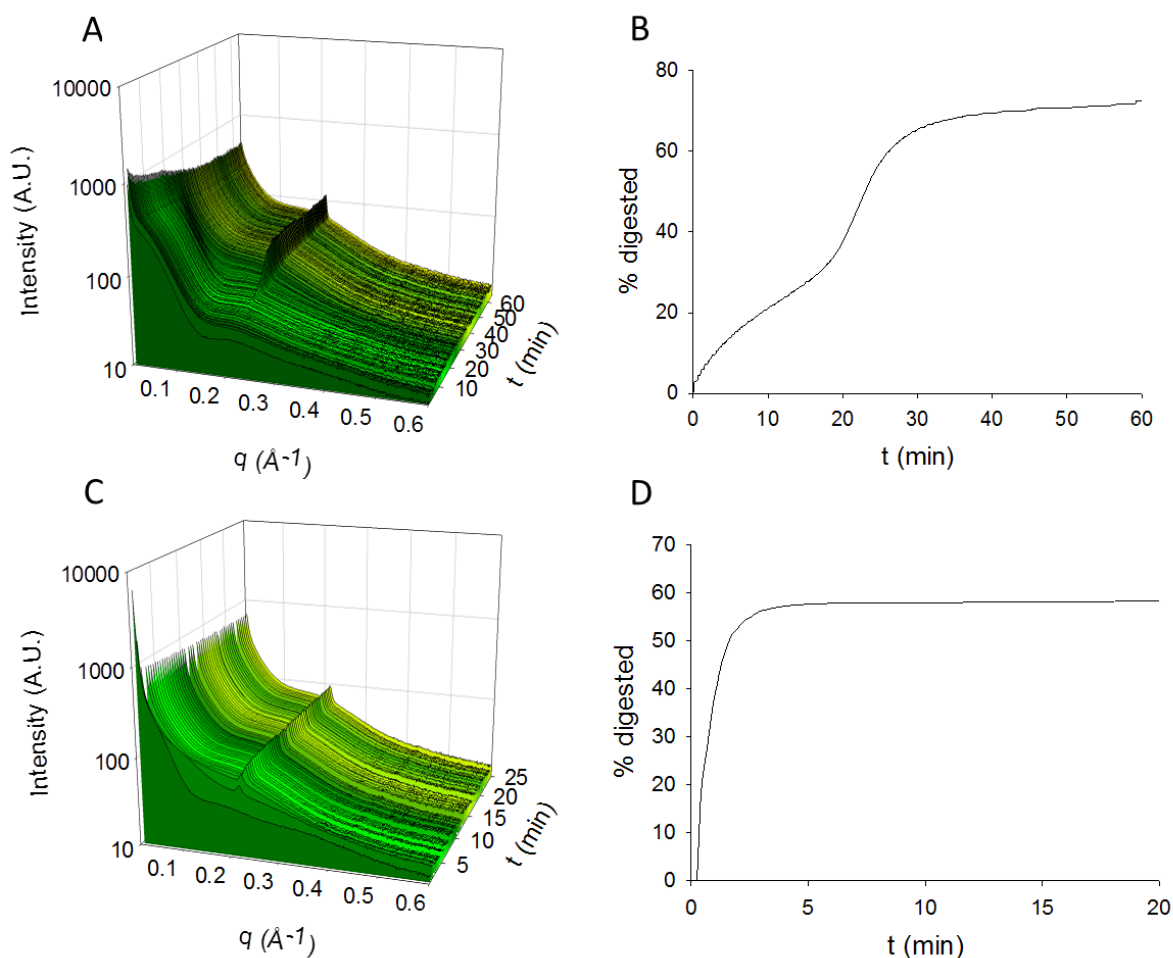


Figure 4.6: Digestion of 50 mM Captex 355 (approx. 250 mg) as a bolus (A) vs. emulsified (B) in the fed state over 60 and 20 min at 37 °C studied by time-resolved SAXS (left) and the corresponding titration profiles (right).

After emulsification, medium and long chain triglycerides existed in the crystalline form prior to initiation of lipolysis, unless emulsions were stored above their melting point to maintain a supercooled state. Digestion of C_{12} TG showed lamellar phase before digestion at low lipid mass (5 mM) in fasted and fed states as a bolus ($d=34.9 \text{ \AA}$) where the intensity of the peak increased during digestion. When the same systems were pre-emulsified, initially an emulsified microemulsion was present, rather than a lamellar phase, and after lipase addition a lamellar phase formed ($d=34.9 \text{ \AA}$) (Figure 4.7).

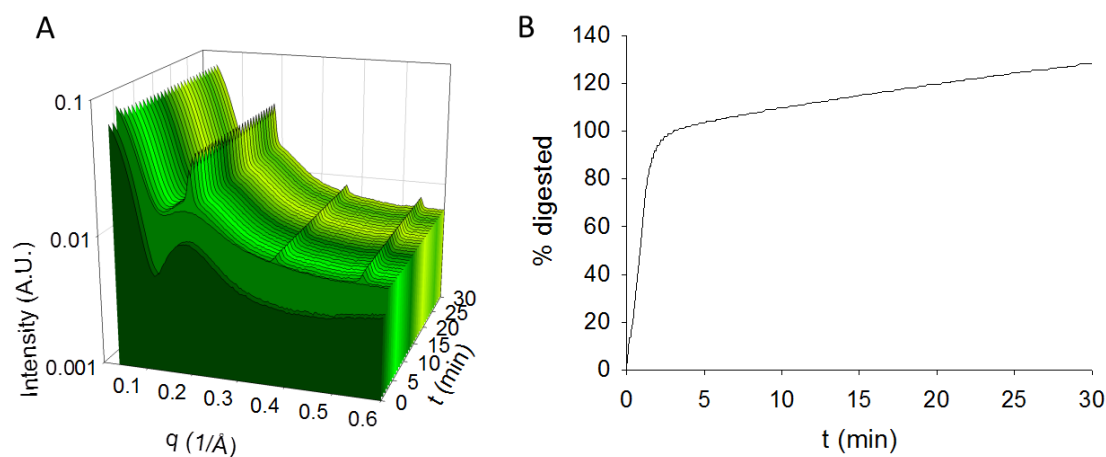


Figure 4.7: Digestion of 5 mM C_{12} TG as an emulsion in the fed state over 30 min at 37 °C studied by time-resolved SAXS (left) and the corresponding titration profile (right).

DSC measurements showed that C_{14} TG emulsions prepared at 70 °C and stored at 37 °C for 24 hr existed in the supercooled state (Figure SI-4.3). During *in vitro* lipolysis, an emulsified microemulsion was present initially, and a lamellar phase formed during lipolysis ($d=39.8$ Å), whereas emulsions stored at 4 °C contained crystalline triglyceride initially ($d=35.7$ Å). During lipolysis of 5 mM C_{14} TG in 0.5 mM micelles, the intensity of the lamellar phase visibly decreased in intensity, whilst a co-existing lamellar phase with larger lattice dimensions ($d=39.8$ Å) formed over time.

Table 4.2: Summary of lattice dimensions of the lamellar phase measured by SAXS in equilibrium systems representing endpoint of triglyceride digestion, and during dynamic lipolysis experiments. “–” indicates systems not studied.

System	Phases	Equilibrium system lamellar d-spacing (Å)	Dynamic system lamellar d-spacing (Å)
C ₈	Micelles, lamellar	29.6	25
C ₁₀	Micelles, lamellar	–	29.9
C ₁₂	Micelles, lamellar	34.6	36.1
C ₁₄	Micelles, lamellar	-	39.8
C ₁₆	Micelles, lamellar	–	44.6
C _{18:1}	Micelles, lamellar	47.5	49.6
Captex 355 (mixed C ₈ /C ₁₀)	Micelles, lamellar	–	30.1

4.6 Discussion

Similarities and differences between equilibrium and dynamic studies

In the literature, model systems representing intestinal contents after lipid digestion consist of lipolytic products such as diglyceride, monoglyceride, fatty acid and fatty acid soaps, which are combined with water, buffer or simulated intestinal fluids [2, 25]. These studies vary in complexity and approach to structural interrogation. Borné *et al.* observed rich phase behaviour including reversed hexagonal, lamellar, micellar and micellar cubic phases in the monoolein:oleic acid:water ternary phase diagram, however these studies did not include bile salt and there was no pH control [3]. With increasing pH, the monoolein:oleic acid:sodium oleate system dispersed in water was seen to reversibly transition from emulsified inverse micellar phase to micellar cubosomes, hexosomes, bicontinuous cubosomes to vesicles within a pH range of 7-8 [26].

In the current study, BS and BS/PL systems representing the gastrointestinal environment prior to lipid digestion revealed the presence of micelles only, which is consistent with previous observations [4, 5, 9]. The DLS measurements revealed a larger hydrodynamic radius for the fasted BS/PL micelles, compared to the fed BS and BS/PL micelles, and fasted BS micelles. BS/PL micelles have been shown to form a variety of structures, whereby with increasing PL content or dilution, spherical micelles transition to rod-like micelles, disc-like micelles and vesicles [27-29]. Therefore elongation of the micelles may explain the larger micellar sizes reported for the fasted state, which is consistent with reports in the literature [30].

The medium and long chain lipolysis products remained solubilised in the fed state BS/PL micelles, similar to previous studies [1, 4, 31], however a co-existing lamellar phase formed in the comparable fasted systems due to the reduced solubilisation capacity of the fasted BS/PL micelles. The broad shape of the lamellar peaks observed in the SAXS data are indicative of short range order, and are attributed to the formation of a fluid lamellar phase, rather than the crystallization of fatty acid out of the mixed micelles, as previously reported [6]. Furthermore, the measurements are performed at physiological temperature, which is above the melting point of the selected lipids [24].

Regardless of the bile salt level, a co-existing lamellar phase was observed in the short chain system at MG:FA > 5:10 mM. This reflects a poorer solubilisation or compatibility for the saturated short chain lipids in BS/PL micelles which is consistent with previous literature comments [4, 32, 33]. In a recent study, short chain fatty acids were shown to be more polar and water-soluble and thus they are less incorporated into mixed micelles than their longer chain counterparts, but in this case also appear to more readily form lamellar structures at higher concentrations [33].

The colloidal structures formed under dynamic lipolysis conditions were the same as those produced at equilibrium in the C₈ TG system. With increasing lipid loading, the minimum in the $I(q)$ shifted to lower q indicating swelling of the mixed micelles to accommodate the lipolysis products. At high lipid (50 mM) in both the fasted and fed states, a co-existing lamellar phase ($d=25.0 \text{ \AA}$) was present after 12 min at 40% digestion, which is comparable to the digestion of Captex 355 despite a difference in triglyceride composition [9]. Percentage digestion was calculated from the number of moles of NaOH added during the reaction, on

the basis that one mole of triglyceride is hydrolysed to produce 1 mole of 2-monoglyceride and 2 moles of fatty acid [34, 35].

Interestingly a digestion of 25 mM C₈ TG in the fed state revealed micelles, which differs from the equilibrium data which indicated the presence of a co-existing lamellar phase. During *in vitro* digestion of 5 mM C₁₂ TG in the fasted and fed state, a lamellar phase was present which correlates with equilibrium data for the fasted state, but not the fed, highlighting differences in the two approaches.

In both approaches, the d-spacing of the lamellar phase increased as triglyceride chain length increased, as summarised in Table 4.2. The study of structures during *in vitro* lipolysis is anticipated to be more *in vivo* relevant than equilibrium systems as in the dynamic system, as there are non-equilibrium effects such as intestinal motility and digestion reactions which change composition during digestion. However, with increasing lipid chain length and lipid loading, the digestion was increasingly incomplete due to crystallisation of the lipid [6]. This is in contrast to the *in vivo* scenario where complete digestion and absorption of dietary lipid occur; hence this is a limitation of the *in vitro* lipolysis model. Despite previous reports in the literature [8, 36-38], more complex phase behaviour was not observed during the digestion of long chain triglycerides, due to the pH and bile salt levels used in the study. However, the vesicles and mixed micelles observed are consistent with studies that have found these to be the dominating structures in equilibrium studies simulating the end of digestion of medium [4, 39, 40] and long chain triglycerides [15, 41-43], and in dynamic studies and *ex vivo* human aspirates [14, 44, 45].

Effect of emulsification on structure formation

The influence of the initial form of the lipid dispersion on structure formation during *in vitro* lipolysis was investigated, because previous *in vitro* digestion protocols using pH stat systems added the lipid as a bolus to the simulated intestinal fluid [8, 12, 38] and the production of a coarse emulsion via magnetic stirring, whereas recent studies measuring structures by *in situ* scattering methods pre-emulsified the lipid [37].

The pH stat titration profile revealed that the onset of lamellar phase formation occurred when 30% of the triglyceride had been digested, indicating a critical degree of digestion to form sufficient lipolysis products to enable structure formation, before the 'end point' of

digestion had been reached. The percentage digested was calculated from the number of moles of NaOH added during the reaction, on the basis that one mole of triglyceride is hydrolysed to produce 1 mole of 2-monoglyceride and 2 moles of fatty acid [34, 35]. After emulsification, an increased rate of digestion and structure formation is observed, which arises from interfacial activation of the pancreatic lipase due to the increased surface area of lipid droplets [46]. *In vivo*, ingested lipids are anticipated to be emulsified in the gastrointestinal fluids by the contractions in the stomach and small intestine, and hence pre-emulsification of the sample prior to the intestinal *in vitro* lipolysis step may be more relevant to the *in vivo* situation.

4.7 Conclusion

Understanding of the self-assembly structure of intestinal contents after lipid digestion is essential for understanding the impact lipid-based formulations have on the fate of drug after oral administration. This study used SAXS and DLS to provide insight into structural aspects of lipid digestion where the addition of phospholipids and lipolysis products was observed to swell bile salt micelles. When the solubilisation capacity for lipids was exceeded, a co-existing lamellar phase was observed. Some differences in structures were apparent between the two approaches used to study structures formed during lipid digestion, highlighting challenges in extrapolation of data from equilibrium to dynamic systems. Emulsification was observed to accelerate the rate of *in vitro* lipolysis and structure formation.

4.8 Supporting Information

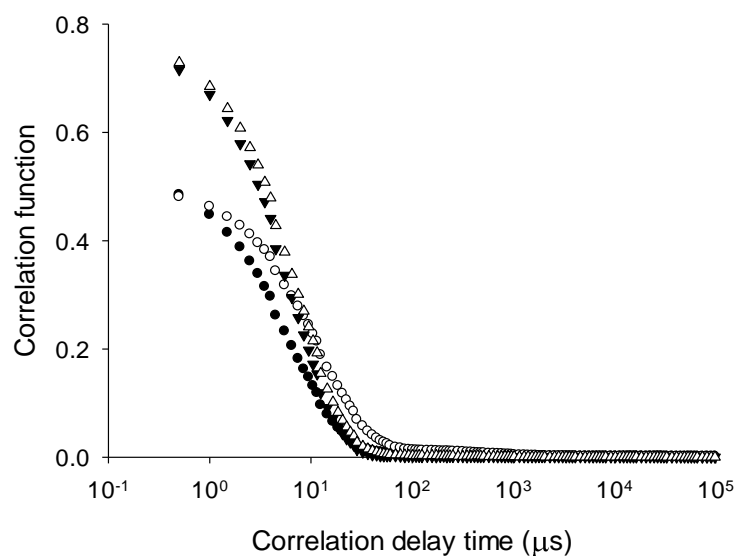


Figure SI-4.1: Intensity correlation functions from DLS for BS micelles in the fasted (closed circles) and fed (closed triangles) state, and BS/PL micelles in the fasted (open circles) and fed (open triangles).

Table SI-4.1: Summary of hydrodynamic radius and PDI for C_8 lipolysis products in fed BS/PL micelles from DLS measurements.

C_8 lipolysis products (monocaprylin:caprylic acid) in BS/PL micelles	Radius (nm)	PDI
5:10 mM (fed)	3.0 ± 1.0	0.20
25:50 (fed)	7.0 ± 3.7	0.16
50:100 (fed)	162.6 ± 117.6	0.46
5:10 mM (fasted)	3.8 ± 1.1	0.29
25:50 (fasted)	56.6 ± 51.3	0.40
50:100 (fasted)	170.3 ± 23.5	0.48

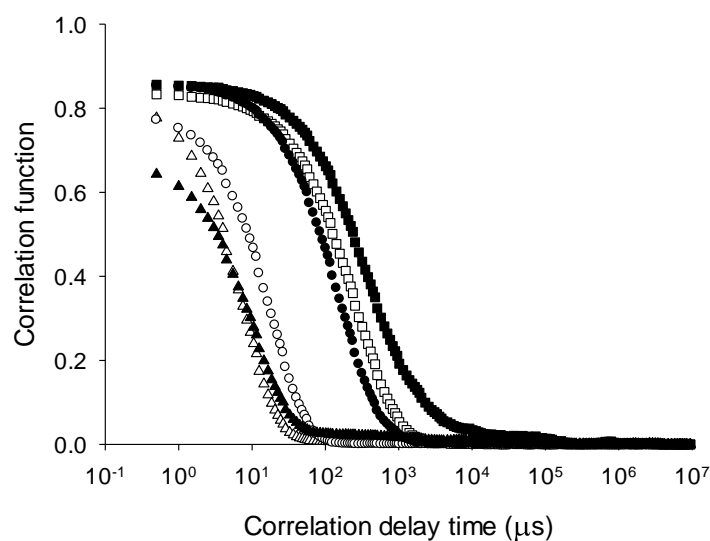


Figure SI-4.2: Intensity correlation functions from DLS for BS/PL micelles with C_8 lipolysis products monocaprylin:caprylic acid in fasted (closed symbols) and fed (open symbols) BS/PL micelles. A shift to longer delay times (i.e. longer diffusion or larger size) with decrease in bile salt, and increase in lipolysis products can be observed where 5:10 mM (triangles), 25:50 mM (circles) and 50:100 mM (squares).

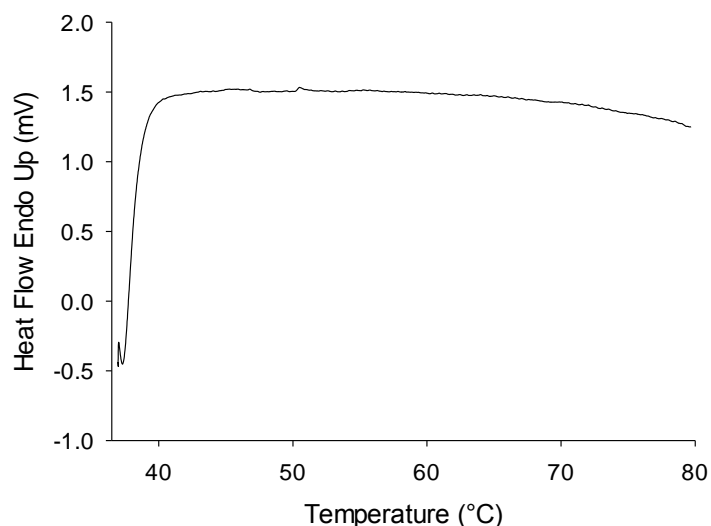


Figure SI-4.3: DSC measurement for C_{14} TG emulsion prepared at $70\text{ }^\circ\text{C}$ and stored at $37\text{ }^\circ\text{C}$ for 24 hr prior to measurement confirms that the emulsion is in a supercooled state. The sample ($10\text{ }\mu\text{L}$) was placed in a $40\text{ }\mu\text{L}$ aluminium pan which was then sealed. The measurement was performed using a Perkin Elmer DSC 8500 (Waltham, MA, USA) and the sample was heated from 37 to $80\text{ }^\circ\text{C}$ at a rate of $10\text{ }^\circ\text{C}/\text{min}$.

4.9 References

1. Hofmann, A.F., *Molecular association in fat digestion: Interaction in bulk of monoolein, oleic acid, and sodium oleate with dilute, micellar bile salt solutions*. *Adv Chem Ser*, 1968(84): p. 53-&.
2. Gustafsson, J., et al., *Phase behavior and aggregate structure in aqueous mixtures of sodium cholate and glycerol monooleate*. *J Colloid Interface Sci*, 1999. **211**(2): p. 326-335.
3. Borné, J., Nylander, T., and Khan, A., *Phase behavior and aggregate formation for the aqueous monoolein system mixed with sodium oleate and oleic acid*. *Langmuir*, 2001. **17**(25): p. 7742-7751.
4. Kossena, G.A., et al., *Separation and characterization of the colloidal phases produced on digestion of common formulation lipids and assessment of their impact on the apparent solubility of selected poorly water-soluble drugs*. *J Pharm Sci*, 2003. **92**(3): p. 634-648.
5. Kleberg, K., et al., *Biorelevant media simulating fed state intestinal fluids: Colloid phase characterization and impact on solubilization capacity*. *J Pharm Sci*, 2010. **99**(8): p. 3522-3532.
6. Phan, S., et al., *Disposition and crystallization of saturated fatty acid in mixed micelles of relevance to lipid digestion*. *J Colloid Interface Sci*, 2015. **449**: p. 160-166.
7. Phan, S., et al., *Self-assembled structures formed during lipid digestion: Characterization and implications for oral lipid-based drug delivery systems*. *Drug Delivery Transl Res*, 2013. **4**(3): p. 245-294.
8. Warren, D.B., et al., *Real time evolution of liquid crystalline nanostructure during the digestion of formulation lipids using synchrotron small-angle X-ray scattering*. *Langmuir*, 2011. **27**(15): p. 9528-9534.
9. Phan, S., et al., *Structural aspects of digestion of medium chain triglycerides studied in real time using sSAXS and cryo-TEM*. *Pharm Res*, 2013. **30**(12): p. 3088-3100.
10. Lee, K.W.Y., Porter, C.J.H., and Boyd, B.J., *The effect of administered dose of lipid-based formulations on the in vitro and in vivo performance of cinnarizine as a model poorly water-soluble drug*. *J Pharm Sci*, 2013. **102**(2): p. 565-578.
11. Porter, C.J.H., et al., *Use of in vitro lipid digestion data to explain the in vivo performance of triglyceride-based oral lipid formulations of poorly water-soluble drugs: Studies with halofantrine*. *J Pharm Sci*, 2004. **93**(5): p. 1110-1121.
12. Sek, L., Porter, C.J.H., and Charman, W.N., *Characterisation and quantification of medium chain and long chain triglycerides and their in vitro digestion products, by HPTLC coupled with in situ densitometric analysis*. *J Pharm Biomed Anal*, 2001. **25**(3-4): p. 651-661.
13. Kaukonen, A.M., et al., *Drug solubilization behavior during in vitro digestion of simple triglyceride lipid solution formulations*. *Pharm Res*, 2004. **21**(2): p. 245-253.
14. Hernell, O., Stammers, J.E., and Carey, M.C., *Physical-chemical behavior of dietary and biliary lipids during intestinal digestion and absorption. 2 Phase-analysis and aggregation states of luminal lipids during duodenal fat digestion in healthy adult human-beings*. *Biochemistry*, 1990. **29**(8): p. 2041-2056.

Chapter 4. How Relevant Are Assembled Equilibrium Samples in Understanding Structure Formation during Lipid Digestion?

15. Fatouros, D.G., et al., *Colloidal structures in media simulating intestinal fed state conditions with and without lipolysis products*. Pharm Res, 2009. **26**(2): p. 361-374.
16. Kaukonen, A., et al., *Drug solubilization behavior during in vitro digestion of suspension formulations of poorly water-soluble drugs in triglyceride lipids*. Pharm Res, 2004. **21**(2): p. 254-260.
17. Sek, L., et al., *Evaluation of the in-vitro digestion profiles of long and medium chain glycerides and the phase behaviour of their lipolytic products*. J Pharm Pharmacol, 2002. **54**(1): p. 29-41.
18. Gargouri, Y., Moreau, H., and Verger, R., *Gastric lipases: Biochemical and physiological studies* Biochimica Et Biophysica Acta, 1989. **1006**(3): p. 255-271.
19. Dressman, J.B., et al., *Upper gastrointestinal (GI) pH in young, healthy men and women*. Pharm Res, 1990. **7**(7): p. 756-761.
20. Kirby, N.M., et al., *A low-background-intensity focusing small-angle X-ray scattering undulator beamline*. J Appl Crystallogr, 2013. **46**: p. 1670-1680.
21. *Small angle X-ray scattering*, ed. Glatter, O.K., O. 1982, London: Academic Press.
22. Koppel, D.E., *Analysis of macromolecular polydispersity in intensity correlation spectroscopy - Method of cumulants*. J Chem Phys, 1972. **57**(11): p. 4814-4820.
23. Phan, S., et al., *Immobilised lipase for in vitro lipolysis experiments*. J Pharm Sci, 2015 **104**(4): p. 1311-1318.
24. Bockisch, M., *Fats and oils handbook*, 1998, AOCS Press.
25. Lindstrom, M., et al., *Aqueous lipid phases of relevance to intestinal fat digestion and absorption*. Lipids, 1981. **16**(10): p. 749-754.
26. Salentinig, S., Sagalowicz, L., and Glatter, O., *Self-assembled structures and pK(a) value of oleic acid in systems of biological relevance*. Langmuir, 2010. **26**(14): p. 11670-11679.
27. Müller, K., *Structural aspects of bile salt-lecithin mixed micelles*. Hepatology, 1984. **4**(5): p. S134-S137.
28. Hjelm, R.P., Thiyagarajan, P., and Alkan, H., *A small-angle neutron-scattering study of the effects of dilution on particle morphology in mixtures of glycocholate and lecithin*. J Appl Crystallogr, 1988. **21**: p. 858-863.
29. Long, M.A., Kaler, E.W., and Lee, S.P., *Structural characterization of the micelle-vesicle transition in lecithin-bile salt-solutions*. Biophys J, 1994. **67**(4): p. 1733-1742.
30. Boni, J.E., et al., *Instant FaSSIF and FeSSIF-Biorelevance meets practicality*. Dissolut Technol, 2009. **16**(3): p. 41-45.
31. Fatouros, D.G., Bergenstahl, B., and Mullertz, A., *Morphological observations on a lipid-based drug delivery system during in vitro digestion*. Eur J Pharm Biopharm, 2007. **31**(2): p. 85-94.
32. Porter, C.J.H., Trevaskis, N.L., and Charman, W.N., *Lipids and lipid-based formulations: Optimizing the oral delivery of lipophilic drugs*. Nat Rev Drug Discov, 2007. **6**(3): p. 231-248.

Chapter 4. How Relevant Are Assembled Equilibrium Samples in Understanding Structure Formation during Lipid Digestion?

33. Salentinig, S., et al., *pH-responsive micelles based on caprylic acid*. Langmuir, 2014. **30**(25): p. 7296-303.
34. Embleton, J.K. and Pouton, C.W., *Structure and function of gastro-intestinal lipases*. Adv Drug Deliv Rev, 1997. **25**(1): p. 15-32.
35. Houde, A., Kademi, A., and Leblanc, D., *Lipases and their industrial applications*. Appl Biochem Biotechnol, 2004. **118**(1-3): p. 155-170.
36. Salentinig, S., et al., *Formation of highly organized nanostructures during the digestion of milk*. ACS Nano, 2013. **7**(12): p. 10904-10911.
37. Salentinig, S., et al., *Transitions in the internal structure of lipid droplets during fat digestion*. Soft Matter, 2011. **7**(2): p. 650-661.
38. Fatouros, D.G., et al., *Structural development of self nano emulsifying drug delivery systems (SNEDDS) during in vitro lipid digestion monitored by small-angle X-ray scattering*. Pharm Res, 2007. **24**(10): p. 1844-1853.
39. Kossena, G.A., et al., *A novel cubic phase of medium chain lipid origin for the delivery of poorly water soluble drugs*. J Control Release, 2004. **99**(2): p. 217-229.
40. Westerman, P.W., *Physicochemical characterization of a model digestive mixture by 2H NMR*. J Lipid Res, 1995. **36**(12): p. 2478-2492.
41. Fatouros, D.G., et al., *Physicochemical characterization of simulated intestinal fed-state fluids containing lyso-phosphatidylcholine and cholesterol*. Dissolution Technol, 2009. **16**(3): p. 47-50.
42. Rigler, M.W., Honkanen, R.E., and Patton, J.S., *Visualization by freeze fracture, in vitro and in vivo, of the products of fat digestion*. J Lipid Res, 1986. **27**(8): p. 836-57.
43. Staggers, J.E., et al., *Physical-chemical behavior of dietary and biliary lipids during intestinal digestion and absorption. 1. Phase behavior and aggregation states of model lipid systems patterned after aqueous duodenal contents of health adult human-beings*. Biochemistry, 1990. **29**(8): p. 2028-2040.
44. Müllertz, A., et al., *Insights into intermediate phases of human intestinal fluids visualized by atomic force microscopy and cryo-transmission electron microscopy ex vivo*. Mol Pharm, 2012. **9**(2): p. 237-247.
45. Armand, M., et al., *Digestion and absorption of 2 fat emulsions with different droplet sizes in the human digestive tract*. Am J Clin Nutri, 1999. **70**(6): p. 1096-1106.
46. Blank, K., et al., *Functional expression of Candida antarctica lipase B in Escherichia coli*. J Biotechnol, 2006. **125**(4): p. 474-83.

Chapter 5. Structural Aspects of Digestion of Medium Chain Triglycerides

Chapter 5. Structural Aspects of Digestion of Medium Chain Triglycerides

The work presented in this chapter has been published as: Phan S., Hawley A., Mulet X, Waddington L., Prestidge C.A., Boyd B.J., *Structural aspects of digestion of medium chain triglycerides studied in real time using sSAXS and cryo-TEM*. Pharm Res, 2013. **30**(12): p.3088-3100.

5.1 Declaration

Declaration by candidate:

In the case of Chapter 5, the nature and extent of my contribution to the work was the following:

Nature of contribution	Extent of contribution
Research design, performance of data collection and analysis, manuscript preparation	80%

The following co-authors contributed to the work:

Name	Nature of contribution
Adrian Hawley	Intellectual input on SAXS operation
Xavier Mulet	Supervision, performance of data collection
Lynne Waddington	Intellectual input on cryo-TEM operation and analysis
Clive A. Prestidge	Input into manuscript preparation
Ben J. Boyd	Supervision, intellectual input, input into manuscript preparation

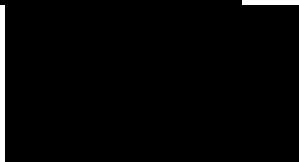
The undersigned hereby certify that the above declaration correctly reflects the nature and extent of the candidate's and co-authors' contributions to this work.

Candidate's signature:



Date: 21/08/15

Main supervisor's signature:



Date: 21/08/15

5.2 Structural Aspects of Digestion of Medium Chain Triglycerides Studied in Real Time using sSAXS and cryo-TEM

Stephanie Phan¹, Adrian Hawley², Xavier Mulet^{1,3}, Lynne Waddington³, Clive A. Prestidge⁴, Ben J. Boyd¹

¹ Drug Delivery, Disposition and Dynamics, Monash Institute of Pharmaceutical Sciences, Monash University (Parkville Campus), 381 Royal Parade, Parkville, VIC 3052, Australia

² SAXS/WAXS Beamline, Australian Synchrotron, Clayton, VIC 3168, Australia

³ CSIRO Materials Science and Engineering, Private Bag 10, Clayton South VIC 3169, Australia

⁴ Ian Wark Research Institute, University of South Australia (Mawson Lakes Campus), SA, Australia

Received 22nd January 2013 and published online 7th August 2013

Citation: Pharm. Res. (2013) 30:3088–3100

DOI: 10.1007/s11095-013-1108-2

Abstract

Purpose: The purpose of this study was to investigate the colloidal structures formed on digestion of medium chain triglyceride (MCT) with a specific objective of identifying and characterizing a previously reported vesicular phase, which has been linked to supersaturation and anomalous digestion kinetics, and to evaluate the influence of lipid mass and enzyme inhibition on self-assembled structure.

Methods: MCT was digested *in vitro* and nanostructure was monitored in real time using synchrotron small angle X-ray scattering (sSAXS), and morphology was studied using cryogenic transmission electron microscopy (cryo-TEM).

Results: Formation of the putative vesicular phase formed on digestion of MCT was confirmed and its structural attributes were determined. Vesicle formation was dependent on lipid mass and bile salt concentration. The use of enzyme inhibitor for offline analysis of lipolysis samples did influence structural aspects of the digestion medium when compared to real time evaluation.

Conclusions: The formation of a vesicle phase was directly linked to the kinetics of lipid digestion. Vesicle formation is linked to lipid mass, or more specifically the ratio of lipid to bile salts present in the digestion mixture. Inhibition of lipase to halt digestion during sampling for offline analysis must be done with caution as structural aspects were shown to differ for the MCT digests with and without inhibitor present.

Keywords: lipid digestion, *in vitro* lipolysis, lipid-based drug delivery, synchrotron small angle X-ray scattering, cryogenic transmission electron microscopy

Abbreviations

Cryo-TEM, cryogenic transmission electron microscopy

LCT, long chain triglyceride

MCT, medium chain triglyceride

SAXS, small angle X-ray scattering

sSAXS, synchrotron small angle X-ray scattering

TBU, tributyrin units

5.3 Introduction

Many new drug compounds are poorly soluble in water, leading to limited dissolution in the gastrointestinal (GI) tract, presenting a barrier to efficient absorption and bioavailability. Lipid-based formulations are increasingly seen to be a solution to address this issue [1].

There are a number of physicochemical and biological mechanisms by which lipid-based formulations may increase the bioavailability of poorly water-soluble drugs. Arguably, of most importance is the ability of lipids to boost the solubilisation capacity of gastrointestinal fluids, providing a mechanism for drug to remain in a solubilized state prior to absorption. When lipids are digested in the GI tract, lipolytic products combine with endogenous amphiphilic molecules (primarily bile salts and phospholipids) to form colloidal phases such as liquid crystals, vesicles and micelles [2-8]. If appropriate quantities and type of lipid are present in the gut, these structures can be critical to maintaining drug in solution rather than precipitating during dispersion of the formulation and digestion of the lipid components. Despite the importance of these structures in determining the fate of drug in the pre-absorption gastrointestinal milieu, the colloidal aspects of lipid digestion and consequent disposition of drug *in vivo* are still not well understood.

Medium chain triglycerides (MCT) have attracted significant attention in the lipid-based drug delivery field, in part because they tend to provide greater solvency for drug in the pre-digested formulation. When MCT formulations are subjected to an *in vitro* lipolysis model [9], they often show a propensity to maintain poorly water-soluble drugs in a solubilized state after complete digestion of the formulation. In fact, for highly lipophilic drugs such as halofantrine and cinnarizine, these formulations can provide an apparently supersaturated state in which the concentration of drug exceeds the solubility of drug in the blank pre-digested formulation [10]. The supersaturation effect is highly dependent on the mass of lipid used in the closed *in vitro* model; reducing the mass of lipid reduces the propensity to support the high concentrations and leads to an increased proportion of drug precipitating during digestion [11]. The effect is also dependent on the concentration of bile salts present and increasing the bile salt to lipid ratio also increases the likely level of drug precipitation. The supersaturation effect is of interest in optimizing lipid-based formulations because engineering formulations to present drug in a state of high thermodynamic activity is an accepted strategy for driving passive drug absorption.

The supersaturation effect has been linked to the colloidal structures present during the digestion of MCT, with the formation of a putative 'vesicular phase' occurring during *in vitro* digestion of high concentrations of MCT [4, 12]. The 'vesicular' phase has been studied indirectly by size exclusion separation of model lipid digests where MCT digestion products were combined with low and high bile salt concentrations [4] and the vesicular phase present at low bile salt concentrations was shown to have high drug carrying capacity [4].

Thus the design of formulations for the generation of the apparent vesicular phase *in vivo* would be expected to be advantageous in terms of optimal conditions for drug solubilisation. Understanding, and more importantly controlling, structure formation *in vivo* is increasingly viewed as a crucial step in transforming lipid-based drug delivery beyond empirical formulation to rational design. However, to our knowledge the presence of the apparent vesicular phase has never been actually demonstrated nor its structure elucidated using contemporary structural techniques such as small angle X-ray scattering (SAXS). SAXS has been employed to characterise colloidal structures in equilibrium systems via a phase diagram approach, and dynamic digesting lipid systems [13, 14]. In recent years, there has been a move to structural studies in real time, by conducting *in vitro* lipolysis studies in a flow through mode at synchrotron facilities [15]. Synchrotron X-rays are advantageous as they enable probing of structures in shorter time scales, have higher resolution, and have the potential for application to *in vivo* studies.

Various other techniques have been used to study digestion of dietary lipids, including light microscopy [2, 16], freeze fracture electron microscopy [17, 18] and quasielastic light scattering techniques [3, 8]. More recently cryogenic transmission electron microscopy (cryo-TEM) has successfully been utilised to observe colloidal structures during digestion of a pharmaceutical lipid-based formulation and also in human intestinal fluids [14, 19-21]. This technique is minimally invasive and advantageous as samples are preserved in their original state in the digested medium, avoiding issues associated with normal electron microscopy techniques, such as artefacts produced by staining, fixation and adsorption [22]. However, the samples taken during digestion in past studies were treated with a lipase inhibitor and then imaged at a later time, leading to the possibility of artefacts.

Consequently, in this study, the structures produced during *in vitro* digestion of MCT have been elucidated using real time synchrotron SAXS (sSAXS), and samples retrieved from digestion for cryo-TEM were immediately vitrified without addition of lipase inhibitor. Specifically a high level of MCT (250 mg, ~50 mM) expected to form the vesicular phase, and low level (50 mg, ~10 mM) expected to form only micelles were investigated. Captex 355 was used as the triglyceride because it has been previously shown to support the supersaturation effect. The molar quantities of lipid stated in the case of Captex 355 are 'nominal' as it is a complex mixture, and were based on the equivalent mass of tricaprylin, as though tricaprylin were the only component. The composition of Captex 355 is elaborated on in the Materials section. Additionally, cryo-TEM was also conducted on digestion samples which were

chemically inhibited to determine whether the presence of the lipase inhibitor induced any artefacts in understanding structural evolution in these digesting systems. The dynamic real time samples have been compared to equilibrium samples prepared by assembly of component monoglycerides and fatty acids for direct comparison of the two approaches.

5.4 Experimental

Materials

Captex 355 (MCT composed of 59% caprylic acid (C_8), 40% capric acid (C_{10}), <1% lauric acid (C_{12}) as stated in the product information) was obtained from Abitec Corporation (Janesville, WI, USA) and used without further purification. Tris maleate (reagent grade), bile salt (sodium taurodeoxycholate >95%), monocaprylin (approx. 99%) and caprylic acid (99+% by capillary gas chromatography) were purchased from Sigma Aldrich (St. Louis, MO, USA). Lipase inhibitor (4-bromophenylboronic acid, 4-BPB, >95% (high performance liquid chromatography)) was obtained from Fluka (Sigma Aldrich, Milwaukee, WI, USA). Phospholipid (dioleoylphosphatidyl choline, DOPC, >94%) was obtained from Trapeze Associates Pty Ltd. (Clayton, Victoria, Australia). Pancreatin extract was purchased from Southern Biologicals (Nunawading, Victoria, Australia) and had USP grade pancreatin activity. Calcium chloride (>99%) was obtained from Ajax Finechem (Seven Hills, NSW, Australia). Sodium chloride (>99%) was purchased from Chem Supply (Gillman, SA, Australia). Water used was sourced from a Millipore water purification system using a QuantumTM EX Ultrapure Organex cartridge (Millipore, Australia).

Lipolysis model and *in vitro* digestion

In vitro digestion studies were performed using a pH-stat auto titrator (Radiometer, Copenhagen, Denmark), illustrated schematically in Figure 5.1, similar to previous reports [9, 10, 15, 23]. Digestion buffer was prepared with 50 mM Tris maleate, 5 mM $CaCl_2 \cdot 2H_2O$, 150 mM NaCl and adjusted to pH 6.5. Bile salt (sodium taurodeoxycholate) and phospholipid (DOPC) concentrations, simulating intestinal fluid in the fasted state and fed state, were 5 mM:1.25 mM and 20 mM:5 mM respectively in digestion buffer, the mean values and 4:1 ratio representing intestinal contents after digestion [8, 20]. Lipid formulations were added to 9 mL of the fasted or fed simulated intestinal fluid in the thermostatted digestion vessel at 37 °C.

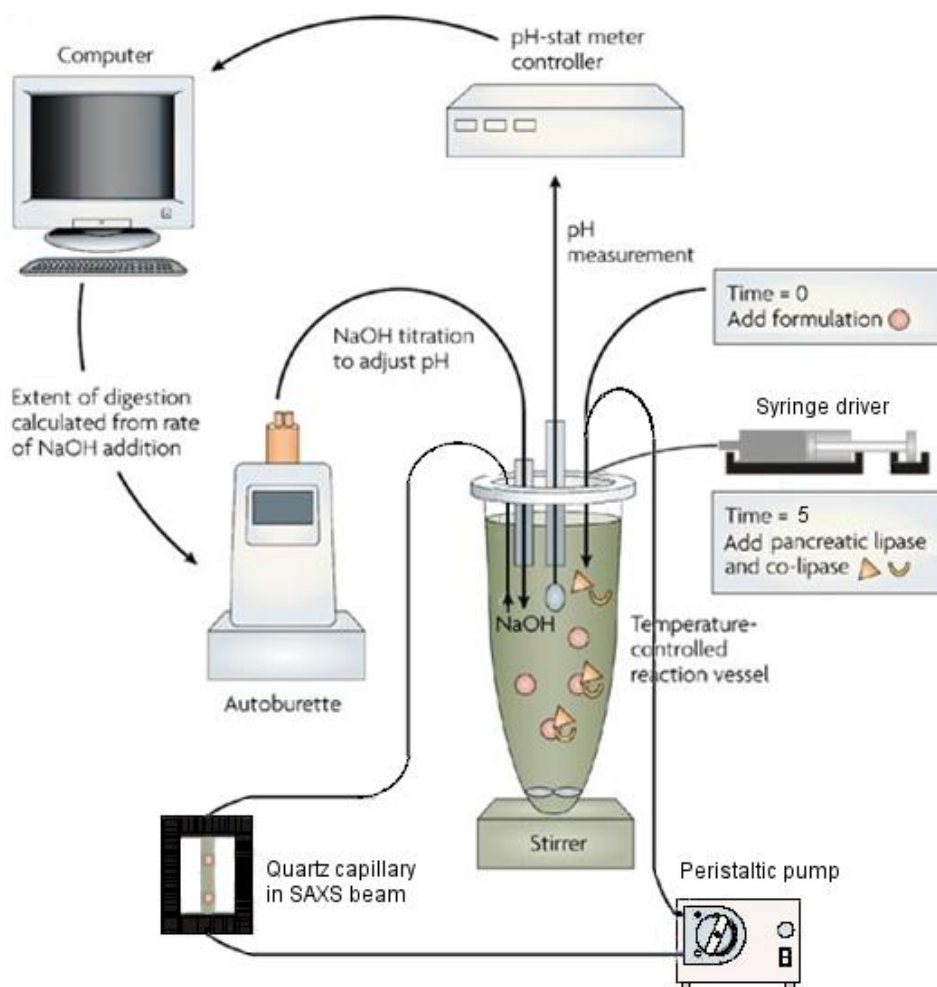


Figure 5.1: Schematic of the *in vitro* digestion apparatus coupled to a synchrotron SAXS flow through cell with syringe driver for enzyme addition. Modified with permission from [15].

Formulations were magnetically stirred for 5 min in simulated intestinal fluid for complete mixing and thermal equilibration and the pH was adjusted to 6.5 ± 0.003 , chosen as a compromise between the optimum for pancreatic lipase activity pH (6 – 10) [24] and duodenal pH (5.0 – 6.5) [25]. On addition of pancreatin (6.94 TBU/mg dry pancreatin powder) the pH-stat titrated the digestion mixture with 0.2 M NaOH in order to maintain the system at $\text{pH } 6.500 \pm 0.003$. Digestion was allowed to proceed for 60 min, in which the degree of enzymatic digestion of the lipid was reflected in the volume of NaOH used to neutralize the fatty acids liberated during the digestion process. A blank digestion without lipid but with bile salt micelles present was performed as a background experiment, to account

for fatty acids that were produced from phospholipids and was subtracted from the profiles for the lipolysis experiments.

Synchrotron small angle X-ray scattering and flow through *in vitro* digestion

SAXS measurements were performed at the Australian Synchrotron. For equilibrium studies, samples were placed in capillaries where they were inserted into a 37 °C thermostatted metal heating block controlled by a Peltier system accurate to ± 0.1 °C. An X-ray beam with a wavelength of 1.1271 Å (11 keV) was selected. The sample to detector distance was 1015 mm, covering a q -range of 0.014 – 0.65 Å⁻¹. The 2D SAXS patterns were collected using a Pilatus 1M detector (active area 169 × 179 mm² with a pixel size of 172 µm). Calibration was performed using silver behenate. Data was normalized the using ScatterBrain Analysis program available at <http://www.synchrotron.org.au/index.php/aussyncbeamlines/saxswaxs/software-saxswaxs>.

The scattering pattern was converted to a plot of intensity versus scattering vector, q , using the equation $q = (4\pi/\lambda)\sin(\theta/2)$ [26]. The periodicity of the lamellar phase was calculated using the equation $d = 2\pi/q$ where q was the location of the lamellar peak. The average of three frames of each sample acquired before enzyme addition was subtracted as background for the dynamic digestions.

To monitor changes in nanostructure in real-time during digestion, the model was fitted with silicone tubing (total volume <1 mL) to enable continuous flow of the digestion medium via peristaltic pump at a rate of 10 mL/min, through a 2 mm diameter quartz capillary. The capillary was fixed in the X-ray beam. A remotely operated syringe driver was used to deliver 1 mL of pancreatin extract over several seconds into the vessel to initiate digestion. A 5 s acquisition time per 30 s for up to 60 min was used to yield the required information in flow through mode depending on the kinetics of digestion. The computer software ScatterBrain Analysis was used to acquire and reduce 2D patterns to 1D curves.

Cryo-TEM studies

A laboratory-built humidity-controlled vitrification system was used to prepare the samples for cryo-TEM. Humidity was kept close to 80% for all experiments, and ambient temperature was 22 °C.

Copper grids (200-mesh) coated with perforated carbon film (Lacey carbon film: ProSciTech, Qld, Australia) were glow discharged in nitrogen to render them hydrophilic. Aliquots (4 μL) of the *in vitro* lipolysis medium were immediately pipetted after sampling onto each grid prior to plunging. After 30 s adsorption time the grid was blotted manually using Whatman 541 filter paper, for approximately 2 s. Blotting time was optimised for each sample. The grid was then plunged into liquid ethane cooled by liquid nitrogen. Frozen grids were stored in liquid nitrogen until required.

The samples were examined using a Gatan 626 cryoholder (Gatan, Pleasanton, CA, USA) and Tecnai 12 Transmission Electron Microscope (FEI, Eindhoven, The Netherlands) at an operating voltage of 120 kV. The sample holder operated at -175.5 ± 1 °C. At all times low dose procedures were followed, using an electron dose of 8-10 electrons/ \AA^2 for all imaging. Images were recorded using a FEI Eagle 4k \times 4k CCD camera at magnifications ranging from 15 000 \times to 50 000 \times .

5.5 Results

Evolution of structure during digestion of Captex 355 under fasted state conditions (sSAXS)

On dispersion in simulated fasted intestinal conditions prior to addition of enzyme, Captex 355 forms a crude oily emulsion. The structural changes during a 60 min digestion of Captex 355 were monitored by sSAXS. For the digestion of 50 mM Captex 355 (250 mg) under fasted conditions, the scattering data in Figure 5.2 Panel A indicated that initially only micelles were present, but that after 20-25 min, two peaks with spacing ratios in q of 1 and 2 became evident, indicating that a lamellar phase was gradually formed. The q -values of the peaks were at 0.2 and 0.4 \AA^{-1} , indicating that the lamellar phase had a repeat distance of 30.1 \AA .

The titration profile, obtained from consumption of NaOH over time due to fatty acid production, describes changes in chemical composition during digestion. Two distinct regimes of behaviour were evident from the solid line in Figure 5.2 Panel B. An initial phase of digestion commencing on enzyme addition but slowed between 10 and 20 min, and a second phase in which at 20 min the digestion inexplicably accelerates with no intervention on the system, and continues until it has almost plateaued at 60 min when the monitoring was discontinued. The time scale of commencement of the second phase of digestion was very

close to that of the appearance of the lamellar phase in the scattering data (Figure 5.2A) suggesting a link between changing structure and the discontinuity in the digestion profile.

To further evaluate the link between structure and digestion kinetics, the intensity of the lamellar phase was calculated from the height of the first lamellar reflection, and plotted against time of digestion (open squares in Figure 5.2 Panel B commencing at 30 min so that the intensity was resolved from the baseline). There was a very clear correlation between the rate of evolution of the lamellar phase, and the digestion kinetics.

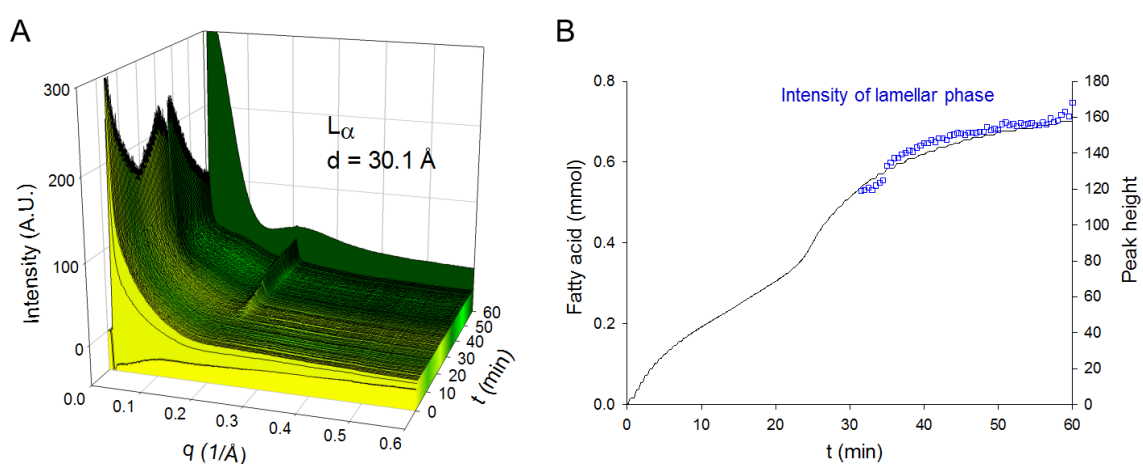


Figure 5.2: Digestion of 50 mM Captex 355 (250 mg) in fasted state over 60 min at 37 °C. Panel A shows the SAXS profiles over time during digestion. Panel B shows the correlation between the digestion kinetics from the titration profile (solid line) and intensity of lamellar phase (open squares). The final frame in Panel A indicates the scattering after addition of extra bile salt to the digestion medium to a final concentration of 55 mM to induce conversion of the lamellar structure to micelles.

At the completion of digestion of 50 mM Captex 355, a high concentration of bile salt was introduced with the expectation that the lamellar phase structures transformed to swollen micellar structures. Indeed on introduction of bile salt to the digestion medium after 60 min (the final frame in Figure 5.2A) such that the final bile salt concentration was 55 mM, the reflections indicating lamellar phase were abolished and a large broad micellar hump was evident.

During a 60 min digestion of 10 mM Captex 355 (50 mg) under the conditions previously described, there was no evidence of lamellar phase formation during digestion at the lower lipid content (Figure 5.3).

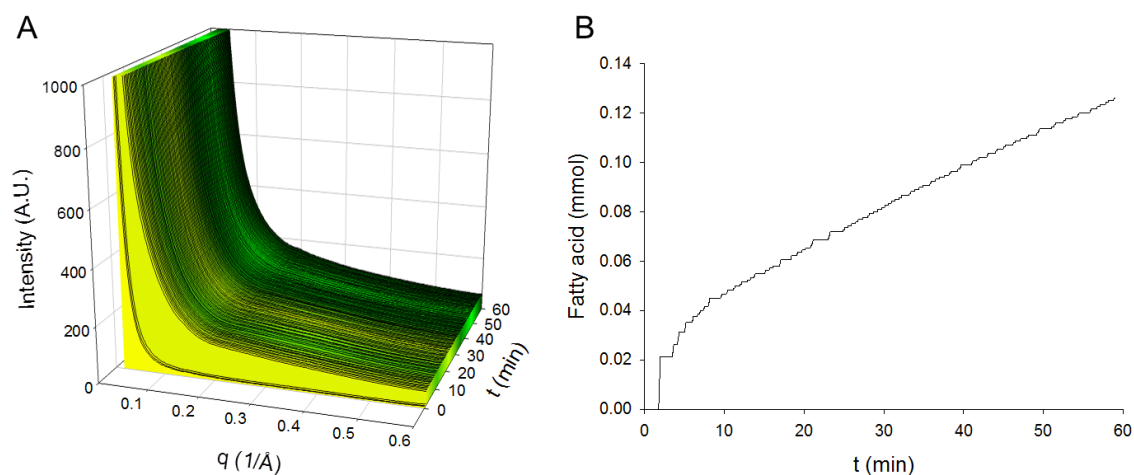


Figure 5.3: Digestion of 10 mM Captex 355 (50 mg) in fasted state over 60 min at 37 °C studied by SAXS (Panel A) and digestion kinetics from the titration profile (Panel B).

Changes in morphology of colloidal structure during digestion of Captex 355 (cryo-TEM)

Digestion buffer and fasted micelles were imaged as blanks, and both samples were clean with only micelles being observed in the fasted micelle sample (Figure 5.4).

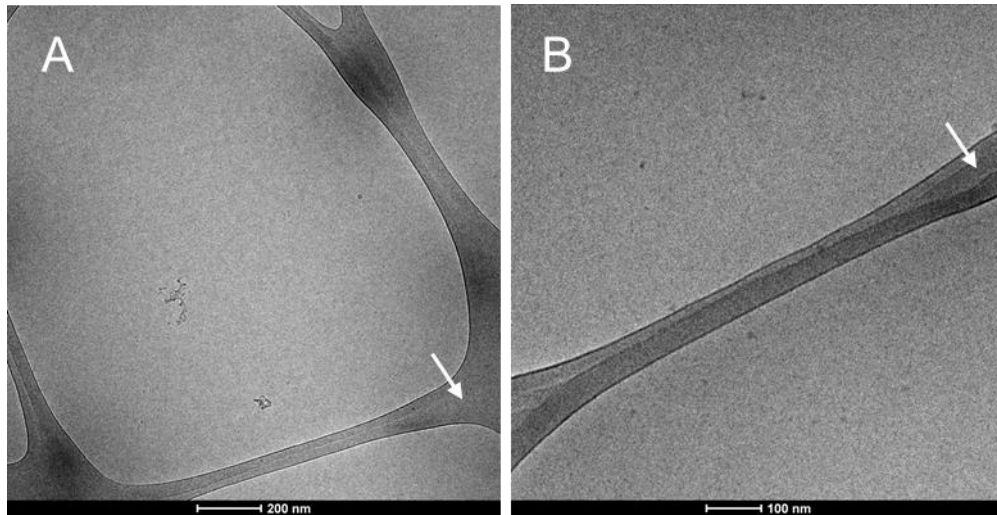


Figure 5.4: Cryo-TEM images of Panel A: digestion buffer (no structures present) and Panel B: Fasted bile salt+phospholipid micelles, where the black dots apparently indicate small micellar structures. Arrows indicate regions of the TEM grid.

The images presented in Figure 5.5 for the 50 mM Captex 355 digestion (250 mg) correlate well with what might be expected from the scattering data. The images are a representative sample of 306 images in total.

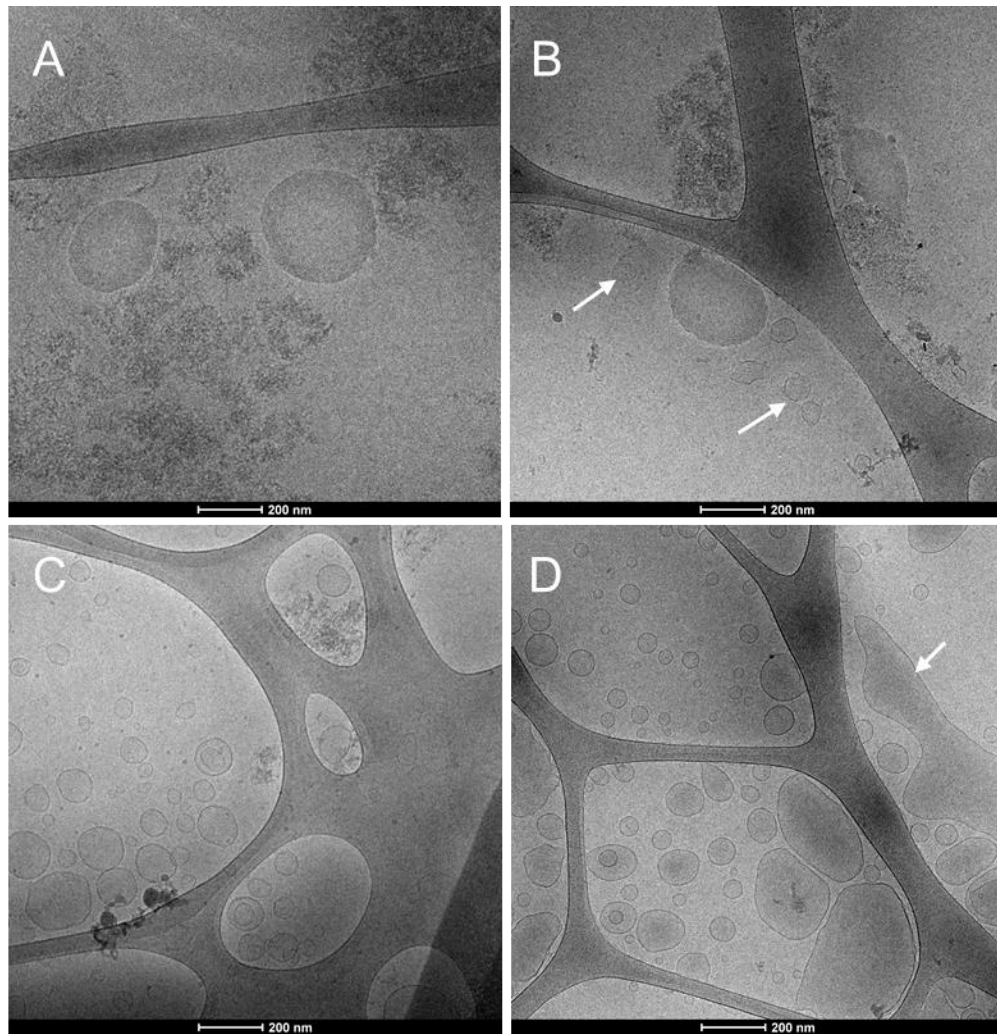


Figure 5.5: Cryo-TEM images of the digestion medium during real time 50 mM Captex 355 (250 mg) digestion. Panel A: at 10 min, oil droplets approximately 200 nm in diameter and protein aggregates are evident. Panel B: at 20 min small faceted unilamellar vesicles 30 – 150 nm were apparent (indicated by arrows) in addition to a 200 nm oil droplet and protein aggregates. Panel C: at 30 min the appearance of unilamellar and bilamellar vesicles 50 – 200 nm increasingly dominate the structures present. Panel D: at 40 min large unilamellar and bilamellar vesicles 50 – 200 nm, and lamellar fragments a few hundred μm in length (indicated by arrow) were observed. Micelles approximately 3 – 4 nm in diameter were seen as small black dots in all samples, which were absent from digestion buffer (Figure 5.4A).

In the samples taken at 10 and 20 min, oil droplets 100 – 600 nm in size were present in close proximity to protein aggregates and long collagen strands several micrometers in length, and 100 nm in width, originating from the pancreatin extract. The collagen originating from the

pancreatin extract was also reported by Fatouros and Müllertz, although they were referred to as “long, well-organised, ladder-shaped structures” [19, 21]. Micelles were also evident, which is in agreement with the scattering data. At the early stage of digestion in Panels A and B, there were no signs of structures that would be consistent with scattering of a lamellar phase.

At 30 and 40 min, unilamellar vesicles and bilamellar vesicles (50 – 200 nm, some very spherical, others irregular/stretched, multicompartment vesicles) and large lamellar fragments a few hundred micrometers in length were visible in large numbers. Vesicles are dispersed lamellar phase, so the vesicles and lamellar fragments provide the scattering indicative of lamellar structures. At 30 min, oil droplet clusters were also present, however they were smaller (50 – 150 nm) and less numerous across the grid than those identified earlier on in the digestion. There were also protein aggregates and collagen strands. 3 – 4 nm micelles were seen as tiny black dots in all samples.

The 50 mM digestion was repeated, and rather than immediately vitrifying the retrieved samples, the lipase inhibitor (0.5 M 4-bromophenylboronic acid in methanol) was added, and the samples vitrified up to 24 hr after digestion. The cryo-TEM images of the inhibited samples taken at the corresponding time points in Figure 5.6 were broadly consistent with those in Figure 5.5 from the real time study, however the abundant liposome structures present towards the end of digestion in the real time sample were less numerous in the inhibited sample. Thus lipase inhibition did appear to have a slight influence on the structures present in inhibited samples.

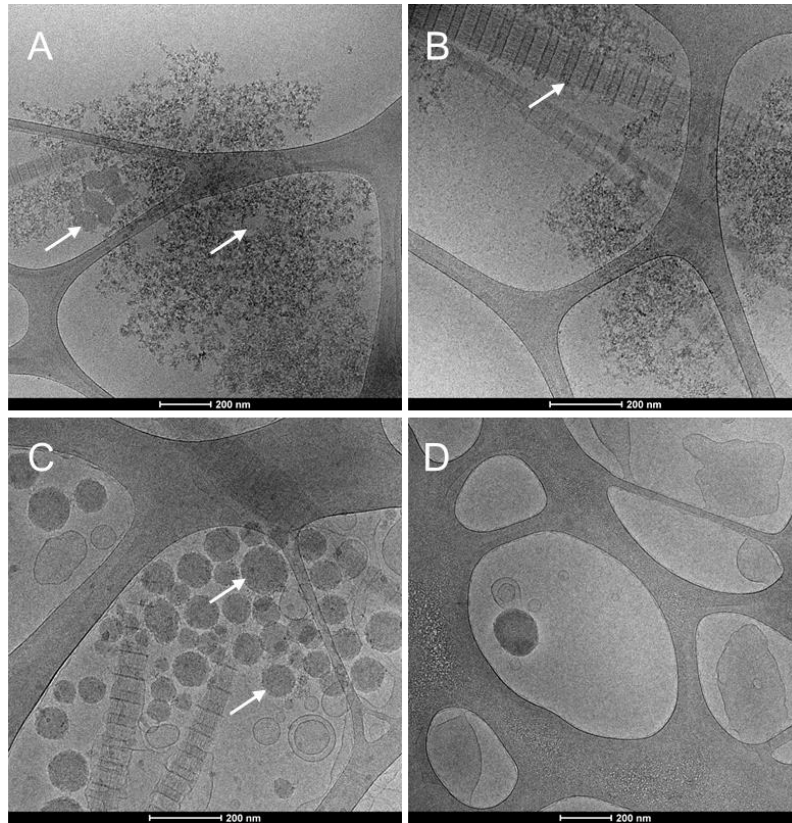


Figure 5.6: Cryo-TEM images of inhibited samples of digestion medium during real time 50 mM Captex 355 (250 mg) digestion. Panel A: at 10 min oil droplets 100 nm in diameter (indicated by arrows) associated with protein aggregates and collagen strands are observed. Panel B: at 20 min oil droplets associated with protein aggregates and collagen strands (indicated by arrow) (present in the pancreatin) still appear to dominate the structures present. Panel C: at 30 min, unilamellar and bilamellar vesicles 50 – 200 nm in diameter, and oil droplets 50 – 150 nm in diameter are seen (indicate by the arrows), and in Panel D at 40 min, lamellar fragments are seen and 150 nm bilamellar vesicles are observed, with one budding off from a 200 nm oil droplet.

Representative images (from 130 in total) obtained during the digestion of 10 mM Captex 355 (50 mg) are shown in Figure 5.7. In the sample taken at 0 min (pre-enzyme addition), only oil droplets up to 2 μ m in diameter were present. Following enzyme addition, collagen and protein aggregates were observed in close proximity in all samples. At 10 min (Panel B), oil droplets 100 – 600 nm in size were present; at 20 min (Panel C), there were 50 – 600 nm oil droplets present, while at 30 min, the oil droplet size had decreased to approximately 50 nm (Panel D). At 40 min, no oil droplets were evident with only micellar structures in the field of

view. As digestion proceeded, the micelle content indicated by the dark dots approximately 3 – 4 nm in diameter, increased.

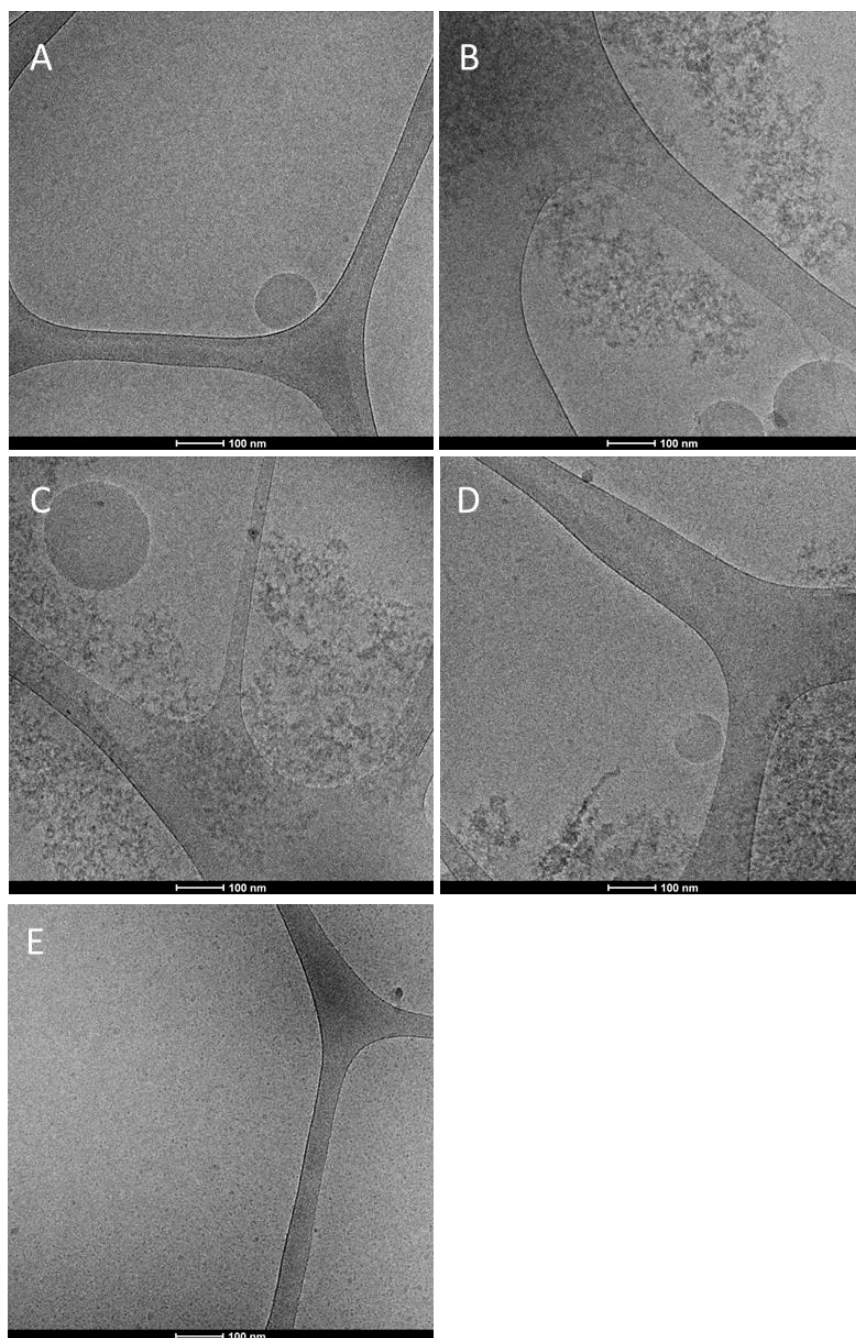


Figure 5.7: Cryo-TEM images of the inhibited samples of digestion medium during real time digestion of 10 mM Captex 355 (50 mg). Panel A = pre-digestion (0 min) showing a 100 nm oil droplet before enzyme addition. Panel B: after 10 min there are 100 – 200 nm oil droplets and protein aggregates. Panel C: at 20 min again 200 nm oil droplet and protein aggregates are present. At 30 min (Panel D) a small residual 100 nm oil droplet remains with protein aggregates, and at 40 min (Panel E) only micelles were evident.

Structure and morphology in equilibrium “assembled” systems representing the endpoint of tricaprylin digestion

Tricaprylin is a major component of Captex 355, and hence the structure formation by ‘pure’ tricaprylin and its digestion products is of interest to compare with the more complex lipid mixture. As a first step, equilibrium structures were prepared by addition of monoglyceride and fatty acid in bile salt and phospholipid mixtures to simulate the anticipated gastrointestinal state on digestion of tricaprylin. Systems were prepared by adding monocaprylin (MC) and caprylic acid (CA), in a 1:2 molar ratio expected on quantitative digestion of the triglyceride.

In both fasted and fed states (low and high bile salt and phospholipid concentrations), bile salt micelles co-existed with a lamellar phase (Figure 5.8). In both the fasted and fed states, with increased lipid loading, the micelle content increased (indicated by the broad hump centred on approximately $q = 0.16 \text{ \AA}^{-1}$) as did the intensity of the sharp lamellar diffraction peaks. This indicates that within the concentration regime studied, there was no change in distribution of structures with increasing lipid load.

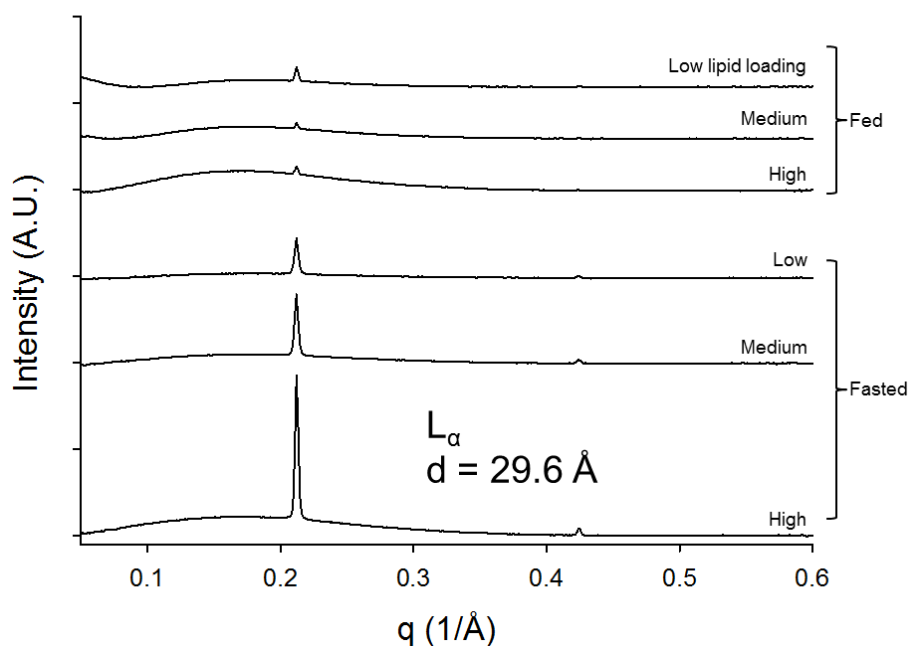


Figure 5.8: SAXS profiles of equilibrium assembled monocaprylin+caprylic acid-containing fed and fasted systems. Systems contained MC+CA in a 1:2 mol ratio at high (50:100 mM), medium (25:50 mM) and low (12.5:25 mM) concentrations respectively. The high and low lipid ‘assembled’ systems are representative of the 250 and 50 mg Captex 355 digestions respectively. The d-spacing of the lamellar (L_{α}) structures present is indicated in the inset.

The low monocaprylin+caprylic acid system in bile salt micelles (12.5:25 mM ratio), prepared in fasted and fed state micellar systems were also analysed by cryo-TEM (Figure 5.9). This system was intended to be indicative of complete digestion of the low Captex 355 digestion, although the concentration was slightly different (12.5 mM of equivalent triglyceride, compared to 10 mM Captex 355, and only C_8 lipids were present). In the fasted state, spherical and elongated liposomes 100 – 200 nm in diameter were present. Large lamellar fragments several hundred micrometers in length were also visible across the grid. This was consistent with the scattering data which a high intensity lamellar phase peak compared to the micellar hump. In the fed state, only micelles were evident which possessed a worm-like or thread-like structure. There was no co-existing lamellar phase observed in the imaging even though there were lamellar structures evident in the scattering profile for the fed low lipid system in Figure 5.8.

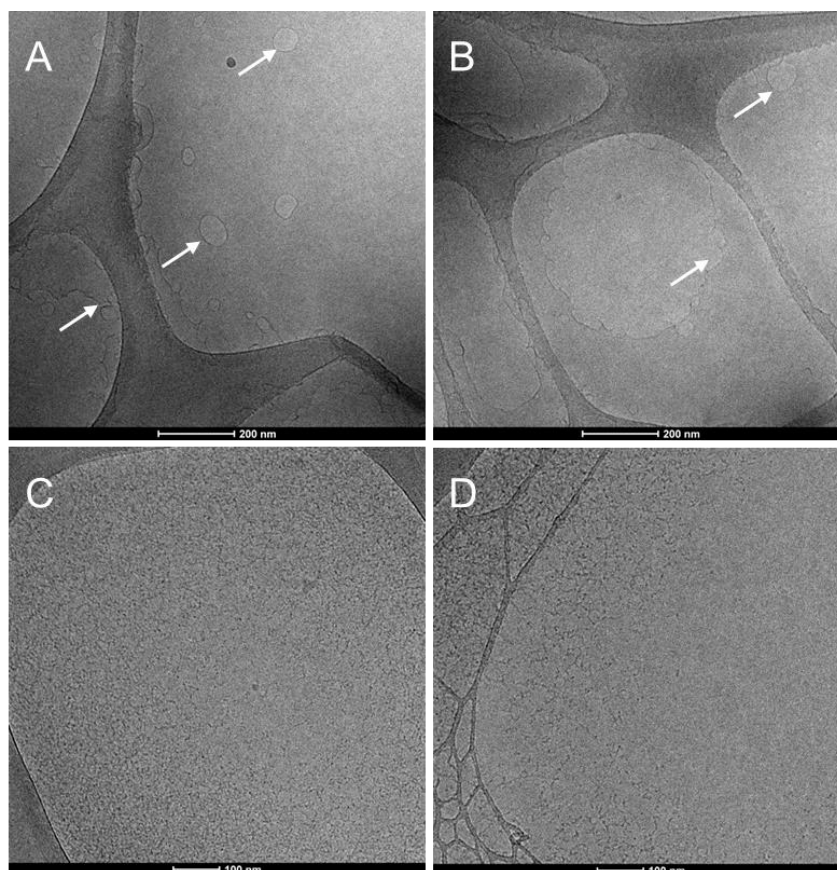


Figure 5.9: Cryo-TEM images of the assembled monocaprylin+caprylic acid system at 12.5:25 mM ratio ('low' lipid ratio). Panels A and B are from samples assembled in the fasted state media, showing lamellar phase, as indicated by liposomes 100 nm in diameter (arrows), and large lamellar fragments. Panels C and D are equivalent samples prepared in the fed state media showing micellar phase, indicated by the presence of worm-like or thread-like micelles.

Evolution of structure during tricaprylin digestion under fasted state conditions

For comparison of the structures present during digestion of Captex to that of 'pure' tricaprylin, tricaprylin was also digested in the flow through synchrotron configuration. The structural changes during a 30 min digestion of 5 mM tricaprylin (equivalent to 23.5 mg/ 10 mL digest) were monitored by SAXS. Micellar content was seen to increase over time, however there was no co-existing lamellar phase (Figure 5.10).

This was consistent with the low lipid digestion with Captex 355 where no lamellar structures were present, whereas the assembled system at the lowest lipid level demonstrated strong lamellar scattering, and it was expected that this may exist at an equivalent lipid concentration

in an assembled system, although the direct comparator system was not studied. Future experiments will determine the impact of increasing lipid load with pure tricaprylin and on lower (eg. 5 mM) assembled systems.

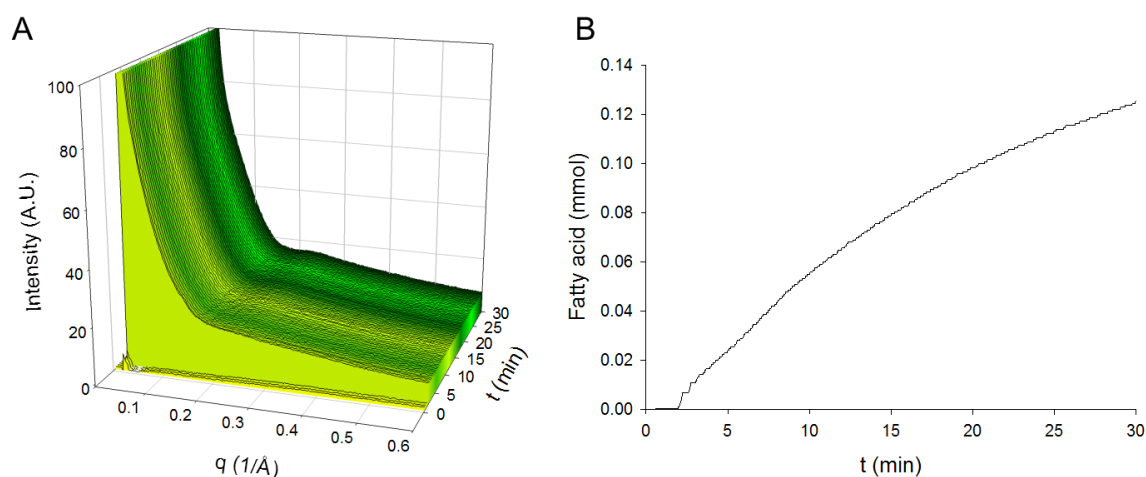


Figure 5.10: Digestion of 5 mM tricaprylin (approx. 25 mg) in the fasted state over 30 min at 37 °C studied by SAXS (Panel A) and titration profile (Panel B).

5.6 Discussion

The colloidal phases generated during lipid digestion are of interest due to their potential role in drug solubilisation, which may have implications for the performance of lipid-based drug formulations. Kossena *et al.* have demonstrated that these intermediate phases are important in drug solubilisation and trafficking [4].

Formation of vesicle phase is linked to digestion kinetics

The lipid content was observed to influence the colloidal structures formed during digestion of Captex 355 in the fasted state. At low lipid level (50 mg, ~10 mM) only micelles were formed (Figures 5.3 and 5.7), whereas a high lipid level (250 mg, ~50 mM) a lamellar phase was evident which was coincident with vesicle formation by cryoTEM (Figures 5.2 and 5.5). This is believed to constitute the first direct evidence of the generation of a vesicular phase during *in vitro* digestion of high concentrations of the MCT Captex 355. The propensity for the vesicle phase to support supersaturated drug concentrations during *in vitro* digestion is

now clear from past studies; only high lipid load digestions exhibit the effect, and in low lipid loads, where micelles are the only colloidal structure present, high drug precipitation occurs. Thus the structure-digestion-performance link in this system was therefore established.

The kinetics of the digestion of Captex 355 shows a two-stage digestion process. This is not normal during triglyceride digestion – neither tributyrin [27], often used to calculate the activity of pancreatin, nor soybean oil [9] (a long chain triglyceride comprised mainly of triolein with C₁₈ unsaturated fatty acid chains) show such behaviour. This interesting phenomenon has been known for over a decade in previous studies [9] but no explanation has been evident prior to the findings in Figure 5.2, where there is a direct temporal relationship between the onset of the lamellar phase formation and the discontinuity in the digestion kinetics.

The morphology of colloidal samples formed during digestion of a lipid-based formulation, and their similarity with *ex vivo* samples of human intestinal fluid has been previously studied by cryo-TEM and AFM [14, 19-21]. The sequence of phase changes observed in the current work was in good agreement with these studies and other reports [17], where at the beginning of lipid digestion, only oil droplets and protein were present, and unilamellar and bilamellar vesicles were seen to develop and dominate at the end of digestion. It has been reported that vesicles co-existing with worm-like mixed micelles should be present at the end of digestion, depending on bile salt levels [8, 28, 29]. Micelles were present throughout digestion, and co-existed with unilamellar and multilamellar vesicles, which is in agreement with previous reports, however previous reports used long chain triglycerides [14, 17, 19].

In the current study, vesicles were seen to ‘bud-off’ from the surfaces of the oil droplets, suggesting the lipid digestion products were removed from the surface and detached to form vesicles and micelles. Müllertz *et al.* also observed a bilayer fragment loosely associated with an oil droplet in *ex vivo* samples [21]. During digestion in the fasted state, only one trilamellar vesicle was observed, and unilamellar vesicles and bilamellar vesicles were found to be dominating. This is in agreement with previous findings, which reported that in the fed state, the higher levels of phospholipid favours formation of multivesicular structures [19, 20]. However, this appears to be in contrast to the SAXS data and cryo-TEM images for the fed-state ‘assembled’ monocaprylin+caprylic acid system in Figures 5.8 and 5.9 which indicate reduced or absence of lamellar phase structures respectively.

The lattice dimensions for the lamellar spacing for the digested Captex 355 was 30.1 Å, which was slightly higher than that shown on Figure 5.8 for the ‘assembled’ monocaprylin+caprylic acid system (29.6 Å). The lattice parameter for the lamellar phase formed in an equivalent ‘assembled’ C₁₀ monoglyceride+fatty acid system was 34.6 Å (data not shown), confirming that the dimensions scaled with average lipid chain length as anticipated.

Segregation of lipids during the digestion process may be possible, for example leading to vesicles composed primarily of monoglyceride, and where fatty acid is incorporated into micellar structures. However, it is likely that the vesicles actually consist of a mixture of monoglyceride and fatty acid – not only because of the agreement with the expected lattice dimensions from the assembled equilibrium mixtures, but also due to the fact that the co-existing oil droplets indicates that it is generation of a separate phase with different local composition to the droplets that constitutes the vesicles, and not a phase change due to a global change in concentration.

“Assembled” equilibrium systems vs. *in vitro* lipolysis and sample inhibition

The dynamic real time Captex 355 digestion samples were compared to equilibrium samples prepared by assembly of component monoglycerides and fatty acids for direct comparison of the two approaches. The low monocaprylin+caprylic acid system in bile salt micelles (12.5:25 mM ratio), prepared in fasted and fed state micellar systems exhibited a micellar phase and co-existing lamellar phase, as indicated in the scattering data. The cryo-TEM results however suggest that whilst there were large lamellar fragments in the fasted state, there were only worm-like or thread-like micelles present in the fed state. This suggests that “assembled” equilibrium systems have their limitations as they are not representative of the dynamic nature of the GI environment, thus dynamic lipolysis experiments measurements are more relevant. The vesicle phase was not apparent in fasted-state low lipid digestions, where the bile salt to lipid ratio was 1:2. The absence of lamellar structure in both the cryo-TEM images in Figure 5.7 and the dynamic scattering data in Figure 5.3 might be expected considering the higher bile salt to lipid ratio compared to the high lipid load digest, where the ratio was 1:10. Previous work has shown further interaction of vesicles with bile salts results in the transition to mixed micelles [4, 8, 17, 28]. The finding is also consistent with the scattering data obtained after addition of 55 mM bile salt to the end point of the 50 mM lipid digestion in Figure 5.2. The ‘assembled’ fed system did show some lamellar phase structure was present in the fed

state where the ratio varied from approximately 1: 0.6 to 1: 2.5. The exact reason for this difference is not yet apparent, again highlighting the difficulties in extrapolation of data from equilibrium assembled systems to predict the likely structures formed during dynamic digestion processes.

The bile salt/phospholipid mixture used in both preparation of the assembled systems and in the dynamic digestion studies is a highly simplified version of the intestinal contents. The use of a complex bile salt mixture to better represent the likely *in vivo* content was of course possible, but studies have shown that increased complexity does not necessarily alter the behaviour of such systems [30] and inter-person variability is high, meaning that the selected complex mixture may not be representative of bile in many cases.

The lipase inhibitor, 4-bromophenylboronic acid is often used to halt digestion when sampling is required during *in vitro* experiments to measure aspects such as drug precipitation or lipid composition. Whilst the inhibitor performs well, there has not been an attempt to directly confirm whether structural aspects are influenced by its presence. Cryo-TEM also revealed subtle differences between samples that were retrieved from digestion and immediately vitrified, compared to samples treated with a lipase inhibitor. Fewer liposome structures were observed in the end stages of digestion in the inhibited sample compared to the corresponding time-points in the real time samples. The lipase inhibitor is typically prepared in methanol. There is potential for the methanol, or less likely the inhibitor, to interact with those structures and either solubilize the lipids comprising the structures or induce a transition to other, likely micellar structures. Although the structure formed in this case were not dramatically different to the real time samples, care must certainly be taken in interpretation of samples containing enzyme inhibitor and the quantity of solvent used should be minimized.

Implications

The solubilization of drug has been shown to critically depend on colloidal structure and lipid comprising the structures [4, 31]. Consequently, an understanding of the structures that are present during digestion that give rise to beneficial effects, such as potential to support supersaturation of drug on digestion, are of interest. This level of structural understanding has potential to lead to rational engineering of formulations to generate specific structures on digestion to optimize the pre-absorptive environment. Until there is a clear understanding of

the complex colloidal behaviour of these relatively simple lipid formulations, development of more advanced and complex approaches such as self-nanoemulsifying systems [32-36] and solid matrix lipid-based formulations [37, 38] will remain empirical by necessity. It remains to be seen whether the dynamic colloidal behaviour observed here and in other similar studies translates to the *in vivo* scenario, potentially leading to increased drug absorption and bioavailability.

5.7 Conclusion

Insights into the structural aspects of the digestion of medium chain triglycerides have been obtained by coupling the *in vitro* lipolysis model with sSAXS and cryo-TEM. A putative vesicular phase formed on digestion of MCT was confirmed and its structural attributes determined. The dependence on bile salt to lipid ratio demonstrated the lipid dependence on formation of the lamellar structures on digestion. Comparison of cryo-TEM images of real time samples compared with inhibited digestion samples demonstrated potential for differing structures to be formed, highlighting the need to conduct real time structural investigations rather than relying on analysis of inhibited samples by offline techniques. The comparison with ‘assembled’ equilibrium samples, representative of the post-digestion environment also indicated some differences in structures formed, again highlighting the caution in interpretation of likely dynamic behaviour from ‘static’ samples.

Acknowledgements

This research was undertaken on the SAXS/WAXS beamline at the Australian Synchrotron, Victoria. Funding is acknowledged from the Australian Research Council under the Discovery Projects scheme DP120104032. BJB is a recipient of an Australian Research Council Future Fellowship (FT120100697).

5.8 References

1. Porter, C.J.H., Trevaskis, N.L., and Charman, W.N., *Lipids and lipid-based formulations: Optimizing the oral delivery of lipophilic drugs*. Nat Rev Drug Discov, 2007. **6**(3): p. 231-248.
2. Patton, J.S. and Carey, M.C., *Watching fat digestion*. Science, 1979. **204**(4389): p. 145-148.
3. Staggers, J.E., et al., *Physical-chemical behavior of dietary and biliary lipids during intestinal digestion and absorption. 1. Phase behavior and aggregation states of model lipid systems patterned after aqueous duodenal contents of health adult human-beings*. Biochemistry, 1990. **29**(8): p. 2028-2040.
4. Kossena, G.A., et al., *Separation and characterization of the colloidal phases produced on digestion of common formulation lipids and assessment of their impact on the apparent solubility of selected poorly water-soluble drugs*. J Pharm Sci, 2003. **92**(3): p. 634-648.
5. Kossena, G.A., et al., *Probing drug solubilization patterns in the gastrointestinal tract after administration of lipid-based delivery systems: A phase diagram approach*. J Pharm Sci, 2004. **93**(2): p. 332-348.
6. Kossena, G.A., et al., *A novel cubic phase of medium chain lipid origin for the delivery of poorly water soluble drugs*. J Control Release, 2004. **99**(2): p. 217-229.
7. MacGregor, K.J., et al., *Influence of lipolysis on drug absorption from the gastro-intestinal tract*. Adv Drug Deliv Rev, 1997. **25**(1): p. 33-46.
8. Hernell, O., Staggers, J.E., and Carey, M.C., *Physical-chemical behavior of dietary and biliary lipids during intestinal digestion and absorption. 2 Phase-analysis and aggregation states of luminal lipids during duodenal fat digestion in healthy adult human-beings*. Biochemistry, 1990. **29**(8): p. 2041-2056.
9. Sek, L., et al., *Evaluation of the in-vitro digestion profiles of long and medium chain glycerides and the phase behaviour of their lipolytic products*. J Pharm Pharmacol, 2002. **54**(1): p. 29-41.
10. Kaukonen, A.M., et al., *Drug solubilization behavior during in vitro digestion of simple triglyceride lipid solution formulations*. Pharm Res, 2004. **21**(2): p. 245-253.
11. Lee, K.W.Y., Porter, C.J.H., and Boyd, B.J., *The effect of administered dose of lipid-based formulations on the in vitro and in vivo performance of cinnarizine as a model poorly water-soluble drug*. J Pharm Sci, 2013. **102**(2): p. 565-578.
12. Embleton, J.K. and Pouton, C.W., *Structure and function of gastro-intestinal lipases*. Adv Drug Deliv Rev, 1997. **25**(1): p. 15-32.
13. Fatouros, D.G., et al., *Structural development of self nano emulsifying drug delivery systems (SNEDDS) during in vitro lipid digestion monitored by small-angle X-ray scattering*. Pharm Res, 2007. **24**(10): p. 1844-1853.
14. Salentinig, S., et al., *Transitions in the internal structure of lipid droplets during fat digestion*. Soft Matter, 2011. **7**(2): p. 650-661.
15. Warren, D.B., et al., *Real time evolution of liquid crystalline nanostructure during the digestion of formulation lipids using synchrotron small-angle X-ray scattering*. Langmuir, 2011. **27**(15): p. 9528-9534.

16. Patton, J.S., et al., *The light-microscopy of triglyceride digestion*. Food Microstruct, 1985. **4**(1): p. 29-41.
17. Rigler, M.W., Honkanen, R.E., and Patton, J.S., *Visualization by freeze fracture, in vitro and in vivo, of the products of fat digestion*. J Lipid Res, 1986. **27**(8): p. 836-57.
18. Rigler, M.W. and Patton, J.S., *The production of liquid-crystalline product phases by pancreatic lipase in the absence of bile salts: A freeze-fracture study*. Biochimica Et Biophysica Acta, 1983. **751**(3): p. 444-454.
19. Fatouros, D.G., Bergenstahl, B., and Mullertz, A., *Morphological observations on a lipid-based drug delivery system during in vitro digestion*. Eur J Pharm Biopharm, 2007. **31**(2): p. 85-94.
20. Fatouros, D.G., et al., *Colloidal structures in media simulating intestinal fed state conditions with and without lipolysis products*. Pharm Res, 2009. **26**(2): p. 361-374.
21. Müllertz, A., et al., *Insights into intermediate phases of human intestinal fluids visualized by atomic force microscopy and cryo-transmission electron microscopy ex vivo*. Mol Pharm, 2012. **9**(2): p. 237-247.
22. Dubochet, J., et al., *Cryo-electron microscopy of vitrified specimens*. Q Rev Biophys, 1988. **21**(2): p. 129-228.
23. Kaukonen, A., et al., *Drug solubilization behavior during in vitro digestion of suspension formulations of poorly water-soluble drugs in triglyceride lipids*. Pharm Res, 2004. **21**(2): p. 254-260.
24. Gargouri, Y., Moreau, H., and Verger, R., *Gastric lipases: Biochemical and physiological studies* Biochimica Et Biophysica Acta, 1989. **1006**(3): p. 255-271.
25. Dressman, J.B., et al., *Upper gastrointestinal (GI) pH in young, healthy men and women*. Pharm Res, 1990. **7**(7): p. 756-761.
26. *Small angle X-ray scattering*, ed. Glatter, O.K., O. 1982, London: Academic Press.
27. Alvarez, F.J. and Stella, V.J., *The role of calcium-ions and bile-salts on the pancreatic lipase-catalyzed hydrolysis of triglyceride emulsions stabilized with lecithin*. Pharm Res, 1989. **6**(6): p. 449-457.
28. Schurtenberger, P., Mazer, N., and Kanzig, W., *Micelle to vesicle transition in aqueous solutions of bile-salt and lecithin*. J Phys Chem, 1985. **89**(6): p. 1042-1049.
29. Hofmann, A.F. and Borgstrom, B., *Intraluminal phase of fat digestion in man: The lipid content of micellar and oil phases of intestinal content obtained during fat digestion and absorption*. J Clin Investig, 1964. **43**(2): p. 247-&.
30. Soderlind, E., et al., *Simulating fasted human intestinal fluids: Understanding the roles of lecithin and bile acids*. Mol Pharm, 2010. **7**(5): p. 1498-1507.
31. Christensen, J.O., et al., *Solubilisation of poorly water-soluble drugs during in vitro lipolysis of medium- and long-chain triacylglycerols*. Eur J Pharm Biopharm, 2004. **23**(3): p. 287-296.

32. Pouton, C.W., *Formulation of poorly water-soluble drugs for oral administration: Physicochemical and physiological issues and the lipid formulation classification system*. Eur J Pharm Biopharm, 2006. **29**(3-4): p. 278-287.
33. Gursoy, R.N. and Benita, S., *Self-emulsifying drug delivery systems (SEDDS) for improved oral delivery of lipophilic drugs*. Biomed Pharmacother, 2004. **58**(3): p. 173-182.
34. Thomas, N., et al., *Influence of lipid composition and drug load on the in vitro performance of self-nanoemulsifying drug delivery systems*. J Pharm Sci, 2012. **101**(5): p. 1721-1731.
35. Gershanik, T. and Benita, S., *Self-dispersing lipid formulations for improving oral absorption of lipophilic drugs*. Eur J Pharm Biopharm, 2000. **50**(1): p. 179-188.
36. Pouton, C.W., *Lipid formulations for oral administration of drugs: Non-emulsifying, self-emulsifying and 'self-microemulsifying' drug delivery systems*. Eur J Pharm Biopharm, 2000. **11**: p. S93-S98.
37. Tan, A., et al., *Silica nanoparticles to control the lipase-mediated digestion of lipid-based oral delivery systems*. Mol Pharm, 2010. **7**(2): p. 522-532.
38. Tan, A., et al., *Hybrid nanomaterials that mimic the food effect: Controlling enzymatic digestion for enhanced oral drug absorption*. Angew Chem Int Ed, 2012. **51**(22): p. 5475-5479.

Chapter 6. Immobilised Lipase for Enhanced Structural Resolution

Chapter 6. Immobilised Lipase for Enhanced Structural Resolution

The work presented in this chapter has published as: Phan S., Salentinig S., Hawley A., Boyd B.J., *Immobilised lipase for in vitro lipolysis experiments*. J Pharm Sci, 2015. **104**(4): p.1311-1318.

6.1 Declaration

Declaration by candidate:

In the case of Chapter 6, the nature and extent of my contribution to the work was the following:

Nature of contribution	Extent of contribution
Research design, performance of data collection and analysis, manuscript preparation	85%

The following co-authors contributed to the work:

Name	Nature of contribution
Stefan Salentinig	Input into manuscript preparation
Adrian Hawley	Intellectual input on SAXS operation
Ben J. Boyd	Supervision, intellectual input, input into manuscript preparation

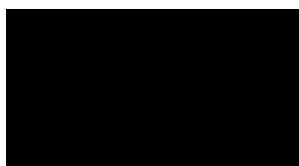
The undersigned hereby certify that the above declaration correctly reflects the nature and extent of the candidate's and co-authors' contributions to this work.

Candidate's signature:



Date: 21/08/15

Main supervisor's signature:



Date: 21/08/15

6.2 Immobilised Lipase for *In Vitro* Lipolysis Experiments

Stephanie Phan¹, Stefan Salentinig¹, Adrian Hawley², Ben J. Boyd^{1,3}

¹ Drug Delivery, Disposition and Dynamics, Monash Institute of Pharmaceutical Sciences, Monash, 381 Royal Parade, Parkville, VIC 3052, Australia

² SAXS/WAXS beamline, Australian Synchrotron, 800 Blackburn Road, Clayton, VIC 3168, Australia

³ ARC Centre of Excellence in Convergent Bio-Nano Science and Technology, Monash Institute of Pharmaceutical Sciences, Monash University (Parkville Campus), 381 Royal Parade, Parkville, VIC 3052, Australia

Received August 27th 2014 and published online 28th January 2015.

Citation: J. Pharm. Sci. (2015) 104:1311-1318

DOI: 10.1002/jps.24327

Abstract

In vitro lipolysis experiments are used to assess digestion of lipid-based formulations, and probe solubilisation by colloidal phases during digestion. However proteins and other biological components in the pancreatin often used as the lipase result in high background scattering when interrogating structures using scattering approaches, complicating the resolution of colloidal structures. In this study, to circumvent this problem, a modified *in vitro* digestion model employing lipase immobilized on polymer beads, which allows for separation of the lipid digestion components during lipolysis, was investigated. Titration of the fatty acids released during digestion of medium chain triglycerides using pancreatin compared to immobilized lipase, combined with HPLC was used to follow the digestion, and small angle X-ray scattering was used to determine colloidal structure formation. Digestion of medium chain triglycerides at the same nominal activity revealed that for the immobilized lipase, a longer digestion time was required to achieve the same extent of digestion. However, the

same structural endpoint was observed, indicating that structure formation was not affected by the choice of lipase used. Lipolysis with immobilized lipase led to the reduction of parasitic scattering, resulting in clearer and more defined scattering from the structures generated by the lipolysis products.

Keywords: immobilised lipase, lipid digestion, *in vitro* lipolysis, lipid-based drug delivery, synchrotron small angle X-ray scattering

Abbreviations:

BS, bile salt

CALB, lipase B from *Candida antarctica*

FA, fatty acid

SAXS, small angle X-ray scattering

TBU, tributyrin units

6.3 Introduction

Lipid-based formulations (LBF) are of interest for the delivery of poorly water-soluble drugs. During the lipolysis of triglycerides, monoglycerides (MG) and fatty acids (FA) are produced. These combine with endogenous amphiphilic molecules in the gastrointestinal tract to form bile salt/phospholipid mixed micelles and other liquid crystalline phases. These structures are important in maintaining drug solubilisation in the gastrointestinal environment, leading to enhanced absorption and bioavailability of co-administered drugs [1, 2].

In vitro lipolysis experiments using a pH stat apparatus are frequently utilised to evaluate digestion of LBF to examine drug disposition, solubilisation and precipitation, with the aim to achieve *in vitro-in vivo* correlations. The study of lipolysis from a compositional aspect remains largely reliant on the titration profile. The pH stat follows the progress of triglyceride digestion, by titrating against the fatty acids liberated.

Understanding structure formation during lipolysis remains a major hurdle, due to lack of real time methods to elucidate structural changes during the dynamic process, and this has recently

been reviewed [3]. Until recently, studies have been limited to microscopy, scattering and spectroscopic techniques to investigate equilibrium structures that are assembled from the individual components representing the end point of lipid digestion. The field has since progressed to the use of *in vitro* lipolysis models coupled to synchrotron small angle X-ray scattering [4, 5], where the digest medium is flowed through a capillary placed in the X-ray beam for probing of nanostructure formation in the millisecond time frame.

The current protocol for *in vitro* digestion studies often utilizes porcine pancreatin extract [4, 6-8] as the lipase source to simulate digestion in the small intestine. However there are many proteins and enzymes in the crude extract which contribute to high undesired scattering from pancreatic components, when using techniques such as small angle X-ray scattering (SAXS) and dynamic light scattering (DLS) to understand the structural evolution caused by lipolysis products in these systems. These may obscure scattering from colloidal species produced on digestion, and complicate the resolution of structures that are present.

Novozym[®] 435 is a commercially available recombinant lipase B from *Candida antarctica* (CALB) manufactured by Novozymes. It is immobilized by physical adsorption to macroporous polyacrylate resin, which has an average particle size of 315-1000 μm , surface area of 130 m^2/g and pore diameter 150 \AA [9, 10]. Immobilized lipases are widely used as biocatalysts in the food, detergent, textile, cosmetic and pharmaceutical industries, for example, hydrolysis of triglycerides to produce fatty acids and esterification, transesterification, aminolysis in organic solvents. Immobilized lipases have been successfully manufactured by ionic binding, covalent binding, cross-linking, entrapment and encapsulation. Advantages of immobilized lipase over free lipase are that they are cost effective and reusable, for continuous large-scale commercial processes, has enhanced chemical and thermal stability and exhibit high enantioselectivity [11]. In the context of *in vitro* lipolysis experiments, having enzyme immobilized on beads enables separation from the digesting medium which may improve the ability to study structural aspects using scattering methods.

Consequently the aim of this study was to investigate the possibility of using lipase immobilised to polymer beads as an alternative to powdered pancreatin to improve the current method for studying structures during lipolysis. To the best of our knowledge immobilized lipase has not been applied to *in vitro* lipolysis experiments. Digestion of medium chain triglycerides (tricaprylin and Captex 355, a commonly used formulation lipid consisting of a mixture of tricaprylin and tricaprln, were assessed to compare the activity, effect of pH,

temperature, and buffer type and resulting structural detail after digestion with immobilized lipase compared to pancreatin extract.

6.4 Experimental

Materials

Captex 355 (MCT composed of 59% caprylic acid (C₈), 40% capric acid (C₁₀), <1% lauric acid (C₁₂) as stated in the product information) was obtained from Abitec Corporation (Janesville, WI, USA) and used without further purification. Tributyrin (>98%) was obtained from TCI Co. Ltd (Kawaguchi City, Saitama, Japan). Tricaprylin (>99%), Tris maleate (reagent grade), bile salt (sodium taurodeoxycholate, >95%) and 4-bromophenylboronic acid (4-BPBA, >95%) were purchased from Sigma Aldrich (St. Louis, MO, USA). Sodium azide was purchased from Merck Schuchardt OHG (Eduard-Buchner-Straße, Hohenbrunn, Germany). Phospholipid (1,2-dioleoyl-sn-glycero-3-phosphocholine, DOPC) was from Trapeze Association Pty Ltd (Clayton, Victoria, Australia). USP grade pancreatin extract was purchased from Southern Biologicals (Nunawading, Victoria, Australia). Novozym[®] 435 was obtained from Novozymes (Bagsvaerd, Denmark). Calcium chloride (>99%) was obtained from Ajax Finechem (Seven Hills, NSW, Australia). Sodium chloride (>99%) was purchased from Chem Supply (Gillman, SA, Australia). HPLC grade methanol (MeOH) was purchased from Merck. Trifluoroacetic acid (TFA) was obtained from Pierce (Rockford, Illinois, USA). Water used was sourced from a Millipore water purification system using a Quantum[™] EX Ultrapure Organex cartridge (Millipore, Sydney, Australia).

Determination of lipolytic activity

The lipolytic activity was determined using the pH stat method, which was used to construct a calibration curve. Digestion buffer was prepared with 50 mM Tris maleate, 5 mM CaCl₂·2H₂O, 150 mM NaCl, 6 mM NaN₃ as anti-microbial agent, and adjusted to pH 6.5. The substrate used was 6 g tributyrin [6, 12] dispersed in 10 mL of digestion buffer for immobilized lipase or 9 mL digestion buffer for pancreatic lipase respectively, which itself was dispersed in 1 mL buffer as below. The quantity of digestion buffer used differed depending on the lipase source to maintain a constant buffer:tributyrin ratio.

Immobilized lipase was added to the test system at different masses; whereas the pancreatic lipase was prepared by weighing the required mass of the pancreatic lipase in a centrifuge tube, adding 5 mL digestion buffer to form a suspension, which was adjusted to pH 6.5 by the addition of NaOH. The suspension was magnetically stirred for 15 min, and centrifuged for 15 min at 3500 rpm at 25 °C as a compromise to prevent a denaturation of the lipase and a decline in activity, and minimize the temperature difference between the lipase suspension and the digestion medium. Fresh pancreatin extracts were prepared each day and the supernatant was kept at room temperature prior to use.

The reaction was typically performed at 37 °C and in Tris buffer pH 7.5 and lipase (mg immobilized or 1 mL pancreatic lipase suspension, containing 10 000 TBU units) was added to initiate digestion and the reaction was titrated with 0.6 M NaOH. In the case where the influence of buffer type (Tris or PBS), temperature (27, 37 or 50 °C) or pH (6.5, 7.5 or 8.5) on activity was studied, these variables were changed accordingly. The activity was defined in Tributyrin Units (TBU) where 1 TBU is the amount of enzyme used to liberate 1 µmol of titratable free fatty acid per minute. A plot of µmol FA titrated per minute yields an initial linear portion, where the slope gives the activity in TBU per mL of digest under the assay conditions.

***In vitro* lipolysis**

A micellar solution was prepared in digestion buffer with bile salt (sodium taurodeoxycholate) and phospholipid (DOPC) at concentrations of 5 mM:1.25 mM as simulated fasted intestinal fluid [13, 14]. The phospholipid was dissolved in chloroform in a round bottom flask and the chloroform was evaporated off under vacuum to leave a thin film. Bile salt and digestion buffer were added and the solution was placed in a sonicator bath for 30 min, before it was stored at 4 °C to equilibrate overnight. Pancreatin extracts were prepared by adding 4 g of porcine pancreatin powder to 5 mL of digestion buffer to achieve an activity of 10 000 TBU/mL. The suspension was magnetically stirred for 15 min, and centrifuged for 15 min at 3500 rpm at 25 °C.

In vitro digestion studies were performed using a pH-stat auto titrator (Metrohm, Switzerland), similar to previous reports [4, 6, 8, 15, 16]. Lipid was added to the fasted simulated intestinal fluid in the thermostatted digestion vessel at 37 °C, and magnetically stirred for 5 min for complete mixing and thermal equilibration. The pH was adjusted to 6.5 ± 0.003 , chosen as a

compromise between the optimum for pancreatic lipase activity pH (6 – 10) [17] and duodenal pH (5.0 – 6.5) [18, 19]. On addition of lipase (~1000 TBU/mL digest) the pH-stat titrated the digestion with 0.6 M NaOH in order to maintain pH 6.500 ± 0.003 . Digestion was allowed to proceed for up to 8 hr, to ensure a similar extent of digestion, in which the degree of enzymatic digestion of the lipid was reflected in the volume of NaOH used to neutralize the fatty acids liberated during the digestion process.

A blank digestion without lipid but with bile salt micelles present was performed as a background experiment, to account for fatty acids that were produced from phospholipids and was subtracted from the profiles for the lipolysis experiments.

Lipid composition in digestion medium

A few techniques have been used to separate and analyze lipid digestion products including HPTLC, GC and HPLC-MS. However these have shortcomings such as long run times, labour intensive, high cost, requirement of specialized equipment and use of volatile solvents. Reversed phase HPLC using refractive index detection has recently been shown to be a useful tool to determine lipid composition following *in vivo* digestion that it is simple and non-destructive [20]. Thus this method was employed to separate and quantify fatty acid analytically during digestion for correlation with total fatty acid produced as indicated by the pH stat titration. Samples (200 μ L) were taken during digestion for analysis of fatty acid content by HPLC. To halt digestion in the sample lipase inhibitor (20 μ L of 0.05 M 4-BPBA in methanol) was added to Eppendorf tubes, where the methanol was evaporated off prior to addition of samples.

Reversed-phase high performance liquid chromatography (HPLC) - Samples were analysed for fatty acid content and separated by an isocratic reversed-phase HPLC method using a 4.6×150 mm Phenomenex Luna C₈ (2) (5 μ m, 100 Å) analytical column, with a 15×3 mm Brownlee RP-18 (7 μ m) guard column. The HPLC system consisted of a Shimadzu CBM-20A system controller, LC-20AD solvent delivery module, SIL-20A auto sampler and a CTO-20A column oven set at 40 °C, coupled to a RID-10A differential refractometric detector (Shimadzu Corporation, Kyoto, Japan). An injection volume of 40 μ L was used to separate caprylic acid and capric acid using a mobile phase consisting of MeOH/water (75:25 v/v) with 0.1% TFA (v/v of total mobile phase) at a flow rate of 1 mL/min. Assay parameters are shown in Table SI-6.1.

Preparation of standards and samples - A stock solution of caprylic and capric acid was prepared at a concentration of 10 mg/mL in methanol. A set of standards containing 0.1, 0.2, 0.5, 1.0 and 2.0 mg/mL of both lipids was prepared by mixing and dilution of the stock solution in the mobile phase. All stock solutions and standards were stored at 4 °C before analysis. Calibration curves were prepared by plotting the area under the curve against known concentration of standard solutions. Lipolysis samples were diluted in mobile phase prior to HPLC analysis. Unknown sample concentrations were calculated from the standard equation $y = mx + c$, as determined by the linear regression of the unweighted standard curve.

Assay validation - Validation of the HPLC assay was run over three days and the results are shown in Table SI-6.2. Intra-assay accuracy was determined by replicate analysis (n=5) of standard solutions of lipids at three concentrations (0.1, 1.0 and 2.0 mg/mL). Inter-assay accuracy was determined on three separate days. The data were expressed as a percentage of the measured concentration over the theoretical concentration, where mean accuracy was within $\pm 15\%$ of the theoretical concentration. Intra-assay precision (repeatability) and inter-assay precision (reproducibility) were calculated in all three runs for each lipid at all three concentrations and expressed as the coefficient of variation (% CV) of replicate assays. Linearity was performed on standard curves for each run and linearity was fulfilled when the correlation coefficient (r^2) of the regression line was >0.99 .

Synchrotron small angle X-ray scattering (SAXS)

SAXS measurements were performed at the SAXS/WAXS beamline [21] at the Australian Synchrotron. An X-ray beam with a wavelength of 1.1271 Å (11 keV) was used. A sample to detector distance of 1588 mm covered the q -range $0.01 < q < 0.7 \text{ \AA}^{-1}$ with q being the magnitude of the scattering vector defined as $q = (4\pi/\lambda)\sin(\theta/2)$, λ being the wavelength and θ , the scattering angle.

Samples were drawn into a capillary which was fixed in a thermostatted metal heating block accurate to $\pm 0.1 \text{ }^\circ\text{C}$, for measurements taken at 37 °C. The 2D SAXS patterns were acquired over 1 s using a Pilatus 1M detector with active area $169 \times 179 \text{ mm}^2$ and with a pixel size of 172 μm . 2D scattering patterns were integrated into the 1D scattering function $I(q)$ using the in-house developed software package scatterBrain. Scattering curves are plotted as a function of relative X-ray intensity, $I(q)$, versus q .

6.5 Results

Lipolytic activity

Activity of the immobilized lipase was very different to that of the pancreatin extract (Figure 6.1). The immobilized lipase displayed consistent lipolytic activity towards tributyrin where it increased linearly with concentration, with approximately 37 TBU/mg immobilized lipase. In contrast, the activity of pancreatic lipase reached a plateau with increasing concentration, approximately 12 TBU/mg dry pancreatin powder at saturation.

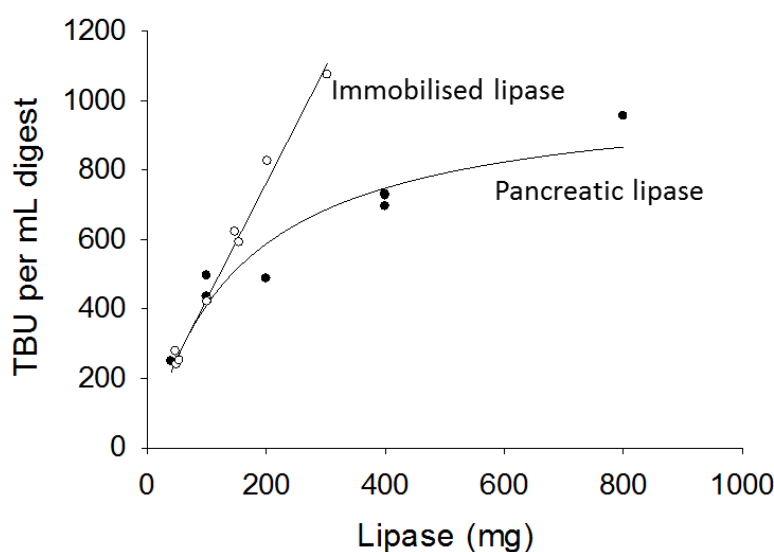


Figure 6.1: Comparison of activity (TBU) of immobilized (open circles) and pancreatic (closed circles) lipase with increasing mass in Tris buffer pH 7.5 at 37 °C

Factors affecting the activity of immobilized lipase

The influence of buffer, temperature and pH on lipolytic activity of immobilized lipase was assessed to further understand the physico-chemical understanding of digestion, as these factors may affect lipase activity. No significant buffer- or pH-dependency was observed on the activity (Figure 6.2A and C). Lipase activity was however observed to vary with temperature as reported in the product information (Figure 6.2B). An increase in activity was observed with increasing temperature as anticipated due to an increase in kinetic energy in the system and lowering of the activation energy required for the reaction, and a decrease in temperature hampered the reaction.

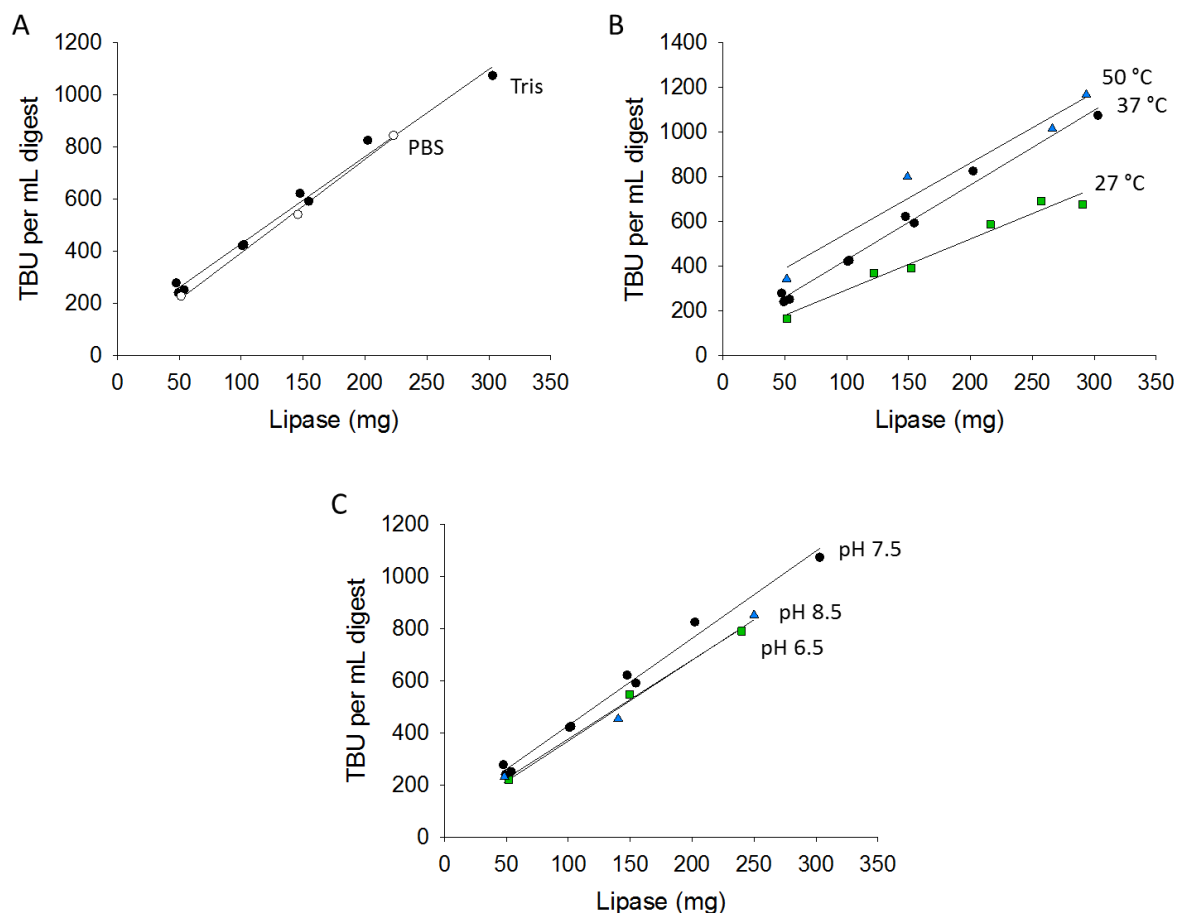


Figure 6.2: Effect of reaction variables on activity of immobilized lipase in A) Buffer type (Tris (closed circles) and PBS (open circles) pH 7.5 at 37 °C). B) Temperature (Tris buffer pH 7.5). C) Buffer pH (Tris buffer pH 6.5, 7.5 and 8.5 at 37 °C).

Digestion kinetics and quantitation of fatty acid released during *in vitro* lipolysis of medium chain triglycerides

The kinetics of digestion when the immobilized lipase was added to initiate digestion of tricaprylin and Captex 355 in the fasted state was slower compared to pancreatic lipase. A longer digestion time was required to achieve a plateau in the titration curve, indicative of the end of lipolysis of ~50 mM medium chain triglyceride, Captex 355 (Figure 6.3A). The percent digested was calculated to be 69.3 and 84.1% for pancreatic and immobilized lipase respectively. This was calculated from the number of moles of NaOH added during the reaction, on the basis that one mole of triglyceride is hydrolysed to produce 1 mole of 2-monoglyceride and 2 moles of fatty acid [22, 23]. Notably, the digestion profiles of Captex 355 for both the lipases had a sigmoidal shape but covered different time scales.

A strong correlation between the moles of fatty acid determined by pH stat titration and HPLC with refractive index detection during lipolysis was observed (Figure 6.3). However, at the endpoint of digestion, the higher fatty acid content determined by HPLC was higher at 92.7 and 90.6% for pancreatic and immobilized lipase respectively.

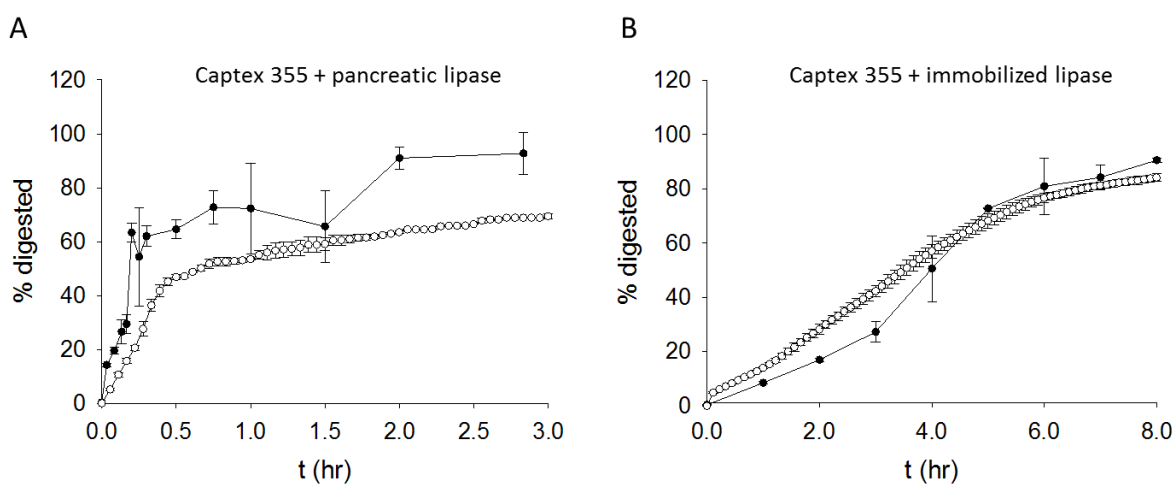


Figure 6.3: Kinetics of digestion, during lipolysis of ~ 50 mM Captex 355 in the fasted state at 37°C with A) pancreatic and B) immobilised lipase, showing fatty acid by HPLC (closed circles) and titration (open circles). Data are mean \pm range ($n=2$).

In the case of lipolysis of 5 mM tricaprylin, digestion proceeded past completion based on the aforementioned assumption of two fatty acids and one monoglyceride (Figure 6.4). For pancreatic lipase, the extent of digestion was calculated to be 178.4% by pH stat titration and 195.6% by HPLC compared to 128.2% by pH stat titration and 116.9% by HPLC for the immobilized lipase.

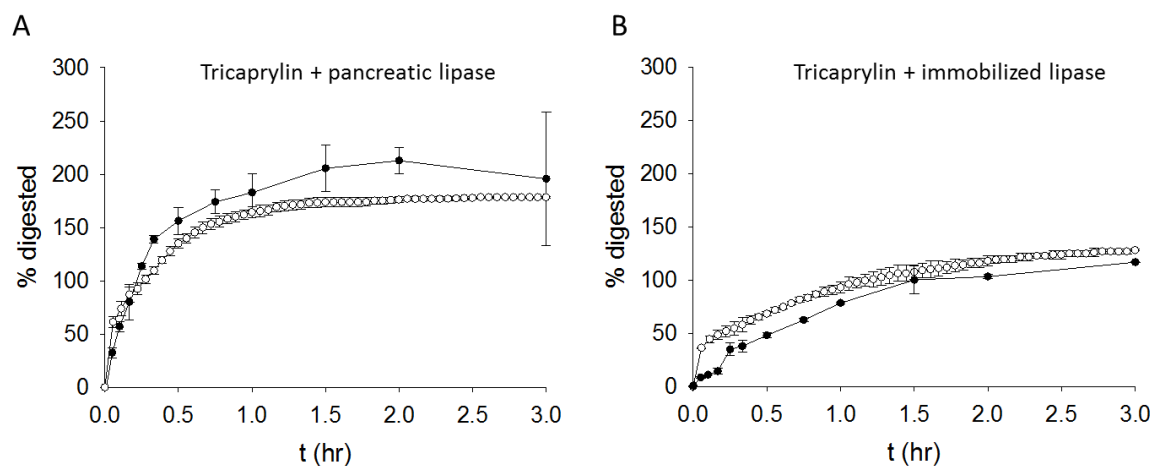


Figure 6.4: Kinetics of digestion, during lipolysis of 5 mM tricaprylin in the fasted state at 37 °C with A) pancreatic and B) immobilised lipase showing fatty acid by HPLC (closed circles) and pH stat titration (open circles). Data are mean \pm range (n=2).

To determine whether separation of immobilised lipase from the digestion medium would be sufficient to halt digestion, samples were removed at predetermined timepoints, without addition of the commonly used inhibitor, 4-BPBA. Correlation of fatty acid content by HPLC and pH stat titration again was observed, confirming that the lipase remains adsorbed to the polymer beads rather than leaching into the digestion medium (Figure SI-6.1).

Structure formation during *in vitro* lipolysis

Synchrotron SAXS was used to determine the structures formed at the completion of digestion to test the hypothesis of reduced scattering from the immobilized lipase, and to confirm independence of structures formed. After subtraction of the buffer as the background, a significant order of magnitude reduction in the scattering was observed in the dispersion of immobilized lipase in digestion buffer compared to pancreatic lipase in digestion buffer (Figure 6.5).

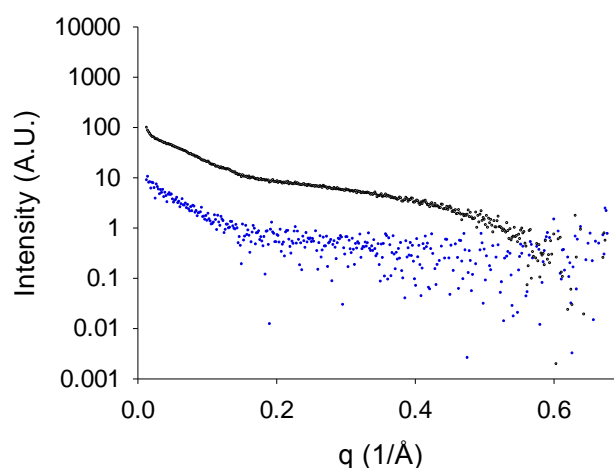


Figure 6.5: SAXS profiles of pancreatic (black) and immobilized (blue) lipase dispersed in digestion buffer pH 6.5 measured at 37 °C.

The two lipases were then used to initiate lipolysis in *in vitro* digestion of formulation lipids and a sample was removed at the endpoint of digestion for structural characterization by SAXS. After 8 hr lipolysis by immobilized lipase, the peaks indicative of a lamellar phase were observed to be more prominent in the scattering profiles after buffer subtraction compared to the sample digested for 3 hr with pancreatic lipase (Figure 6.6A). The lamellar phase had a repeat distance of 29.6 Å. Similarly, better structural resolution of the micellar structure was achieved using immobilised lipase following lipolysis of 5 mM tricapylin under the same digestion conditions (Figure 6.6B).

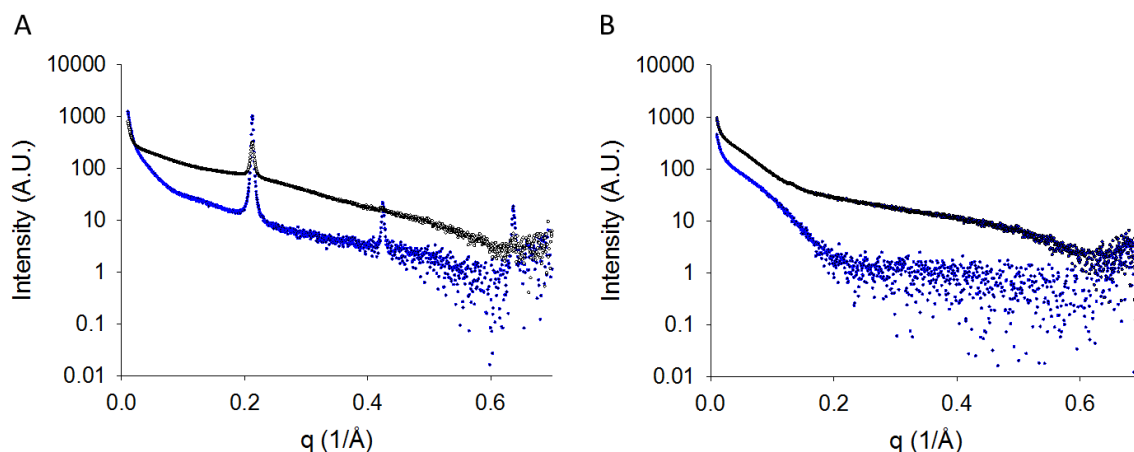


Figure 6.6: SAXS profiles of end point of lipolysis of A) ~ 50 mM Captex 355 and B) 5 mM tricaprylin in the fasted state at 37°C reveal formation of lamellar phase and micelles respectively. Lipolysis was performed with pancreatic (upper) and immobilized (lower) lipase.

6.6 Discussion

Lipases have been employed in the food, dairy, pharmaceutical, detergent, textile, pulp and paper, animal feed, leather and cosmetics industry. The application of immobilised lipases is increasing due to advantages over the free form such as enantioselectivity, increased chemical and thermal stability, cost efficiency and ability for reuse in continuous large-scale commercial processes. Significant resources have been deployed in recent times to attempt to improve and standardize *in vitro* digestion experiments to assist the development of LBFs [8]. It is therefore surprising that immobilized lipases have not been investigated in these activities.

Factors affecting lipase activity

The lipolytic activity of the immobilised lipase was characterized to determine the influence of buffer, pH and temperature. The independence of lipase activity on pH and buffer type opens new avenues for improved and more versatile versions of the ‘accepted’ *in vitro* digestion models. Specifically, more intestinally-relevant buffer systems, at pH values closer to those expected in the duodenum, rather than those traditionally employed in such test methods, would be expected to not deviate from the enzyme activity and structure formation while adding versatility to the choice of model variables. The adherence to past protocols may be claimed to have to a degree actually held back the research field through restricted access to

components such as pancreatic lipase and specific bile components. Challenging these accepted norms through alternative approaches to the models will help to broaden our understanding of the lipid-based formulation field.

Immobilised lipase displays differences in digestion kinetics

This is the first description of immobilised lipases used for *in vitro* lipolysis. Formerly, the definition of a ‘true’ lipase included the presence of a lid and activation by the presence of an interface, such that increased activity is observed when the substrate is present as an emulsion [24]. However this definition has been revised to carboxylesterases that catalyse the hydrolysis and synthesis of acylglycerols of chain length of 10 carbon atoms or more [23-25].

Pancreatic lipase is a typical lipase in that the active site is shielded from solvent, but when it is exposed to a hydrophobic interface it undergoes a conformational change to expose the active site. This is known as interfacial activation [26-29]. Co-lipase is also required to bind to pancreatic lipase to allow it to act at the oil/water interface to hydrolyse triglycerides, and remove bile acids from the interface which could inhibit further digestion [30]. In the current study, the immobilized lipase used, CALB, has a typical lipase α/β hydrolase fold, and the active site consists of a serine, aspartic acid and histidine catalytic triad and no typical lid domain. The amino acids are the same as those found in human and porcine pancreatic lipase [31]. Despite this difference, the current work confirms the lipolytic activity of CALB, and is in agreement with literature reports of little or no interfacial activation [24, 29]. It was found to display enhanced lipolytic activity against tributyrin compared to pancreatic lipase. This is potentially due to differences in conformation; immobilized lipase is adsorbed onto hydrophobic support, which resembles the substrate, thus rendering the lipase in a fixed ‘on’ conformation [32, 33].

The difference in extent of digestion by the two lipases for tricaprylin could be due to the specificity of the lipase. Novozym[®] 435 can show positional specificity, according to the product specifications, whereas the porcine pancreatic extract contains other enzymes such as Pancreatic Lipase-Related Protein 2, Pancreatic Phospholipase A2, colipase and cholesterol esterase so it is possible that further digestion occurs as a result. It has also been previously reported that after digestion, the MG:FA ratio could be as high as 1:6 [35-37]. The lipid composition during digestion of Captex 355 with pancreatic lipase is in agreement with quantification of lipid content during medium chain digestion by HPTLC [34]. Interestingly

the FA content measured by HPLC was higher than by pH stat titration. In the latter, only ionised FA are neutralised with the addition of NaOH, whereas HPLC is expected to detect all fatty acid making it more reliable.

Captex 355 is a mixture of medium chain triglycerides commonly used in lipid based formulations [38, 39]. Digestion of Captex 355 with immobilised lipase was slower than with pancreatin. This could be attributed to the lack of access of the lipase active site to the substrate due to confinement to the polymer beads compared to the pancreatic lipase dispersed freely in solution. The likely mechanism of triglyceride digestion by immobilized lipase is at the droplet interface, as the majority of the triglyceride is in the emulsion droplets due to their low solubility in water. If this is the case, it would be reasonable to expect that if the bead size was reduced and the surface area was increased at a nominal enzyme activity, then the rate of digestion with longer chain triglycerides would increase.

Interestingly, the immobilized lipase was found to be very effective in digesting the short chain lipid, tributyrin, compared to tricaprylin. It has been proposed in literature that lipolysis is dependent on solubility of substrate in the solvent [29]. The difference in activity can be explained by the solubility of the lipid in the solvent; tributyrin is more water soluble than tricaprylin [40]. This is in accordance with previous studies that demonstrated a higher specificity constant of CALB [29, 41], and other lipase [42] for a short chain substrates compared to long chain counterparts.

The product information states that the method of lipase immobilization is by physical adsorption to a macroporous polyacrylic resin, but does not give specific information about their immobilization process. The adsorption technique has weaker linkages between the enzyme and support than expected for covalent linkage [11, 33], thus it was of importance to determine whether desorption of lipase could occur. It has previously been demonstrated that physical desorption or leaching of CALB can occur in the presence of detergent such as Triton-X and organic solvents, leading to the conclusion that CALB is most likely physisorbed onto the support by hydrophobic interactions [10, 43]. Absence of leaching into the medium was confirmed due to correlation of fatty acid by HPLC and pH stat titration during lipolysis, indicating that the removal of immobilised lipase halts digestion. Consequently, unlike pancreatic lipase, inhibition with a molecular inhibitor such as 4-BPBA is not required [5].

Immobilized lipase provides reduced background scattering during *in vitro* lipolysis

SAXS measurements indicated a clear reduction in parasitic scattering in a dispersion of immobilised lipase compared to porcine pancreatin extract, which contains other digestive enzymes such as amylase, trypsin, ribonuclease, deoxyribonuclease, gelatinase and elastase. Interestingly, in the case of the immobilized lipase sample, an upturn was observed at low q . This indicates the presence of some larger particles in the scattering volume which may originate from fragments of the polymer particles.

The SAXS results following *in vitro* lipolysis of Captex 355 and tricaprylin demonstrated that the structural change that occurs at the “kink” in the sigmoidal profile previously attributed to vesicle formation is retained regardless of lipase used [5]. The decreased parasitic scattering observed during lipolysis with immobilized lipase renders it a better lipase for structural studies. It is not straightforward to simply subtract the buffer and lipase curve from the overall scattering data, as the composition of the bulk phase changes due to the formation of new interfaces and adsorption of these materials during the digestion. Application to time-resolved structural determination through improved quality of scattering data is expected to now be enabled by this discovery.

6.7 Conclusion

This study provides insight into the use of immobilised lipase for *in vitro* lipolysis experiments. The digestion kinetics of the immobilised lipase depended on the chain length of the substrate, lipid loading and temperature. The structural and compositional changes during *in vitro* lipolysis were maintained regardless of lipase used, however the decreased background scattering observed with immobilised lipase renders it advantageous over lipase sourced from porcine pancreatic extract for understanding structure formation during lipolysis.

Acknowledgements

This research was undertaken on the SAXS/WAXS beamline at the Australian Synchrotron, Victoria. Funding is acknowledged from the Australian Research Council under the Discovery Projects scheme DP120104032. BJB is a recipient of an Australian Research Council Future Fellowship (FT120100697).

6.8 Supporting Information

Reversed-phase high performance liquid chromatography (HPLC) assay

Table SI-6.1: HPLC assay parameters for lipid analysis.

Compound	Column	Mobile phase	Retention time (min)	Run time (min)	Calibration range (mg/mL)	LOQ (mg/mL)
Caprylic acid	4.6 × 150 mm Phenomenex Luna C ₈ (2) (5 μm, 100 Å)	75:25 MeOH/water (0.1% TFA)	4	7.5	0.10-2.0	0.10
Capric acid	4.6 × 150 mm Phenomenex Luna C ₈ (2) (5 μm, 100 Å)	75:25 MeOH/water (0.1% TFA)	6.3	7.5	0.10-2.0	0.10

HPLC assay validation

Table SI-6.2: Intra- and inter- assay accuracy (%) and precision (CV %) for the quantification of caprylic and capric acid.

Lipid	Concentration (mg/mL)	Intra-assay (n=5)		Inter- assay (n=3)	
		Accuracy (%)	Precision (% CV)	Accuracy (%)	Precision (% CV)
Caprylic acid	0.1	97.0	3.7	98.3	2.6
	1.0	102.3	2.3	99.9	4.1
	2.0	100.4	1.1	98.7	1.0
Capric acid	0.1	98.5	4.3	101.1	3.5
	1.0	102.7	1.7	100.6	3.8
	2.0	101.8	0.6	99.5	1.5

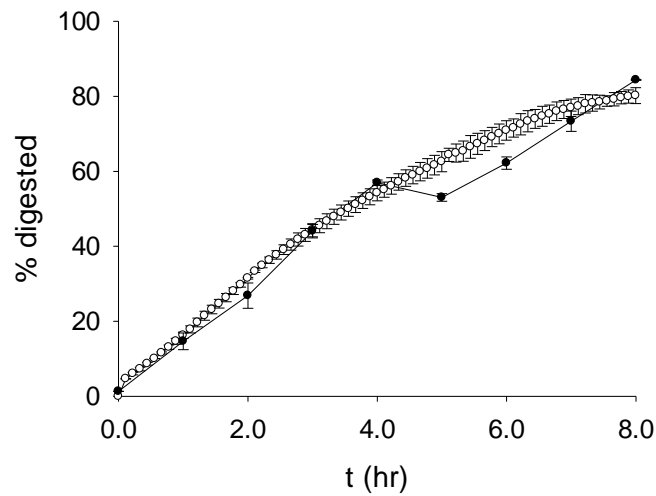
Removal of immobilised lipase halts digestion

Figure SI-6.1: Further digestion inhibited by removal of sample from digestion medium and separation from immobilised lipase. Sample taken at each time point stored at room temperature for duration of digestion – if enzyme has desorbed and was present in sample then would expect 80-90% digestion at all time points. Correlation of fatty acid determined by HPLC (closed circles) and pH stat titration (open circles) during lipolysis of ~50 mM Captex 355 in the fasted state at 37 °C without inhibition with 4-BPBA. Data are mean \pm range (n=2).

6.9 References

1. Kossena, G.A., et al., *Probing drug solubilization patterns in the gastrointestinal tract after administration of lipid-based delivery systems: A phase diagram approach*. J Pharm Sci, 2004. **93**(2): p. 332-348.
2. Kossena, G.A., et al., *Influence of the intermediate digestion phases of common formulation lipids on the absorption of a poorly water-soluble drug*. J Pharm Sci, 2005. **94**(3): p. 481-492.
3. Phan, S., et al., *Self-assembled structures formed during lipid digestion: Characterization and implications for oral lipid-based drug delivery systems*. Drug Delivery Transl Res, 2013. **4**(3): p. 245-294.
4. Warren, D.B., et al., *Real time evolution of liquid crystalline nanostructure during the digestion of formulation lipids using synchrotron small-angle X-ray scattering*. Langmuir, 2011. **27**(15): p. 9528-9534.
5. Phan, S., et al., *Structural aspects of digestion of medium chain triglycerides studied in real time using sSAXS and cryo-TEM*. Pharm Res, 2013. **30**(12): p. 3088-3100.
6. Sek, L., et al., *Evaluation of the in-vitro digestion profiles of long and medium chain glycerides and the phase behaviour of their lipolytic products*. J Pharm Pharmacol, 2002. **54**(1): p. 29-41.
7. Fatouros, D.G. and Mullertz, A., *In vitro lipid digestion models in design of drug delivery systems for enhancing oral bioavailability*. Expert Opin Drug Metab Toxicol, 2008. **4**(1): p. 65-76.
8. Williams, H.D., et al., *Toward the establishment of standardized in vitro tests for lipid-based formulations, part 1: Method parameterization and comparison of in vitro digestion profiles across a range of representative formulations*. J Pharm Sci, 2012. **101**(9): p. 3360-3380.
9. Poojari, Y. and Clarson, S.J., *Thermal stability of Candida antarctica lipase B immobilized on macroporous acrylic resin particles in organic media*. Biocatal Agric Biotechnol, 2013. **2**(1): p. 7-11.
10. Chen, B., et al., *Candida antarctica Lipase B chemically immobilized on epoxy-activated micro- and nanobeads: Catalysts for polyester synthesis*. Biomacromolecules, 2008. **9**(2): p. 463-471.
11. Murty, V.R., Bhat, J., and Muniswaran, P.K.A., *Hydrolysis of oils by using immobilized lipase enzyme: A review*. Biotechnol Bioprocess Eng, 2002. **7**(2): p. 57-66.
12. MacGregor, K.J., et al., *Influence of lipolysis on drug absorption from the gastro-intestinal tract*. Adv Drug Deliv Rev, 1997. **25**(1): p. 33-46.
13. Hernell, O., Staggers, J.E., and Carey, M.C., *Physical-chemical behavior of dietary and biliary lipids during intestinal digestion and absorption. 2 Phase-analysis and aggregation states of luminal lipids during duodenal fat digestion in healthy adult human-beings*. Biochemistry, 1990. **29**(8): p. 2041-2056.
14. Fatouros, D.G., et al., *Colloidal structures in media simulating intestinal fed state conditions with and without lipolysis products*. Pharm Res, 2009. **26**(2): p. 361-374.

15. Kaukonen, A., et al., *Drug solubilization behavior during in vitro digestion of suspension formulations of poorly water-soluble drugs in triglyceride lipids*. Pharm Res, 2004. **21**(2): p. 254-260.
16. Kaukonen, A.M., et al., *Drug solubilization behavior during in vitro digestion of simple triglyceride lipid solution formulations*. Pharm Res, 2004. **21**(2): p. 245-253.
17. Gargouri, Y., Moreau, H., and Verger, R., *Gastric lipases: Biochemical and physiological studies* Biochimica Et Biophysica Acta, 1989. **1006**(3): p. 255-271.
18. Dressman, J.B., et al., *Upper gastrointestinal (GI) pH in young, healthy men and women*. Pharm Res, 1990. **7**(7): p. 756-761.
19. Bergström, C.A.S., et al., *Early pharmaceutical profiling to predict oral drug absorption: Current status and unmet needs*. Eur J Pharm Biopharm, 2014. **57**(0): p. 173-199.
20. Lee, K.W., Porter, C.J., and Boyd, B.J., *A simple quantitative approach for the determination of long and medium chain lipids in bio-relevant matrices by high performance liquid chromatography with refractive index detection*. AAPS PharmSciTech, 2013. **14**(3): p. 927-34.
21. Kirby, N.M., et al., *A low-background-intensity focusing small-angle X-ray scattering undulator beamline*. J Appl Crystallogr, 2013. **46**: p. 1670-1680.
22. Embleton, J.K. and Pouton, C.W., *Structure and function of gastro-intestinal lipases*. Adv Drug Deliv Rev, 1997. **25**(1): p. 15-32.
23. Houde, A., Kademi, A., and Leblanc, D., *Lipases and their industrial applications*. Appl Biochem Biotechnol, 2004. **118**(1-3): p. 155-170.
24. Jaeger, K.E. and Reetz, M.T., *Microbial lipases form versatile tools for biotechnology*. Trends Biotechnol, 1998. **16**(9): p. 396-403.
25. Jaeger, K.E., Dijkstra, B.W., and Reetz, M.T., *Bacterial biocatalysts: molecular biology, three-dimensional structures, and biotechnological applications of lipases*. Annu Rev Microbiol, 1999. **53**: p. 315-51.
26. Ferreira, G.C. and Patton, J.S., *Inhibition of lipolysis by hydrocarbons and fatty alcohols*. J Lipid Res, 1990. **31**(5): p. 889-897.
27. Verger, R. and Dehaas, G.H., *Interfacial enzyme-kinetics of lipolysis*. Annu Rev Biophys Bioeng, 1976. **5**: p. 77-117.
28. Brady, L., et al., *A serine protease triad forms the catalytic centre of a triacylglycerol lipase*. Nature, 1990. **343**(6260): p. 767-70.
29. Blank, K., et al., *Functional expression of Candida antarctica lipase B in Escherichia coli*. J Biotechnol, 2006. **125**(4): p. 474-83.
30. Wickham, M., et al., *Modification of a phospholipid stabilized emulsion interface by bile salt: Effect on pancreatic lipase activity*. J Lipid Res, 1998. **39**(3): p. 623-32.
31. Luthi-Peng, Q., Marki, H.P., and Hadvary, P., *Identification of the active-site serine in human pancreatic lipase by chemical modification with tetrahydrolipstatin*. FEBS Lett, 1992. **299**(1): p. 111-5.

32. *Immobilization of enzymes and cells*, Guisan, J.M., Editor 2006, Humana Press: New Jersey.
33. Knežević, Z.D., Šiler-Marinković, S.S., and Mojović, L.V., *Immobilized lipases as practical catalysts*. Acta Periodica Technologica, 2004(35): p. 151-164.
34. Sek, L., Porter, C.J.H., and Charman, W.N., *Characterisation and quantification of medium chain and long chain triglycerides and their in vitro digestion products, by HPTLC coupled with in situ densitometric analysis*. J Pharm Biomed Anal, 2001. **25**(3-4): p. 651-661.
35. Kalantzi, L., et al., *Canine intestinal contents vs. simulated media for the assessment of solubility of two weak bases in the human small intestinal contents*. Pharm Res, 2006. **23**(6): p. 1373-1381.
36. Persson, E.M., et al., *The effects of food on the dissolution of poorly soluble drugs in human and in model small intestinal fluids*. Pharm Res, 2005. **22**(12): p. 2141-2151.
37. Kleberg, K., et al., *Biorelevant media simulating fed state intestinal fluids: Colloid phase characterization and impact on solubilization capacity*. J Pharm Sci, 2010. **99**(8): p. 3522-3532.
38. Pouton, C.W., *Formulation of poorly water-soluble drugs for oral administration: Physicochemical and physiological issues and the lipid formulation classification system*. Eur J Pharm Biopharm, 2006. **29**(3-4): p. 278-287.
39. Porter, C.J.H. and Charman, W.N., *In vitro assessment of oral lipid based formulations*. Adv Drug Deliv Rev, 2001. **50**: p. S127-S147.
40. Kan, P., et al., *Development of nonionic surfactant/phospholipid o/w emulsion as a paclitaxel delivery system*. J Control Release, 1999. **58**(3): p. 271-8.
41. Adamczak, M., *Synthesis, properties, and application of lipase from Candida antarctica for high yield monoacylglycerol biosynthesis*. Pol J Food Nutr Sci, 2003. **12**(4): p. 3-8.
42. Anguita, J., Rodriguez Aparicio, L.B., and Naharro, G., *Purification, gene cloning, amino acid sequence analysis, and expression of an extracellular lipase from an Aeromonas hydrophila human isolate*. Appl Environ Microbiol, 1993. **59**(8): p. 2411-7.
43. Cabrera, Z., et al., *Novozym 435 displays very different selectivity compared to lipase from Candida antarctica B adsorbed on other hydrophobic supports*. J Mol Catal B: Enzym, 2009. **57**(1-4): p. 171-176.

Chapter 7. Summary and Perspectives

Chapter 7. Summary and Perspectives

7.1 Summary of Findings

Lipid-based formulations are increasingly of interest for the oral delivery of poorly water-soluble drugs and bioactive molecules. These molecules have limited solubility in the aqueous system of the gastrointestinal tract, leading to low absorption and variable bioavailability. The digestion of lipids is a dynamic process with continuous changes in composition and colloidal structure. The lipolysis products are dispersed in the gastrointestinal environment and self-assemble into colloidal phases. These phases enable drug solubilisation, and are important in the digestion process and the nutritional and drug delivery fields. In the case of lipid-based drug delivery, formulation design is still empirical due to a lack of complete understanding of the link between formulation variables, digestion process, lipid self-assembly structures and drug behaviour under dynamic lipolysis conditions. This thesis presents approaches to understanding colloidal structure formation during lipid digestion.

In Chapter 3, the equilibrium structure of bile salt-phospholipid mixed micelles upon incorporation of monoglycerides and fatty acids was studied. Scattering and microscopy techniques revealed an increase in the micellar size and shape upon inclusion of these lipolysis products of increasing lipid chain length. At low pH, elongated particles were present which transitioned to spherical particles at elevated pH. Thus the influence of pH on structure formation could be attributed to the ionisation state of the incorporated fatty acid. The saturated fatty acids were determined to be in the core of the micelle, which was surrounded by a shell composed of monoglyceride, bile salt and phospholipid. Crystallisation was observed when the solubility limit in the micelles was exceeded; however increasing pH and temperature increased the solubility of saturated fatty acids. Crystallisation of lipids and drugs is not ideal as they are expected to be excreted from the body rather than being absorbed in the small intestine. The studies undertaken provided a basis to understand digesting lipid systems in a controlled manner, before progression to studies under non-equilibrium conditions.

The formation of colloidal structures under equilibrium and non-equilibrium conditions was investigated in Chapter 4. SAXS measurements revealed that the colloidal structures depend on monoglyceride and fatty acid chain length, lipid loading, bile salt concentration and whether the lipid was present as an emulsion or crude oil. Long chain lipolysis products were more readily solubilised in mixed bile salt/phospholipid micelles compared to medium chain

counterparts, which are more polar and water soluble. The lattice dimensions of the lamellar phases formed on digestion increased with increasing carbon chain length of the lipolysis products. Furthermore, in Chapter 5 the link between the fatty acid composition and formation of particular uni- and multilamellar vesicles during lipolysis was determined for a medium chain system using HPLC, pH stat titration and SAXS.

The potential for immobilised lipase to address drawbacks in the use of porcine pancreatic lipase for *in vitro* lipolysis, particularly in terms of scattering measurements, was examined in Chapter 6. Pancreatic lipase contains many proteins that scatter in the same size range as the colloidal structures, whereas the immobilised lipase can be separated from the digestion medium prior to SAXS measurement, enabling improved resolution of the scattering for colloidal structures. The activity of the immobilised lipase was buffer- and pH-independent, and its digestion kinetics was dependent on the solubility of the substrate in water, hence it could be used in a simplified approach to *in vitro* lipolysis studies. Correlation of colloidal structure and product formation (fatty acid composition) during lipolysis was determined by HPLC and pH stat titration.

Overall the studies have provided new approaches and insights into structure formation during lipid digestion and build our understanding of how composition and conditions can be manipulated to target specific structural types towards the long term goal of enabling rational design of lipid-based drug formulations.

7.2 Future Directions

The work in this thesis naturally points to areas of further research into lipid-based drug delivery systems. In this thesis, the use of deuterated fatty acids in the equilibrium studies was limited to saturated fatty acids, primarily due to limitations in available materials from the Australian National Deuteration Facility. A significant part of dietary lipid intake is from unsaturated fats, thus the studies in Chapter 3 can be extended by using long- chain unsaturated fatty acids. For instance triglycerides in food products such as oils have oleic acid (C_{18:1}) as a major component. Using the triolein system would be a natural extension of this work.

The likely *in vivo* relevance of the model equilibrium systems could be increased with the inclusion of additional components to the simplified systems used in these studies. Sodium

taurodexycholate is only one of the bile salts present in the complex mix, and although some studies use one bile salt for economic reasons and for greater batch-to-batch consistency [1-3], others use a porcine bile extract [4-7]. Further important endogenous lipids such as cholesterol and lyso-phosphatidyl choline, both of which are expected to be present in colloidal structures after digestion of lipid formulations or a fatty meal were not included, but could influence the phase behaviour.

As the food bolus progresses through the gastrointestinal tract, it is subject to changes in pH and exposure to different enzymes and secretions. In Chapters 3 and 4 and elsewhere, pH has been shown to influence colloidal structure formation [8-10]. A more *in vivo* relevant approach to the *in vitro* lipolysis model could include infusion of the bile salt solution and pancreatic lipase into the digestion vessel, followed by a gradual increase in pH over time to better simulate *in vivo* conditions, with simultaneous structural evaluation using SAXS. Furthermore, a limitation of the model is that it does not include an absorption step, whereby lipolysis products and drug molecules are removed from the system. This lack of sink condition leads to a build-up of lipolysis products and incomplete digestion, which is not reflective of the efficient lipid digestion process *in vivo*. The use of Caco-2 cells [11] or polymers [12, 13] to absorb lipids, could be applied to the current work to address this, enabling a more relevant analyses of the restructuring of colloidal structures formed.

The 'end game' is to understand what colloidal structures are formed during lipid digestion, how they influence delivery of active compounds in terms of solubilisation, precipitation and absorption, with the aim of enabling the rational design of lipid-based formulations. Hence, the release of incorporated poorly water-soluble drugs during digestion of lipid-based formulations could be investigated. The behaviour of drug in these systems under digesting conditions is not well understood and traditionally precipitation has been believed to limit drug absorption. Recent studies suggest this may not be the case if precipitation occurs in an amorphous form [14]. An early direction in this work was to examine the solid state of precipitated drug during digestion of lipid systems using wide angle X-ray diffraction, and to quantify drug in the aqueous and pellet phase. It was observed that danazol and fenofibrate, both non-ionic drugs precipitate crystalline, but halofantrine, a basic drug did not precipitate. Hence, the modified thermodynamic environment in self-assembled structures formed during the digestion of co-administered lipids impacts drug solubilisation, and controls precipitation. Furthermore, formulations could be developed that can be manipulated to on-demand structural transitions during digestion for controlled-release systems.

The immobilised lipase provides an opportunity to simplify and standardise the *in vitro* lipolysis model as the lipolytic activity was demonstrated to be independent of buffer type and pH, and moderate activity was maintained at ambient temperature. It can be applied to time-resolved structural determinations to improve the quality of scattering data.

It remains to be seen whether equilibrium and dynamic experiments translate to the *in vivo* scenario. A limited number of *ex vivo* studies report the presence of vesicles and mixed micelles in human aspirates after lipid administration, however no cubic or hexagonal phases were observed [15-17]. It is anticipated that application of structure-revealing techniques in real-time with high resolution and fast kinetic studies, to an *in vivo* scattering model would negate the shortcomings of current approaches, such as artefacts induced by sampling and inhibition protocols. This online *in vivo* model could consist of a section of quartz capillary surgically inserted into the intestine of a rat, which is then fixed in the path of an X-ray beam during *in situ* SAXS/WAXS experiments. Such advancement will be the ultimate goal in understanding and controlling self-assembled structures and their implications for delivery of pharmaceutically active molecules.

7.3 References

1. Williams, H.D., et al., *Toward the establishment of standardized in vitro tests for lipid-based formulations, part 1: Method parameterization and comparison of in vitro digestion profiles across a range of representative formulations.* J Pharm Sci, 2012. **101**(9): p. 3360-3380.
2. Warren, D.B., et al., *Real time evolution of liquid crystalline nanostructure during the digestion of formulation lipids using synchrotron small-angle X-ray scattering.* Langmuir, 2011. **27**(15): p. 9528-9534.
3. Sek, L., Porter, C.J.H., and Charman, W.N., *Characterisation and quantification of medium chain and long chain triglycerides and their in vitro digestion products, by HPTLC coupled with in situ densitometric analysis.* J Pharm Biomed Anal, 2001. **25**(3-4): p. 651-661.
4. Fatouros, D.G., Bergenstahl, B., and Mullertz, A., *Morphological observations on a lipid-based drug delivery system during in vitro digestion.* Eur J Pharm Biopharm, 2007. **31**(2): p. 85-94.
5. Fatouros, D.G., et al., *Structural development of self nano emulsifying drug delivery systems (SNEDDS) during in vitro lipid digestion monitored by small-angle X-ray scattering.* Pharm Res, 2007. **24**(10): p. 1844-1853.
6. Zangenberg, N.H., et al., *A dynamic in vitro lipolysis model I. Controlling the rate of lipolysis by continuous addition of calcium.* Eur J Pharm Sci, 2001. **14**(2): p. 115-122.

7. Christensen, J.O., et al., *Solubilisation of poorly water-soluble drugs during in vitro lipolysis of medium- and long-chain triacylglycerols*. Eur J Pharm Biopharm, 2004. **23**(3): p. 287-296.
8. Salentinig, S., Sagalowicz, L., and Glatter, O., *Self-assembled structures and pK(a) value of oleic acid in systems of biological relevance*. Langmuir, 2010. **26**(14): p. 11670-11679.
9. Salentinig, S., et al., *Formation of highly organized nanostructures during the digestion of milk*. ACS Nano, 2013. **7**(12): p. 10904-10911.
10. Phan, S., et al., *Disposition and crystallization of saturated fatty acid in mixed micelles of relevance to lipid digestion*. J Colloid Interface Sci, 2015. **449**: p. 160-166.
11. Vors, C., et al., *Coupling in vitro gastrointestinal lipolysis and Caco-2 cell cultures for testing the absorption of different food emulsions*. Food Funct, 2012. **3**(5): p. 537-46.
12. Boyd, B.J., Porter, C.J., and Charman, W.N., *Using the polymer partitioning method to probe the thermodynamic activity of poorly water-soluble drugs solubilized in model lipid digestion products*. J Pharm Sci, 2003. **92**(6): p. 1262-71.
13. Sallee, V.L., *Determinants of fatty acid and alcohol monomer activities in mixed micellar solutions*. J Lipid Res, 1978. **19**(2): p. 207-14.
14. Sassene, P.J., et al., *Precipitation of a poorly soluble model drug during in vitro lipolysis: Characterization and dissolution of the precipitate*. J Pharm Sci, 2010. **99**(12): p. 4982-4991.
15. Hernell, O., Staggars, J.E., and Carey, M.C., *Physical-chemical behavior of dietary and biliary lipids during intestinal digestion and absorption. 2 Phase-analysis and aggregation states of luminal lipids during duodenal fat digestion in healthy adult human-beings*. Biochemistry, 1990. **29**(8): p. 2041-2056.
16. Müllertz, A., et al., *Insights into intermediate phases of human intestinal fluids visualized by atomic force microscopy and cryo-transmission electron microscopy ex vivo*. Mol Pharm, 2012. **9**(2): p. 237-247.
17. Armand, M., et al., *Digestion and absorption of 2 fat emulsions with different droplet sizes in the human digestive tract*. Am J Clin Nutri, 1999. **70**(6): p. 1096-1106.